

“Barley HIPP protein HvFP1 functions in a crosstalk between abiotic stress responses and developmental signaling pathways, including leaf senescence”

Dissertation

To obtain the academic degree
doctor rerum naturalium (Dr. rer. nat.)

submitted to

Faculty of natural sciences I – Biosciences –
Martin-Luther-University Halle-Wittenberg



Submitted by

Athina Parasyri

Born on 09 October 1991

in Rethymnon, Greece

Reviewer 1: Prof. Dr. Klaus Humbeck
Reviewer 2: Prof. Dr. Nicolaus von Wirén
Reviewer 3: Prof. Dr. Karin Krupinska

Date of public defense: 04 April 2023

Table of Contents

Abbreviations	V
Summary.....	1
Zusammenfassung	2
1. Introduction	3
1.1. Plant photosynthesis and leaf senescence: two processes for nutrient distribution.....	3
1.2. Plant development under unfavorable conditions	4
1.2.1. Plant adaptation strategies under biotic and abiotic stress	5
1.2.2. The role of ABA in abiotic stress response signaling pathways	8
1.2.3. The role of other phytohormones in plant response signaling pathways	10
1.3. Heavy metal associated Isoprenylated Plant Protein family	11
1.3.1. HIPP proteins in model plants <i>Arabidopsis thaliana</i> and <i>Oryza sativa</i>	13
1.3.2. HIPP proteins in other plant species	16
1.4. Barley as model plant.....	17
1.5. Goal of dissertation	19
2. Results	20
2.1. Expression level of <i>HvFPI</i> in barley primary leaves during abiotic stress, phytohormone treatment and developmental leaf senescence.....	20
2.1.1. The effect of abiotic stress treatments on transcript level of <i>HvFPI</i>	20
2.1.2. Expression of <i>HvFPI</i> during developmental leaf senescence	22
2.1.3. Effect of phytohormone treatments on <i>HvFPI</i> expression level	22
2.2. Transgenic lines of <i>Hordeum vulgare</i> L. cv. Golden promise	23
2.2.1. Establishment of overexpression lines 21.3I and 21.2A	24
2.2.2. Establishment of knock out lines 20.1At and 20.17M	24
2.2.3. Transcript and protein level of <i>HvFPI</i> in OE and KO lines	25
2.2.4. Phenotypic analysis of transgenic lines.....	26
2.3. Study of barley WT and <i>HvFPI</i> OE lines under various abiotic stress conditions and during developmental leaf senescence.....	27
2.3.1. Drought stress	27
2.3.2. Combined cold and high light stress	30
2.3.3. Salt stress.....	32
2.3.4. Dark stress (Dark induced leaf senescence).....	34
2.3.5. Developmental leaf senescence.....	36
2.4. Study of WT and <i>HvFPI</i> KO barley lines under drought stress and developmental leaf senescence	39
2.4.1. Drought stress	39
2.4.2. Developmental leaf senescence.....	42
2.5. RNA Seq analysis.....	45
2.5.1. Senescence Associated Genes of <i>Hordeum vulgare</i>	46
2.5.2. Genes possibly regulated downstream of <i>HvFPI</i>	52
2.5.2.1. Validation of differential expression of selected candidate genes in two <i>HvFPI</i> OE lines	55
3. Discussion.....	57
3.1. <i>HvFPI</i> is induced during abiotic stress and developmental leaf senescence	57
3.2. Phytohormone regulation of <i>HvFPI</i>	58
3.3. <i>HvFPI</i> knock out plants behave similar to wild type during stress treatments and developmental leaf senescence	59

3.4. Overexpression of <i>HvFPI</i> causes distinct changes in ABA-related gene expression and in the course of leaf senescence	60
3.5. Transcriptomic analysis of developmental leaf senescence in <i>Hordeum vulgare</i>	62
3.5.1. Senescence Associated Genes (SAGs).....	63
3.5.1.1. Transcription factors	63
3.5.1.2. Anabolic and catabolic enzymes.....	64
3.5.1.3. Carbon remobilization and cell wall organization	66
3.5.1.4. Transporters	67
3.5.1.5. Phytohormones and signaling cascades	68
3.5.1.6. Redox regulation.....	70
3.5.1.7. Stress responses and other genes	72
3.5.2. Senescence Downregulated Genes (SDGs)	73
3.5.2.1. Transcription factors	73
3.5.2.2. Components of photosynthetic apparatus	75
3.5.2.3. Anabolic and catabolic enzymes.....	75
3.5.2.4. Carbon remobilization and cell wall organization	76
3.5.2.5. Transporters	77
3.5.2.6. Phytohormones and signaling cascades	77
3.5.2.7. Redox regulation.....	79
3.5.2.8. Stress responses and other genes	80
3.6. Identification of target genes in <i>HvFPI</i> regulatory pathways	81
3.6.1. Differentially expressed genes in <i>HvFPI</i> OE lines in both control and senescing states	81
3.6.2. Differentially expressed genes in <i>HvFPI</i> OE lines in either control or senescing states.....	83
3.7. Proposed model for the function of <i>HvFPI</i>	84
4. Materials and Methods	88
4.1. Materials.....	88
4.1.1. Chemicals, solvents, kits and enzymes	88
4.1.2. Vectors	88
4.1.3. Microorganisms	88
4.1.4. Primers	88
4.1.5. Plant material	89
4.1.5.1. Overexpression lines 21.3I and 21.2A.....	89
4.1.5.2. Knock out lines 20.1At and 20.17M.....	89
4.2. Methods.....	89
4.2.1. Barley plant cultivation.....	89
4.2.2. Phenotypic characterization of barley plants	90
4.2.3. Experimental Design/ Abiotic Stress Treatments	90
4.2.3.1. Drought stress	90
4.2.3.2. Cold and high light stress.....	90
4.2.3.3. Salt stress	90
4.2.3.4. Dark induced leaf senescence	90
4.2.3.5. Developmental leaf senescence	91
4.2.3.6. Phytohormone treatments	91
4.2.4. Measurement of physiological parameters.....	91
4.2.4.1. Photosystem II efficiency	91
4.2.4.2. Chlorophyll content	91
4.2.5. Isolation of total RNA.....	91
4.2.6. Synthesis of complementary DNA.....	92

4.2.7. Quantitative Real-Time PCR	92
4.2.8. DNA isolation	92
4.2.9. Polymerase Chain Reaction	93
4.2.10. Agarose gel.....	93
4.2.11. Gel extraction and DNA sequencing.....	93
4.2.12. Protein isolation.....	93
4.2.13. Protein quantification	94
4.2.14. SDS Polyacrylamide Gel Electrophoresis	94
4.2.15. Antibody production/ Western blot analysis	94
4.2.16. RNA Sequencing.....	95
4.2.16.1. Sample preparation	95
4.2.16.2. Library preparation and sequencing.....	95
4.2.16.3. Data Analysis.....	96
4.2.16.3.1. Quality control.....	96
4.2.16.3.2. Mapping to reference genome, novel gene prediction and quantification.....	96
4.2.16.3.3. Differential expression analysis.....	96
4.2.16.3.4. Functional analysis	97
4.2.17. Statistical analysis	97
5. References	98
6. Appendix	VIII
6.1. Additional information for barley <i>H. vulgare</i> L. cv. Golden promise transgenic lines.....	VIII
6.1.1. The constructs for the establishment of OE and KO lines	VIII
6.1.2. Polymerase Chain Reaction (PCR) for genotyping of OE and KO lines.....	IX
6.1.3. Phenotypic characterization of OE and KO lines.....	XI
6.2. Additional information for RNA Seq analysis in barley primary leaves	XII
6.2.1. Example of quality control of the RNA samples with a Bioanalyzer	XII
6.2.2. Number of reads and total mapping rate of the 12 samples	XIII
6.2.3. Complete lists of SAGs and SDGs.....	XIV
6.2.4. Lists of five DEGs groups in control and/or senescence samples of <i>HvFPI</i> OE line	XXV
6.3. The relative transcript level of six members of barley HIPP family during developmental leaf senescence in WT, OE and KO lines	XXVIII
6.4. Additional information for the primers and vectors used in Materials and Methods.....	XXIX
6.4.1. Vectors for genetic transformation of barley embryos.....	XXIX
6.4.2. List of primers and oligos used in PCR, qRT-PCR and CRISPR protocols	XXIX
List of Figures.....	XXXII
List of Tables.....	XXXIV
Acknowledgements	XXXV
Curriculum Vitae	XXXVI
Statutory declaration.....	XXXVII

Abbreviations

ABA	Abscisic Acid		Millions base pairs
Amp ^R	Ampicillin Resistance		sequenced
Appx.	Appendix	F _v	Variable Fluorescence
APS	Ammonium Persulfate	Fw	forward primer
BAM	Binary Alignment Map	F ₀	Minimum Fluorescence
bp	base pair	GA	Gibberellins
C	Control sample	h	hour
CaMV	Cauliflower Mosaic Virus	HIPP	Heavy metal associated Isoprenylated Plant Protein
Ca	Calcium	HL	High Light
Cd	Cadmium	HMA	Heavy Metal Associated domain
cDNA	complementary DNA	H ₂ O ₂	Hydrogen Peroxide
Chl	Chlorophyll	i.e.	id est (Latin), that is
CK	Cytokinin	Kan ^R	Kanamycin Resistance
cm	centimeter	kDa	kilodalton
Cm ^R	Chloramphenicol Resistance	kg	kilogram
CRISPR	Clustered Regularly Interspaced Short Palindromic Repeats	KO	Knock Out
Cu	Copper	KOH	Potassium Hydroxide
DAS	Days After Sowing	L	Liter
DEG	Differentially Expressed Genes	LSD	Leaf Senescence Database
DEPC	Diethyl Pyrocarbonate	log	logarithm
DNA	Deoxyribonucleic Acid	m	meter
dNTP	Deoxynucleoside Triphosphate	M	Molar concentration
DTT	Dithiothreitol	(Me)JA	(Methyl) Jasmonate
EDTA	Ethylenediaminetetraacetic Acid	mg	milligram
e.g.	exempli gratia (Latin), for example	min	minute
ERAD	Endoplasmic Reticulum Associated Degradation	ml	milliliter
et al.	et alia (Latin), and others	mM	millimolar
ETI	Effector-Triggered Immunity	mmol	millimole
EtOH	Ethanol	mRNA	messenger RNA
FC	Fold Change	NaCl	Sodium Chloride
Fig.	Figure	ng	nanogram
F _m	Maximum Fluorescence	NLS	Nuclear Localization Signal
FPKM	Fragments Per Kilobase of transcript sequence per	NTP	Nucleoside Triphosphate
		°C	grad Celcius
		OE	Overexpression
		PAM	Pulse Amplitude Modulation
		PCR	Polymerase Chain Reaction
		PMSF	Phenylmethylsulfonyl Fluoride
		pol	polymerase

pre-mRNA	premature messenger RNA	vol.	volume
PSI	Photosystem I	vs	versus
PSII	Photosystem II	WBB	Western Blotting Buffer
PTI	Pattern Triggered Immunity	WT	Wild Type
PVDF	Polyvinylidene Difluoride	w/v	weight per volume
qRT-PCR	quantitative Real-Time PCR	ZmCas9	<i>Zea mays</i> CRISPR associated 9
rcf	relative centrifugal force	ZmUbi1p	<i>Zea mays</i> Ubiquitin 1
REST	Relative Expression Software Tool	Zn	Zinc
Rev	reverse primer	µg	microgramm
RIN	RNA Integrity Number	µl	microliter
RNA	Ribonucleic Acid	µM	micromolar
RNase	Ribonuclease	µmol	micromole
ROS	Reactive Oxygen Species	6-BAP	6-Benzyl-Aminopurine
rpm	revolutions per minute	6-His	Hexahistidine tag
rRNA	ribosomal RNA		
RT	Room Temperature		
RWC	Relative Water Content		
R ²	square of the Pearson correlation coefficient		
S	Senescing sample		
SA	Salicylic Acid		
SAG	Senescence Associated Gene		
SDG	Senescence Downregulated Gene		
SDS	Sodium Dodecyl Sulfate		
SDS-PAGE	SDS-polyacrylamide gel electrophoresis		
s	second		
Seq	Sequencing		
sgRNA	single guide RNA		
SPAD	Soil Plant Analysis Development		
Spec ^R	Spectinomycin Resistance		
TA	Transcription Activator		
TAE	Tris-Acetic acid-EDTA buffer		
TBS(T)	Tris-buffered saline (with Tween20)		
TE	Tris-EDTA buffer		
TEMED	Tetramethylethylenediamine		
TF	Transcription Factor		
T _m	Melting Temperature		
v	version		

Abbreviations of gene/protein names

ABC	ATP-Binding Cassette	Hsp17	Heat Shock Protein 17
ABF	ABA-responsive Binding Factor	HvFP1	<i>Hordeum vulgare</i> Farnesylated protein 1
ABI	Abscisic Acid Insensitive	IPT	Isopentyl-transferase
ACBD/P	Acyl-CoA-Binding Domain/Protein	JAZ	Jasmonate ZIM-Domain
ACC	1-Aminocyclopropane-1-Carboxylic acid	LEA	Late Embryogenesis Abundant
AP2	APETALA2	LRR	Leucine-Rich Repeat
AREB	ABA-Responsive Element Binding factor	MSANTD	Myb/SANT-like DNA-binding domain protein
ARF	Auxin Response Factor	NCED	9- <i>cis</i> -Epoxy-carotenoid Dioxygenase
AtFP	<i>Arabidopsis thaliana</i> Farnesylated protein	NOL	NonYellow Coloring 1-Like
ATP	Adenosine Triphosphate	NYC	NonYellow Coloring
bHLH	basic Helix-Loop-Helix	OPDA	12-Oxo-Phytodienoic Acid
CKF	Cytokinin response factor	OST1	Open Stomata 1
CKX	Cytokinin oxidases/ dehydrogenases	PAO	Polyamine Oxidase
Cor(14b)	Cold Regulated (14b)	PFBS	Phytochromobilin:ferredoxin oxidoreductase/ PFB synthase
CPK	Ca ²⁺ -dependent Protein Kinases	PMTV	Potato Mop-Top Virus
CRT	C-Repeat	PP2A	Protein Phosphatase 2A
Cytb ₆ f	Cytochrome b ₆ f	PP2C	Protein Phosphatase 2C
C3H-	CCCH domain-containing protein -	PYL	PYR-Like proteins
Dhn1	Dehydrin 1	PYR1	Pyrabactin Resistance Protein 1
DRE	Dehydration-Responsive Element	P5CS	delta 1-Pyrroline-5-Carboxylate Synthetase
DREB	DRE-/CRT-binding protein	RCAR	Regulatory Components of ABA Receptor
EBP	Ethylene Binding Protein	RCC	Regulator of Chromosome Condensation
EIN	Ethylene Insensitive	RD	Response to Dehydration
EM	Early Methionine Labelled	RuBisCO	Ribulose-1,5-Bisphosphate Carboxylase/Oxygenase
ERA	Enhanced Response to ABA	SAM	S-adenosyl-L-methionine
ERF	Ethylene Responsive Factor	SAUR	Small Auxin Up RNA
FRS	FAR1-related sequence	SBT	Subtilisin protease
GCN5	General Control Non-repressed 5	SnRK2s	Sucrose non-fermenting 1-Related protein Kinase 2s
GS2	Glutamine Synthetase 2	TPR	Tetratricopeptide Repeat
HAB	Hypersensitive to ABA	VNI	Vascular-related NAC-domain-Interacting
Hpt	Hygromycine Phosphotransferase	2OG	2-oxoglutarate

Summary

Plants' sessile lifestyle exposes them to a number of adverse conditions. The environmental factors, which may cause severe stress to plants, are categorized as biotic and abiotic. Biotic stress derives from living organisms, such as fungi, bacteria, insects and others, while abiotic stress is caused by physicochemical factors and includes water deprivation, high or low temperature, high salinity, high or low light intensity and complete darkness. Plants have the ability to sense those factors and, through signaling cascades, activate specific responses for their adaptation and survival. The multiple signaling networks involve many components, which may act autonomously in a specific pathway or in interaction with components of other signaling cascades. This fine-tuned crosstalk among stress response pathways, as well as regulatory developmental processes determine the adaptability and survival rate of plants. Thus, unraveling and studying factors, which act in a crosstalk and regulate many aspects of plant life may improve their performance and overall yield. In the present work, it is proposed that barley *Hordeum vulgare* Farnesylated Protein 1 (HvFP1), which belongs to family of Heavy metal associated Isoprenylated Plant Proteins, has such crosstalk mode of action. This protein possesses one heavy metal associated domain, one isoprenylation site at the C'-end and one nuclear localization signal. In a transcriptomic analysis, it was shown that *HvFP1* was induced after exposure to various abiotic stress conditions and application of abscisic acid, which is known to regulate abiotic stress responses. Furthermore, this gene was induced at the final stage of developmental leaf senescence, while cytokinins, which are negative regulators of this process, suppressed *HvFP1*. Establishment and study of barley *HvFP1* overexpression (OE) and knock out (KO) lines showed that the OE lines exhibited a modified expression of stress- and senescence-related genes, which are regulated by abscisic acid, and delayed the course of developmental leaf senescence. On the other hand, the KO lines behaved similar to wild type (WT) plants. In order to unravel the mode of action and detect possible interaction partners of HvFP1, an RNA Seq transcriptomic analysis was performed in barley WT and OE primary leaves in control and senescing state. On one hand, the analysis of WT samples revealed a long list of senescence up- or downregulated genes, creating a novel comprehensive leaf senescence database for barley. On the other hand, a comparison between WT and OE samples resulted in a number of differentially expressed genes, which were mostly upregulated and might act downstream of HvFP1 in specific plant processes. It is worth mentioning that many of those differentially expressed genes corresponded to Zn²⁺ finger binding domain proteins. Thus, it is proposed that HvFP1 acts directly through its heavy metal associated domain in providing Zn²⁺ to those proteins for their downstream activation. Another interesting observation was the positive regulation of other multifunctional genes, including many HvFRS5 proteins and a member of the HvACBD family. Thus, HvFP1 may act indirectly by positively influencing the expression of those genes, which then regulate multiple aspects of plant responses and development.

Zusammenfassung

Die sessile Lebensweise von Pflanzen setzt sie einer Reihe von widrigen Bedingungen aus. Die Umweltfaktoren, die Pflanzen stark belasten können, werden in biotische und abiotische Faktoren eingeteilt. Biotischer Stress geht von lebenden Organismen wie Pilzen, Bakterien, Insekten und anderen aus, während abiotischer Stress durch physikalisch-chemische Faktoren wie Wasserentzug, hohe oder niedrige Temperatur, hoher Salzgehalt, hohe oder niedrige Lichtintensität und völlige Dunkelheit verursacht wird. Pflanzen sind in der Lage, diese Faktoren zu erkennen und über Signalkaskaden spezifische Reaktionen für ihre Anpassung und ihr Überleben zu aktivieren. An den multiplen Signalnetzwerken sind viele Komponenten beteiligt, die autonom in einem bestimmten Signalweg oder in Wechselwirkung mit Komponenten anderer Signalkaskaden wirken können. Dieses fein abgestimmte Zusammenspiel zwischen Signalwegen, die sowohl Stressantworten als auch Entwicklungsprozesse steuern, determinieren die Anpassungsfähigkeit und Überlebensrate von Pflanzen. Die Entschlüsselung und Untersuchung von Faktoren, die in einem Wechselspiel wirken und viele Aspekte des Pflanzenlebens regulieren, ist eine wichtige Voraussetzung, um pflanzliche Leistung und ihren Gesamtertrag verbessern. In der vorliegenden Arbeit wird postuliert, dass das Gerstenprotein *Hordeum vulgare* Farnesylated Protein 1 (HvFP1), das zur Familie der schwermetallassozierten isoprenylierten Pflanzenproteine gehört, einen solchen Crosstalk-Wirkungsmechanismus aufweist. Dieses Protein besitzt eine schwermetallassozierte Domäne, eine Isoprenylierungsstelle am C'-Ende und ein Kernlokalisierungssignal. Mittels qRT-PCR wurde gezeigt, dass *HvFP1* bei verschiedenen abiotischen Stressbedingungen und nach Applikation von Abscisinsäure, die bekanntermaßen abiotische Stressreaktionen reguliert, induziert wurde. Außerdem wurde dieses Gen im Endstadium der Blattseneszenz induziert, während Cytokinine, die diesen Prozess negativ regulieren, *HvFP1*-Expression unterdrückten. Die Etablierung und Untersuchung von Gersten-*HvFP1*-Überexpressions- (OE) und Knock-Out- (KO) Linien zeigte, dass die OE-Linien eine veränderte Expression von stress- und seneszenzbezogenen Genen aufwiesen, die durch Abscisinsäure reguliert werden, und einen verzögerten Verlauf der entwicklungsbedingten Blattseneszenz zeigen. Andererseits verhielten sich die KO-Linien ähnlich wie Wildtyp-Pflanzen (WT). Um die Wirkungsweise von HvFP1 zu entschlüsseln und Zielgene der HvFP1-Regulation aufzuspüren, wurde eine RNA-Seq-Transkriptomanalyse in Gersten-WT- und OE-Primärblättern im Kontroll- und Seneszenzstadium durchgeführt. Einerseits ergab die Analyse der WT-Proben eine lange Liste von Genen, die in der Seneszenz hoch- oder herunterreguliert wurden, so dass erstmalig eine umfassende Datenbank der Blattseneszenz bei Gerste erstellt werden konnte. Andererseits ergab ein Vergleich zwischen WT- und OE-Proben eine Reihe von unterschiedlich exprimierten Genen, die zumeist hochreguliert waren und möglicherweise bei bestimmten Pflanzenprozessen downstream von HvFP1 wirken. Andererseits ergab ein Vergleich zwischen WT- und OE-Proben eine Reihe von unterschiedlich exprimierten Genen, die zumeist hochreguliert waren und möglicherweise bei bestimmten Pflanzenprozessen downstream von HvFP1 wirken. Es ist erwähnenswert, dass viele dieser unterschiedlich exprimierten Gene mit Zn²⁺-Finger-Bindungsdomänenproteinen korrespondieren. Es wird daher vermutet, dass HvFP1 direkt über seine Schwermetall-assozierte Domäne Zn²⁺ für diese Proteine bereitstellt, damit sie downstream aktiviert werden können. Eine weitere interessante Beobachtung war die positive Regulierung anderer multifunktionaler Gene, darunter viele HvFRS5-Proteine und ein Mitglied der HvACBD-Familie. Somit könnte HvFP1 indirekt wirken, indem es die Expression dieser Gene positiv beeinflusst, die dann mehrere Aspekte der Pflanzenreaktionen und der Entwicklung regulieren.

1. Introduction

1.1. Plant photosynthesis and leaf senescence: two processes for nutrient distribution

Plants and single cell photosynthetic organisms are defined as autotrophs, meaning that they require sunlight as energy input, water as reducing agent and CO₂ as carbon source to produce complex organic compounds, such as carbohydrates, through photosynthesis. Their ability to use sunlight as energy source and their limited demand in raw materials makes them the primary producers and the basis of food chain of all living organisms. This fascinating life style depends on the photosynthetic apparatus, which is located in thylakoid membranes of chloroplasts. Basic components in this chain are the photosystem I (PSI) and photosystem II (PSII), the cytochrome b₆f (Cytb₆f) complex and an ATP synthase (Rochaix, 2011). Both photosystems consist of a number of proteins, some of which are harbouring chlorophyll (Chl) molecules, organized in a core reaction center and surrounding light-harvesting complexes. In photosynthesis, driven by light energy, electrons are transferred along the photosynthetic chain and the energy fluctuation during this process resembles a Z scheme, as first proposed by Hill & Bendall (1960). Photosynthesis provides the basis for energy acquisition and complex macromolecule synthesis in plant cells. Then, its products are transferred from source to sink tissues through phloem vascular system (Lemoine *et al.*, 2013). That ensures enough carbon molecules for non-photosynthetic cells, including those in root system and new developing leaves.

During maturation, leaves synthesize many complex macromolecules, such as proteins that form the photosynthetic machinery in the chloroplasts. When the photosynthetic performance of a specific leaf is no more needed, due to a developmental or stress-induced shift from vegetative to reproductive state, the last phase of leaf development is activated, which is known as leaf senescence. This process is the final point in cell life, where major metabolic procedures are ceased and all nutrients are redistributed to other tissues and organs (Krieger-Liszkay *et al.*, 2019). In fact, among the first obvious signs of leaf senescence is the degradation of Chl molecules and chloroplasts, resulting in color change of leaves (Pružinská *et al.*, 2005). The execution of this process determines the efficient recycling of macromolecules and other substances from older cells and tissues to new developing ones, in order to avoid any loss in nutrients. Thus, it is a highly regulated process, accompanied by a massive reprogramming of gene expression. All genes, which are induced during developmental leaf senescence, are known as Senescence Associated Genes (SAGs), while those, who are downregulated, are known as Senescence Downregulated Genes (SDGs) (Ahmad & Guo, 2019). After extensive research in the field of leaf senescence, databases are created and constantly updated, including all known SAGs and SDGs in model plants, such as *Arabidopsis thaliana* (Li *et al.*, 2020). A functional analysis of those differentially regulated genes has appointed them with a specific mode of action and the same functional groups are found among various plant species. Each group has a specific function during leaf senescence, although there are still open questions and missing points regarding the fine-tuning of this process.

The main process during leaf senescence is the recycling of nutrients from older to younger tissues. For that, multiple catabolic enzymes for degradation of proteins, lipids and nucleic acids are activated and the resulting nitrogen, phosphorus, carbon and other nutrients

are transferred and used in sink organs for the formation of macromolecules, as well as in fruit maturation and seed filling (Yu *et al.*, 2015). It is obvious that the optimal completion of this process is very important, especially for plants of economic interest. To that belong crop plants, such as rice, maize, wheat and barley, which are the basis of human nutritional chain (Zhang *et al.*, 2018; Sakellariou & Mylona, 2020). As human population increases and it is estimated to reach up to 10 billion by 2050 (Gupta *et al.*, 2020), the yield of cereals, not only needs to be ensured, but also to reach a maximum level. Stress-induced premature leaf senescence can lead to insufficient nutrient recycling and incomplete grain filling, thus the overall crop yield will be reduced. There are many factors, which may affect the well-orchestrated completion of leaf senescence, such as restriction in water and nutrient availability, light deprivation or pathogen attack. Unfortunately, the predictions regarding water availability are pessimistic, as more and more people will live in areas with limited access to fresh water by 2050 (Gupta *et al.*, 2020). So, not only the demand of crops is increasing, but also the environmental conditions become limiting factors in plant development and overall crop yield. Thus, scientists focus on unraveling the highly regulatory process of leaf senescence during optimal plant development, as well as under adverse, stressful conditions, with long term goal the establishment of resistant lines and the improvement of plant performance.

1.2. Plant development under unfavorable conditions

Plants have the exceptional trait of completing their life cycle as sessile organisms in a hostile and ever-changing environment. Many studies aim to understand the strategies and mechanisms, which are utilized by plants in order to ensure their successful development and reproduction even under stressful conditions. After decades of research, there are still many questions regarding key processes, but now the rapid climate change adds an additional level of complexity. Human civilization depends on plants for maintaining a habitable and balanced natural environment, but also for agriculture, nutrition, animal feed, medicine and other industrial purposes. In the recent years, the drastic climate change and natural disasters raise great concerns about their effect on sustainable agriculture and global food security, as human population is expanding. Besides global warming, i.e. high temperature, climate change also results in extreme temperature fluctuations, heavy precipitations, prolonged periods of drought and shifts in atmospheric compositions (Gray & Brady, 2016). The aforementioned factors create an imbalance on plant environment, leading to other secondary effects, including rising of pathogen infections and stress vulnerability. This creates a great pressure to prevent climate change and extreme disasters, but also to improve plant tolerance to such unfavorable conditions.

As mentioned before, the knowledge around stress avoidance and adaptation strategies and mechanisms, which are used by plants and make them thrive in adverse conditions is still rather incomplete. One reason is the complexity of stress response pathways, which include the perception of environmental stimuli, a complex signal transduction network through phytohormones, changes in ion influx and antioxidant systems, recruitment of specific signaling molecules and proteins, biosynthesis of secondary metabolites and finally the differential regulation of appropriate genes (Mitra *et al.*, 2021). In addition, plants are normally exposed to multiple stressors simultaneously and it is

challenging to investigate the mechanisms regarding the integration, coordination and fine-tuning of the different signaling pathways and responses during co-stress. There is increasing evidence that regulatory proteins, which are able to act in different stress-responsive and development-dependent pathways, function as hubs, integrating complex environmental triggers and fine-tuning the balance among the different responses (Ranty *et al.*, 2016; Garcia-Molina *et al.*, 2017; Fichman & Mittler, 2020). Such molecular regulators acting in crosstalk between developmental and stress-related pathways are of high interest and subject of the current research.

1.2.1. Plant adaptation strategies under biotic and abiotic stress

Stress factors are defined as unfavorable conditions, which disturb the homeostasis of an organism. Focusing on plants, they may be generated from environmental changes and from anthropogenic actions (Baweja & Kumar, 2020). The latter is associated with human actions, such as the release of pollutants in ecosystems, the use of pesticides and other chemicals and the overall climate change. The present work focuses on environmental factors, which are further categorized as biotic and abiotic. As summarized in Fig. 1 (adapted from Baweja & Kumar, 2020), biotic factors originate from bacteria, fungi, nematodes, viruses and other living organisms. On the other hand, abiotic stress is caused by physicochemical factors like water deficit, flooding, low or high temperature fluctuations, high salinity, high light intensity or light deprivation. Any of those conditions has the potential to disturb the life cycle of plants and their effect depends on the intensity and duration of stress. A brief and mild

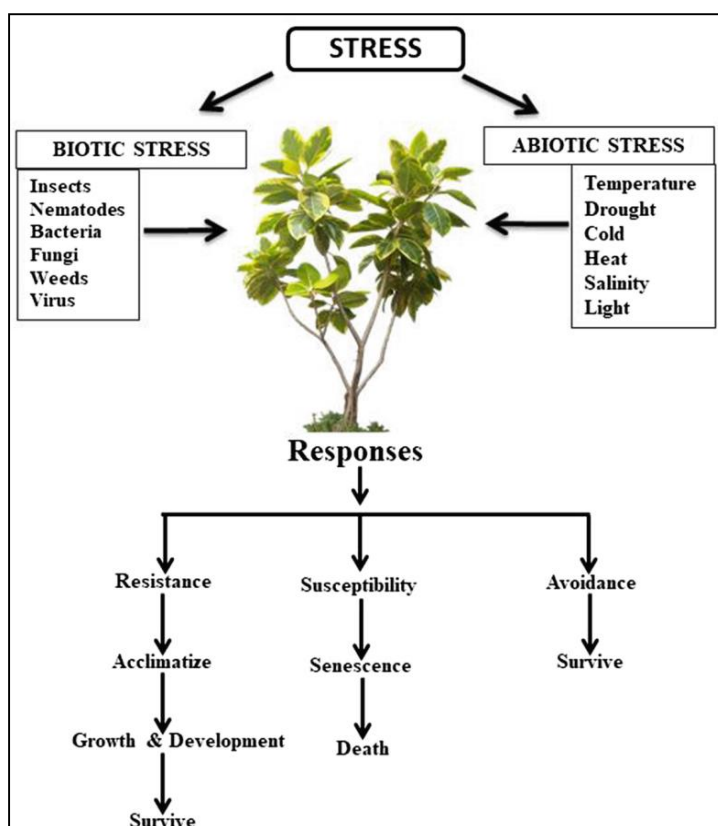


Figure 1: A synopsis of abiotic and biotic stress factors and their possible effects on plant development (adapted from Baweja & Kumar, 2020).

stress has small impact on plants, while a severe and prolonged stress can lead to compromised flowering, irregular seed and fruit maturation and even to premature senescence.

Extensive research in the field of plant physiology and phytopathology unraveled a number of smart strategies, which are utilized by plants in order to fight a stressful condition. In the case of biotic stress, plants recruit mechanisms in order to avoid the penetration and infection of pathogens. Physical barriers on leaf surface include the cuticle, stomata and cell wall. Their role is not limited in keeping the pathogens outside plant cells, but also in sensing the pathogen attack and activating a signaling pathway for the appropriate

defense responses. Besides the physical barriers, there are pathogen specific immune responses, which function in two steps (reviewed in Jones & Dangl, 2006). Briefly, the pathogen-associated molecular patterns are recognized by plant cell surface-localized pattern-recognition receptors and a pattern-triggered immunity (PTI) is promoted. Pathogens respond back with the secretion of virulence-associated molecules, such as effectors that are secreted via bacterial type III secretion system. Then, plants recognize specific intracellular nucleotide-binding domain leucine-rich repeat containing receptors and the second layer of plant immunity is activated, which is known as effector-triggered immunity (ETI). ETI involves the regulation of pathogenesis related proteins and the hypersensitive response, which may lead to programmed cell death at the site of infection. Another mechanism involves the accumulation of antimicrobial substances on the site of pathogen penetration, changes in cellular metabolic profile, as well as enzymes for the degradation of pathogens' cell wall (Kissoudis *et al.*, 2014). It is interesting that biotic stress responses are often influenced by abiotic stress responses. One representative example is the stomatal closure due to water deprivation, which also prevents a possible infection by fungi (reviewed in Mitra *et al.*, 2021). Other plant strategies for avoiding or resisting abiotic stresses are described in the next paragraphs.

One adverse condition, which imposes a great threat due to climate change and overpopulation, is water deficit (Gupta *et al.*, 2020). Plants recruit mechanisms to avoid this situation, including the elongation and expansion of root system in order to implement more efficient water uptake and to obtain other water sources. At the same time, the elimination of water loss, due to respiration, is necessary. Thus, plants respond with accumulation of K^+ and NO in guard cells for a rapid stomatal closure on leaf surface, followed by the reduction of transpiration rate (T.-H. Kim *et al.*, 2010). On a cellular level, a structural integrity is ensured by maintaining the turgor pressure with the accumulation of osmolytes, like proline, mannitol, sorbitol, trehalose, fructans and osmoprotectant proteins, like dehydrins and other Late Embryogenesis Abundant (LEA) proteins (Verma *et al.*, 2013). In addition, the redox homeostasis remains stable by the deployment of an antioxidant system, which includes peroxidases and other enzymes functioning in cellular damage prevention and membrane integrity preservation (Gupta *et al.*, 2020). Depending on the severity of stress, plants may sustain their growth with low internal water content or promptly switch into their reproductive phase to avoid the severe effect of drought (Gupta *et al.*, 2020).

A drought response is observed, not only due to water deprivation, but also in case of high salinity in soil, which inhibits the water uptake from plant roots and results in osmotic stress (Mahlooji *et al.*, 2018). A second form of stress is caused by the accumulation of toxic amounts of salt ions in plant cells, which leads to nutrient imbalance (Munns, 2005). Depending on the nature of stress, plants follow appropriate strategies, which include the inhibition of salt transportation to vascular tissues, the increase of cell storage volume in order to maintain a constant salt concentration or the distribution of salt, in the forms of Na^+ and Cl^- , from leaves to other organs through phloem (Acosta-Motos *et al.*, 2017). On a physiological level, plant growth is inhibited due to stomatal closure and impaired photosynthesis. The effect of osmotic stress is mitigated by osmolytes like carbohydrates (sucrose, sorbitol, mannitol, glycerol, arabinitol, pinitol), nitrogen compounds (proteins, amino acids, betaine, glutamate, choline, putrescine, 4-gamma aminobutyric acid) and organic

acids (malate and oxalate) (Acosta-Motos *et al.*, 2017). In some cases, ions are transferred from younger to older leaves, in order to ensure the optimal development of young leaves and overall plants (Munns, 2005).

Another limiting factor in plant growth and development is the deviation from an optimum temperature. A higher than optimum temperature has drastic effects on plant phenotype, as sun scabs, abrasions and scorching appears on leaves and fruits. In a cellular level, membranes and cytoskeleton structure become unstable, proteins are misfolded, enzymes are inactivated and the whole cellular metabolic profile is compromised (Baweja & Kumar, 2020). The main response of plants to heat stress is the recruitment of heat shock proteins, which are highly induced under elevated temperatures and function as molecular chaperones in maintaining the structure of other proteins and enzymes (Nakamoto & Víg, 2007). In this way, cellular metabolism is preserved until the temperature is back to the optimal range for plant development. The opposite tendency, i.e. a temperature below the optimal, has also adverse effect on plant processes. Here, two scenarios are possible: a chilling temperature between 0-15 °C and a freezing temperature below 0 °C (Baweja & Kumar, 2020). Freezing temperatures cause the transition of liquid water to solid ice crystals, which results in water deprivation, but also in damage of tissues and macromolecules. Then, chilling stress affects membrane fluidity and metabolic processes, like respiration and photosynthesis. In addition, plant growth is limited, curling or necrosis of leaves is observed, the transition to reproductive phase is changed and the ripening of fruits is irregular (Baweja & Kumar, 2020). Plants overcome those threats by producing antifreeze and cryoprotectant molecules, including dehydrins, cold regulated (Cor) proteins, chaperones and other stress specific proteins, as well as osmolytes, like proline, glycine, betaine and polyols, soluble sugar molecules and sugar alcohols (Janská *et al.*, 2009). As for cellular membranes, the lipid composition is enriched in unsaturated fatty acids phosphatidylcholine and phosphatidylethanolamine in order to ensure its fluidity (Heidarvand & Maali Amiri, 2010).

Plants require a specified range of conditions in order to complete major metabolic processes and light intensity is one important component. There are appropriate receptors in plant cells, which absorb light in the spectrum of blue (400-500 nm), red (600-700 nm) and far-red (600-700 nm) pulses (Fiorucci & Fankhauser, 2017). Interestingly, plants sense the reduction in light availability, for example, in the case of neighboring plants, from the increased perception of far-red light reflection and consequently a lower red to far-red ratio. As a response, they invest energy for stem elongation without increase in branches, chloroplast accumulation, leaf elevation and faster transition to reproductive phase (Fiorucci & Fankhauser, 2017). In the unfavorable case of prolonged shading or complete darkness, plant responses are abrupt and a fast senescence is observed. In the opposite case of excess light intensity, plant responses also follow an opposite trend. These include cells with a thicker wall and asparse organization of chloroplasts, changes in leaf orientation in order to minimize light absorption, leaf surface is covered with a layer of trichomes and photoprotective pigments are accumulated (Baweja & Kumar, 2020). Regarding the photosynthetic performance under high light stress, the inactivation of PSII reaction center due to excess of reactive oxygen species (ROS) is observed, which leads to photoinhibition of PSII. Plants recruit strategies to avoid this phenomenon, including the increase in thermal dissipation of excess energy, the cyclic electron flow in PSI, the induction of ROS scavenging

enzymes, the xanthophylls cycle and the photorespiratory pathway (Szymańska *et al.*, 2017). The aforementioned responses vary among plant species according to their demands in light intensity.

Finally, another form of abiotic stress is the high concentration of heavy metals in soil. Some heavy metals are not necessary for plants and considered toxic, while other heavy metals are essential for plant developmental processes, but become toxic if their concentration is elevated above a specific threshold (Dykema *et al.*, 1999.). It is known that heavy metals cause the production and accumulation of ROS, the oxidative damage of lipids in cellular membranes, nucleic acids and other macromolecules, while some specific heavy metals substitute essential ions in enzymes and proteins leading to their inactivation (Yadav, 2010). As a result, vital processes, including photosynthesis and respiration are compromised. One strategy to avoid the accumulation of heavy metals involves the filtering of the type and amount of heavy metals absorbed in the root system and transferred to shoot tissues (Baweja & Kumar, 2020). When this mechanism fails, plant cells activate detoxification strategies, such as the recruitment of heavy metal transporters and amino acids, glutathione, phytochelatin, metallothioneins and enzymes such as superoxide dismutase and peroxidases for the sequestration of those heavy metals in vacuoles (Yadav, 2010; Ghori *et al.*, 2019).

Even though each stressor causes specific adaptation strategies, a common ground has been observed. That includes the stress perception and transduction from roots to shoots and the recruitment of signaling components, such as phytohormones, calcium cations (Ca^{2+}) and Ca^{2+} -binding proteins, accumulation of ROS, protein kinases and phosphatases. Various signaling cascades lead to the activation of transcription factors (TFs) and transcription regulatory elements for the induction of stress responsive genes. Through this process, specific cellular and morphological responses are observed, including the biosynthesis of secondary metabolites and osmoprotectants and changes in root and leaf phenotype, respectively.

1.2.2. The role of ABA in abiotic stress response signaling pathways

Studies of the different abiotic stress responses unravel an overlap in plant strategies and defense mechanisms under these conditions. This is the case, for example, for drought, salt, heat and cold stress, as all conditions limit the water availability in plant tissues, resulting in an osmotic stress effect and, as a response, in accumulation of osmoprotectant molecules (Janská *et al.*, 2009; Verma *et al.*, 2013; Acosta-Motos *et al.*, 2017). The aforementioned stress factors are perceived by plants and trigger the activation of specific signaling cascades and the differential regulation of the corresponding stress responsive genes. It is known that abscisic acid (ABA) is the main phytohormone, which regulates abiotic stress responses, but also developmental processes like flowering, seed development and leaf senescence (Dar *et al.*, 2017). Under stress conditions, it functions as a long distance endogenous messenger to promote tolerance to water deficit, high salinity and extreme temperatures (Dar *et al.*, 2017).

Different environmental conditions may lead to similar plant responses, which start with a fast biosynthesis and accumulation of ABA and its translocation through ATP-dependent transporters. Then, the RCARs/PYR1/PYLs (Regulatory Components of ABA Receptor/ Pyrabactin Resistance Protein1/ PYR-Like proteins) receptors perceive ABA and downstream suppress some Protein Phosphatases 2C (PP2Cs), like various Abscisic Acid

Insensitive (ABI) and Hypersensitive to ABA (HAB) proteins (Lim & Lee, 2020), which are considered negative regulators of ABA pathway (Raghavendra *et al.*, 2010). As a result, the signal is transduced via secondary messengers, including the Open Stomata 1 (OST1)/sucrose non-fermenting 1-related protein kinase 2s (SnRK2s) and Ca²⁺-dependent protein kinases (CPK) (Lim & Lee, 2020), leading to the downstream phosphorylation and activation of other targets, including TFs and ion channels. In some cases, kinases function for the phosphorylation of a plasma membrane localized NADPH oxidase that generates hydrogen peroxide (H₂O₂), for promoting a positive feedback loop for stomatal closure and downstream activation of stress responses. Other secondary messengers involve phosphatases, heterotrimeric G proteins and G-protein-coupled receptors, cyclic nucleotides, phospholipases, an increase in Ca²⁺ concentration due to the activation of Ca²⁺ channels and an accumulation of ROS (Cutler *et al.*, 2010; T.-H. Kim *et al.*, 2010).

The differential regulation of stress responsive genes is promoted by ABA-responsive binding factors (ABFs) and ABA-responsive element binding factors (AREBs), which are phosphorylated and activated by the ABA-activated kinases SnRKs (Dar *et al.*, 2017). These transcription regulators induce genes, such as the dehydration responsive gene *RD29B* (Nakashima *et al.*, 2006) and late embryonic and abundant gene EARLY METHIONINE-LABELED (*EM*) (Lim & Lee, 2020). In parallel, the ABA dependent pathway is crossed with an ABA independent pathway, which involves the dehydration-responsive element/C-repeat (DRE/CRT) and DRE-/CRT-binding protein 2 (DREB2). The latter belongs to Apetala2/Ethylene-Responsive-Factor (AP2/ERF) plant specific TFs and, under normal conditions, they are suppressed by the ubiquitin E3 ligase proteolytic pathway (Yoshida *et al.*, 2014). During abiotic stress conditions, they are activated and regulate stress responsive genes, such as many *Cor* genes, the proline biosynthesis gene delta 1-pyrroline-5-carboxylate synthetase (*P5CS1*), LEA and heat shock proteins (Hsiao *et al.*, 2014). Other targets are members of NAC, WRKY, bZIP, MYB and MYC/bHLH TF families (Raghavendra *et al.*, 2010; Dar *et al.*, 2017). A model of the ABA-dependent and ABA-independent signaling cascades under a general osmotic stress is summarized in Fig. 2 (adapted from Yoshida *et al.*, 2014).

The role of ABA in plant life cycle is not limited in stress responses, but it involves developmental processes like embryogenesis, seed germination and maturation, fruit ripening, abscission and leaf senescence (Jibrán *et al.*, 2013). Focusing on the latter, the most prevalent mode of action involves a crosstalk among ABA dependent and independent pathways with the senescence signaling cascades. This is supported by the induction of ABA biosynthesis genes, the accumulation of ABA in senescing leaves and the acceleration of senescence after exogenous application of ABA (Jibrán *et al.*, 2013). Additionally, the senescence associated gene *SAG113* encodes for a PP2C, which is a negative regulator of ABA dependent signaling cascade for stomatal closure (Zhang & Gan, 2012). On the other hand, ABA induces the expression of specific genes, which are known to be involved in developmental leaf senescence. This is the case for the NAC TF VND-INTERACTING 2 (*VNI2*), which then regulates various *Cor* and RESPONSE TO DEHYDRATION (*RD*) genes during stress responses and leaf senescence (Yang *et al.*, 2011). Then, the *S40* gene is established as developmental and stress induced senescence marker gene, as it is highly expressed under those conditions and it was shown that it is regulated downstream of ABA

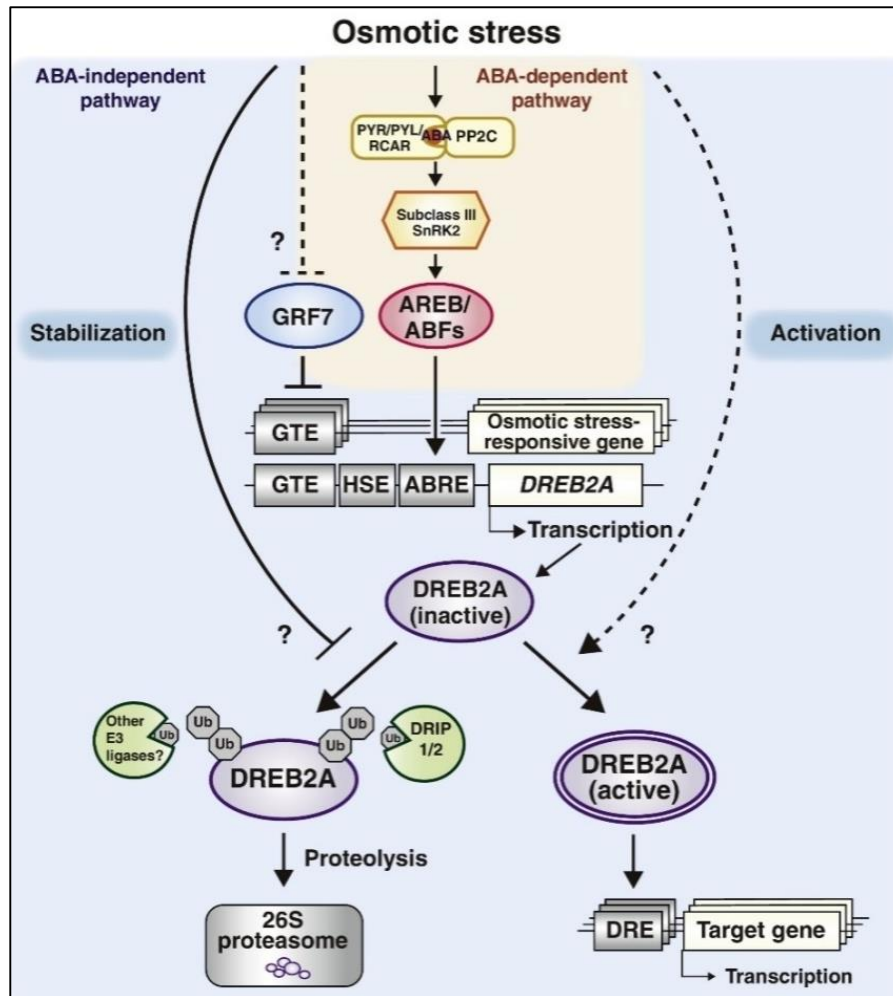


Figure 2: The ABA-dependent and ABA-independent pathways under osmotic stress. In the ABA-dependent pathway, ABA is perceived by RCARs/PYR1/PYL receptors and PP2Cs are suppressed. That leads to the activation of SnRKs, which phosphorylate and activate AREB/ABFs transcription factors for the regulation of stress responsive genes and the induction of DREB2A, which is a key transcription factor in ABA-independent pathway, as well. In this pathway, DREB2A and DRE/CRT factors induce stress-responsive genes in an ABA-independent manner. Under normal conditions, DREB2A is suppressed by the ubiquitin E3 ligase and the ubiquitin proteolytic system in proteasome (Adapted from Yoshida *et al.*, 2014).

(Jehanzeb *et al.*, 2017). These are only two examples of the complicated network, which orchestrates the responses to environmental stresses, but also the onset and progress of developmental leaf senescence.

1.2.3. The role of other phytohormones in plant response signaling pathways

It is worth mentioning that ABA is not the only phytohormone, which is implicated in stress responses and plant development. It is known that salicylic acid (SA) and jasmonic acid (JA) are involved in biotic stress perception and downstream responses. Then, under normal conditions, SA and JA, as well as ABA, ethylene and auxin positively regulate the onset of leaf senescence, while cytokinins (CK) and gibberellins (GA) have the opposite effect (reviewed in Luoni *et al.*, 2019). It was shown that *Arabidopsis* leaf senescence involves an accumulation of JA in senescing leaves, while exogenous application of JA led to the acceleration of this process (He *et al.*, 2002). Then, Jing *et al.* (2005) clearly showed

that when *Arabidopsis* plants are exposed to ethylene, a premature leaf senescence is observed. On the other hand, CK level is decreased during senescence and exogenous application of CKs inhibits chloroplast degradation, thus delaying leaf senescence (Gan & Amasino, 1995). The decrement of CKs is due to suppression of CK biosynthesis genes, i.e. CK synthase and adenosine phosphate isopentenyl-transferase (IPT), and upregulation of a CK oxidase, which acts in CK degradation (Lim *et al.*, 2007). These are only single observations in the mode of action of phytohormones during plant development and especially leaf senescence.

Important intermediates in the crosstalk among different phytohormone pathways are TFs. Most of them belong to NAC, MYC, MYB, WRKY and bHLH families (Y. Guo *et al.*, 2021), which regulate multiple aspects of plant life. As for the phytohormone associated TFs, it is well-established that ethylene induces the ETHYLENE-INSENSITIVE 2 (EIN2) and EIN3 for the downstream activation of other TFs and catabolic enzymes, which promote leaf senescence (J. Kim *et al.*, 2015). Then, similar action is noted for JA, which is normally suppressed by JASMONATE ZIM-DOMAIN (JAZ) TFs, but accumulated during leaf senescence by the action of MYC2. The latter is a negative regulator of EIN3, but mediator between JA and ethylene signaling cascades, although this reciprocal mode of action is not clear. Furthermore, JA regulates the biosynthesis of ethylene through its interaction with 1-Aminocyclopropane-1-carboxylic acid (ACC) (J. Kim *et al.*, 2015). On the contrary, an antagonistic effect is observed between ABA and CK. In general, CK biosynthesis gene IPT is regulated by SAG12 during leaf senescence. Then, CK is perceived by CK receptor AHK3 and leads to the activation of CK response factors (CKF) for the inhibition of leaf senescence (Y. Guo *et al.*, 2021). Zhang *et al.* (2021) showed that the accumulation of CK leads to reduction of ABA levels, by a positive regulation of ABA degradation genes and negative regulation of ABA biosynthesis genes in rice.

So far, it is clear that plant developmental processes and their responses to biotic and abiotic stress factors are regulated by multiple signaling cascades. The diverse role of phytohormones and TFs in these processes was briefly introduced in the above chapters, but there are more components, which ensure the maintenance of plant homeostasis and optimal development. One protein family with such functions, is that of Heavy metal associated Isoprenylated Plant Proteins. Even though little is known about their role in plants, recent publications justified a multifunctional mode of action. Their discovery and the studies about their function under control and stressful conditions are introduced in the next chapter.

1.3. Heavy metal associated Isoprenylated Plant Protein family

The importance of heavy metal binding proteins in various organisms is well-established. Focusing on plants, they transfer necessary heavy metals, such as copper (Cu), zinc (Zn), manganese (Mn), nickel (Ni) and iron (Fe), from soil to plant tissues in order to be used in vital processes, in which TFs, enzymes and other proteins require heavy metals for their structure and function (Cobbett & Goldsbrough, 2002). On the other hand, excess amount of those or other toxic heavy metals, including cadmium (Cd), aluminium (Al) and lead (Pb), have a detrimental effect on plant metabolism and development (Dykema *et al.*, 1999). Especially for Cd, it is known that it resembles the chemical structure of essential heavy metals, such as Ca, Zn and Fe and replaces them in cellular processes, resulting in toxic

effects for plants (DalCorso *et al.*, 2008). Specific groups of heavy metal binding proteins, such as metallochaperones (Tehseen *et al.*, 2010), phytochelatins and metallothionins (Cobbett & Goldsbrough, 2002) are responsible for preventing the intake of toxic heavy metals, transferring essential heavy metals among plant tissues and maintain the overall heavy metal homeostasis. It is known that heavy metal binding proteins possess at least one Heavy Metal Associated (HMA, pfam00403.6) domain in an I/L/MXCXXC core (where 'I' is isoleucine, 'L' is leucine, 'M' is methionine, 'C' is cysteine and 'X' is any amino acid), with cysteines being the necessary amino acids for heavy metal binding (Dykema *et al.*, 1999; Cobbett & Goldsbrough, 2002).

Another protein process, which requires the presence of a cysteine residue, is isoprenylation. Isoprenylation is a posttranslational modification, which adds a hydrophobic tail to proteins and enables their interaction with cellular membranes or other proteins. This tail corresponds to an isoprenoid lipid, which is attached by an isoprenyltransferase/farnesyltransferase to a cysteine residue, close to the C-terminus of a protein (Crowell, 2000). The interaction is stabilized by a cysteinyl thioether covalent bond. This process involves various physiological roles in eukaryotes, such as regulation of cell division, cytoskeletal organization, signal transduction and vesicular transport. Especially for plants, isoprenylation of proteins was linked with membrane biogenesis during bacteria symbiosis, floral meristem identity, CK biosynthesis, auxin regulation and ABA signal transduction (Crowell, 2000; Crowell & Huizinga, 2009). The latter expands the role of isoprenylation to other plant processes, including abiotic and biotic stress responses. Interestingly, one subunit of an isoprenyltransferase/ farnesyltransferase is encoded by the ENHANCED RESPONSE TO ABA 1 (*ERA1*) gene and is identified as negative regulator of ABA signaling. In a number of studies, *loss-of-function* of *ERA1*, led to higher ABA activity and drought tolerant plants due to enhanced anion channel activity and reduced water loss (Pei *et al.*, 1998) and increased lateral roots (Brady *et al.*, 2003). Nevertheless, there are various forms of isoprenylation, depending on the type of hydrophobic tail attached to the target proteins. This makes more complicated the understanding of this posttranslational modification in plants and other organisms.

The presence of both HMA domain and isoprenylation motif in one protein sequence was first reported by Dykema *et al.* (1999) when they showed that isoprenylated plant proteins are capable of transition metal ion binding. Interestingly, the existence of this protein family only in vascular plants has been noted (Dykema *et al.*, 1999; de Abreu-Neto *et al.*, 2013). After this observation, the *Arabidopsis thaliana* Farnesylated protein 3 (AtFP3; Dykema *et al.*, 1999) and the *Hordeum vulgare* Farnesylated protein 1 (HvFP1; Barth *et al.*, 2004) were the first candidates of this new protein group to be studied and, a few years later, the family of Heavy metal associated Isoprenylated Plant Proteins (HIPPs) was established (Barth *et al.*, 2009). Each member of the HIPP family is defined by the presence of at least one HMA domain and one isoprenylation site. As mentioned above, the HMA domain exhibits two cysteines in an I/L/MXCXXC motif for heavy metal binding. Then, the isoprenylation of HIPPs is carried out by a farnesyltransferase or a geranylgeranyltransferase, which respectively adds a 15-carbon farnesyl or a 20-carbon geranylgeranyl group to the cysteine residue of a C'-terminal CaaX motif (where 'C' is cysteine, 'a' is an aliphatic amino acid, and 'X' is usually methionine, glutamine, serine, alanine, or cysteine; Crowell & Huizinga,

2009). In addition, some members of HIPP family have a nuclear localization signal (NLS), which implies localization and probably a function in the nucleus. A general illustration of HIPP sequence with the key motifs is presented in Fig. 3.

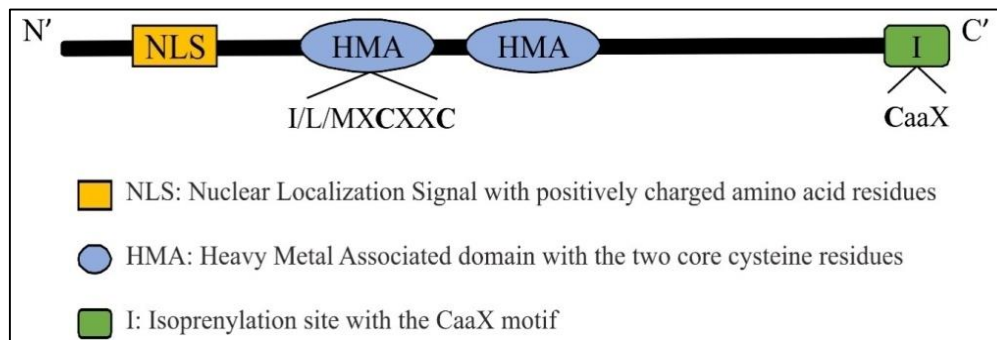


Figure 3: Model sequence of HIPP proteins with the two key components and the optional nuclear localization signal. Yellow box: nuclear localization signal; blue box: heavy metal associated domain(s), green box: isoprenylation site.

At first, the focus of HIPP proteins was mainly on heavy metal binding and their subsequent function in maintaining heavy metal homeostasis and responding to heavy metal stress (Dykema *et al.*, 1999; Tehseen *et al.*, 2010; Zhao *et al.*, 2013; Cheng *et al.*, 2018; Khan *et al.*, 2019). However, barley *HvFP1* was discovered as a cold and high light response gene, shedding light on a new functional aspect of this protein family. This specific member is a 155 amino acid protein with one HMA domain and one NLS (Fig. 4A). Briefly, Barth *et al.* (2004) detected a high and transient expression of *HvFP1* under combined cold and high light stress, by using a northern blot (Fig. 4C). In fact, the light parameter had low impact on gene expression, while the low temperature is the main trigger factor for the upregulation of *HvFP1*. Furthermore, the same technique showed an increased transcript amount of this gene in shoot axes under normal conditions, in shoot axes, primary and secondary leaves, leaf sheaths and roots after cold and high light stress (Fig 4B) and in primary leaves during drought stress treatment, ABA application and developmental leaf senescence (Fig. 4D, E and F). Interestingly, exposure to Cu and Cd heavy metals had small or no effect on the induction of this gene (Fig. 4F). As for the isoprenylation motif, its function is not clear, but confocal microscopy showed that it is necessary for the localization of *HvFP1* in the nucleus (Barth *et al.*, 2004). This comprehensive study unraveled a diverse function of HIPP family, beyond the heavy metal binding. Afterwards, much research was performed in other members of HIPP family with popular model plant species, like *A. thaliana* and rice *Oryza sativa*.

1.3.1. HIPP proteins in model plants *Arabidopsis thaliana* and *Oryza sativa*

The role of HIPP proteins in heavy metal regulation has been well-established, as well as their ability to confer resistance to heavy metal exposure, when they are overexpressed in plants or ectopically expressed in yeast (Gao *et al.*, 2009; Tehseen *et al.*, 2010; Zhao *et al.*, 2013; Zhang *et al.*, 2015; Khan *et al.*, 2019; Khan *et al.*, 2020; Manara *et al.*, 2020; B. Zhang *et al.*, 2020; H. Zhang *et al.*, 2020; Liu *et al.*, 2022). Their function in other aspects of plant life, other than heavy metal regulation, is drawing the attention of many researchers. The main focus is on the model plant *A. thaliana*, although studies have been done with other

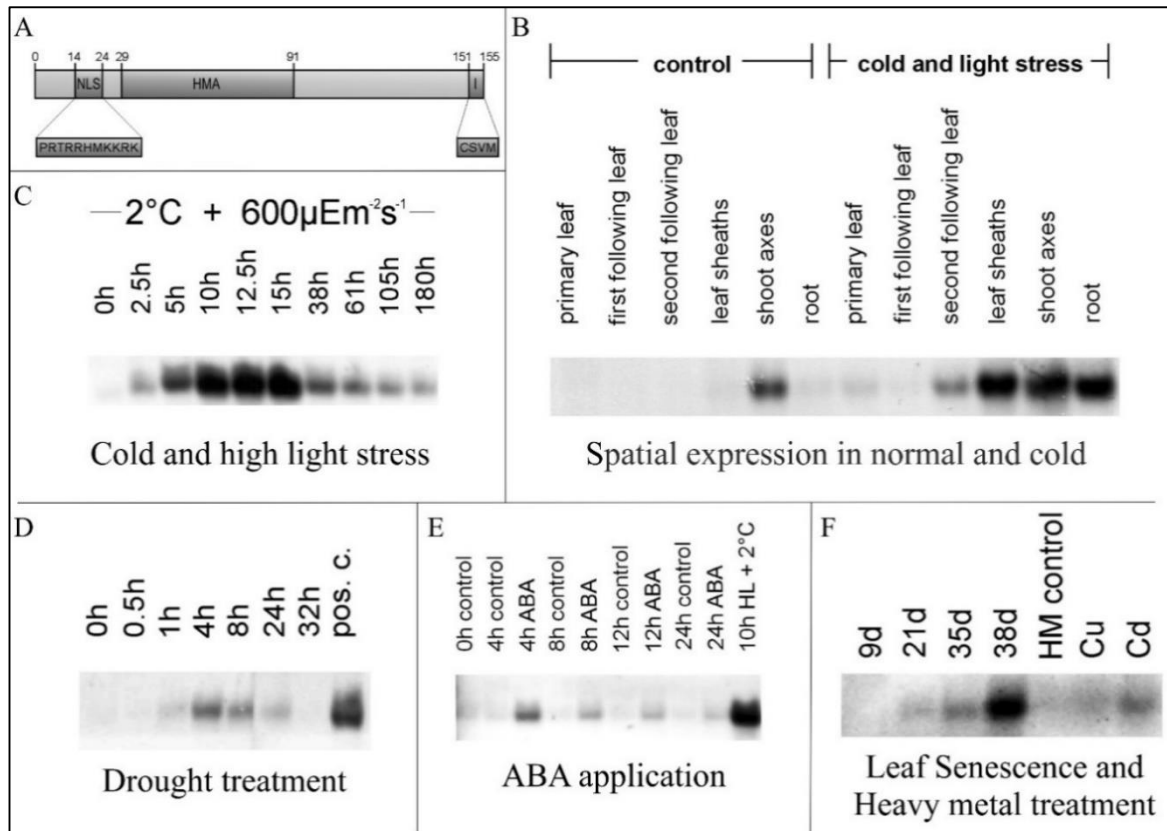


Figure 4: Study of HvFP1 under various conditions. (A) Schematic representation of HvFP1 protein sequence with one Heavy Metal Associated (HMA) domain, the isoprenylation site and one Nuclear Localization Signal (NLS); (B) Northern analysis of spatial expression of *HvFP1* under control and cold/high light conditions; (C) Northern analysis of the expression of *HvFP1* at various time points after cold/high light stress; (D) Northern analysis of the expression of *HvFP1* under drought stress; (E) Northern analysis of the expression of *HvFP1* after ABA treatment and (F) Northern analysis of the expression of *HvFP1* during developmental leaf senescence and after treatment with copper (Cu) and cadmium (Cd) (adapted from Barth *et al.*, 2004).

plant species, as well. A research of this multigene family in databases revealed at least 45 genes in *A. thaliana*, 44 in *O. sativa*, 114 in *Triticum aestivum*, 74 in *Populus trichocarpa*, 58 in *Triticum dicoccoides*, 51 in *Setaria italica*, 40 in *Aegilops tauschii*, 33 in *Triticum urartu*, 34 in *Chenopodium quinoa*, 33 in *H. vulgare* and only 5 putative HIPP genes in *Selaginella moellendorffii* (Barth *et al.*, 2009; de Abreu-Neto *et al.*, 2013; Khan *et al.*, 2019; H. Zhang *et al.*, 2020; Sun *et al.*, 2022). According to some unique features, they are classified in 5 distinguished groups (de Abreu-Neto *et al.*, 2013). Specifically, group I includes HIPPs with two HMA domains in their sequence, while most members of group III have additional glycine-rich repetitions and proline-rich motifs. The presence of proline-rich motifs hints a function in signaling cascades. Then, small HIPPs with or without proline-rich motifs belong to groups II and V, respectively and group IV includes larger HIPPs with proline-rich motifs.

Focusing on *A. thaliana* and *O. sativa*, many studies implied a function of HIPPs in heavy metal transport, but also in developmental and stress response processes. Starting from the homologous to HvFP1 protein, the nuclear localized AtHIPP26 of group II is induced under cold, drought and in addition salt stress, but not after ABA treatment or during leaf senescence (Barth *et al.*, 2009). Furthermore, it was shown that it interacts with the Zn^{2+}

finger-homeodomain TF ATHB29 (Barth *et al.*, 2009), which regulates drought responsive genes (Tran *et al.*, 2006). This finding implies a possible role of AtHIPP26 as transporter of necessary heavy metals, in this case Zn^{2+} , to TFs for the regulation of stress responsive genes. In the same year, Gao *et al.* (2009) proved via the yeast two-hybrid system the interaction of AtFP6, which was later named AtHIPP26, with the Acyl-CoA Binding Protein 2 (AtACBP2). The latter is localized in plasma membrane (Li & Chye, 2003) and belongs to the family of acyl-CoA-binding proteins, which are capable of binding and transporting long-chain acyl-CoA esters and are involved in phytohormone dependent and independent signaling cascades during exposure to stress (reviewed in Lai & Chye, 2021). Especially for AtACBP2, it possesses ankyrin repeats, which seem to be necessary for the interaction with AtFP6 (Gao *et al.*, 2009) and the Ethylene-Binding Protein (AtEBP) (Li & Chye, 2004). After this finding, Gao *et al.* (2009) proposed that AtFP6 is involved in heavy metal stress responses and AtACBP2 acts in phospholipid repair, caused by this type of stress. Another assumption is that AtACBP2 and AtFP6 participate in heavy metal transfer and especially in Cu^{2+} -mediated ethylene signaling through their interaction partner AtEBP. In any case, both proteins are induced in response to abiotic stress, as drought responsive elements (Barth *et al.*, 2009; Du *et al.*, 2013).

Other studies in *A. thaliana* HIPP family supported its role in stress responses and plant development. One example is the AtHIPP3, which is capable of binding Zn^{2+} and possesses two HMA domains (Zschiesche *et al.*, 2015); hence it is classified in group I (de Abreu-Neto *et al.*, 2013). The expression pattern of *AtHIPP3* contradicts that of *AtHIPP26*, as it is downregulated by drought stress and ABA treatment, but it is highly induced after inoculation with *Pseudomonas syringae* pv. *tomato* culture (Zschiesche *et al.*, 2015). The same team confirmed the role of AtHIPP3 in regulation of stress mechanisms by a transcriptomic analysis, in which overexpression of *AtHIPP3* resulted in differential regulation of stress responsive genes and a suppression of the biotic stress regulatory SA pathway. At the same time, those plants exhibit a delay in flowering time, proving a simultaneous role in major developmental processes. Another member of *A. thaliana* HIPP family, which is involved in biotic stress response, is AtHIPP27. This protein was characterized as a susceptibility factor, which is induced in *A. thaliana* roots and it is necessary for plant infection by cyst nematodes and the development of syncytium (Radakovic *et al.*, 2018). This role is specific for an infection by this pathogen and does not implicate with phytohormone regulation of plant basal defense. On the contrary, *loss-of-function* of *AtHIPP27* led to less susceptible plants and accumulation of starch grains in syncytia of nematodes after their infiltration in *loss-of-function* mutants.

The above results confirm diverse and distinct functions of *Arabidopsis* HIPP family in plant stress responses and development. Thus, a question is raised about this protein family in crops and other plants of economic interest. It is important to understand the role of HIPPs in plant development and stress adaptation strategies, in order to optimize their efficiency and overall yield. One major crop plant is rice *O. sativa*, which is among the top cultivated cereals worldwide. In the recent years, rice has become a popular model plant due to its small, diploid genome, the acquisition of high-precision genome sequences, the identification of many genes and quantitative trait loci (QTL) and its efficient genetic transformation (Xing & Zhang, 2010). In the study of de Abreu-Neto *et al.* (2013), total 59 genes encoding for HIPP

members were identified, while a few years later, another team found 44 HIPP genes in the genome of *O. sativa* (Khan *et al.*, 2019). Nevertheless, the diversification among the members of the same protein family is interesting. Focusing on the homologous to *HvFP1* and *AtHIPP26* gene *OsHIPP41*, it is highly induced in rice seedlings during drought and cold stress treatment (de Abreu-Neto *et al.*, 2013). It is worth mentioning that this protein, but also *OsHIPP42*, are localized in the nucleus and in the cytosol (de Abreu-Neto *et al.*, 2013; Khan *et al.*, 2020), implying that the function of some HIPPs require a translocation between those cellular compartments. Even though most studies in rice focus on the role of HIPPs on heavy metal responses and detoxification of plants (Cheng *et al.*, 2018; de Abreu-Neto *et al.*, 2013; Khan *et al.*, 2019; Khan *et al.*, 2020), it is clear that they are involved in other forms of stress responses and in developmental processes. In the recent years, many researchers focus their interest in this particular protein family of other plant species, which are analyzed in the next chapter.

1.3.2. HIPP proteins in other plant species

The advancement of scientific methods has facilitated the sequencing of whole genome of organisms and enabled the establishment of a genetic database, even for less popular species, which would otherwise require many resources for their research. This made possible to study the HIPP family in other organisms, including various *Triticeae* (Zhang *et al.*, 2015; H. Zhang *et al.*, 2020), *Solanaceae* (Cowan *et al.*, 2018; Manara *et al.*, 2020) and *Musaceae* (Villao *et al.*, 2019) species.

The common wheat *T. aestivum* has 114 genes encoding for HIPPs (H. Zhang *et al.*, 2020). Of that, *TaHIPPI1* is 99% homologous to barley *HvFP1* (Zhang *et al.*, 2015). Interestingly, *TaHIPPI1* follows similar expression pattern as *HvFP1*, with a high induction of this gene by ABA and exposure to cold, but also salt treatment (Zhang *et al.*, 2015). The same team tested the effect of biotic stress on the expression of *TaHIPPI1* and confirmed a differential regulation in response to *Pseudomonas striiformis*. A specialized role of *TaHIPPI1* as susceptibility factor was detected, as this gene is significantly upregulated by a compatible host-pathogen strain of *Pseudomonas*, while the opposite expression pattern was observed for an incompatible strain. This finding was confirmed when *loss-of-function* of *TaHIPPI1* led to an upregulation of pathogenesis related genes and to more resistant wheat plants after *Pseudomonas* infection. One interesting hypothesis is that *TaHIPPI1* is involved in a signaling cascade, which regulates the basal defense against biotic stress, but also the responses to abiotic stress through ABA signaling and farnesylation events (Zhang *et al.*, 2015). So far, a negative regulation of ABA signaling by farnesylation has been noted (Crowell & Huizinga, 2009), but how this process is regulated in HIPP family and how this affects stress responses is unclear.

The *Solanaceae* family includes plants with great importance in human nutrition, including tomato *Solanum lycopersicum* and potato *Solanum tuberosum* and in research and pharmaceutical industry, such as tobacco *Nicotiana benthamiana*. One threat in their cultivation is the biotic stress, caused by pathogenic bacteria, fungi, nematodes and viruses. Plants can be resistant or susceptible to such biotic stress factors, depending on multiple levels of defense and PTI and ETI immune responses (reviewed in Jones & Dangl, 2006). In a series of studies, members of the HIPP family were connected with plant responses against virus

infection. More specifically, it was shown that HIPP26 paralogs are involved in biotic and abiotic stress responses through interaction with the potato mop-top virus (PMTV) movement protein TGB1 (Cowan *et al.*, 2018) or the tomato metallocarboxypeptidase inhibitor-1 (Manara *et al.*, 2020), respectively. More specifically, Cowan *et al.* (2018) performed experiments with *N. benthamiana* plants and described HIPP26 as a vascular-expressed plant stress sensor, which is involved in long distance movement of PMTV by interacting with its movement protein TGB1. So far, most studies focus on the ability of HIPP proteins to interact with heavy metals, while the C-terminal isoprenylation motif seems to be important for spatial localization of those proteins. This is one of the few studies considering posttranslational modifications, in this case isoprenylation and *S*-acylation, important for the function of HIPP26. They suggested that the prenyl group is a prerequisite for TGB1 binding with HIPP26 in plasma membrane and plasmodesmata, after a PMTV infection. This subjects HIPP26 to a conformational change and makes one *S*-acyl thioester accessible for cleavage, which releases HIPP26 from plasma membrane and, through microtubule, to the nucleus for the transcriptional regulation of stress-responsive factors.

Only one year later, the importance of prenylation in HIPP function was further supported by T. Guo *et al.* (2021). The posttranslational modification promotes the interaction of some specific HIPPs with FAD-containing CK oxidases/dehydrogenases (CKXs). This event involves the Endoplasmic Reticulum Associated Degradation (ERAD) of proteins and modulates the apoplastic CK pool in plant cells. The hypothesis that there is a connection between HIPPs and CKs was reinforced when the latter resulted in a downregulation of specific HIPP members. Eventually, it was proposed that this mechanism controls the responses of plants to specific stimuli through changes in CK homeostasis and triggering of specific signaling cascades. T. Guo *et al.* (2021) studied the cluster I HIPP1, 6 and 7 and proposed that they regulate the CKX-ERAD process in order to maintain the CK balance in plant cells or change this balance for the downstream activation of CK dependent signaling pathways. The role of CKs in major plant developmental processes, such as leaf senescence, and their antagonistic function with ABA have been discussed above. Future studies could unravel how ABA and CKs are involved with HIPPs in signaling pathways for the regulation of multiple aspects of plant life.

1.4. Barley as model plant

The present work deals with one member of the HIPP family in model crop plant barley. Domesticated barley *H. vulgare* belongs to Poaceae grass family and its cultivation started around 10,000 years ago in Fertile Crescent (Badr *et al.*, 2000). It is evolved from its wild ancestor *H. spontaneum* and morphologically has two- or six-row spikes, shorter stems and awns and wider leaves, while it can be hulled or hullless (Badr *et al.*, 2000; Harwood, 2019). In a genetic aspect, this annual grass is self-pollinating, with haploid genome size of 5.3 Gbp and more than 39,000 genes, organized in a diploid chromosome number of $2n=14$ (Harwood, 2019). The cultivation of barley plants depends on the spring or winter type of cultivars, as the latter are sowed in autumn and require a period of low temperature before the anthesis. In general, it is considered a robust crop with high resistance against stress factors, making a good model plant (Harwood, 2019).

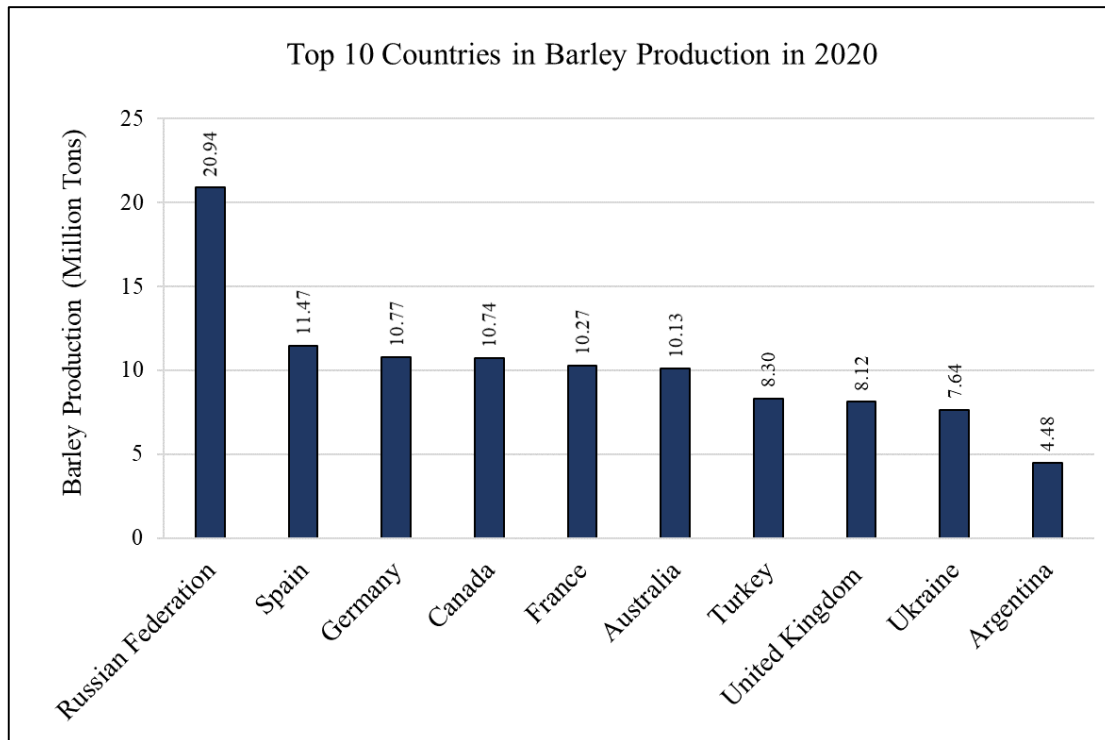


Figure 5: Top ten producers and total barley production in million tons worldwide for the year 2020.

Source: FAOSTAT (<https://www.fao.org/faostat/en/#data/QCL/visualize>).

Barley is the fourth most cultivated crop plant worldwide, with a production of 158 million tons in 2020 (source FAOSTAT). Of that, 10.8 million tons come from Germany, making it the 3rd country in barley production worldwide for the year 2020 (Fig. 5; source: FAOSTAT). The main purpose of barley cultivation is animal feed and malting industry, while its consumption is limited to certain regions, even though it has a high nutritional value and it is a good source of β -glucan (Harwood, 2019). Besides the fact that barley has been replaced by wheat in human diet due to the higher number of grains and lack of threshing in wheat (Giraldo *et al.*, 2019), it is still urgent to establish improved cultivars due to the increasing human population and the climate change, which threatens crop cultivation and yield. That means, that barley cultivars need to be resistant to a number of abiotic and biotic stress factors in order to avoid a premature leaf senescence, which leads to insufficient nutrient transportation for the formation of flag leaf, ears and seed filling. As a result, losses in barley yield and production are expected. The members of HIPP family are good candidates for studying the impact of stress factors on barley senescence, as they are involved in the regulation of both processes.

1.5. Goal of dissertation

The ability of plants and other organisms to maintain an optimal functioning state is called homeostasis and is important for survival, development and reproduction. Plants have a complex and well-coordinated network, which regulates all aspects of their life cycle. During development, the homeostasis of plants can be interrupted by internal or external abiotic and biotic factors. Factors, which cause abiotic stress, are nonliving, environmental extremes, such as drought, low or high temperature, high salinity and low or high light. Biotic stress is caused by living organisms, such as bacteria, fungi, viruses, insects and others. An inadequate response to those factors can have an impact on plant performance, leading to premature senescence. When this highly regulated process is interrupted, huge losses in the yield of crop plants are monitored. Various members of HIPP family were found to be regulated under various stress and developmental conditions. The exact mode of function of those proteins is not known, but they could have a regulatory role in the interplay among different signaling pathways. Most studies have been performed in model plant *A. thaliana*, while little is known about HIPPs in crop plants and especially in *H. vulgare*. The present dissertation focuses on the study of *HvFPI*, which belongs to barley HIPP family. The following questions are addressing:

- 1. Which factors determine the differential regulation of *HvFPI* in primary leaves of barley plants?** To answer this question, barley plants were monitored after exposure to a number of abiotic stress conditions, phytohormones and during plant development. Primary leaves were used in order to estimate the expression of *HvFPI* via quantitative Real-Time PCR (qRT-PCR).
- 2. Is the overexpression or knock out of *HvFPI* influencing the performance of barley plants under abiotic stress conditions and during their development?** For this question, the first step was to establish barley homozygous transgenic lines which either overexpress or are knocked out for the gene of our interest. The OE lines were produced after transformation of barley embryos with *Agrobacterium tumefaciens* culture, carrying a cassette with *HvFPI* under the regulation of double enhanced constitutive promoter CaMV35S. The KO lines were produced via the CRISPR-Cas9 transformation system. Then, the transgenic lines were exposed to abiotic stress conditions or were monitored during their development. The performance of primary leaves was monitored in regards of the Chl content and PSII efficiency, while the expression of specific genes was estimated via qRT-PCR.
- 3. Which genes are differentially expressed during developmental leaf senescence in barley primary leaves? Is the overexpression of *HvFPI* reprogramming the expression of genes under control or senescing conditions?** This question is addressed by performing an RNA Seq analysis of total 12 samples. Those include samples of control (mature) and senescing primary leaves of WT and *HvFPI* OE lines in three independent biological replicates. Then, the lists of senescence associated genes in WT leaves and the differentially expressed genes in *HvFPI* OE lines were analysed.

2. Results

2.1. Expression level of *HvFPI* in barley primary leaves during abiotic stress, phytohormone treatment and developmental leaf senescence

Plants are exposed to a number of adverse factors during their development. Each factor constitutes a signal, which is perceived by plants and triggers a signaling cascade for the activation of the corresponding stress response. As described in detail in the introduction, HIPP proteins, including barley *HvFPI* (Barth *et al.*, 2004), are expressed in plants in response to various stresses. This finding was further investigated in the present work, by studying the regulation of *HvFPI* transcript level under our controlled conditions in growth chamber, including drought, combined cold and high light, salt and dark stress. Additionally, the regulation of this gene at different stages of leaf senescence was estimated. Both stress and developmental responses are highly regulated by the action of specific phytohormones. For that, the effect of different phytohormones on the expression of *HvFPI* was also unraveled.

2.1.1. The effect of abiotic stress treatments on transcript level of *HvFPI*

Drought stress is caused by reduction in water availability and may have a big impact on plant development. Especially for crop plants, it leads to massive losses in yield. The response of barley plants to drought stress was part of the present study. A reproducible drought stress system was established. Barley seeds were sowed in 1.5 kg soil and grown in greenhouse cabinets, under controlled, long-day conditions, as described in “Materials and Methods” section. The relative water content (RWC) of soil was 65 % at the beginning of the experiment. After the 11th day after sowing (DAS), natural drought was simulated by withholding the water supply from plants. Control plants were irrigated every two days in order to maintain the RWC of soil at 65 %. The experiment was conducted three times. The mean values with standard deviation of relative expression level of *HvFPI* during stress is presented in Fig. 6A. The results from qRT-PCR clearly showed that drought triggered an increased expression of *HvFPI* in primary leaves at different time points.

Low temperatures may have a severe impact on plant growth and development. In combination with a high light environment, the excess excitation energy in the photosynthetic apparatus causes a rise in detrimental ROS (Huner *et al.*, 1998). The differential regulation of *HvFPI* by combined cold and high light stress was studied here. More specifically, barley plants were grown as described above and on the 11th DAS half of the plants were exposed to combined cold (4 °C) and high light (780 $\mu\text{mol m}^{-2} \text{s}^{-1}$) stress in a growth chamber. Control plants remained in the optimal conditions of the greenhouse cabinets. The regulation of *HvFPI* was monitored by qRT-PCR at specific time points. *HvFPI* was significantly induced after already 4 h of cold and high light treatment (Fig. 6B). The expression was at the highest level after 7 and 10.5 h and then a small reduction was observed at 12.5 h. At 31 and 52 h, both control and stressed plants showed the same transcript amount of *HvFPI*.

Another stress factor, which resembles drought and has an adverse effect on plant growth, is high salinity. It may cause various physiological disturbances, such as ion-specific stress, which leads to leaf senescence, or osmotic effects, which lead to inhibition of water uptake (Mahlooji *et al.*, 2018). Here, the effect of salt on the regulation of *HvFPI* was

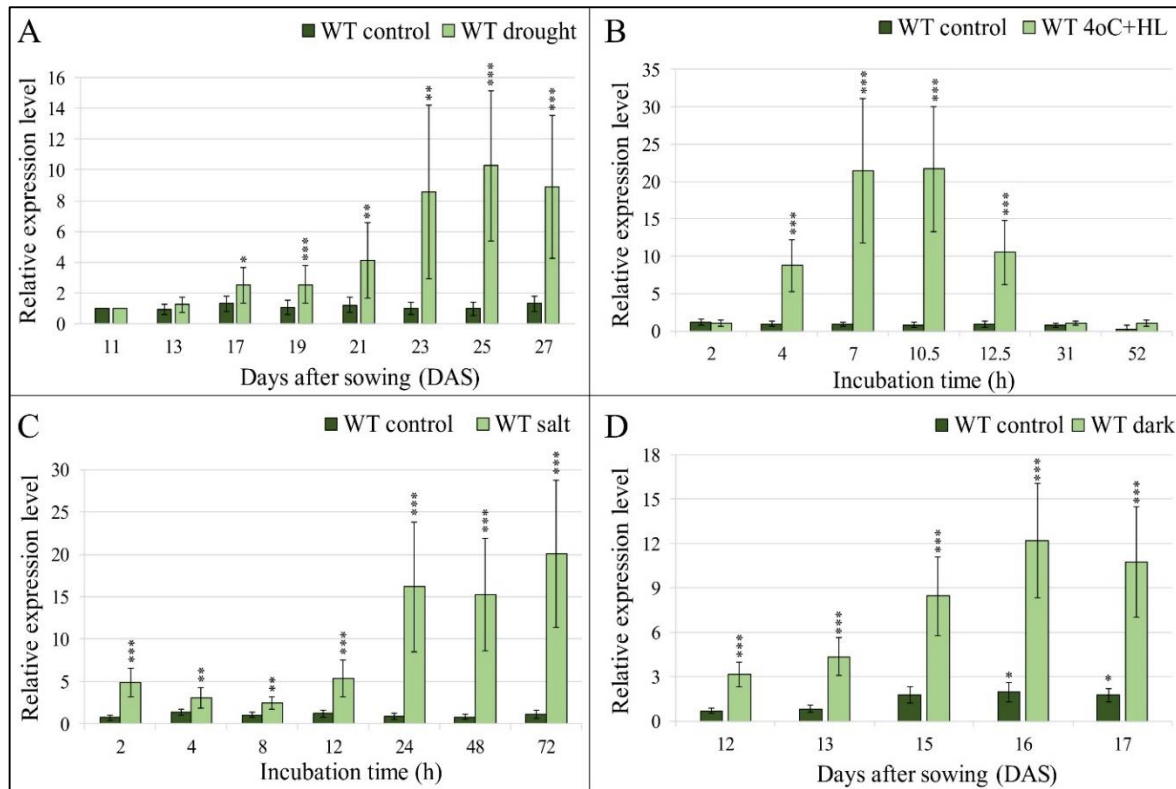


Figure 6: The relative transcript level of *HvFPI* at different time points of abiotic stress. (A) drought stress, compared with samples of 11th DAS; **(B)** cold (4°C) and high light (HL) stress, compared to untreated samples; **(C)** salt stress, compared to untreated samples and **(D)** dark stress, compared with primary leaves of 11th DAS. Mean relative expression level of three independent biological replicates, standard deviations and *p*-values were determined by REST-384 © 2006 (Pfaffl *et al.*, 2002) and normalized against *HvPP2A*, *HvActin* and *HvGCN5*. Statistically significant differences between control and stressed samples in comparison with untreated primary leaves on 11th DAS are indicated by asterisks: *p* < 0.05 (*), *p* < 0.01 (**), *p* < 0.001 (***).

observed. Specifically, barley plants were cultivated, as described before, and on the 11th DAS half of the plants were treated with 250 mmol salt (NaCl) per kg well-watered soil, while control plants were irrigated with fresh water. Then, samples of primary leaves were taken at specific time points and the expression of *HvFPI* was determined by qRT-PCR. The effect of salinity on barley plants was already obvious after 2 h of stress, when *HvFPI* was induced 5-fold (Fig. 6C). The relative expression level was higher at 24, 48 and 72 h after salt application. After 72 h, plants were senescing due to exposure to high salinity.

One factor that stresses the plants and leads to premature leaf senescence is light deprivation. Dark-induced leaf senescence is an extreme example of shading that induces the senescence of leaves in a way similar to normal plant development (Sobieszczuk-Nowicka *et al.*, 2016). The possible implication of *HvFPI* in this extreme form of leaf senescence was studied here. Seeds of barley plants were handled as described above and, on the 11th DAS, plants were subjected to dark stress by covering the primary leaves with aluminum foil. Then, samples of primary leaves were taken at specific time points and the expression of *HvFPI* was calculated by qRT-PCR. A 3-fold upregulation of *HvFPI* was already observed after one day of dark application (Fig. 6D). This induction was significant at every time point and led to 10- to 12-fold higher relative expression level by the 17th DAS. On this time point, the primary leaves were completely senescent.

2.1.2. Expression of *HvFPI* during developmental leaf senescence

The induction of *HvFPI* in response to various abiotic stresses was confirmed. These stress conditions may lead to a premature, stress-induced leaf senescence. Therefore, the relative transcript level of *HvFPI* at different stages of developmental, and not stress-induced, senescence of barley primary leaves was estimated here. The different stages of leaf senescence were defined by changes in Chl content of mature primary leaves. The maximum Chl content (100 %) in mature leaves was observed approximately on 21st DAS and started to decline at the onset of leaf senescence (data not shown). Very early stages of senescence were defined by a reduction in Chl content to 90-95 % of that in mature leaves. In the middle stage, the Chl content was reduced to 80-75 % and in late stages it was less than 50 %.

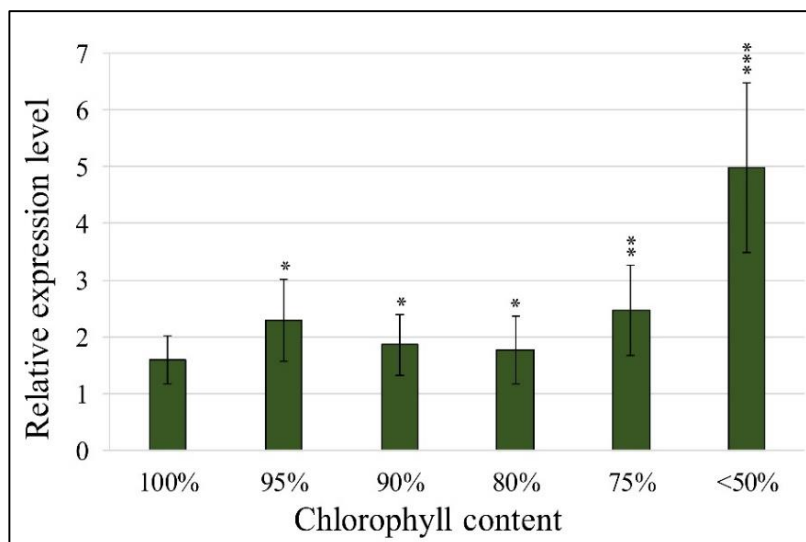


Figure 7: The relative transcript level of *HvFPI* at various developmental stages, compared with samples of 13th DAS. Mean relative expression level of three independent biological replicates, standard deviations and *p*-values were determined by REST-384 © 2006 (Pfaffl *et al.*, 2002) and normalized against *HvPP2A*, *HvActin* and *HvGCN5*. Statistically significant differences between samples on various developmental stages in comparison to samples on 13th DAS are indicated by asterisks: *p* < 0.05 (*), *p* < 0.01 (**), *p* < 0.001 (***).

The relative gene expression was compared with samples of 13th DAS, when the primary leaves had reached the maximum length. The results showed a significant induction of *HvFPI* in all stages of leaf senescence and the maximum expression level observed at the later stage, when the Chl content was less than 50 % (Fig. 7).

2.1.3. Effect of phytohormone treatments on *HvFPI* expression level

Phytohormones act as systemic messengers within plants, activating signaling cascades in target cells for plant stress responses and developmental processes. In this work, the regulation of *HvFPI* by ABA, SA, Methyl-Jasmonate (MeJA) and the three CKs: kinetin, zeatin and 6-benzyl-aminopurine (6-BAP), was monitored. Primary leaves of barley plants were cut and incubated in different phytohormone solutions with their corresponding controls, as described in “Materials and Methods” section. The regulation of *HvFPI* was studied after 4 h and 24 h and compared with samples, which were treated only with the appropriate control solvent (EtOH for ABA, SA and MeJA and KOH for CKs; Fig. 8).

Treatments with the control solvents EtOH or KOH alone did not cause significant changes in *HvFPI* expression (data not shown).

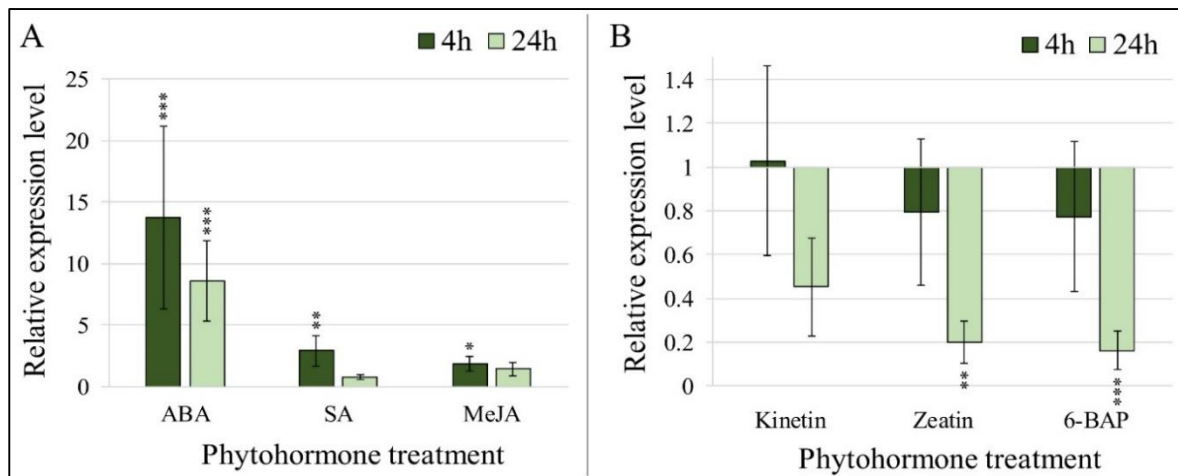


Figure 8: The relative transcript level of *HvFPI* in barley primary leaves after treatment with various phytohormones. (A) Abscisic acid (ABA), Salicylic acid (SA) and Methyl-Jasmonate (MeJA) in comparison to respective control treatment, and (B) Kinetin, Zeatin and 6-benzylaminopurine (6-BAP) in comparison to respective control treatment. Mean relative expression level of three independent biological replicates, standard deviations and *p*-values were determined by REST-384 © 2006 (Pfaffl *et al.*, 2002) and normalized against *HvPP2A*, *HvActin* and *HvGCN5*. Statistically significant differences between samples after treatment with phytohormones in comparison to samples after treatment with corresponding control are indicated by asterisks: *p* < 0.05 (*), *p* < 0.01 (**), *p* < 0.001 (***).

The results showed that ABA, SA and MeJA were positive regulators of *HvFPI* expression (Fig. 8A). Specifically, ABA was the main regulator, as it strongly induced *HvFPI*, after 4 h and 24 h of treatment. SA and MeJA induced *HvFPI* in the first 4 h, but the expression level was not different than the control after 24 h. On the other hand, the group of CKs resulted in downregulation of *HvFPI* after 24 h of treatment (Fig. 8B).

2.2. Transgenic lines of *Hordeum vulgare* L. cv. Golden promise

In the present study, the regulation of *HvFPI* under various abiotic stresses, phytohormone treatments and during leaf senescence was confirmed. This suggests a function of *HvFPI* in these processes. Reverse genetic approaches causing *gain-of-function* and *loss-of-function* are powerful tools to investigate the mode of action of novel genes. Here, in order to functionally characterize *HvFPI*, transgenic overexpression (OE) and knock out (KO) lines were established and analyzed. Barley cultivar *H. vulgare* L. cv. Golden promise was used, due to its higher transformation rate, which results in successful genetic modification (Marthe *et al.*, 2015; Schreiber *et al.*, 2020). Barley embryos were transformed with the *A. tumefaciens* system, carrying the appropriate construct for OE or KO of *HvFPI*. The procedure for the OE lines was carried out by Stefan Ehnert, while the KO lines were produced during the present work with assistance from the group of Prof. Dr. Edgar Peiter (Plant Nutrition Lab, Institute of Agricultural and Nutrition Sciences, Martin Luther University, Halle-Wittenberg), who has established a barley transformation platform.

2.2.1. Establishment of overexpression lines 21.3I and 21.2A

The construct for the OE lines of *HvFPI* is presented in Fig. 38 in appx. 6.1.1. The whole genomic sequence of *HvFPI*, with two exons and one intron under the regulation of the double enhanced constitutive viral promoter CaMV35S, was inserted in barley embryos. One StrepII® tag sequence (Schmidt & Skerra, 2007), which encodes for 8 amino acids, and a bridge sequence of 5 amino acids were inserted at the 5'-end of the gene of interest. The construct included the hygromycin phosphotransferase (*Hpt*) gene for hygromycin resistance, under the regulation of *Zea mays* Ubiquitin 1 promoter (*ZmUbi1p*). The hygromycin resistance was used as selection marker for the successfully transformed embryos and the formation of calli was induced.

Plants of the first generation (T_0) were examined for the presence of the transgenic construct (data not shown). In T_1 and T_2 generations, the plants carrying the transgenic *HvFPI* and the *Hpt* gene were selected for further analysis and establishment of homozygous OE lines. An example of this analysis in T_1 generation is shown in Fig. 40 in appx. 6.1.2., for the candidate lines 21.3I and 21.2A. First, DNA was isolated from leaf tissue and a PCR reaction was performed for the detection of whole inserted gene. Appropriate primers were designed, which were specific for the vector sequence and amplified the whole insert, in order to distinguish between the WT and the transgenic *HvFPI*. The inserted *HvFPI* with the strep tag was 744 bp and the PCR product was estimated at 886 bp. Total 6 plants of 21.3I and 5 plants of 21.2A lines were analysed and those with the transformation construct were used for the establishment of two independent homozygous lines in the next generation. The detected products were purified and sequenced, confirming the presence of the insertion (data not shown). These results were verified with PCR for the selection marker gene *Hpt* (data not shown).

2.2.2. Establishment of knock out lines 20.1At and 20.17M

In the present work, the type II Clustered Regularly Interspaced Short Palindromic Repeats (CRISPR) system was used, as described by Kumar *et al.* (2018), to establish barley *HvFPI* KO lines. Barley embryos were transformed with a construct, which contains two main components: The *Zea mays* CRISPR associated 9 (*ZmCas9*) nuclease and synthetic single guide RNAs (sgRNA), which were complementary to the target gene, together with a scaffold sequence. The positions of three sgRNAs for targeting *HvFPI* are presented in Fig. 39 in appx. 6.1.1. Again, the *Hpt* gene under the regulation of *ZmUbi1* promoter was used as a selective marker, as described above. The successfully transformed embryos were selected via hygromycin resistance and the formation of calli was induced. In the present work, total 24 plants of T_0 generation were screened for mutations in *HvFPI* gene. First, total DNA was extracted from leaf tissue and a PCR reaction was carried out in order to detect *HvFPI* gene. The WT PCR product corresponds to 819 bp. Plants 1 and 17 exhibited a shorter product, as shown in the gel provided in Fig. 42 in appx. 6.1.2., and both were extracted from the gel and sequenced (data not shown). Plant 1 carries a homozygous deletion, with a product of 483 bp. This product was a result of cleavage at sgRNA1 and sgRNA2 positions and failure to repair the double strand breaks. Plant 17 showed a strong product of 374 bp, but also a weak product of 819 bp. The 374 bp product resulted from cleavage at sgRNA1 and sgRNA3 positions and failure to repair the double strand breaks. At the end, plants 1 and 17 were chosen for further

cultivation. In the next generations, plants with a homozygous deletion for *HvFP1*, but without carrying the transformation cassette with the *ZmCas9* nuclease were chosen and the KO homozygous lines 20.1At (from plant 1) and 20.17M (from plant 17) were established.

2.2.3. Transcript and protein level of *HvFP1* in OE and KO lines

The successful transcription of the transgene was determined for both OE lines. For this, RNA was isolated from leaf tissue of the aforementioned plants and cDNA was synthesized. The cDNA was used as a template in a PCR reaction, where appropriate primers were designed in order to detect the full-length transcribed product (size 771 bp), but also the functional spliced product of *HvFP1* (size 468 bp). Indeed, the samples, which were positive for the inserted *HvFP1*, showed products of both transcripts, one of unspliced product (~800 bp) and one of spliced product (~500 bp) (Fig. 41 in appx. 6.1.2.).

Furthermore, the transcription of a functional product was confirmed via qRT-PCR. For that, total RNA was extracted from leaf tissue of plants of WT, OE and KO lines, cDNA was synthesized and then used as template for a qRT-PCR reaction in order to quantify the transcripts of *HvFP1*. The expression level in transgenic lines was compared with samples of WT plants. The relative expression level was significantly higher in OE lines. Specifically, the amount of *HvFP1* transcripts, when compared to WT, was over 150 times higher for 21.3I line and close to 200 times higher for 21.2A line (Fig. 9A). The significant downregulation of *HvFP1* in the two KO lines is shown in the same figure (Fig. 9B), with the amount of *HvFP1* being 0.004 for 20.1At line and close to 0.01 for 20.17M line, when compared to WT, which was set as 1.

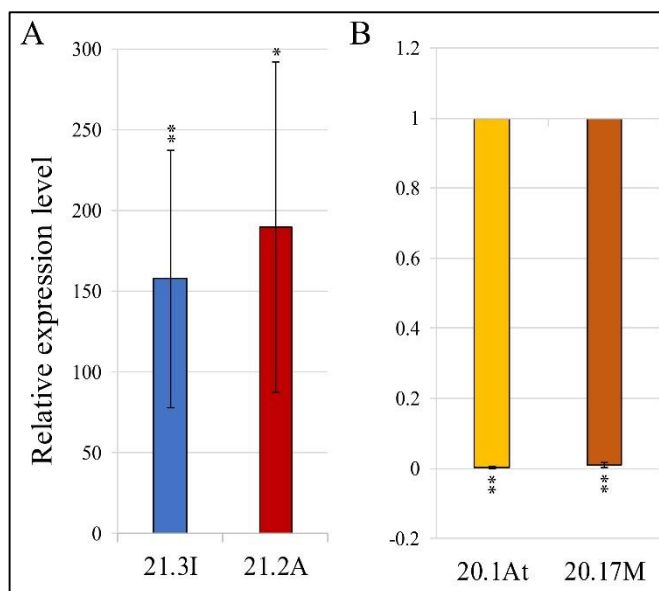


Figure 9: The relative transcript level of *HvFP1* in barley transgenic lines. (A) Overexpression lines 21.3I and 21.2A and (B) Knock out lines 20.1At and 20.17M in comparison to WT samples. Mean relative expression levels of at least three samples, standard deviations and *p*-values were determined by REST-384 © 2006 (Pfaffl *et al.*, 2002) and normalized against *HvPP2A*, *HvActin* and *HvGCN5*. The statistical significance between samples of transgenic lines in comparison to WT samples is indicated by asterisks: *p* < 0.05 (*), *p* < 0.01 (**).

For the detection of *HvFP1* protein by using specific polyclonal antibodies, leaf tissue of barley WT and transgenic lines was used for protein extraction. Specifically, 60 µg of total protein samples were separated in an SDS-PAGE and transferred to a PVDF membrane for detection of *HvFP1* with western blot (Fig. 10). The size of WT *HvFP1* was estimated at 17.3 kDa, while the size of Strep-*HvFP1* in two OE lines was estimated at 18.8 kDa. The bands of Strep-*HvFP1* were clearly shown in OE lines 21.3I and 21.2A. In WT and KO lines, no band of *HvFP1* was visible, but only weak signals at around 15 kDa were detected in all samples.

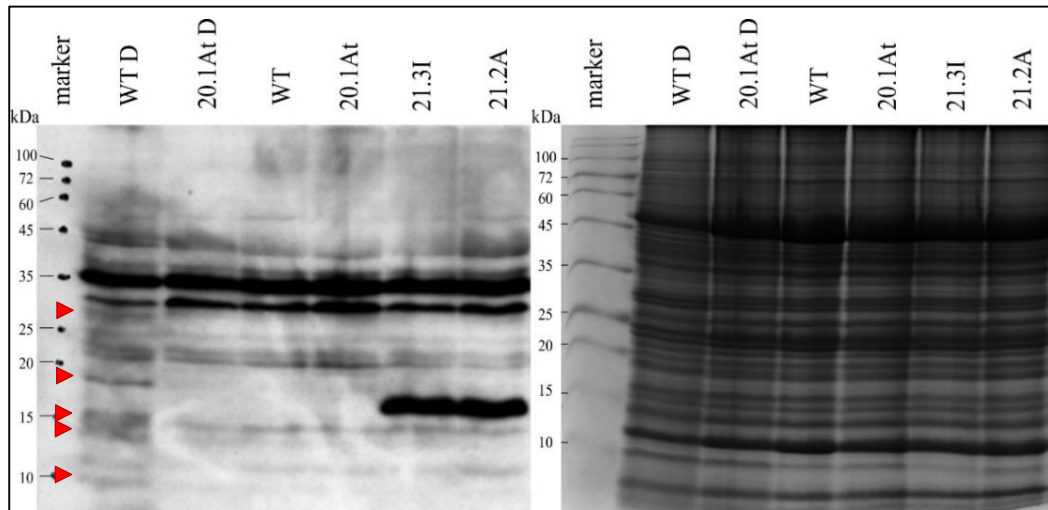


Figure 10: Western blot analysis for detection of HvFP1 in WT, both OE and one KO lines using purified polyclonal α -HvFP1 antibodies. One sample of WT drought (WT D) and one of KO drought (20.1At D) were also included. The expected size of WT protein was 17.3 kDa and the size of strep-HvFP1 in OE line was 18.8 kDa. A Coomassie stained SDS-PAGE gel of the same protein samples was also shown, proving the equal loading amount of 60 μ g of total proteins. Red triangles demonstrated the signals detected exclusively in drought stressed WT samples (WT-D).

This was expected for KO line. The lack of a band in WT could reflect a low protein level under control conditions. Therefore, one sample of WT and one of 20.1At during drought stress, when HvFP1 was induced, were also loaded. The WT D sample exhibited additional bands at approximately 10, 13, 16, 18 and 30 kDa (Fig. 10; red triangles), which were not observed for KO D sample. However, there was no clear proof, that any of this band corresponded to HvFP1, which should be at 17.3 kDa. Thus, it was difficult to make a conclusion for WT samples.

2.2.4. Phenotypic analysis of transgenic lines

A genotypic analysis of transgenic lines showed the successful genetic transformation of barley *H. vulgare* L. cv. Golden promise plants. Lines 21.3I and 21.2A overexpress *HvFP1*, leading to a higher amount of functional HvFP1 protein. The opposite effect was observed in lines 20.1At and 20.17M, where deletion events led to inactive transcripts of *HvFP1*. The effect of both genetic transformations on plant phenotype was also monitored in the present work. To investigate effects of *gain-* or *loss-of-function* of *HvFP1* on plant development, ten plants of all five lines, i.e., WT, 21.3I, 21.2A, 20.1At and 20.17M, were monitored throughout their development, until the flowering time and the maturation of seeds. Photos of plants on the 43rd DAS showed no obvious phenotypic difference during their development (Fig. 43 in appx. 6.1.3.).

The growth of WT, OE and KO plants was further characterized by monitoring the length of primary leaves on 13th DAS, the time point of flag leaf formation and the plant height of total 10 individuals from each line. Besides normal variation, no significant differences between WT and transgenic lines were detected, indicating that plant development under the normal conditions was not affected (Fig. 11A, B and D). After the

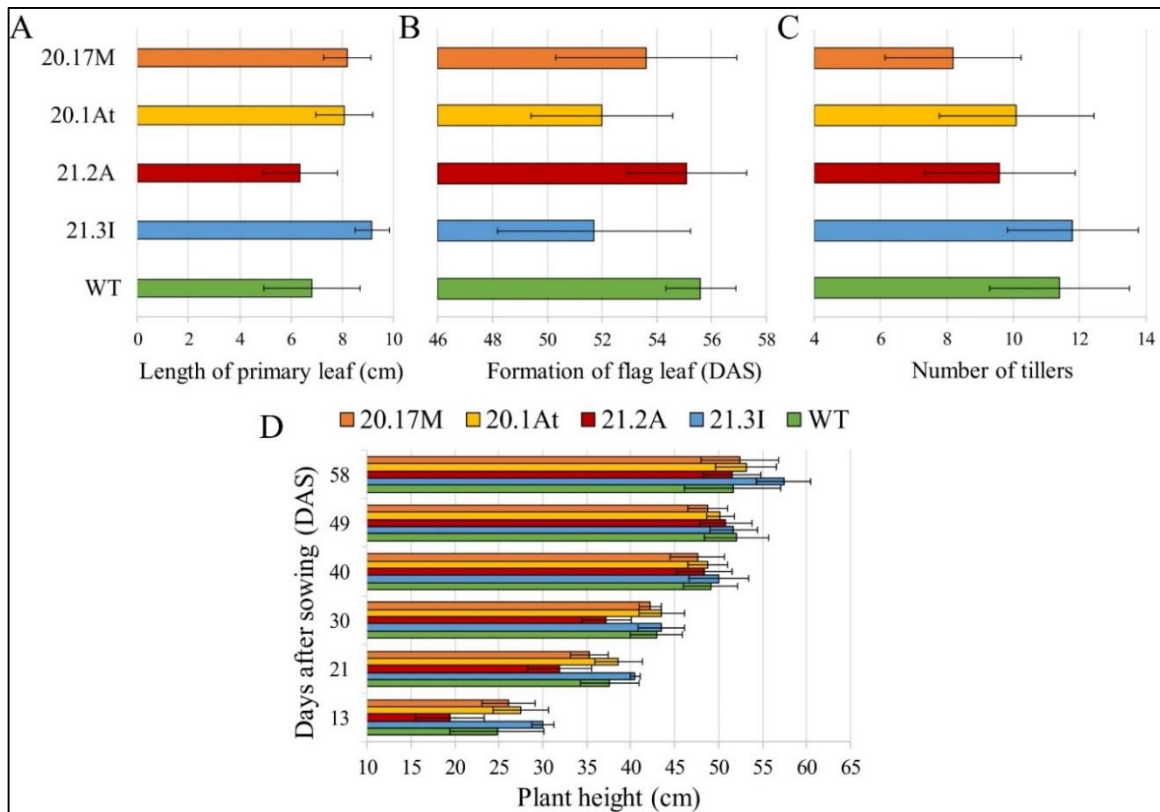


Figure 11: Phenotypic analysis of total 10 plants of each transgenic line. (A) Length of primary leaf on 13th day after sowing (DAS); **(B)** Day after sowing (DAS) of flag leaf formation; **(C)** Number of tillers and **(D)** Total height of plants at various time points.

formation of flag leaf, each plant develops tillers, which is an important trait for the yield. Here, the WT and 21.3I plant lines exhibited the highest number of tillers, up to 14 (Fig. 11C). The other three lines had slightly less tillers, but this follows the natural variation among the individuals.

2.3. Study of barley WT and *HvFPI* OE lines under various abiotic stress conditions and during developmental leaf senescence

As shown before, *HvFPI* was strongly induced under drought, combined cold and high light and salt stress, but also in dark-induced and developmental leaf senescence, indicating a role in these processes. In order to get a better understanding about the function of *HvFPI*, the responses of WT, OE and KO barley lines to these conditions were studied in more detail. For each condition, the expression of known stress marker genes was evaluated in order to confirm the success of the experimental design. Possible effects on stress responses and leaf senescence were analysed via two parameters, related to photosynthesis: Chl content and maximum PSII quantum efficiency (F_v/F_m). Both parameters are known to sensitively respond to various abiotic stress conditions and at the onset of leaf senescence (Krieger-Liszkay *et al.*, 2019).

2.3.1. Drought stress

The experimental design for drought stress was the same as described above. Shortly, barley seeds of WT and two OE lines 21.3I and 21.2A were sowed in soil with 65 % RWC and grown in greenhouse cabinets under controlled, long-day conditions. Drought stress was

applied by stopping the irrigation of the plants, while control plants were irrigated every two days. The experiment was conducted three times for each line. The RWC of soil was reduced to 55 % after four days of water deprivation and reached only 10 % at the end of the experiment in all lines (Fig. 12A). The primary leaves of drought stressed plants started to turn yellow on the 25th DAS (Fig. 12B), when the RWC of soil was at 20 %. The drought induced leaf senescence was observed on the 31st to 33rd DAS, with leaves being completely dry (Fig. 12B). The progress of drought-induced leaf senescence was monitored by changes in photosynthetic parameters of leaves. The PSII efficiency was approximately 0.8 at the beginning of the experiment and remained stable in control plants (Fig 12C). Water deficit affected the photosynthetic performance, which was shown by the reduction of F_v/F_m value to 0.4-0.6 on the 27th to 29th DAS, when the RWC of soil was less than 20 %. The relative Chl content was affected more drastically and the reduction started on the 19th to 21st DAS, when the RWC of soil was less than 40 % (Fig. 12D). The values of both physiological parameters were close to 0 on the 33rd DAS. The same observations were made for all lines, showing that the OE of *HvFPI* did not affect the drought induced, premature shift from a photosynthetically active to a senescing chloroplast.

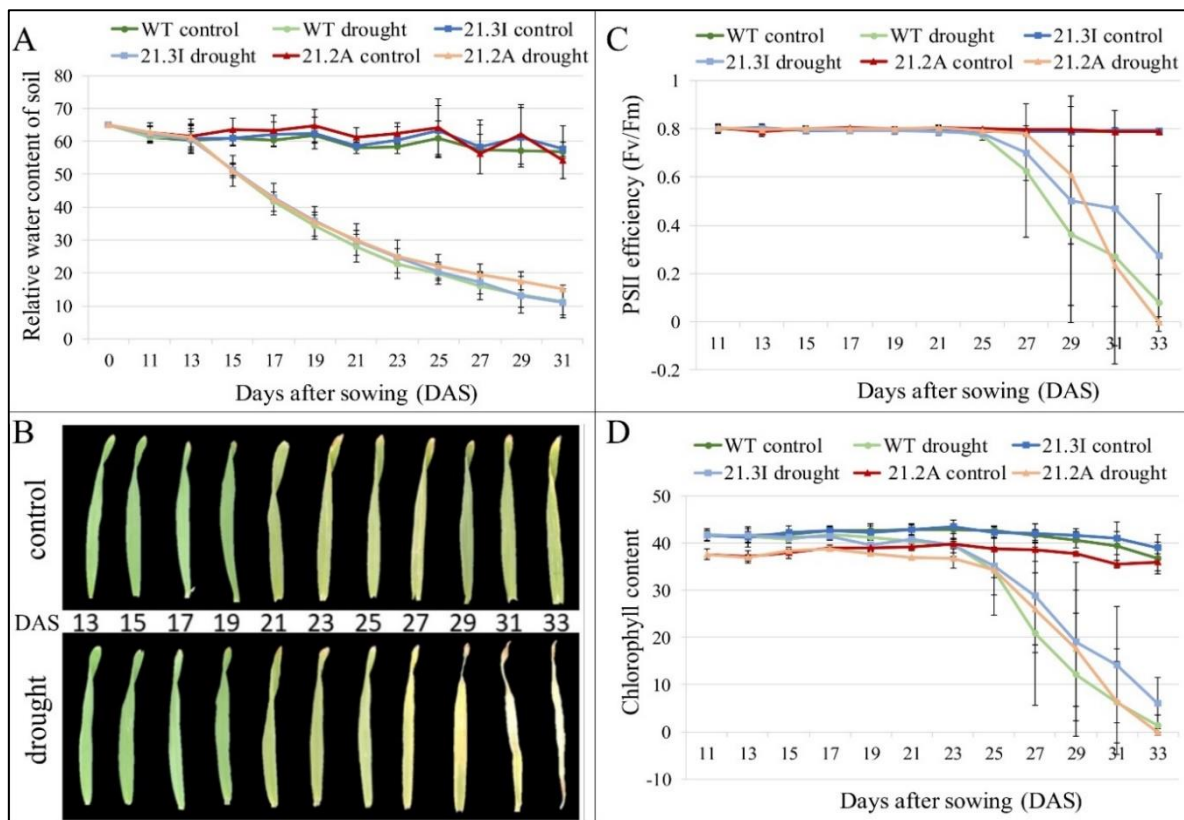


Figure 12: Study of barley *HvFPI* OE lines under drought stress. (A) The relative water content of soil during the drought stress approaches, which was 65 % at the beginning of the experiment; (B) Example of the progress of drought-induced senescence of primary leaves in WT plants; (C) The photosynthetic activity of primary leaves, expressed as PSII efficiency (F_v/F_m) and (D) The relative Chl content of primary leaves, expressed in SPAD units. All data are mean values of three independent biological replicates.

Plants respond to drought stress by activating a number of strategies, in order to avoid or adapt to water deficit (Gupta *et al.*, 2020). These strategies are highly regulated by a number

of genes, which are known to be induced in response to drought stress and are considered as drought stress marker genes. In the present work, the effect of OE of *HvFPI* on drought related expression of *HvS40*, 9-*cis*-epoxycarotenoid dioxygenase (*HvNCED*), dehydrin 1 (*HvDhn1*) and heat shock protein 17 (*HvHsp17*) genes was investigated at various time points and for all lines. *HvS40* is a well-known ABA-dependent senescence associated gene, which was induced during developmental leaf senescence, but also during drought-induced leaf senescence (Jehanzeb *et al.*, 2017). Furthermore, *HvNCED* and *HvDhn1* are two well-known drought stress marker genes. *HvNCED* is an important enzyme in biosynthesis of ABA (Iuchi *et al.*, 2001) and the important role of ABA in plant defense against drought stress was already mentioned in the introduction. Then, *HvDhn1* encodes for a LEA Group II protein, which was upregulated in response to dehydration in an ABA-dependent way (Suprunova *et al.*, 2004). Finally, it is known that *HvHsp17* was also regulated in response to drought (Temel *et al.*, 2017), but it is not clear if its expression was dependent on ABA (Zou *et al.*, 2009).

A significant induction of all drought stress marker genes during drought treatment in all lines was observed. This is documented in Fig. 13, where the expression level of each gene in OE lines was compared to that of WT on the 11th DAS, which was the last irrigation time point, before drought was applied. Interestingly, clear differences between WT and both OE lines were noted. Significant induction of *HvS40*, *HvNCED* and *HvDhn1* was observed for

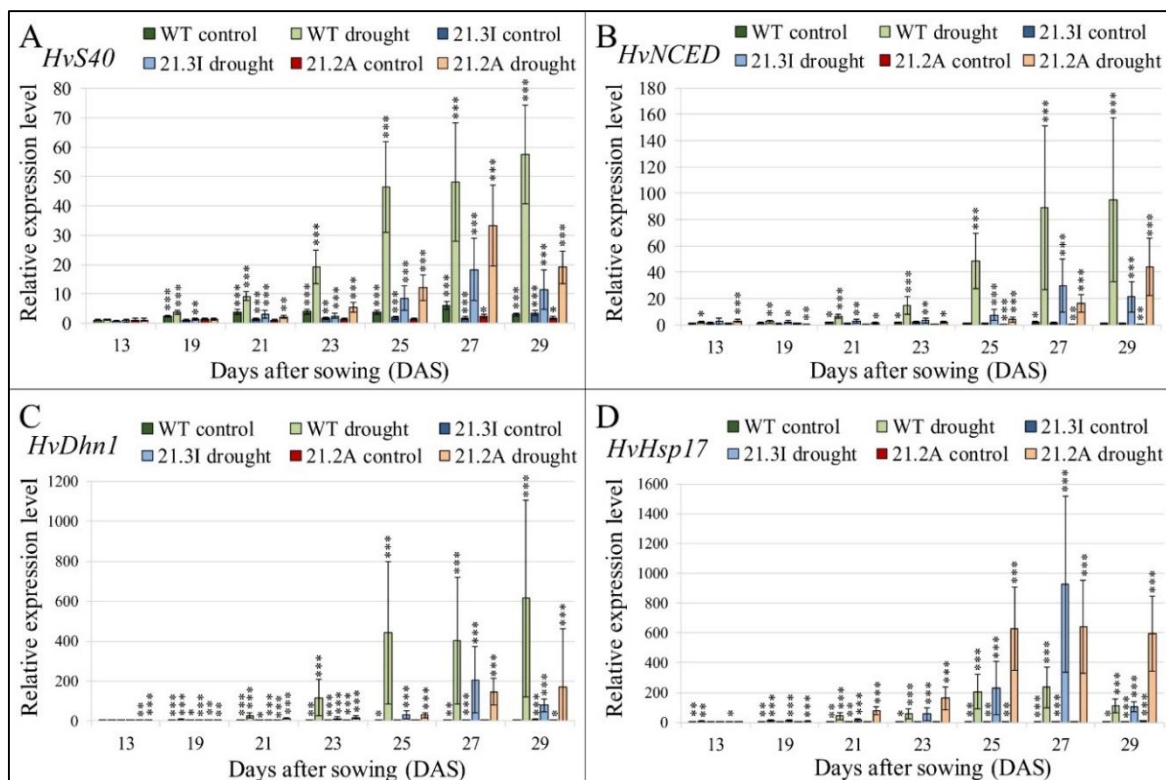


Figure 13: The relative transcript level of drought stress marker genes at different time points of drought stress, compared with samples of WT on 11th DAS (set as 1). (A) *HvS40*; (B) *HvNCED*; (C) *HvDhn1* and (D) *HvHsp17*. Mean relative expression level of three independent biological replicates, standard deviations and *p*-values were determined by REST-384 © 2006 (Pfaffl *et al.*, 2002) and normalized against *HvPP2A*, *HvActin* and *HvGCN5*. Statistically significant differences between samples of WT and OE lines, in control and drought treatments, at various time points in comparison to WT samples on the 11th DAS are indicated by asterisks: *p* < 0.05 (*), *p* < 0.01 (**), *p* < 0.001 (***)

WT senescing leaves on 23rd and 25th DAS, while this was clearly noted only in later phases (27th and 29th DAS) for OE lines and did not reach as high expression levels as in WT (Fig. 13A, B and C). This was better illustrated when the relative expression level of those genes in drought samples of both OE lines was compared with drought samples of WT plants at the same time points (Fig. 14A, B and C). The results clearly showed that drought-related induction of the three ABA-dependent genes *HvS40*, *HvNCED* and *HvDhn1* was repressed in both OE lines. Interestingly, the expression of *HvHsp17*, which is not necessarily under the regulation of ABA, was not repressed in OE samples, but rather highly induced at specific time points (Fig. 13D and 14D). The above results indicated a possible function of *HvFPI* in the regulatory pathway of typical drought-response genes, in an ABA-dependent manner.

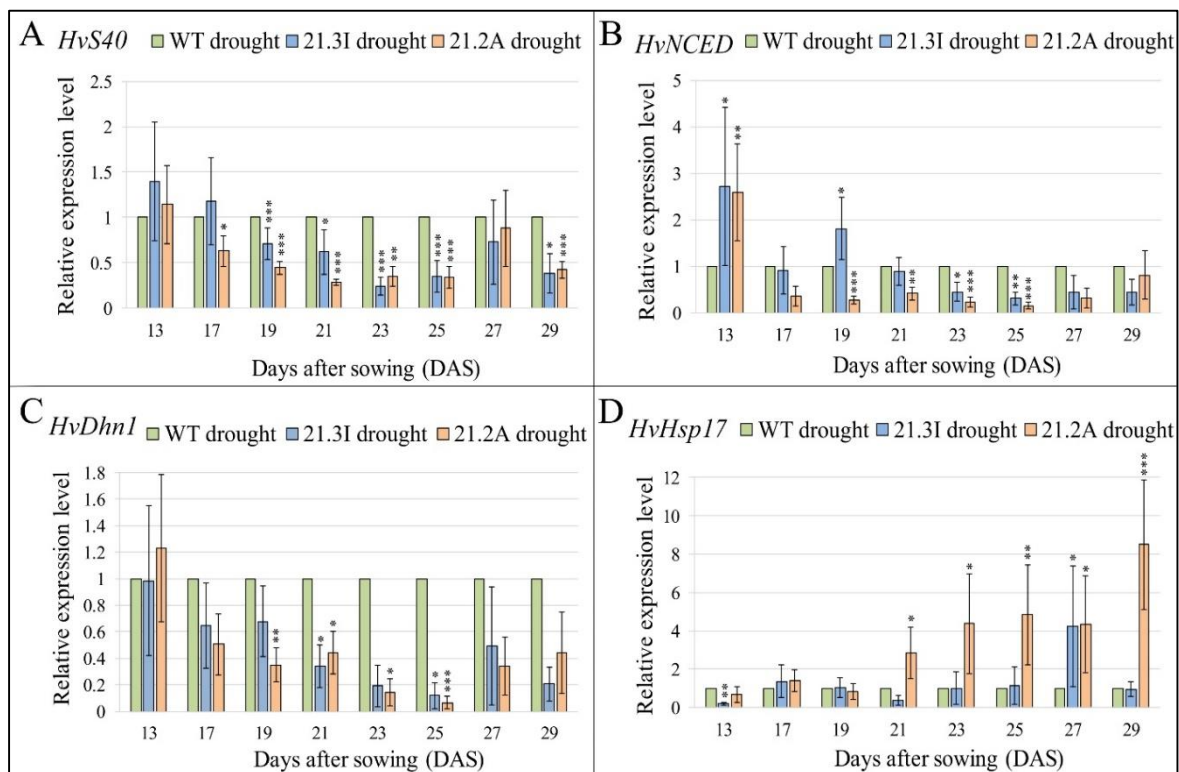


Figure 14: The relative transcript level of drought stress marker genes in drought samples of OE lines at different time points, compared with drought samples of WT at each time point. (A) *HvS40*; (B) *HvNCED*; (C) *HvDhn1* and (D) *HvHsp17*. Mean relative expression levels of three independent biological replicates, standard deviations and p -values were determined by REST-384 © 2006 (Pfaffl *et al.*, 2002) and normalized against *HvPP2A*, *HvActin* and *HvGCN5*. Statistically significant differences between drought samples of OE lines at each time point in comparison with drought samples of WT on the same time point are indicated by asterisks: $p < 0.05$ (*), $p < 0.01$ (**), $p < 0.001$ (***)).

2.3.2. Combined cold and high light stress

It was shown that *HvFPI* was induced in response to combined cold and high light stress (Fig 6B). The effect of the OE of *HvFPI* on plant responses to the combination of these two stress factors was studied in a similar way, as described before for drought stress. Seeds of WT and OE lines were handled as described above and, on the 13th DAS, cold and high light was applied to half of the plants, while the rest remained in the greenhouse cabinets.

During the experiment, changes in physiological parameters of primary leaves and the relative expression of *Cold Regulated gene 14b* (*Cor14b*) were determined.

Plants of both WT and OE lines responded to the combination of cold and high light treatment by a quick decrease in PSII efficiency (Fig. 15A). This fast response within the first hours reflected a reorganization of the photosynthetic machinery under the excess excitation energy caused by combined cold and high light (Huner *et al.*, 1998). This was exhibited here, as the PSII efficiency, which was approximately 0.8 at the beginning of the experiment, was reduced to 0.7 during the first 2 h of stress and to 0.5 after 10.5 h, but then it remained stable, reflecting a cold acclimation in all lines (Fig. 15A). In contrast, Chl content stayed rather high during the treatment, with a small reduction by 10 % to 20 % in the first hours and then it remained stable, in all lines (Fig. 15B). This indicated that the short-term experimental setup, used in this experiment, did not cause severe damages in chloroplasts, but allowed us to investigate the effect of *HvFPI* OE on the quick cold acclimation response. Since there were no phenotypic differences between WT and OE lines, *HvFPI* seemed not to be directly involved in this process.

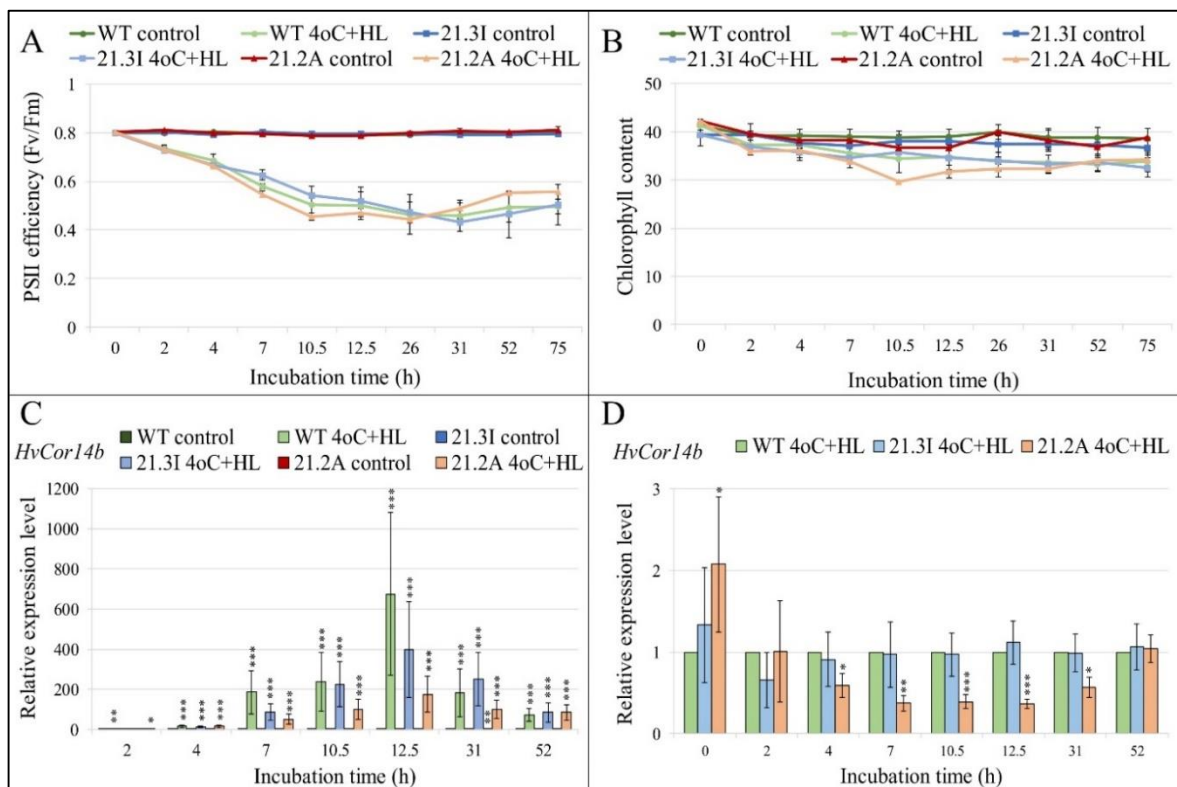


Figure 15: Study of barley *HvFPI* OE lines under cold and high light (4°C+HL) stress. (A) The photosynthetic activity, expressed as PSII efficiency (F_v/F_m); **(B)** The relative Chl content, expressed in SPAD units; **(C)** The relative transcript level of cold stress marker gene *HvCor14b* at different time points of 4°C+HL stress, compared with WT samples before the treatment and **(D)** The relative transcript level of *HvCor14b* in 4°C+HL samples of OE lines compared with the corresponding WT samples at each time point. Mean relative expression levels of three independent biological replicates, standard deviations and *p*-values were determined by REST-384 © 2006 (Pfaffl *et al.*, 2002) and normalized against *HvPP2A*, *HvActin* and *HvGCN5*. Statistically significant differences between **(C)** control and 4°C+HL samples of WT and both OE lines, at all time points, in comparison to WT untreated samples, and **(D)** 4°C+HL samples of both OE lines in comparison to 4°C+HL WT samples at each specific time point, are indicated by asterisks: *p* < 0.05 (*), *p* < 0.01 (**), *p* < 0.001 (***)

Besides the changes in physiological parameters, exposure to cold and high light stress caused the induction of stress response gene *HvCor14b*. It is known that *HvCor14b* is induced in response to cold stress, under the regulation of CRT-binding TF (Gilmour *et al.*, 1998). Here, there was a significant induction of *HvCor14b* in stress samples of WT and the two OE lines, starting already after 4 h of stress application (Fig. 15C). This induction was higher between 10.5 h and 31 h after treatment in all cold and high light samples and then a small reduction was observed. A comparison between stress samples of OE lines with the corresponding samples of WT for each time point showed a significant lower expression of *HvCor14b* in 21.2A line (Fig 15D). Interestingly, this was not confirmed for the second OE line 21.3I. These results did not give a clear conclusion on whether *HvFPI* was involved in the regulation of this cold-regulated gene.

2.3.3. Salt stress

The possible effect of *HvFPI* OE on barley responses to salt stress was determined. Plants of all lines were sowed in soil, grown in greenhouse cabinets and treated with 250 mmol NaCl per kg soil, as described before. In order to determine the responses of barley plants to salt stress, the physiological parameters of primary leaves were measured. During the first 48 h after the salt application, the F_v/F_m ratio remained unchanged in all lines and started to reduce at 72 h post treatment (Fig. 16A). Similar observation was made for the Chl content of primary leaves, which was reduced by ~10 % after 48 h and by ~20 % after 72 h in all lines (Fig. 16B).

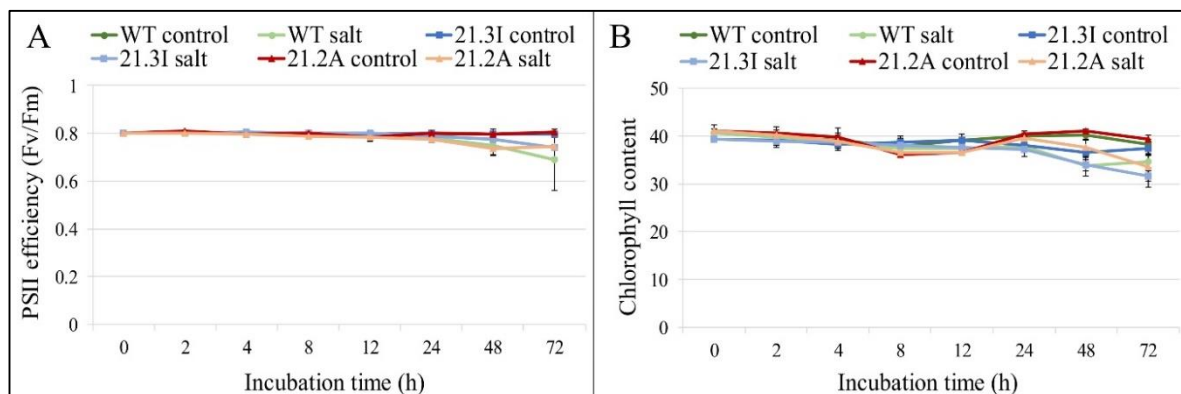


Figure 16: Study of barley *HvFPI* OE lines under salt stress. (A) The photosynthetic activity, expressed as PSII efficiency (F_v/F_m) and (B) The relative Chl content, expressed in SPAD units. All data are mean values of three independent biological replicates.

The application of salt treatment, in this experimental design, had no direct impact on the photosynthetic efficiency of primary leaves individually, but rather to whole plants after 72 h post treatment. Nevertheless, it clearly induced the expression of three well-known salt stress marker genes. These were the *HVA1* and *HvDhn1*, which both are members of LEA family (Chandra Babu *et al.*, 2004; Kumar *et al.*, 2014), and the *HvP5CS2*, which encodes a central enzyme for proline biosynthesis (Turchetto-Zolet *et al.*, 2009). All three genes showed a significant upregulation in WT and both OE samples during the 72 h of salt treatment (Fig.17A, B and C). However, the time scale of induction of salt stress marker genes in OE leaves seemed to be different from that in WT leaves. Specifically, salt stress marker genes showed higher induction after 12 h in WT primary leaves, while OE samples exhibited higher

induction after 24 h to 48 h, and a faster decrease at 72 h. A comparison between salt treated samples of both OE lines with the corresponding WT samples at each time point did not show a clear difference in the expression of salt stress marker genes (Fig. 17D, E and F). In specific

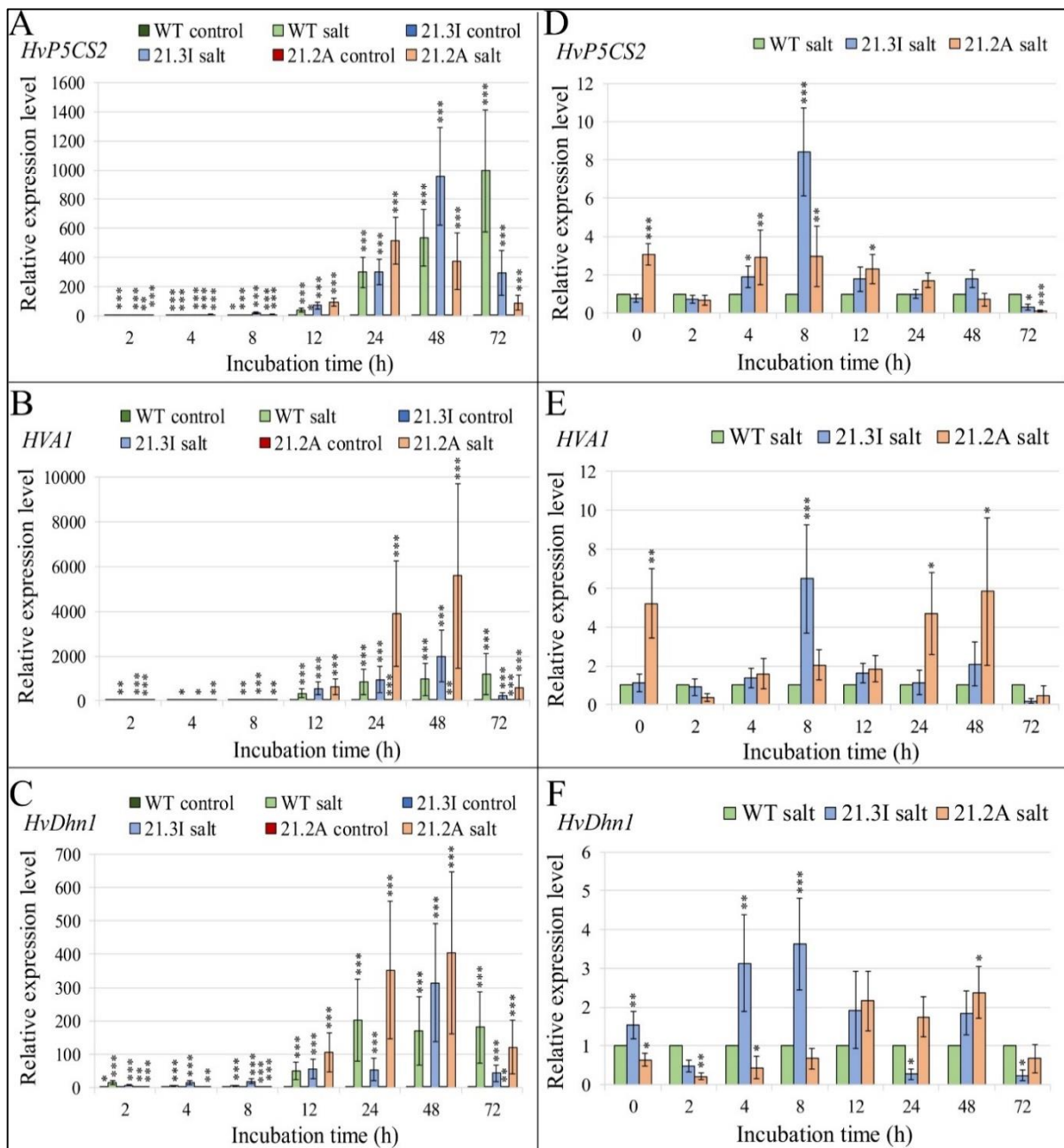


Figure 17: The relative transcript level of salt stress marker genes at different time points after salt application. The relative transcript level of (A) *HvP5CS2*; (B) *HVA1* and (C) *HvDhn1* at different time points of salt stress, compared with WT untreated samples. The relative expression level of (D) *HvP5CS2*; (E) *HVA1* and (F) *HvDhn1* in salt treated OE samples in comparison to WT at each time point. Mean relative expression levels of three independent biological replicates, standard deviations and *p*-values were determined by REST-384 © 2006 (Pfaffl *et al.*, 2002) and normalized against *HvPP2A*, *HvActin* and *HvGCN5*. Statistically significant differences between (A); (B); (C) control and salt samples of WT and both OE lines, at all time points, in comparison to WT untreated samples, and (D); (E); (F) salt samples of both OE lines in comparison to WT salt samples at each specific time point, are indicated by asterisks: *p* < 0.05 (*), *p* < 0.01 (**), *p* < 0.001 (***).

time points, one or both OE lines showed significant up- or downregulation of marker genes, but not a clear common expression pattern.

2.3.4. Dark stress (Dark induced leaf senescence)

Dark-induced leaf senescence is often used for brief studies of this process, as it leads to fast and premature leaf senescence. Here, barley plants responded fast to extreme dark application and leaves were senescing after only 6 days. Briefly, seeds of barley WT and both OE lines were sowed in soil and, on the 11th DAS, plants were subjected to dark by covering the primary leaves with aluminum foil, as described before. The photosynthetic efficiency of primary leaves was estimated every two days, in at least three independent biological replicates. The response of plants to dark was rapid and the PSII efficiency was reduced from 0.8 to 0.6-0.5 in the first four days (Fig. 18A). After six days, the F_v/F_m ratio was less than 0.2 in the dark treated leaves of all lines. Same pattern was observed for the Chl content. On the 13th DAS, the Chl content was reduced by 20 % and on the 17th DAS was reduced by 75 % (Fig. 18B). The dark induced leaf senescence of primary leaves was observed on the 17th DAS for all lines.

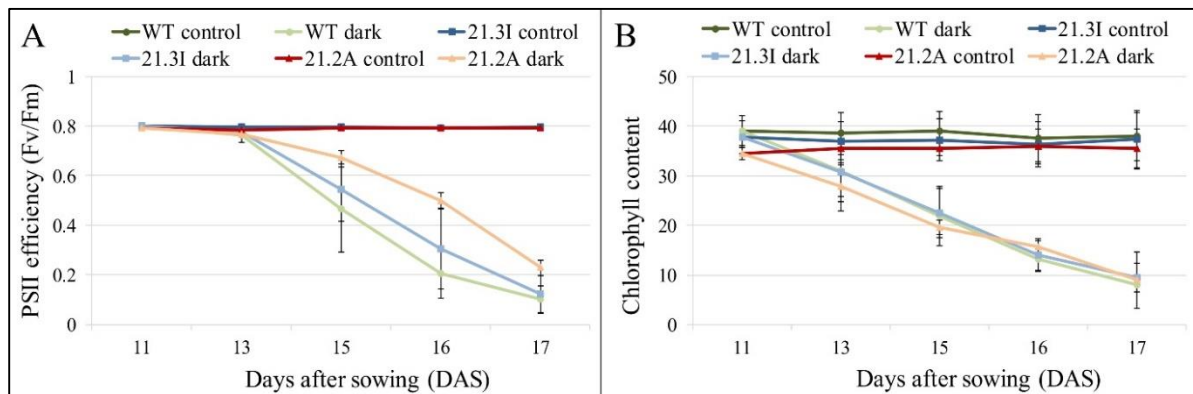


Figure 18: Study of barley *HvFPI* OE lines under dark stress. (A) The photosynthetic activity, expressed as PSII efficiency (F_v/F_m) and (B) The relative Chl content, expressed in SPAD units. All data are mean values of at least three independent biological replicates.

The plant responses to dark were also determined on a molecular level. It is known that *HvS40*, glutamine synthetase (*HvGS2*) and *HvHsp17* genes were regulated during developmental leaf senescence. In fact, *HvS40* and *HvHsp17* were upregulated (Jehanzeb *et al.*, 2017; Orendi *et al.*, 2001), while the plastidic *HvGS2* was downregulated (Avila-Ospina *et al.*, 2015). Here, it was shown that dark induced leaf senescence had the same effect, with *HvS40* being significantly induced in dark treated samples of all lines after 24 h (Fig. 19A). This induction was stronger during the advancement of leaf senescence in all lines. The opposite was observed for *HvGS2*, which was strongly downregulated already after 24 h of dark application, in all lines and remained downregulated in later time points (Fig. 19B). Since *HvGS2* was also downregulated during developmental senescence, a small downregulation of this gene was observed in the control samples of all lines, as well. A transient expression pattern was observed for *HvHsp17*. This gene was highly upregulated in the first 4 days after dark application, while the transcript level was less, but still significantly high on the 16th and 17th DAS (Fig. 19C). Among the three dark stress marker genes, *HvS40* exhibited a significant lower transcript level in both OE lines than in WT dark treated samples

(Fig. 19D). This was in line with previous results for the expression of *HvS40* under drought stress (Fig. 13A and 14A). As for *HvGS2* and *HvHsp17*, no significant difference between WT and OE lines was detected here (Fig. 19E and F).

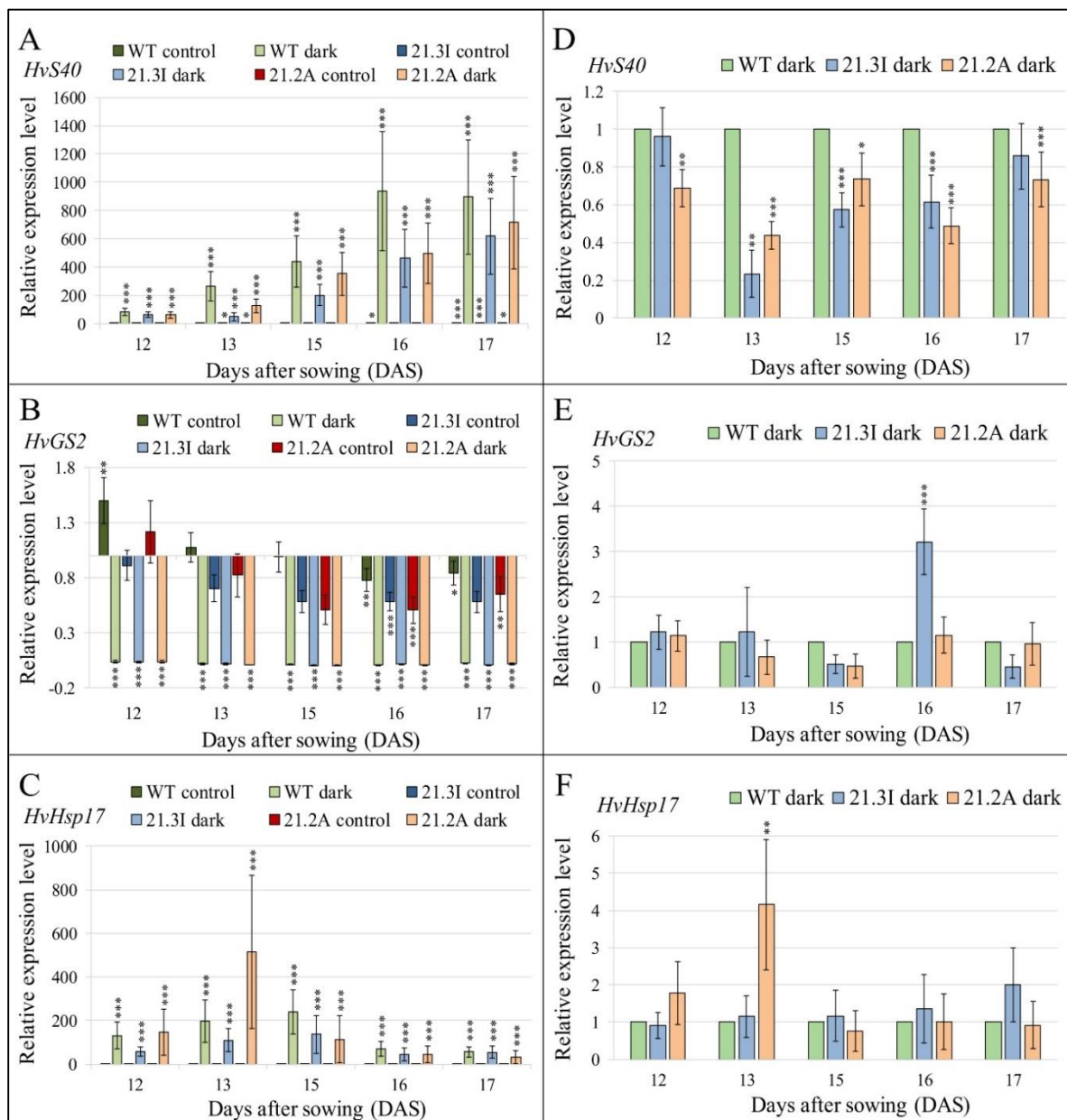


Figure 19: The relative transcript level of dark stress marker genes at different time points after dark application. The relative transcript level of (A) *HvS40*; (B) *HvGS2* and (C) *HvHsp17* at different time points, compared with samples of WT on 11th DAS. The relative transcript level of (D) *HvS40*; (E) *HvGS2* and (F) *HvHsp17* in OE stress samples in comparison to corresponding WT stress samples at each time point. Mean relative expression levels of three independent biological replicates, standard deviations and *p*-values were determined by REST-384 © 2006 (Pfaffl *et al.*, 2002) and normalized against *HvPP2A*, *HvActin* and *HvGCN5*. Statistically significant differences between (A); (B); (C) control and dark samples of WT and both OE lines, at all time points, in comparison to WT samples on 11th DAS, and (D); (E); (F) dark samples of both OE lines in comparison to dark WT samples at each specific time point, are indicated by asterisks: *p* < 0.05 (*), *p* < 0.01 (**), *p* < 0.001 (***)

Taking the above results together, it was clear that there was no phenotypic difference between WT and OE lines under drought, combined cold and high light, salt and dark stress.

The physiological parameters followed the same trend under stress in all lines. On a molecular level, though, the expression of specific stress marker genes was different in OE lines, indicating a role of *HvFP1* in stress-induced reprogramming of gene expression.

2.3.5. Developmental leaf senescence

The effect of *HvFP1* OE on developmental leaf senescence was also determined in the present study. Seeds of barley WT and both OE lines were sowed in soil and grown in greenhouse cabinets, under controlled long-day conditions. The development of plants was monitored until the senescence of the primary leaves in two independent sets of experiments, one for comparison of 21.3I line with WT (Fig. 20A and B) and one for comparison of 21.2A line with WT (Fig. 20C and D). Good markers of development and senescence were the photosynthetic efficiency and the Chl content of leaves. Here, the PSII efficiency, expressed as F_v/F_m ratio and the Chl content of primary leaves were measured every two to four days, in at least three independent biological replicates for both experimental approaches.

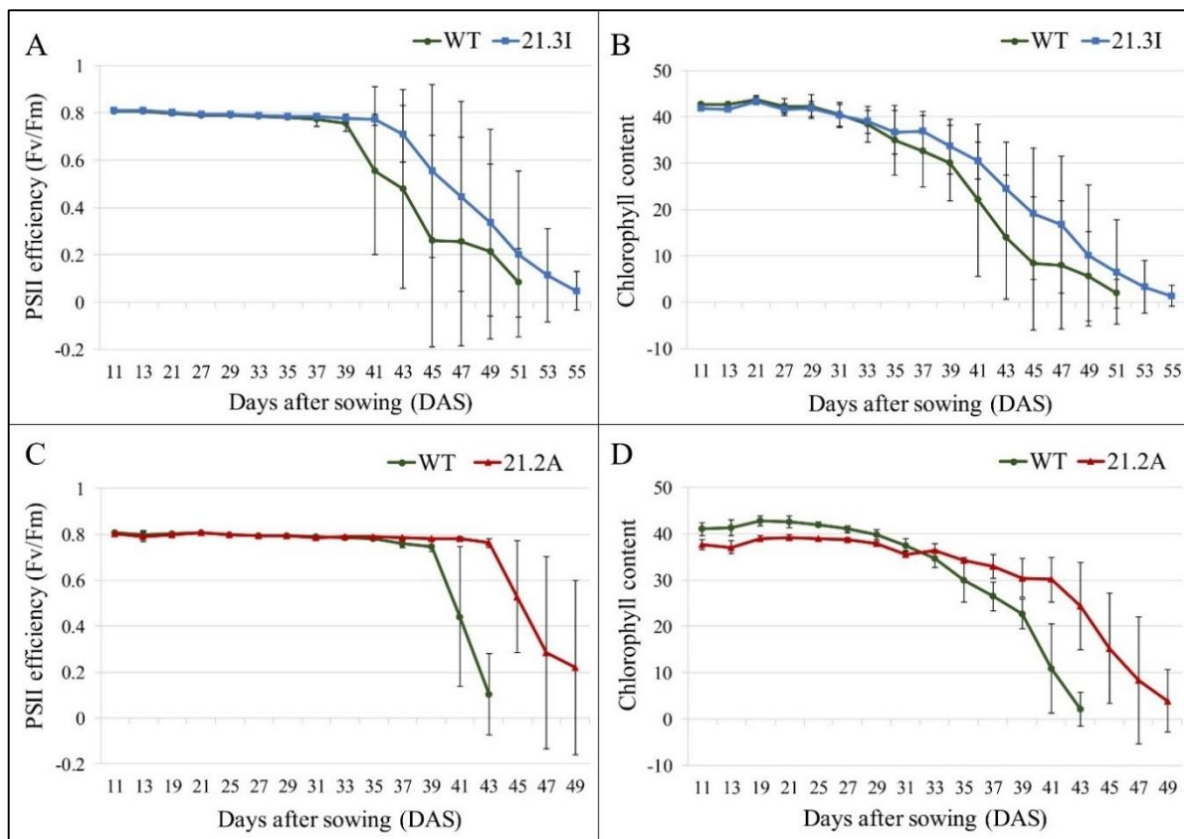


Figure 20: Study of barley *HvFP1* OE lines during developmental leaf senescence. (A) The photosynthetic activity, expressed as PSII efficiency (F_v/F_m) for WT and 21.3I approaches; (B) The relative Chl content, expressed in SPAD units for WT and 21.3I approaches; (C) The photosynthetic activity, expressed as PSII efficiency (F_v/F_m) for WT and 21.2A approaches and (D) The relative Chl content, expressed in SPAD units for WT and 21.2A approaches. All data are mean values of three independent biological replicates.

The PSII efficiency started to decrease on the 39th DAS in WT plants and on the 41st to 43rd DAS in OE lines 21.3I and 21.2A, respectively (Fig. 20A and C). The Chl content reached the maximum value on 21st DAS for all lines and then it started to reduce (Fig. 20B and D). This reduction was faster in WT plants. The results of both OE lines from the

independent experiments clearly showed that senescence of primary leaves was delayed in plants with high levels of *HvFPI* in comparison to WT plants. An example of WT and OE primary leaves during barley development and leaf senescence is presented in Fig. 21. The delay in onset of leaf senescence in OE plants was obvious.

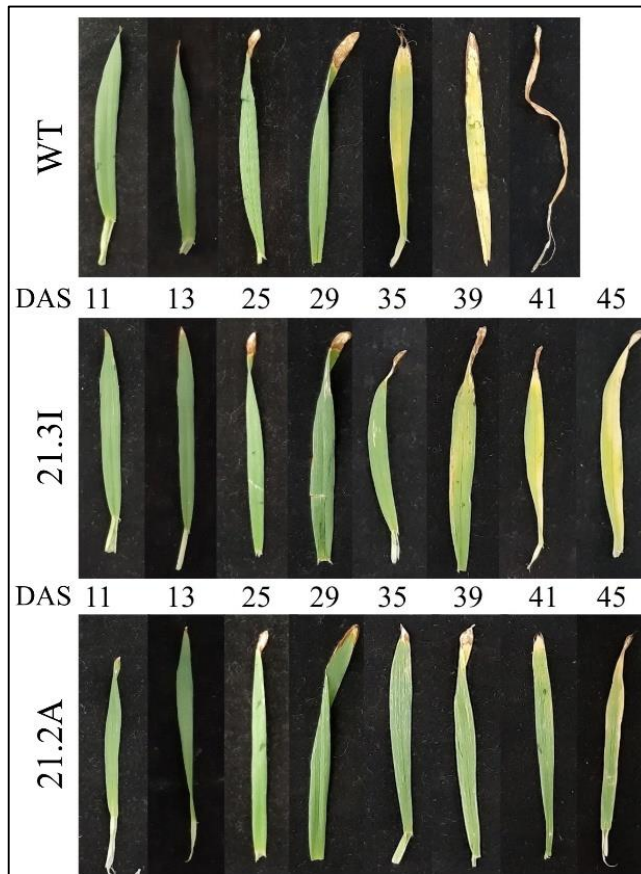


Figure 21: Primary leaves of WT, 21.3I and 21.2A lines during the course of developmental leaf senescence.

The effect of *HvFPI* OE on leaf senescence was observed, not only on the physiological parameters, but also on a molecular level. As described above, *HvS40* is a well-known senescence associated gene (Jehanzeb *et al.*, 2017). It was upregulated in stress-induced and developmental leaf senescence. Additionally, both, *HvSAG39*, which encodes for a cysteine protease and *HvSBT*, which encodes for a subtilisin protease, are well-known senescence associated genes and were both upregulated during developmental leaf senescence (Liu *et al.*, 2010; Roberts *et al.*, 2017). Here, the expression of these three senescence associated genes at different stages of leaf senescence was estimated, for all lines. The developmental stages were defined by the Chl content in primary leaves of WT plants. The maximum Chl content (100 %) was observed approximately on 21st DAS (Fig. 20B

and D) and started to reduce to 95 % and 90 % at the onset of leaf senescence. In the late stage, it was reduced to 80 % and 75 % and at the final stage was less than 50 %. The gene expression was compared with WT samples on 13th DAS, when the primary leaves had reached the maximum length. Then, the expression of *HvS40*, *HvSAG39* and *HvSBT* in OE lines, on the corresponding days, was monitored.

The differential expression of all three genes is presented in Fig. 22. *HvS40*, *HvSAG39* and *HvSBT* were significantly induced when the Chl content dropped to 90% in WT leaves and their expression level clearly increased during the senescence process (Fig. 22A, B and C). In both OE lines, all three senescence marker genes were also induced, but this induction was much lower and delayed when compared to WT. All three genes showed a repressed induction in the two OE lines. This difference was more obvious when samples of 21.3I and 21.2A were compared with the corresponding WT sample at each developmental stage (Fig. 22D, E and F). The relative gene expression in WT samples was set as 1 and all three genes have a relative expression level below 1 in the middle and later stages of leaf senescence in the two OE lines.

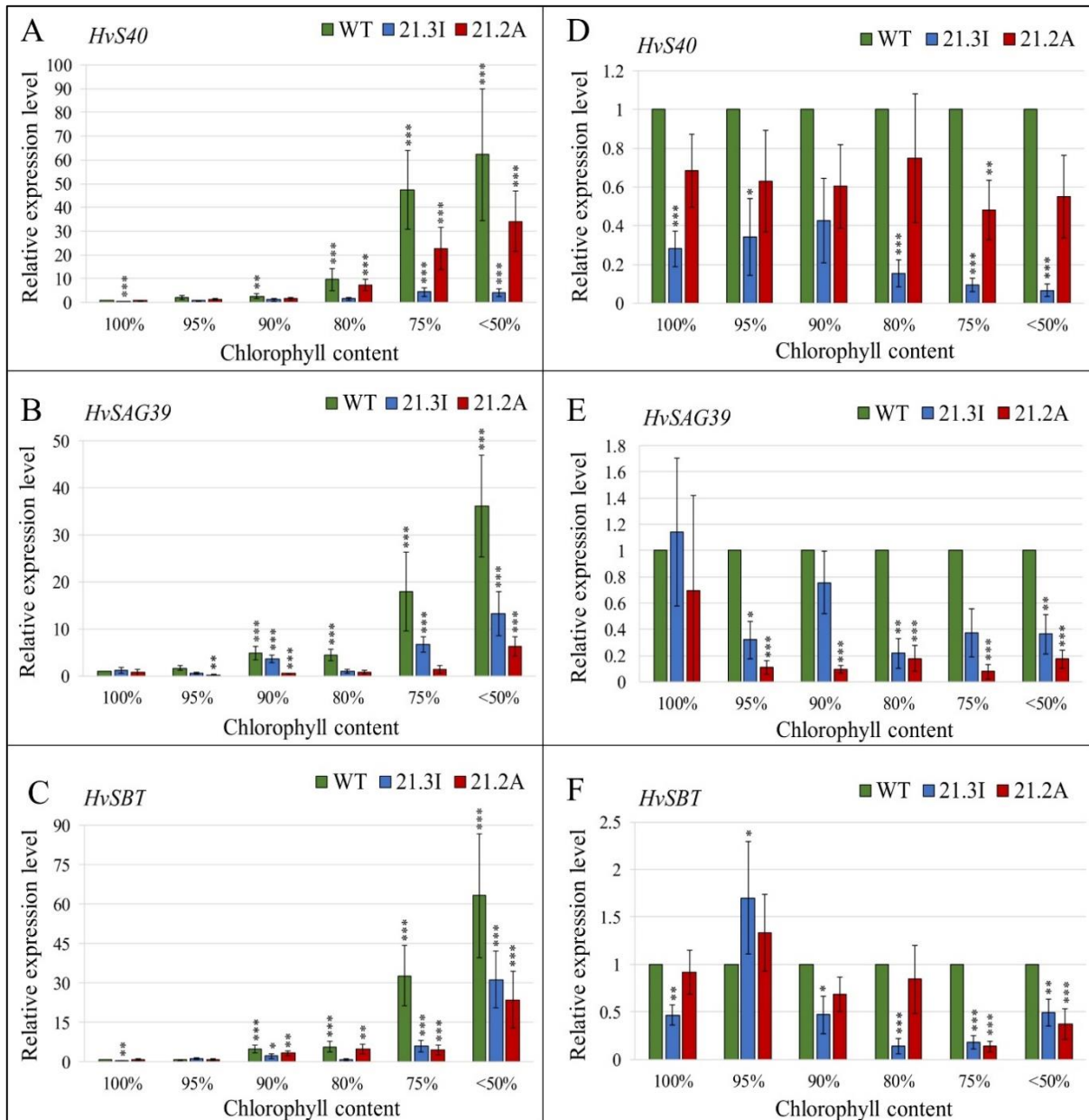


Figure 22: The relative transcript level of senescence marker genes at various developmental stages, as defined by the Chl content of WT primary leaves. The relative transcript level of (A) *HvS40*; (B) *HvSAG39* and (C) *HvSBT*, at each developmental stage of WT samples and corresponding days of 21.3I and 21.2A lines, compared with WT samples on 13th DAS. The relative transcript level of (D) *HvS40*; (E) *HvSAG39* and (F) *HvSBT* in 21.3I and 21.2A lines in comparison to corresponding WT samples at each developmental stage. Mean relative expression levels of three independent biological replicates, standard deviations and p -values were determined by REST-384 © 2006 (Pfaffl *et al.*, 2002) and normalized against *HvPP2A*, *HvActin* and *HvGCN5*. Statistically significant differences between (A); (B); (C) WT samples at various developmental stages and OE samples on the corresponding days in comparison to WT samples on 13th DAS, and (D); (E); (F) OE samples of the corresponding days in comparison to WT samples of each developmental stage are indicated by asterisks $p < 0.05$ (*), $p < 0.01$ (**), $p < 0.001$ (***)).

2.4. Study of WT and *HvFP1* KO barley lines under drought stress and developmental leaf senescence

As described above, the barley HIPP protein *HvFP1* was induced in response to abiotic stress and during leaf senescence. While OE of *HvFP1* affected the course of developmental leaf senescence, it did not result in a clear phenotype under several abiotic stress treatments. However, an altered expression pattern of drought stress and senescence marker genes was observed in *HvFP1* OE lines. In order to investigate whether *loss-of-function* of *HvFP1* counteracts the observed effects of *gain-of-function*, responses of WT and KO mutant 20.1At to drought and leaf senescence were monitored.

2.4.1. Drought stress

An efficient protocol for drought stress was applied on WT and KO lines after the 11th DAS, as described above. The changes in RWC of soil are shown in Fig. 23A. In control pots, the RWC of soil was kept around 65 % during the experiment. After application of drought stress, there was a stable reduction in RWC of soil, which reached 10 % on the 29th DAS in both WT and KO plants. The effect of water deficit on the physiological parameters of barley leaves was measured in terms of PSII efficiency, presented as F_v/F_m ratio, and relative Chl content. Both parameters reflected the stress-induced onset of senescence. The PSII efficiency started to decrease after 23rd DAS with a small, but not significant, delay in KO mutant (Fig. 23B). The relative Chl content started to decrease on the 17th DAS in drought stressed samples of both lines (Fig. 23C). The progress of drought-induced leaf senescence is presented in Fig. 23D. The yellow color of stressed plants appeared between the 21st to 23rd DAS, when the RWC of soil was 20% or less.

The above results implied a similar physiological response of WT and *HvFP1* KO plants to drought stress. Besides the phenotypic study, the possible effect of *HvFP1 loss-of-function* on the expression of drought stress marker genes was investigated. For that, samples of primary leaves were collected from control and stressed plants from both, WT and KO lines, at the same time points and the transcript levels of *HvS40*, *HvNCED*, *HvDhn1* and *HvHsp17* were estimated via qRT-PCR. All four genes were significantly induced on about 8 days after the last irrigation of plants and were highly expressed during the whole experiment in all drought samples (Fig. 24). There was no difference in the expression of those genes between the WT and KO lines. This was more obvious when their transcript level in drought samples of KO line was compared with the respective WT samples at each time point (Fig. 24E, F, G and H). Only the relative expression level of *HvNCED* seemed to differentiate in KO primary leaves. More specifically, on 23rd and 25th DAS, there was a significant lower amount of *HvNCED* in KO samples, while the opposite pattern was observed on 27th DAS (Fig. 24F). For the other three drought stress marker genes, no significant difference was noted. It seemed that in contrast to OE lines of *HvFP1* (Fig. 13 and 14), KO line 20.1At did not exhibit an altered expression of drought stress marker genes.

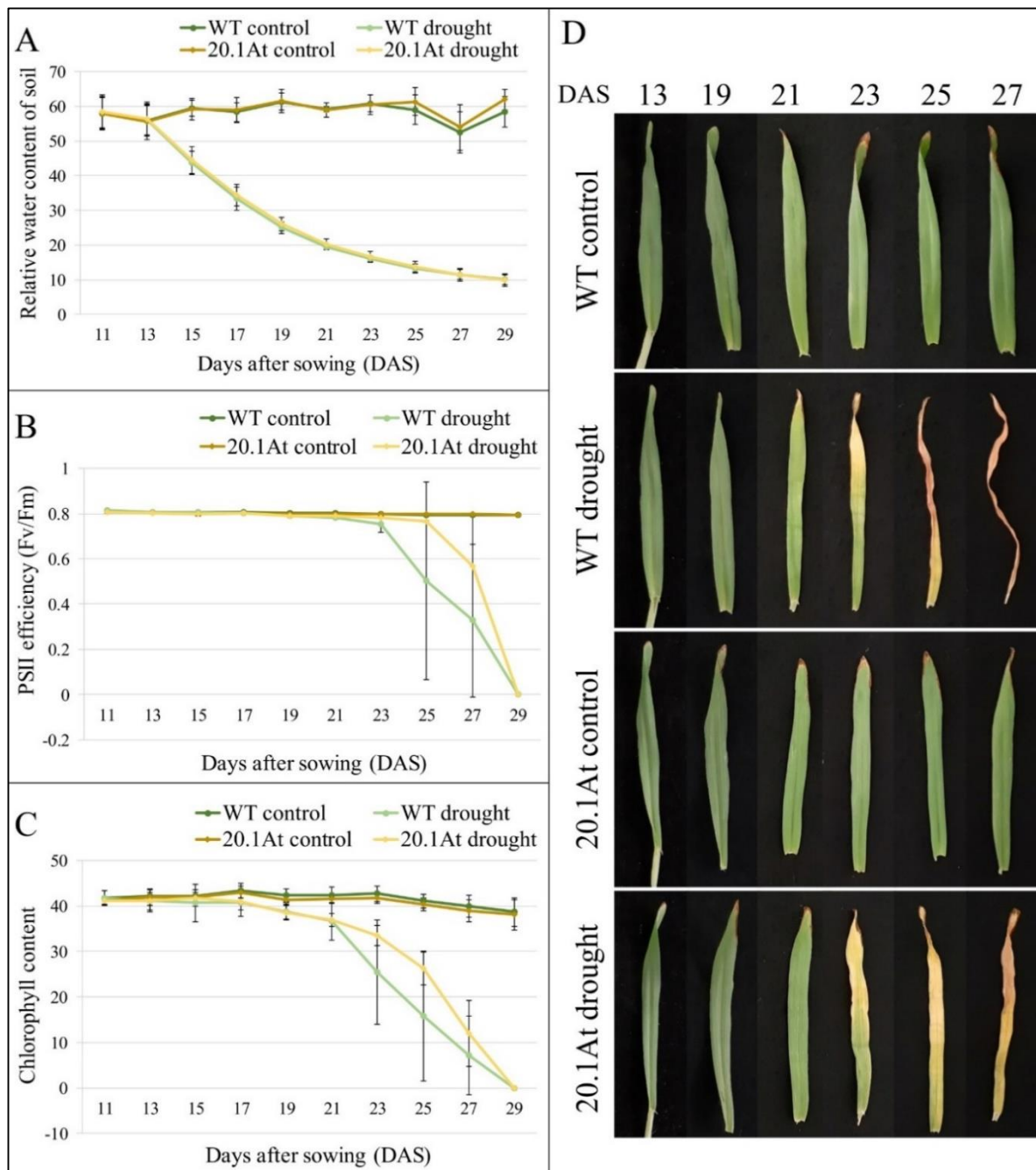


Figure 23: Study of barley *HvFPI* KO line under drought stress. (A) The relative water content of soil during the drought stress approaches. It was set at 65 % at the beginning of the experiment; (B) The photosynthetic activity of primary leaves, expressed as PSII efficiency (F_v/F_m); (C) The relative Chl content of primary leaves, expressed in SPAD units and (D) The progress of drought induced leaf senescence in primary leaves of WT and 20.1At lines. All data are mean values of three independent biological replicates.

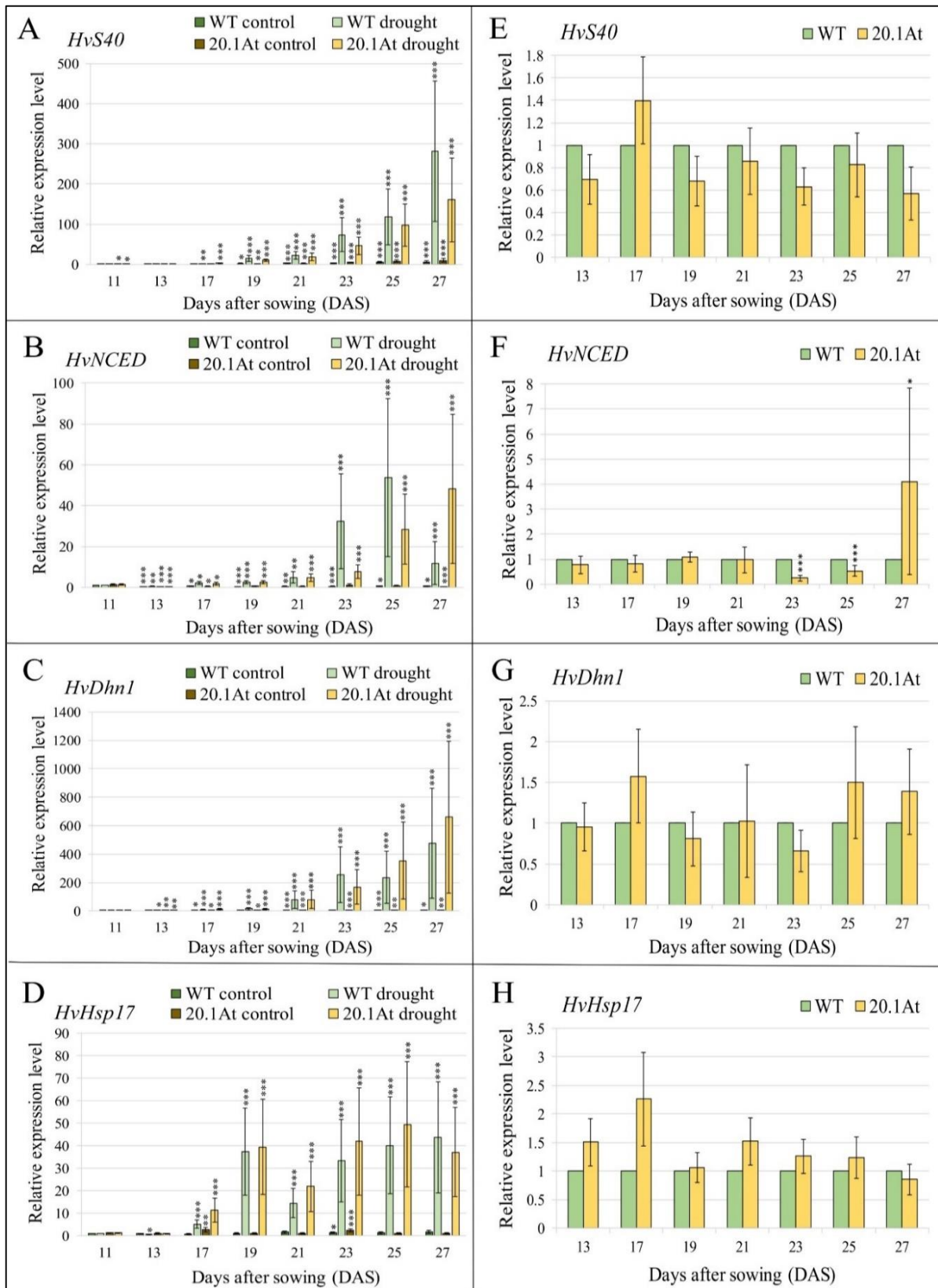


Figure 24: The relative transcript level of drought stress marker genes in WT and *HvFPI* KO lines at different time points. The relative transcript level of (A) *HvS40*; (B) *HvNCED*; (C) *HvDhn1* and (D) *HvHsp17* compared with samples of WT on the 11th DAS. The relative transcript level of (E) *HvS40*; (F) *HvNCED*; (G) *HvDhn1* and (H) *HvHsp17* in drought samples of 20.1At line in comparison to WT drought sample at each time point. Mean relative expression levels of three independent biological replicates, standard deviations and *p*-values were determined by REST-384 © 2006 (Pfaffl *et al.*, 2002) and normalized against *HvPP2A*, *HvActin* and *HvGCN5*. Statistically significant differences between (A); (B); (C); (D) samples of WT and KO lines, in control and drought treatments, at various time points in comparison to WT samples on the 11th DAS, and (E); (F); (G); (H) drought samples of KO line in comparison with drought samples of WT on each time point, are indicated by asterisks *p* < 0.05 (*), *p* < 0.01 (**), *p* < 0.001 (***)

2.4.2. Developmental leaf senescence

The primary leaves of barley were used for monitoring the developmental leaf senescence in WT and KO line 20.1At. According to the above results, OE of *HvFPI* had a beneficial effect and delayed developmental leaf senescence. The expected observation for *HvFPI* KO line was the opposite effect, i.e., early senescence of barley primary leaves. Interestingly, this was not the case. The senescence of primary leaves, monitored as a decrease in PSII efficiency, started on the 35th DAS in WT plants and between 37th and 39th DAS in KO line (Fig. 25A). The content of Chl also changed drastically during leaf development. The maximum Chl content was observed between the 21st and 23rd DAS (Fig. 25B). Then, it was reduced gradually as the senescence process was evolved. Both lines had the same Chl content

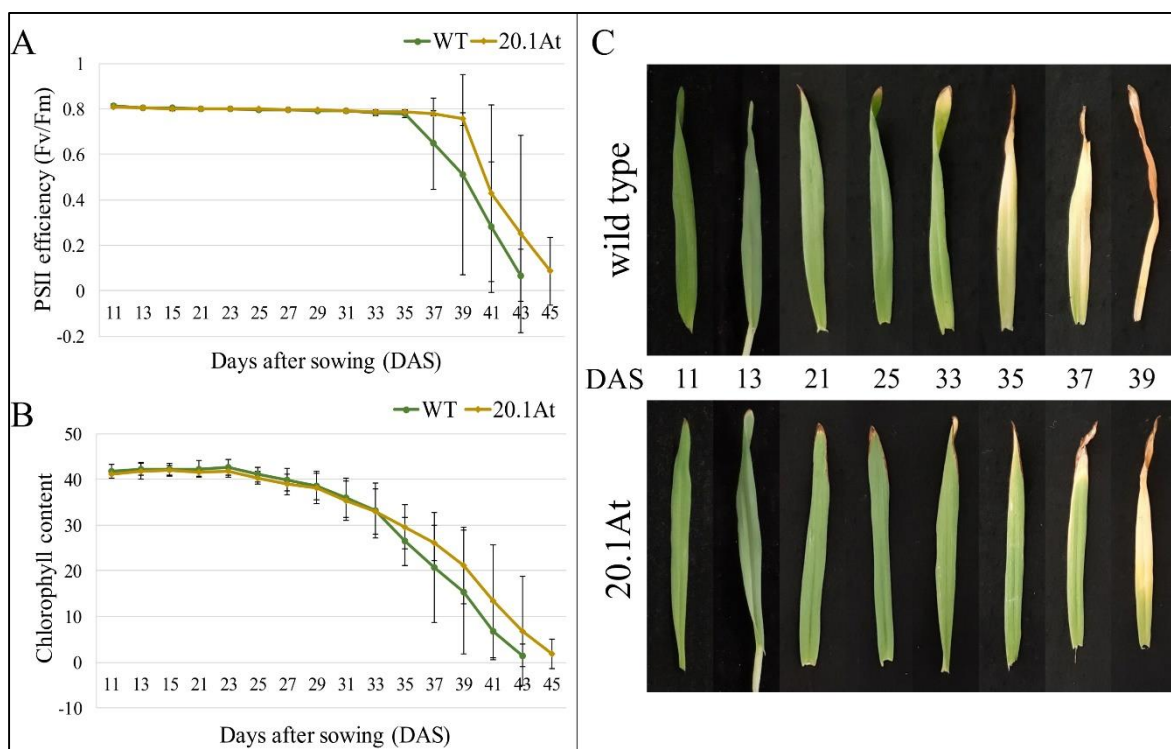


Figure 25: Study of barley *HvFPI* KO line during developmental leaf senescence. (A) The photosynthetic activity of primary leaves, expressed as PSII efficiency (Fv/Fm); (B) The relative Chl content of primary leaves, expressed in SPAD units and (C) Primary leaves of WT and 20.1At lines during the course of developmental leaf senescence. All data are mean values of three independent biological replicates.

until the 33rd DAS. The WT samples exhibited a slightly faster Chl degradation and the developmental leaf senescence was observed two days faster than the 20.1At plants. However, this difference was not observed in all three biological replicates. An example of the progress of leaf senescence is presented in Fig. 25C, where primary leaves started to turn yellow on the 35th DAS and senescence occurred on the 39th DAS. Overall, in contrast to what was expected, *loss-of-function* of *HvFPI* did not accelerate the senescence of primary leaves, but rather delayed leaf senescence, as observed in OE lines, although this result was not significant.

The effect of *HvFPI* KO on the expression of well-known senescence marker genes was also investigated. As described before, the gene expression was studied at defined developmental stages, according to the Chl content in WT primary leaves and compared with WT samples on the 13th DAS. Then, samples of the corresponding days of 20.1At primary leaves were used for a comparative study. The expression of *HvS40* was significantly induced at the early stage of leaf senescence, where the Chl content was reduced to 95-90 % (Fig. 26A). In the middle and late stages, this induction was even stronger in both WT and KO lines. Same pattern was observed for the cysteine protease *HvSAG39* and subtilisin protease *HvSBT*. The *HvSAG39* gene was induced when the Chl content was at 95 %, similarly as *HvS40* (Fig. 26B). The advancement of leaf senescence led to an upregulation of this gene, which was induced 100 times more at the final stage of leaf senescence, in both WT and 20.1At lines. Finally, the subtilisin protease *HvSBT* was induced in the middle stage of leaf senescence, when the Chl content was at 80 % (Fig. 26C). The induction was higher in the WT samples at the stage of 75 %, but appeared similar at the final stage in both lines. The transcript level of all three genes in KO line was compared with that of WT at each developmental stage in order to detect any significant changes between those lines (Fig. 26D, E and F). Overall, both lines exhibited similar expression of senescence marker genes and regulation in the process of leaf senescence in a physiological and molecular level.

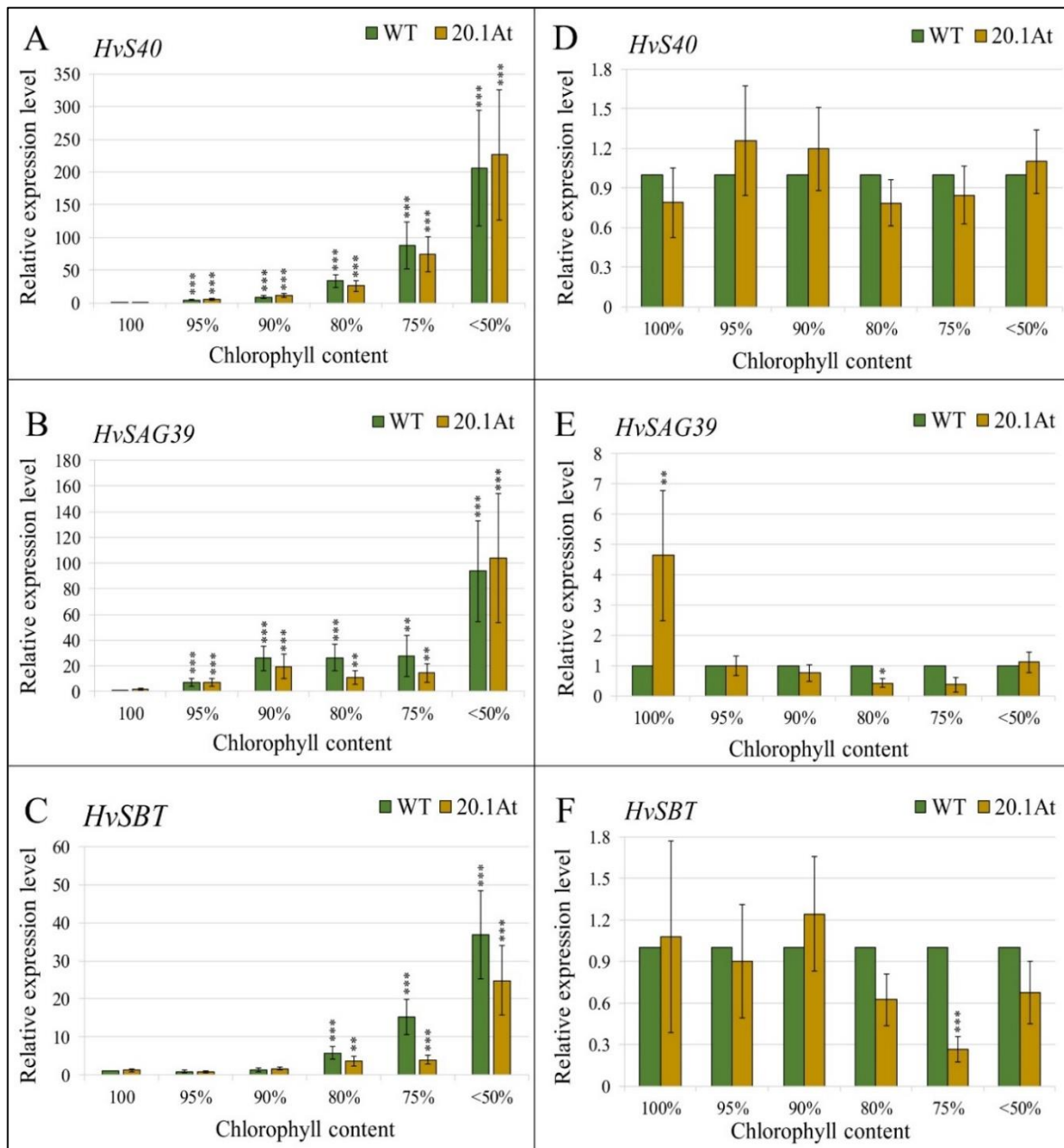


Figure 26: The relative transcript level of senescence marker genes at various developmental stages, as defined by the Chl content of WT primary leaves. The relative transcript level of (A) *HvS40*; (B) *HvSAG39* and (C) *HvSBT* at each developmental stage of WT samples and corresponding days of 20.1At line, compared with WT samples on 13th DAS. The relative transcript level of (D) *HvS40*; (E) *HvSAG39* and (F) *HvSBT* in 20.1At line in comparison to corresponding WT samples at each developmental stage. Mean relative expression levels of three independent biological replicates, standard deviations and p -values were determined by REST-384 © 2006 (Pfaffl *et al.*, 2002) and normalized against *HvPP2A*, *HvActin* and *HvGCN5*. Statistically significant differences between (A); (B); (C) WT samples at various developmental stages and KO line on the corresponding days in comparison to WT samples on the 13th DAS, and (D); (E); (F) KO samples of the corresponding days in comparison to WT samples of each developmental stage are indicated by asterisks $p < 0.05$ (*), $p < 0.01$ (**), $p < 0.001$ (***)).

2.5. RNA Seq analysis

Transgenic barley plants, which overexpress *HvFPI*, showed a delay in developmental leaf senescence and a delay in expression of some senescence and stress associated marker genes (Fig. 13A, B and C; 14A, B and C; 20; 21 and 22). In order to identify genes affected by *HvFPI* OE on a global scale, an RNA Seq analysis of WT and OE samples of primary leaves in mature (further on mentioned as control samples wt-C, oe-C) and senescing (wt-S, oe-S) state was performed, in three independent biological replicates. The control samples corresponded to barley mature primary leaves, on the 21st DAS, when the Chl content was at the highest value (100 % - Fig. 20B). The second time point corresponded to senescing (S) barley primary leaves, with 70-78 % Chl content, in comparison to 21st DAS. These time points corresponded to 41st - 44th DAS in the three independent biological replicates. Total RNA was extracted from the selected samples. A quality control of the samples was performed with a Bioanalyzer 2100 (Agilent Technologies). One example of the electropherogram profile, as originated from the Bioanalyzer for the ladder and two RNA samples is provided in Fig. 44 in appx. 6.2.1. High quality samples were sent to Novogene Co., Ltd (United Kingdom) for sequencing and bioinformatic analysis.

Following the library preparation and sequencing, the quality control showed a 93.92-95.93 % of clean and high-quality reads (Table 2 in appx. 6.2.2). Then, the raw data were aligned with the reference genome *H. vulgare* L. cv. Morex v2 (Mascher 2019), by using the HISAT2 software (D. Kim *et al.*, 2015; Kim *et al.*, 2019). The number of total reads was between 45,085,782 to 66,197,098 in all 12 samples, with 92.41 % to 95.95 % total mapping rate (Table 3 in appx. 6.2.2). Of that, 89.74 % to 93.83 % corresponded to unique mapping. In addition, the mapped reads were classified as exonic, intronic or intergenic. The exonic regions were the most abundant, reflecting 81.26 % to 94.5 % of mapped reads (Table 3 in appx. 6.2.2). The intronic regions were derived due to the presence of pre-mRNA or intron-retention from alternative splicing and covered 0.67 % to 4.80 %. Finally, intergenic regions constituted 0.71 % to 16.65 % of total mapped reads (Table 3 in appx 6.2.2).

Among the various possibilities of the RNA Seq analysis, the present work focused on the differential gene expression analysis, which was estimated by the abundance of transcripts that mapped to genome or exon. Here, the FPKM (Fragments Per Kilobase of transcript sequence per Millions base pairs sequenced) value was calculated for the estimation of gene expression, as described in “Materials and Methods”. In the present work, there were samples from three independent biological replicates. Due to that, a correlation analysis was necessary for the verification of the reliability and sample selection, in order to ensure the repeatability of the experiment and estimate the differential gene expression analysis. In the case of a Pearson correlation coefficient (R^2) close to 1, a higher similarity among the samples was implied. Here, the values for the three wt_C samples ranged between 0.824 to 0.907 and for wt_S from 0.760 to 0.840 (Fig. 27). As for the OE line, the three oe_C samples had an R^2 between 0.886 and 0.951 and oe_S between 0.776 and 0.855. The R^2 values were above the recommended range for all control leaves and slightly lower for the senescing samples. Even lower values were observed among samples with different genetic background, i.e. WT or OE line, and developmental stage, i.e. control or senescing state.

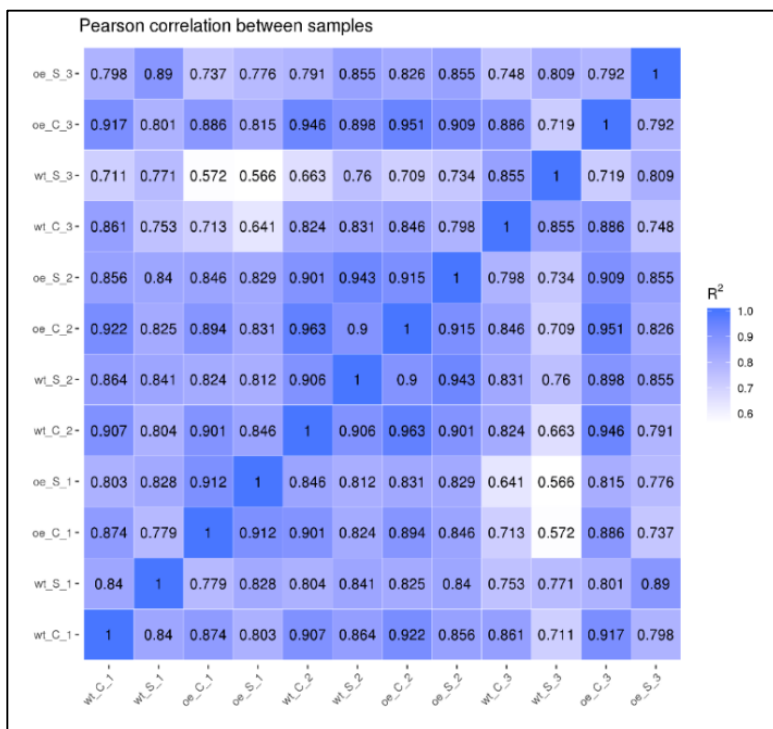


Figure 27: Correlation coefficient matrix among different treatments, lines and biological replicates. R^2 : Square of Pearson correlation coefficient (R).

After the correlation analysis, the differentially expressed genes (DEG) in three biological replicates were estimated by using the DESeq2 R package (Anders & Huber, 2010), with adjusted p -values according to Benjamini and Hochberg's approach for controlling the false discovery rate. The resulting lists contained the DEGs after the comparison of the following samples: wt_C vs wt_S, oe_C vs oe_S, oe_C vs wt_C and oe_S vs wt_S. By analyzing the RNA Seq results, it was possible to compare C with S samples of two lines, in order to have a list of DEGs in senescing samples, also known as SAGs and SDGs. Furthermore, a comparison between OE and WT samples of control and senescing state resulted in genes that may be regulated downstream of HvFP1.

2.5.1. Senescence Associated Genes of *Hordeum vulgare*

A first group of analyses involved the comparison of wt-S with wt-C samples and oe-S with oe-C. The DEGs during the senescence process are known as SAGs and SDGs. The results included the significantly DEGs in the three independent replicates, with adjusted p -value < 0.05 and $\log_2\text{FoldChange} > 2$ ($\log_2\text{FC} > 2$). The comparison between wt-S with wt-C samples resulted in total 671 DEGs. Of them, 439 genes were upregulated and 232 genes were downregulated (Fig. 28A). On the other hand, the comparison of the respective OE samples resulted in only 445 DEGs. Total 269 genes were upregulated and 176 genes were downregulated (Fig. 28B). The obviously reduced number of SAGs in OE line correlates with the observed delay in developmental leaf senescence. In addition, the overlap between the up- and downregulated genes of both lines was examined. In the senescence state, total 184 genes were upregulated and 92 genes were downregulated in both lines (Fig. 29). However, 255 genes were upregulated and 140 genes were downregulated only in WT senescing samples, while 85 genes were upregulated and 84 genes were downregulated only in OE senescing samples. Focusing on DEGs only in WT line, an extensive set of SAGs and SDGs

could be obtained for barley plants for the first time, specifically for the version 2 of genome annotation (Mascher 2019).

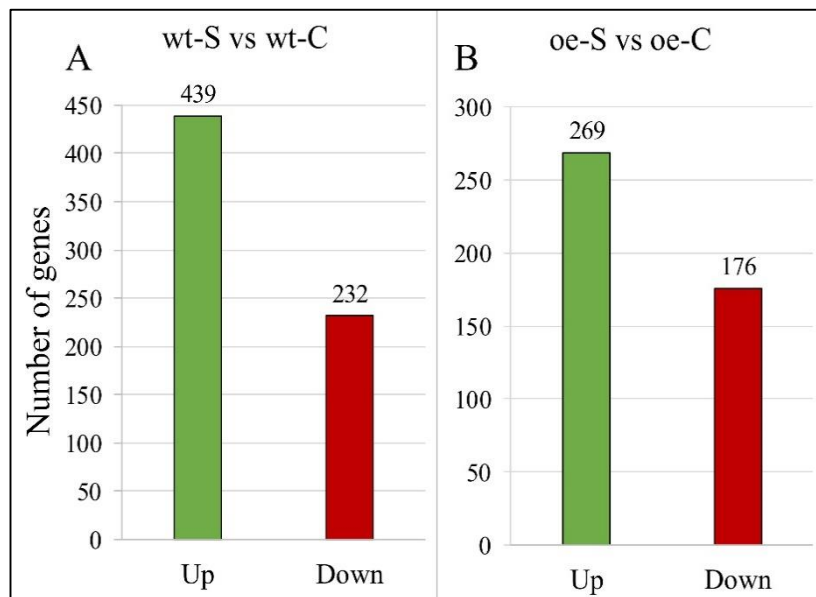


Figure 28: Total number of differentially expressed genes in WT and *HvFPI* OE lines, in (A) wt-S vs wt-C and (B) oe-S vs oe-C analysis from three independent biological replicates. Upregulated genes are presented in green and downregulated genes are presented in red.

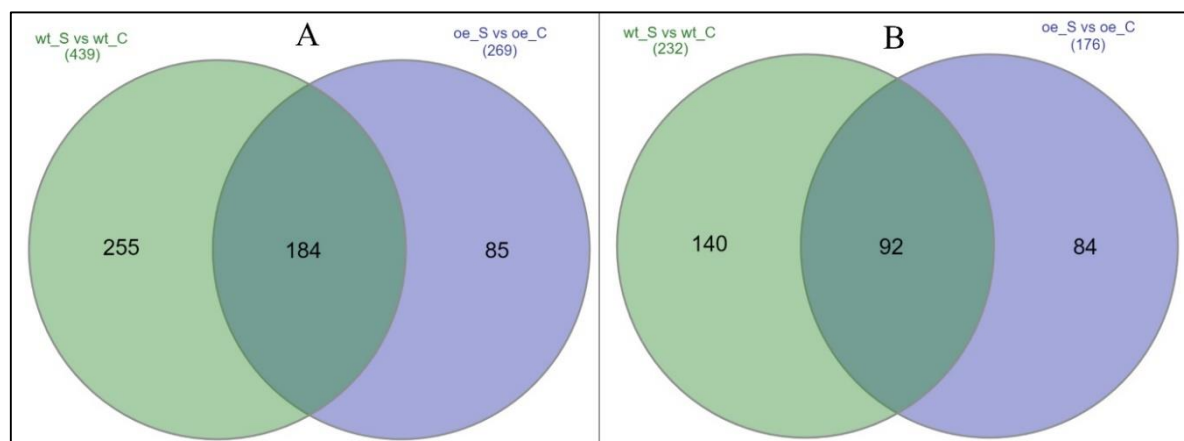


Figure 29: Venn diagrams of (A) senescence upregulated (associated) genes and (B) senescence downregulated genes in WT and/or OE line.

Starting with the 439 upregulated and 232 downregulated genes in wt-S, the differential gene regulation during developmental leaf senescence in barley WT plants could be monitored. The complete lists with SAGs and SDGs are provided in supplementary data (Tables 4 and 5 in appx. 6.2.3). The functional groups, as derived from the manual sorting of the upregulated genes, are presented in the graph of Fig. 30A. The main representative genes for each functional group are shown in the graph of Fig. 31 and discussed in more details later. A comparison of barley SAGs with the established Leaf Senescence Database 3.0 (LSD; Li *et al.*, 2020) showed that during leaf senescence in barley, similar classes of genes were differentially regulated as in *A. thaliana*. The biggest group, clearly upregulated after the onset of senescence was functionally annotated as regulatory genes, including TFs and transcriptional regulators (59 genes in barley of total 505 genes annotated in this class in *Arabidopsis*; 59|505), genes related to phytohormones (15|129), signaling cascades (42|349) and epigenetic regulators (methyltransferases, cell and chromosome organization, DNA

replication and transcription, translational and posttranslational modifications - total 49|184). This high number of total 165 DEGs reflected the massive reprogramming of gene expression during leaf senescence. In addition, genes involved in recycling of resources during senescence were also upregulated, including carbon metabolism and cell wall organization (37|108), photosynthetic apparatus degradation (7|39), amino acid and protein metabolism (29|112), lipid metabolism (13|65), nucleic acid metabolism (13|24) and transporters (39|178). Strikingly, also 29|87 genes belong to the group of stress-related genes, 55|256 genes regulate the redox state and 7|25 genes regulate plant development.

Working in a similar way, the barley SDGs were classified according to their functional classes, as presented in the graph of Fig. 30B, while the main representative genes for each functional group were shown in the graph of Fig. 32. Again, specific regulatory genes including TFs and transcriptional regulators (14|505), genes involved in phytohormone regulation (11|129), signaling cascades (11|349 and epigenetic regulators (17|184) were found. Then, some genes of carbon metabolism and cell wall organization (22|108), protein and amino acid metabolism (22|112), lipid metabolism (11|65) and nucleic acid metabolism (4|24) were also downregulated in leaf senescence, together with specific transporters (27|178), genes of redox regulation (39|256), genes involved in stress (13|87) and development (5|25). As for genes encoding for structural components of the photosynthetic apparatus (23|39), e.g., Chl *a/b* binding proteins, they were downregulated here, reflecting the degradation of photosynthetic machinery during leaf senescence.

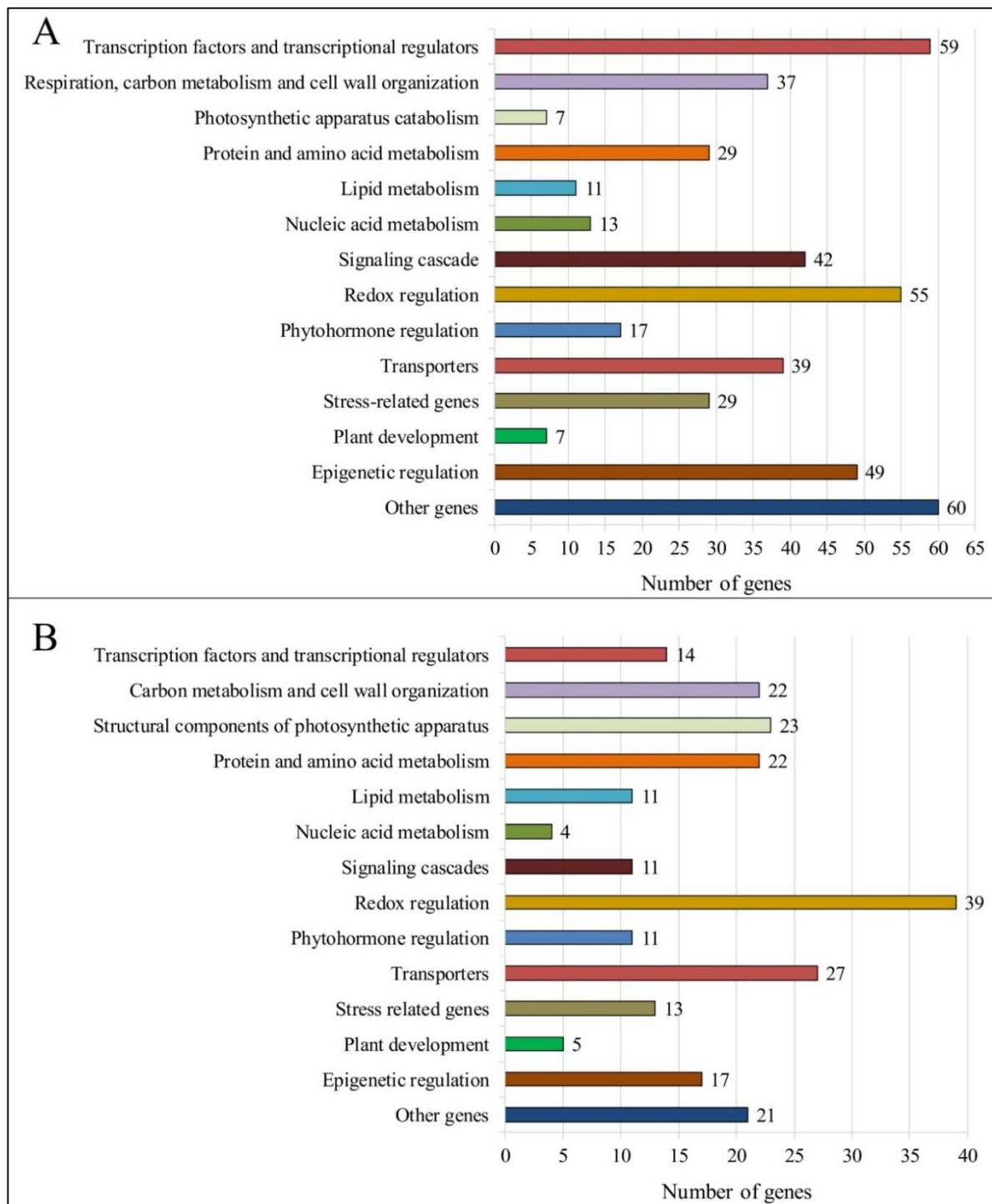


Figure 30: The major groups of functional annotation and the number of genes in each group for (A) Senescence Upregulated (Associated) Genes and (B) Senescence Downregulated Genes.

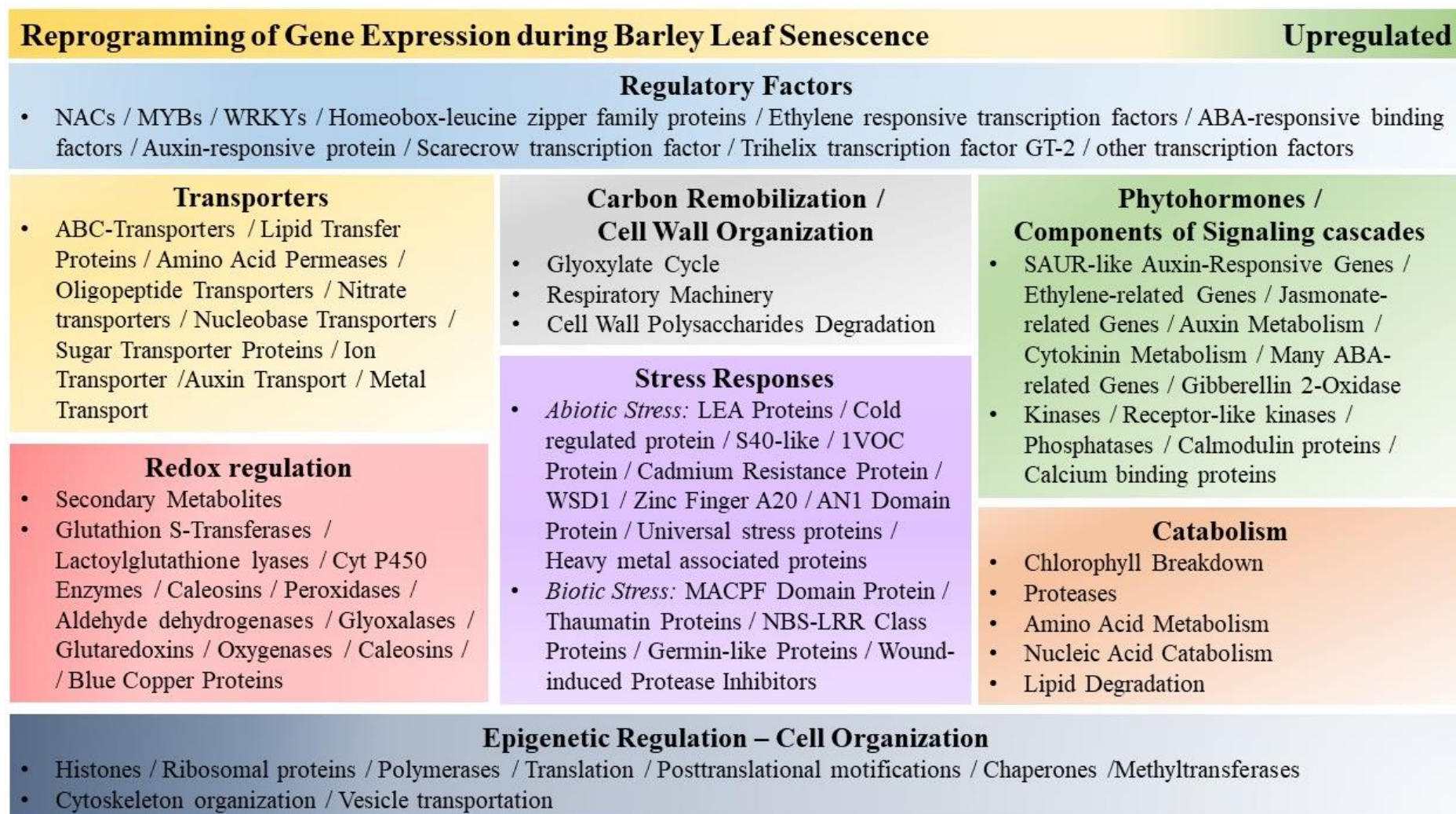


Figure 31: A summary of functional groups and representative genes, which were upregulated during the reprogramming of gene expression in response to developmental leaf senescence in barley.

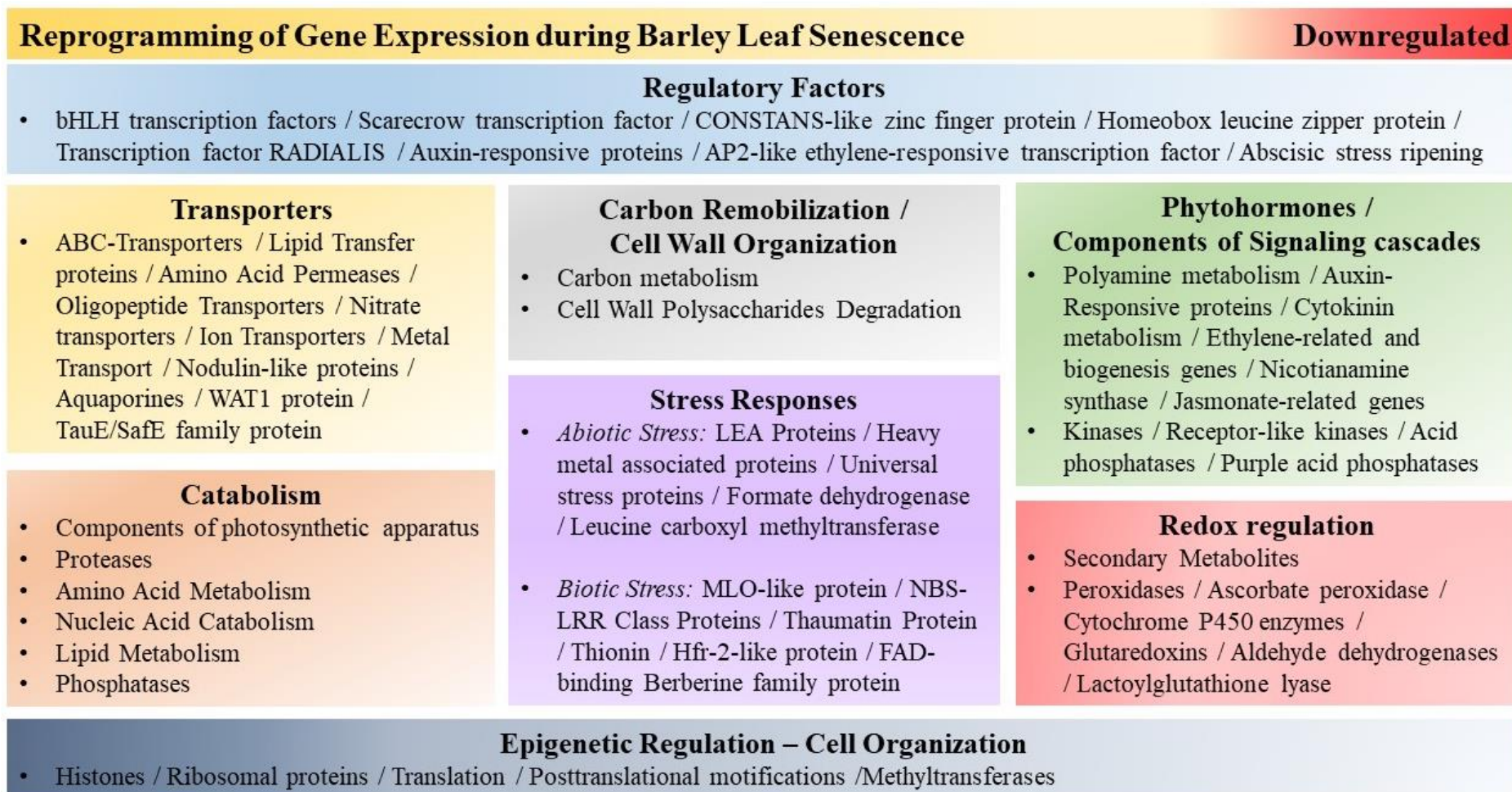


Figure 32: A summary of functional groups and representative genes, which were downregulated during the reprogramming of gene expression in response to developmental leaf senescence in barley.

2.5.2. Genes possibly regulated downstream of HvFP1

A second group of analyses involved the comparison of oe-C with wt-C and oe-S with wt-S samples. This comparison revealed the differential regulation of genes as a response to *HvFP1* OE in control and senescent leaves and enabled the identification of genes acting downstream of *HvFP1* in signaling pathways. With the high stringency applied to identify the DEGs, there were in total only 70 DEGs in oe-C compared to wt-C, with 68 genes being upregulated and only 2 genes downregulated (Fig. 33A). On the other hand, there were 105 DEGs in oe-S compared to wt-S, with only 12 genes being downregulated and 93 genes upregulated (Fig. 33B). It is obvious that the great majority of DEGs in this comparison were induced in response to *HvFP1* OE. This indicated a possible positive function of HvFP1 in transcriptional regulation via downstream signaling cascades.

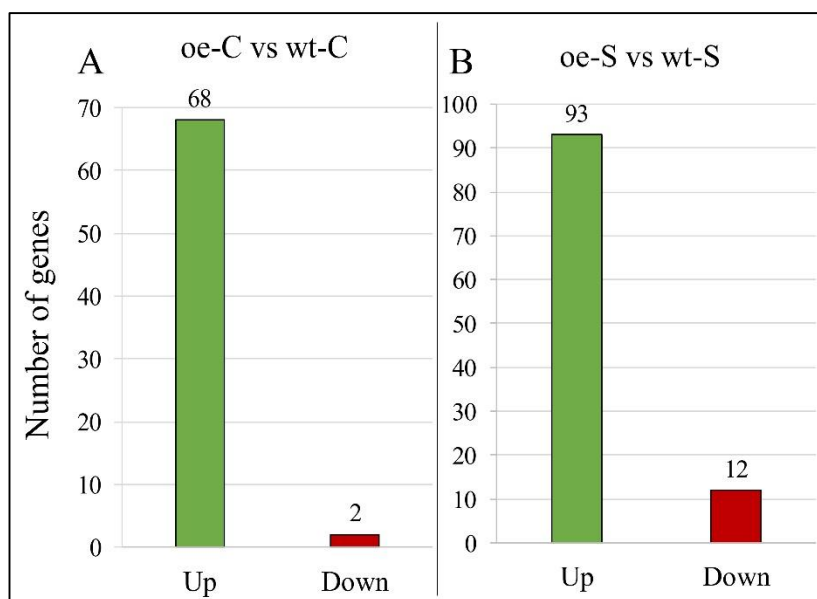


Figure 33: Total number of genes, which were up- or downregulated in (A) oe-C compared with wt-C samples and (B) oe-S compared with wt-S samples. Upregulated genes are presented in green and downregulated genes are presented in red.

In Venn diagram of Fig. 34, the upregulated genes after OE of *HvFP1* in control samples were compared with those in senescent stage. Total 50 genes were found to be differentially expressed due to *gain-of-function* of HvFP1 independently of leaf developmental stage, while 18 genes were upregulated only in control stage and 43 genes only in senescent stage. From the 12 downregulated genes, 2 were found in both control and senescing states and 10 were specifically downregulated in senescent leaves. The RNA Seq analysis resulted in identification of five specific sets of genes, assigned from A to E, which were differentially regulated after OE of *HvFP1* (Table 1). A brief analysis of the function of those genes is given below, while the detailed lists of each set are provided in supplementary data (Tables 6 - 10 in appx. 6.2.4).

Table 1: The five groups, in which the differentially regulated genes of OE line are classified.

Set	Differential Gene Expression	Number of genes
A	Downregulated in control and senescence stage	2
B	Downregulated only in senescence stage	10
C	Upregulated in control and senescence stage	50
D	Upregulated only in control stage	18
E	Upregulated only in senescence stage	43

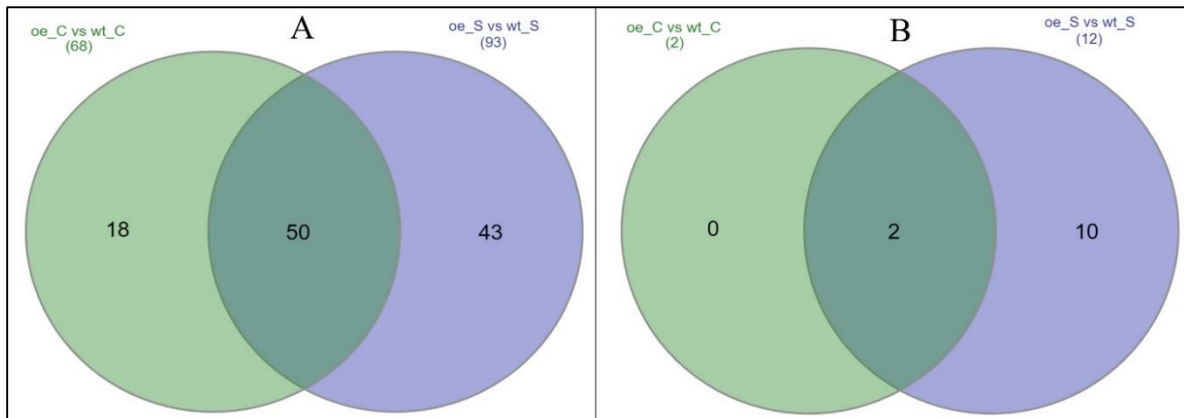


Figure 34: Venn diagrams of: (A) Upregulated genes in oe-C and oe-S samples in comparison to wt-C and wt-S, respectively and (B) Downregulated genes in oe-C and oe-S samples in comparison to wt-C and wt-S, respectively.

Starting with the downregulated groups, only two genes could be identified in control and senescent stage (set A): one F-box family protein and the protein DETOXIFICATION (Table 6 in appx. 6.2.4). Then, there were 10 more genes downregulated only in oe-S samples (set B; Table 7 in appx. 6.2.4). Briefly, these included two genes of RNA polymerase II mediators, two senescence associated genes, the histone H3, an rRNA N-glycosidase, one FGGY family of carbohydrate kinase, the ras-related protein RHN1, the peroxidase 2 and a GA 3-beta-dioxygenase 1.

The groups of upregulated genes included more interesting information. The 50 upregulated genes in both control and senescent stages of *HvFPI* OE leaves (set C) are provided in Table 8 in appx. 6.2.4. Those genes could be further classified according to their function, as shown in graph of Fig. 35. Of them, the TFs and transcriptional regulators were of great interest. Here, the TF Zinc finger CCCH domain-containing protein 12 (*C3H12*), Myb/SANT-like DNA-binding domain protein (*MSANTD*), Auxin response factor 10 (*ARF10*), the Zn²⁺ finger binding transcription regulator FAR1-related sequence 5 (*FRS5*),

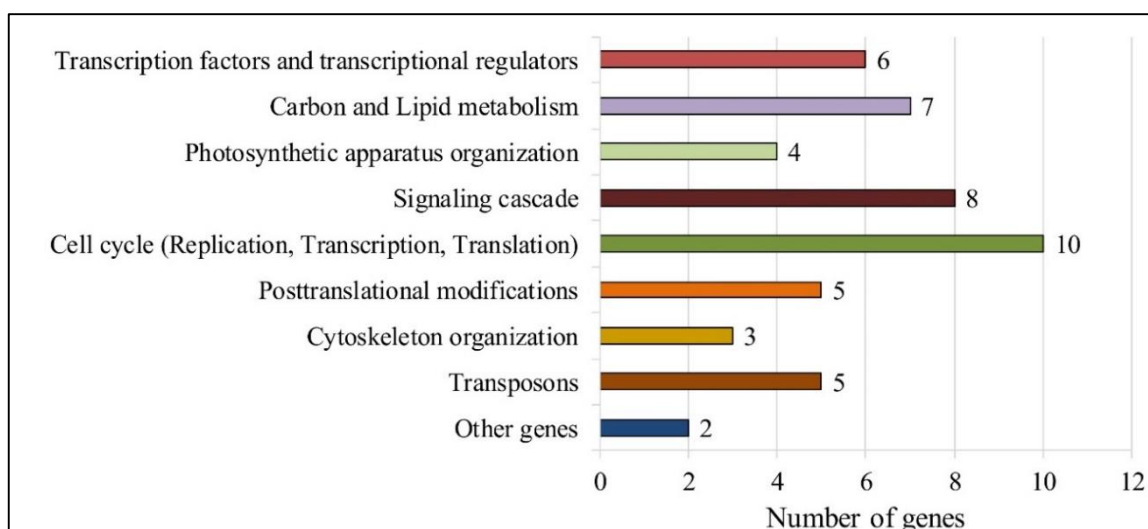


Figure 35: The groups of functional annotation and the number of genes in each group for upregulated genes in *HvFPI* OE line.

the Fibronectin type III domain protein and a CheY-like two-component responsive regulator protein were upregulated in OE samples.

Besides the TFs and regulators, there were additionally 44 genes in the list of upregulated genes in OE samples compared to WT. Many of these genes were involved in cell cycle, specifically in DNA replication, transcription, translation and protein modification, like a 40S ribosomal protein, the beta subunit of proteasome, a DNA ligase, the histone H3, an elongation factor, the subunit B of DNA polymerase alpha, the DEAD-box ATP-dependent RNA helicase, the RNA polymerase Rpb1 and an ATP-dependent DNA helicase MER3 homolog. Then, some genes were involved in protein stability and posttranslational modifications, like a chaperone DnaJ-domain protein, the DNL-type domain-containing protein, the DHHC-type Zn²⁺ finger family protein, a SUMO-activating enzyme and a sentrin-specific protease.

Interestingly, in the same group, genes related to photosynthesis and light response were found, such as a phytochromobilin:ferredoxin oxidoreductase (*PFBS*), a NAD(P)H-quinone oxidoreductase, a tetratricopeptide repeat (TPR)-like protein and the subunit PSI-N of PSI reaction center. Then, there were genes from carbohydrate metabolism, like a callose synthase, a laccase, a phosphoenolpyruvate carboxylase, a glycosyl hydrolase protein, a phospho-N-acetylmuramoyl-pentapeptide-transferase homolog and a 1,4-alpha-D-glucan maltohydrolase.

Members of signaling pathways were also included in the list, such as protein kinases (a wall-associated receptor kinase, a serine/threonine protein kinase, a putative cysteine-rich receptor-like protein kinase), the 1-phosphatidylinositol 4,5-bisphosphate phosphodiesterase epsilon-1, one glutamate receptor, one muscarinic acetylcholine receptor M3, an SH3 domain-binding protein and a regulator of chromosome condensation (RCC1) family with FYVE Zn²⁺ finger domain-containing protein. Another upregulated gene was the acyl-[acyl-carrier-protein] desaturase, which is involved in fatty acid metabolism. There were also many members of transposons, a HAT dimerisation domain-containing protein-like, cytoskeleton organization factors (a dynein assembly factor, a microtubule-associated protein RP/EB, a kinesin heavy chain), a pyridoxal-5'-phosphate-dependent enzyme, a XH/XS domain-containing protein and a binding protein.

The upregulated genes, which were differentially expressed only in oe-C or oe-S, i.e. genes of sets D and E, were of great interest. These genes were upregulated due to *HvFPI* OE, but this upregulation depended on developmental stage of leaf. The specificity of the induction of these genes by *HvFPI* OE could give information about the mode of their action and interaction with *HvFPI* during developmental leaf senescence.

Focusing on the 18 upregulated genes in oe-C (set D; Table 9 in appx. 6.2.4.), there was an induction of two transporters, the subunit alpha-1 of muscle calcium channel and one nitrate transporter NRT. Then, some genes were involved in nucleic acid and protein modification, such as the Werner syndrome-like exonuclease, one La-related protein and members of the ubiquitin catabolic process. Important regulators were also disease resistance genes, like Rp1-like protein and disease resistance protein RPM1, enzymes of flavonoid metabolism, like sterol 3-beta-glucosyltransferase and dihydroflavonol-4-reductase and well-known members of signaling cascades, like a leucine-rich repeat receptor-like protein kinase and a rho GTPase-activating protein. Dynamin-1 is involved in cytoskeleton formation, the

subunit C of NADH-quinone oxidoreductase in photosynthetic electron transport in PSI and an alpha/beta-hydrolase in hydrolation events. Interestingly, another member of the FRS5 transcription regulator family was represented here, as well as another HIPP member, with homology to *AtHIPP27*.

The list of 43 upregulated genes in oe-S samples (set E; Table 10 in appx. 6.2.4.) included TFs and TAs, like two FRS5 representatives, one Zn²⁺ finger C3H- protein, one F-box protein, one ARIA-interacting double AP2 domain protein, one dentin sialophosphoprotein-related protein and SEN1 helicase. Again, genes involved in nucleic acid and protein modification were found, such as a helicase-like protein, DNA topoisomerase 2, one probable staphylococcal-like nuclease CAN3, one tRNA pseudouridine synthase D and one tRNA (guanine-N(7)-)-methyltransferase, then an inter-alpha-trypsin inhibitor heavy chain H3 and a sentrin-specific protease and members of the ubiquitin catabolic process. Many genes were related to cell cycle structure, including a kinesin-like protein KIN-14T, a replication protein A, an animal RPA1 domain protein, one MAR-binding filament-like protein 1-1, two proteins for structural maintenance of chromosomes and the cell division cycle and an apoptosis regulator protein. Representatives of signaling cascades and vesicle formation and transfer were also upregulated. These were three protein kinases (a receptor kinase-like protein, a kinase protein family and a cysteine-rich receptor-like protein kinase), calmodulin 1, an auxilin-like protein and protein GRIP for vesicle formation and transfer. The TPR-like protein and a NAD(P)H-quinone oxidoreductase, the endoglucanase 11 and the ACBD4 were involved in photosynthesis, carbohydrate metabolism and lipid modification, respectively. Other upregulated genes in OE samples during senescence were one MLO-like protein, one tripartite terminase subunit, a modifier of snc1,4 and one disease resistance RPP13-like protein. All those genes were involved in plant defense against biotic stress. Finally, multiple representatives of transposons were completing this list, like transposon protein Pong sub-class, HAT family dimerization domain containing protein, a putative transposon protein (Mutator sub-class), a putative CACTA transposon protein (En/Spm sub-class), a retrovirus-related Pol polyprotein from transposon TNT 1-94 and one transposase.

2.5.2.1. Validation of differential expression of selected candidate genes in two *HvFP1* OE lines

The RNA Seq analysis was performed in control and senescing samples of WT and one OE line 21.3I. The analysis of the DEGs in “OE vs WT” samples resulted in a list of candidate genes, which were potentially regulated downstream of *HvFP1*. In this work, two OE lines have been established. Samples of control and senescing leaves were used to perform qRT-PCR in order to validate the differential expression of selected genes in both OE lines. Here, the relative expression level in all samples was compared to wt-C, which was set as 1.

Total 6 genes were chosen for qRT-PCR validation, including four TFs or TAs and according to the RNA seq results, they were significantly upregulated in both control and senescing samples of line 21.3I. The Zn²⁺ finger *HvC3H12* TF was significantly upregulated in both OE lines 21.3I and 21.2A (Fig. 36A). In fact, the expression was slightly higher in control leaves. Similar pattern was observed for the *HvMSANTD* TF (Fig. 36B). There, the expression was significantly higher in the second OE line 21.2A. Then, one gene with TF activity was the *HvARF10*. This gene was induced at least 50 times more in 21.3I line and

100-150 times more in 21.2A line (Fig. 36C). On the other hand, the *HvFRS5* TA was more than 50 times upregulated in lines 21.3I and between 150-300 times more in line 21.2A (Fig. 36E). Overall, it was clear that all TF or TA genes were significantly induced in both OE lines in comparison to WT samples, confirming the findings of RNA seq analysis.

The other three genes, which were validated via qRT-PCR here, encoded for proteins or enzymes with various cellular functions. *HvACBD4* was significantly induced in oe-S samples of RNA Seq analysis. Here, the relative transcript level was significantly high in both control and senescing samples of 21.3I and 21.2A lines (Fig. 36F). Same procedure was followed for the *HvPFBS*, which was found in similar biosynthetic pathways with *HvFRS* for the biosynthesis of phytochromobilin. The latter was the necessary chromophore for the activation of phytochromes. Both OE lines showed a strong upregulation of this gene, which was at least 100 times more than the wt-C samples (Fig. 36D). The expression was similar in C and S samples of both OE lines.

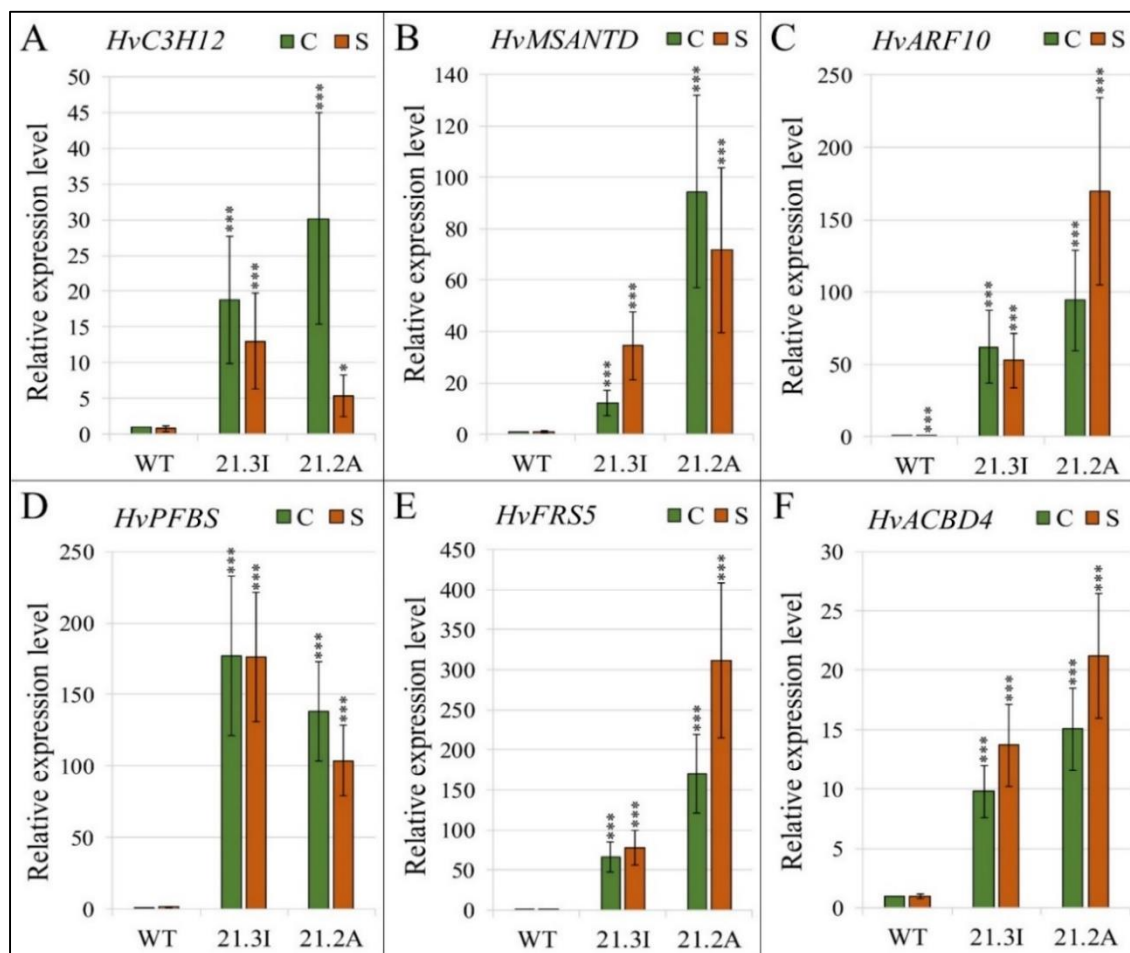


Figure 36: The relative transcript level of selected genes for RNA Seq validation. (A) Zn²⁺ finger CCCH domain containing protein 12 (*HvC3H12*); (B) Myb/SANT-like DNA binding domain (*HvMSANTD*); (C) Auxin Response Factor 10 (*HvARF10*); (D) PFB synthase (*HvPFBS*); (E) FAR1-Related Sequence 5 (*HvFRS5*) and (F) Acyl-coA binding domain 4 (*HvACBD4*) in WT, 21.3I and 21.2A lines, at control (C) and senescing (S) leaves. Mean relative expression levels of three independent biological replicates, standard deviations and *p*-values were determined by REST-384 © 2006 (Pfaffl *et al.*, 2002) and normalized against *HvPP2A*, *HvActin* and *HvGCN5*. Statistically significant differences between C samples of OE lines and S samples of WT and OE lines in comparison to WT C samples are indicated by asterisks *p* < 0.05 (*), *p* < 0.001 (***)

3. Discussion

The *Hordeum vulgare* Farnesylated protein 1 (HvFP1) belongs to the family of Heavy metal associated Isoprenylated Plant Proteins (HIPPs). This protein family was recently discovered in vascular plants and its members are characterized by two domains: at least one Heavy Metal Associated (HMA) domain and one C-terminal isoprenylation motif (Dykema *et al.*, 1999; Barth *et al.*, 2009). Most HIPPs have nuclear localization signals, which indicate a localization and function of those proteins in the nucleus. Indeed, a number of HIPP members, including HvFP1, are known to be localized in the nucleus (Barth *et al.*, 2004, Barth *et al.*, 2009; Zschiesche *et al.*, 2015). The presence of HMA domains implied a function in heavy metal detoxification or maintenance of heavy metal homeostasis (Dykema *et al.*, 1999; Zhao *et al.*, 2013; Khan *et al.*, 2019; Khan *et al.*, 2020; Manara *et al.*, 2020; B. Zhang *et al.*, 2020; Liu *et al.*, 2022). Recent studies found a connection between HIPP proteins and stress responses of plants, establishing a more complex function of this protein family (Barth *et al.*, 2004; Barth *et al.*, 2009; Zhang *et al.*, 2015; Zschiesche *et al.*, 2015; Radakovic *et al.*, 2018; Cowan *et al.*, 2020; Manara *et al.*, 2020). The aim of the present work was to investigate the function of *HvFP1* by analysing its expression patterns under various conditions and studying the effects of *gain-* and *loss-of-function* of *HvFP1* on plant responses to different stress conditions and leaf senescence on physiological and transcriptomic levels.

3.1. *HvFP1* is induced during abiotic stress and developmental leaf senescence

The expression level of *HvFP1* was analyzed under three abiotic stress conditions, i.e., drought, combined cold and high light and salt stress, and during dark-induced and developmental leaf senescence. The effect of drought stress on barley plants was tested by withholding the water supply after the 11th DAS. This experimental setup reflected natural drought stress conditions, with a slow decrease in RWC of soil during a prolonged dry period. Under these conditions, plants exhibited the first physiological stress responses by decreasing their photosynthetic efficiency (Fig. 12C and D), proportionally with the reduction in RWC (Fig. 12A). The expression of *HvFP1* in control and drought samples of primary leaves was monitored every two days throughout the experiment, showing a clear induction of *HvFP1* gene expression during the drought treatment (Fig. 6A). This indicates a function of HvFP1 in the complex response of barley plants to drought. A possible regulatory function of other HIPP members during drought stress has already been recorded in *A. thaliana*. In fact, *AtHIPP26*, which is the closest homolog of *HvFP1* in *Arabidopsis*, was also induced under drought stress conditions (Barth *et al.*, 2009). In that work, Barth *et al.* (2009) used the yeast two hybrid system and found that *AtHIPP26* interacts with the Zn²⁺ finger homeodomain TF ATHB29, which regulates stress responsive genes (Tran *et al.*, 2006). In fact, the presence of a functional HMA domain in *AtHIPP26* was necessary for this interaction. *Loss-of-function* of *AtHIPP26* resulted in the suppression of drought stress regulated genes, which were normally induced by ATHB29.

HvFP1 was first reported as a cold and high light induced gene in winter barley *H. vulgare* L. cv. Trixi (Barth *et al.*, 2004). In the present work, the upregulation of *HvFP1* under these stress conditions was also confirmed for spring barley *H. vulgare* L. cv. Golden promise. *HvFP1* was transiently expressed in primary leaves under this stress treatment, with

the highest induction of *HvFPI* being observed between 4 and 12.5 h after exposure to cold and high light (Fig. 6B). At these time points, the PSII efficiency was significantly reduced, while the Chl content of primary leaves remained relatively high (Fig. 15A and B). After 31 h, the transcript level of *HvFPI* in stressed samples was not different than the one in control samples (Fig. 6B). Taken the above results together, barley plants underwent changes in physiological parameters and in the expression of specific genes in the first 7 to 12.5 h post treatment. After that time point, the physiological parameters were stabilized, reflecting a cold acclimation, while the transcript level of *HvFPI* was reduced. Many members of HIPP family in *Arabidopsis* were found to have a transient regulation in response to cold stress. Barth *et al.* (2009) showed that *AtHIPP23*, *AtHIPP25* and *AtHIPP26* were induced after 6 h of cold application and their expression was decreased after 24 h. On the contrary, *AtHIPP24* was induced only after 24 h of cold stress, while *AtHIPP27* was downregulated in both time points, reflecting a diverse role of this protein family in stress responses. Similarly, rice *OsHIPP41*, which is homologous to *AtHIPP26* was strongly induced in response to drought and cold, but the exact mode of action was not clear (de Abreu-Neto *et al.*, 2013).

Salt can be considered as another form of drought stress. Application of high concentrations of NaCl to barley plants highly increased the expression level of *HvFPI* in primary leaves (Fig. 6C). This expression pattern correlates with that of *Arabidopsis* homolog *AtHIPP26*, which was reported to be strongly upregulated under salt stress, as well (Barth *et al.*, 2009). Here, *HvFPI* was fast induced even 2 h after salt application and the relative transcript level was increased with the time past salt treatment. Zhang *et al.* (2015) also showed that wheat *TaHIPP1*, which is 99% identical to *HvFPI*, was strongly induced in response to cold and salt stress. Especially for salt stress, they ectopically expressed *TaHIPP1* in yeast cells and observed an enhanced yeast tolerance under heavy metal and high salinity. This indicated a regulatory function of *HvFPI* in plant responses to salt stress, as well.

The function of *HvFPI* was obviously not limited in abiotic stress responses, but involved particular aspects of plant development. This was supported by the significant induction of *HvFPI* in dark- and age-dependent leaf senescence. The strong induction of this gene in response to dark was reported in the present work for the first time. A 3-fold upregulation was detected after 24 h of dark application and increased up to 12-fold at the end stages of dark-induced leaf senescence (Fig. 6D). In general, dark application was often used as a tool for the acceleration of developmental leaf senescence in order to facilitate the study of this process. As expected, a strong expression of *HvFPI* was observed at the end stage of developmental leaf senescence (Fig. 7), as well. At this stage, the Chl content was less than 50% (Fig. 20B and D). Interestingly, the homologous to *HvFPI* gene *AtHIPP26* had a different expression pattern, as it was downregulated during developmental leaf senescence (Barth *et al.*, 2009).

3.2. Phytohormone regulation of *HvFPI*

The expression data indicated that *HvFPI* was involved in pathways related to stress-responses and leaf senescence. These pathways are upstream regulated via the action of specific phytohormones. The effect of those molecules on the expression of *HvFPI* was also investigated here. For that, barley primary leaves were incubated with three stress-related phytohormones, ABA, SA and MeJA (Wani *et al.*, 2016), and with three CK variants, known

to suppress stress-related and developmental leaf senescence (Zwack & Rashotte, 2015; Hönig *et al.*, 2018). It has already been reported that the abiotic stress phytohormone ABA (Danquah *et al.*, 2014) was the main regulator of *HvFP1* (Barth *et al.*, 2004) and its wheat homolog *TaHIPPI* (Zhang *et al.*, 2015), but had no effect on the expression of *AtHIP26* (Barth *et al.*, 2009). Here, *HvFP1* was strongly and quickly upregulated by ABA, while the biotic stress phytohormones SA and MeJA (Wasternack, 2007; An & Mou, 2011) had a smaller impact on the induction of this gene (Fig. 8A). Zhang *et al.* (2015) reported that SA and MeJA led to a negative regulation of *TaHIPPI* after 24 h of treatment and discussed the antagonistic function of ABA and SA, especially under biotic stress. In the present work, the negative effect of SA and MeJA on *HvFP1* expression was not confirmed.

It is worth mentioning that kinetin, zeatin and 6-BEP, which belong to isoprene or aromatic classes of CKs (Hönig *et al.*, 2018), downregulated *HvFP1* after 24 h of treatment (Fig. 8B). CKs are involved in many aspects of plant development, including leaf senescence. It has been reported that exogenous application of CKs or OE of CK biosynthesis genes led to delay in senescence (reviewed in Hönig *et al.*, 2018). Actually, *trans*-zeatin had the highest effect in delaying wheat leaf senescence, followed by kinetin and 6-BAP (Holub *et al.*, 1998). On the other hand, these phytohormones were endogenously decreased under stress (Hare *et al.*, 1997), while ABA, SA and MeJA increased in response to abiotic or biotic stress (Du *et al.*, 2013; Khan *et al.*, 2015; Dar *et al.*, 2017). It is well established that the interplay among various phytohormones, such as ABA and CKs (Zwack & Rashotte, 2015), determined plant responses under specified conditions. Here, one assumption is that under abiotic stress, the increase of ABA in combination with decrement in CKs favored the induction of *HvFP1*.

Targeted expression of *HvFP1* under stress conditions, including the combination of cold and high light and high salinity, and also during developmental and stress-related senescence, driven by drought and dark, was well-established in the present work. In addition, it could be shown that expression of *HvFP1* was positively regulated via stress-related phytohormones, most prominently by ABA, but downregulated by CKs. This complex expression pattern might reflect a more general role of *HvFP1* in different stress- and senescence-related pathways, similarly to hubs involved in crosstalk between different pathways. Plants have developed complex and highly flexible signaling pathways, interconnected for balancing specific processes, such as stress responses with growth and development. Despite increasing efforts to identify components of these interconnected pathways and to unravel their mode of action, there are still many open questions. Here, the role of barley *HvFP1* was investigated in more detail in a genetic approach by analyzing *gain-* and *loss-of-function* barley mutants of *HvFP1*.

3.3. *HvFP1* knock out plants behave similar to wild type during stress treatments and developmental leaf senescence

The CRISPR-Cas9 technology was utilized to create transgenic barley lines lacking full-length *HvFP1*. The successful KO of *HvFP1* was observed on a molecular level, where qRT-PCR showed a low transcript level of KO lines in comparison to WT samples (Fig. 9B). Possible effects of *HvFP1 loss-of-function* on stress responses and developmental leaf senescence were analyzed by comparing the KO lines with WT plants in terms of stress-related decrease of Chl content and PSII efficiency and increase of the expression of stress

marker genes. The transgenic plants used in this study did not show a significant difference compared to WT, in both drought stress treatment and developmental leaf senescence (Fig. 23 to 26). The reason for that “lack of phenotype” is not known and one can only speculate. One possibility might be that other barley HIPP proteins similar to HvFP1 (e.g. HvFP2 or HvFP3) were able to substitute the missing HvFP1. Expression analysis of six other members of barley HIPP family showed that some of them were also differentially regulated during developmental leaf senescence, but their expression did not differentiate in KO line (Fig. 45 in appx. 6.3). However, estimation of transcript level of more members of barley HIPP family and further experiments with double or triple mutants are needed to clarify that point. Establishment of those barley mutants was not possible in this work, due to time limitation. Another reason for the above observation could be that the CRISPR-Cas9 approach resulted in a truncated version of HvFP1 which was still somehow active. This shorter version of HvFP1 should still have part of the HMA domain and the C-terminal isoprenylation motif, while the expected protein size was 13.7 kDa instead of 17.3 kDa. Further experiments on protein level are needed to understand the lack of phenotype. Due to lack of significant effect, the KO lines were not further investigated in this study.

3.4. Overexpression of *HvFP1* causes distinct changes in ABA-related gene expression and in the course of leaf senescence

The hypothesis that barley protein HvFP1 is a good candidate for acting in the crosstalk among different response pathways was further investigated by studying *HvFP1* OE lines, as well. More specifically, plant responses to stress and the course of leaf senescence were analyzed in two *HvFP1* OE lines, named 21.3I and 21.2A. OE of *HvFP1* in the two lines was clearly proven on transcript and protein level (Fig. 9A and 10). Interestingly, OE of *HvFP1* affected the stress-related reprogramming of gene expression. This was most obvious under drought condition, where induction of typical drought stress-related genes, such as *HvNCED*, *HvDhn1* or *HvS40*, was clearly delayed when compared to WT (Fig. 13 and 14). The expression of those well-established drought regulated genes depends on the magnitude of the stress (Iuchi *et al.*, 2001; Tommasini *et al.*, 2008; Krupinska *et al.*, 2014; Temel *et al.*, 2017). In fact, it is known that nuclear localized HvS40 was regulated by HvWHIRLY1 during age- and dark-dependent senescence and under various stress conditions, including water deficit and its expression was highly influenced by ABA (Krupinska *et al.*, 2014; Janack *et al.*, 2016). Here, *HvS40* was induced on the 19th DAS in drought stressed samples of WT leaves and the amount of transcript increased with the progress of water deprivation (Fig. 13A). Interestingly, in both *HvFP1* OE lines, induction of *HvS40* was clearly delayed (Fig. 14A). Same observation was made for the drought stress marker genes *HvNCED* and *HvDhn1*. The first encodes for a 9-*cis*-epoxycarotenoid dioxygenase, which is a key rate-limiting enzyme in ABA biosynthesis (Iuchi *et al.*, 2001). It was shown that rice plants overexpressing *OsNCED3* exhibited enhanced drought tolerance (Huang *et al.*, 2018). Then, *HvDhn1*, which belongs to LEA group II family, was induced under drought stress and encoded for proteins with protective function against the deleterious effects of dehydration (Suprunova *et al.*, 2004). Both genes were upregulated in WT drought samples on the 21st DAS (Fig. 13B and C), when the RWC of soil was reduced by half (Fig. 12A). Then, the transcript amount increased proportionally with the days after sowing and by the 29th DAS,

HvNCED and *HvDhn1* had 100 and 600 times more transcript level in drought leaves, respectively. Similar to *HvS40*, induction of these two genes was clearly suppressed in both OE lines 21.3I and 21.2A (Fig. 14B and C).

Interestingly, expression of another drought-stress related gene, *HvHsp17*, was not affected by OE of *HvFP1*. It was shown that ABA treatment could affect the expression of some heat shock proteins in rice, but had no impact on small heat shock protein Hsp17 (Zou *et al.*, 2009). Then, Sun *et al.* (2016) noted even a suppression of *AsHsp17* in *Agrostis stolonifera* leaves after treatment with ABA and the downregulation of ABA biosynthesis genes in *AsHsp17* OE lines, which implied a negative regulation of ABA on the expression of *AsHsp17*. They proposed an *AsHSP17*-mediated ABA-independent stress signaling under abiotic stress through the DREB1/CBF- and DREB2-related TFs. In independent studies, it was shown that small HSPs stabilize other proteins and membranes in order to prevent damages of water deficit (Guo *et al.*, 2009), while drought tolerant barley cultivars accumulate *HvHsp17* transcripts and proteins (Temel *et al.*, 2017). Here, *HvHsp17* was induced in WT after the 21st DAS and this induction was higher with the progress of drought stress (Fig. 13D). In fact, the transcript level in OE lines was equal or even higher than the WT samples on the same time points (Fig. 14D).

In addition to drought, effects on cold and high light, salt and dark stress responses were analyzed. In general, under these stress conditions, *HvFP1* OE lines showed a similar decrease in PSII efficiency and in Chl content as WT. There were only some smaller effects on the expression of specific stress marker genes in *HvFP1* OE samples (Fig. 15C and D, 17 and 19), however these effects were not as pronounced as in drought stress. Despite the delay in expression of some ABA-related drought stress marker genes, the general time course of early stress-induced leaf senescence was not affected. This indicated that premature and drastic induction of Chl breakdown and decrease in photosynthetic activity during stress was triggered by a fast higher order mechanism, overrunning the pathway where *HvFP1* is involved. However, in contrast to the drastic and fast stress induction of senescence in response to drought, the slower process of developmental leaf senescence was delayed in *HvFP1* OE lines (Fig. 20 and 21).

Developmental leaf senescence aims for the recycling of nutrients from older to younger leaves and organs. Due to its great importance, senescence is a highly regulated process, which has to be fine-tuned in response to a changing environment to balance growth and photosynthesis on one hand, and recycling of nutrients during senescence on the other hand, increasing fitness in an ever-changing environment. The switch from a photosynthetically active to a senescing leaf, which is a source of valuable resources to be recycled, is a major developmental step. This step is accompanied by massive reprogramming of gene expression. As already described, genes induced at onset of senescence are known as SAGs, while genes downregulated in this process are called SDGs (Ahmad & Guo, 2019). To follow the onset of leaf senescence on molecular level, the expression levels of three well-known senescence marker genes, *HvS40*, *HvSAG39* and *HvSBT*, were analyzed during leaf development. As mentioned before, *HvS40* is a strongly induced drought and dark stress marker gene. A number of studies describe *HvS40* as an SAG as well (reviewed in Jehanzeb *et al.*, 2017), which was localized in the nucleus and induced by ABA. Mutants of *AtS40* showed a delayed leaf senescence and downregulation of senescence associated genes

(Krupinska *et al.*, 2002; Fischer-Kilbiński *et al.*, 2010). A small upregulation of *HvS40* was observed in WT samples, when the Chl content was reduced below 90 % (Fig. 22A). The highest relative expression level was observed in the middle and later stages of leaf senescence. The two *HvFPI* OE lines exhibited significantly lower expression levels at each stage, which was clearly shown in Fig. 22D, where the expression in 21.3I and 21.2A lines was compared with the expression of WT samples at each specific stage. The lower expression level of *HvS40* in the OE samples was in line with the delayed progress of leaf senescence in these plants. Similar pattern was observed for two senescence regulated proteases. One cysteine protease is known as *HvSAG39*, its transcript was induced at the late stage of leaf senescence and functions in protein degradation during this process (Liu *et al.*, 2010). Here, *HvSAG39* was already significantly upregulated in WT samples, when the Chl content drops to 90 % (Fig. 22B). In the next stages, WT samples exhibited stronger regulation, as expected, and this induction was always higher in comparison to the two OE lines, as presented in Fig. 22E. Lastly, another proteolytic enzyme involved in leaf senescence is the subtilisin-like protease. This is a serine protease which contributes to nitrogen remobilization to new developing organs by degradation of proteins in senescing organs (Roberts *et al.*, 2017). Here, *HvSBT* gene was upregulated at the onset of developmental leaf senescence, when the Chl content decreases to 90 % (Fig. 22C). The highest expression level was observed at 75 % and less than 50 % Chl content. At these stages, 21.3I and 21.2A exhibited a much lower relative expression level in comparison to WT samples (Fig. 22F). The regulation of these proteases further supports that OE of *HvFPI* favors a delay in the onset of leaf senescence.

3.5. Transcriptomic analysis of developmental leaf senescence in *Hordeum vulgare*

The last stage of leaf development is called senescence and involves the remobilization of nutrients to new developing leaves and reproductive organs (Krieger-Liszkay *et al.*, 2019). In crop plants, the successful remobilization of those nutrients is important for the survival of plants, but also for achieving the highest yield. The process of leaf senescence is highly regulated on a molecular level and there are numerous studies focusing on this topic and especially on the genetic regulation of its onset, middle and final stages (Guo *et al.*, 2004; Thomas *et al.*, 2009; Woo *et al.*, 2019). Understanding the environmental sensitive and efficient regulation of leaf senescence is also of high economic interest, since premature leaf senescence might impair grain filling and overall yield of plants (Gregersen *et al.* 2013). Thus, crop cultivars or transgenic plants with a stay-green phenotype, as observed with *HvFPI* OE lines, are of particular interest. Most studies focus on the model plant *A. thaliana*, since a complete genome sequence and annotation have been available. Recently, Li *et al.* (2020) updated the third version of Leaf Senescence Database (LSD), where 5,853 SAGs and SDGs from 68 species were included. Of that, 3,852 come from *A. thaliana* and only 19 are found in barley *H. vulgare*. One major obstacle in barley transcriptomic studies is the incomplete annotation of its genome. Currently, there are three versions available and some databases are still not updated. Even though there are some stay-green phenotypes of barley, in which specific SAGs are characterized (Gregersen *et al.*, 2008; Kucharewicz *et al.*, 2017), there is not a complete barley senescence database with the newest annotation available. In the present work, a transcriptomic analysis of barley primary leaves

during the middle stage of leaf senescence was carried out and the version 2 of genome annotation (Mascher, 2019) was used for the differential gene expression annotation and analysis.

The analysis of WT barley senescing primary leaves in three independent biological replicates resulted in total 671 significantly DEGs with $\log_2FC > 2$. The majority of those genes were induced, with 439 genes being upregulated and only 232 genes being downregulated (Fig. 28A). In general, the genetic reprogramming during senescence in barley followed a similar pattern as observed in *A. thaliana*, with upregulation of genes involved in degradation of chloroplasts and macromolecules and recycling of released biomolecules via catabolic enzymes and transport systems to bring the nitrogen, carbohydrate and lipid degradation products to new developing parts of the plant. This involves the action of many regulatory factors and components of signaling cascades, including TFs, phytohormone-related factors, kinases and epigenetic regulators, but also a set of stress-related genes, which were upregulated during barley leaf senescence. On the other hand, there were also typical downregulated genes, for example genes encoding components of the photosynthetic apparatus, which were degraded during senescence, and genes, encoding regulatory proteins involved in maturation and growth of a leaf. The barley SAGs and SDGs are discussed below in more details.

3.5.1. Senescence Associated Genes (SAGs)

3.5.1.1. Transcription factors

The successful remobilization of nutrients during developmental leaf senescence requires a well-coordinated network, which is regulated by TFs and phytohormones. The families of NAC, MYB and WRKY TFs have well-established functions in developmental leaf senescence (Zhang *et al.*, 2012; Podzimska-Sroka *et al.*, 2015; Zhang *et al.*, 2016; reviewed in Luoni *et al.*, 2019). The substantial family of NAC TFs has diverse functions in a crosstalk with phytohormones and environmental signals (Breeze *et al.*, 2011). Depending on the interaction partners, some members promote and others delay the process of leaf senescence (reviewed in Luoni *et al.*, 2019). Similar multifunctional roles of MYB family have been unveiled in many plant species (Zhang *et al.*, 2012). Many members are regulated by ABA in response to abiotic stress (Dubos *et al.*, 2010; Zhang *et al.*, 2012) and leaf senescence (Jaradat *et al.*, 2013). In addition, members of WRKY family are induced by ABA, stress and senescence (Rushton *et al.*, 2010), confirming a complex response network of different signaling pathways. Here, six members of NAC, seven MYB and four WRKY TFs were upregulated in senescing leaves of barley. Then, there were 23 TFs and transcriptional regulators with distinguished sequence domains and nine phytohormone related TFs. Of them, six correspond to ethylene responsive TFs and three are ABA responsive factors or ABA binding proteins. The role of ethylene at the onset of leaf senescence is well-known. Numerous studies showed that ethylene functions upstream of a signaling cascade, which promotes the process of senescence. Exogenous application or early induction of ethylene leads to premature senescence, while inhibition of ethylene synthesis leads to delayed leaf senescence (Koyama, 2014). Similar pattern was observed for ABA. This phytohormone was strongly induced under abiotic stress conditions, as a positive

regulator of leaf senescence (Breeze *et al.*, 2011). Finally, an auxin-responsive protein was induced here, which is known to promote plant development (Kohno *et al.*, 2012).

3.5.1.2. Anabolic and catabolic enzymes

The first sign of senescence on leaf phenotype is the yellow colour, as chloroplasts are degraded and Chl molecules are broken down (Luoni *et al.*, 2019). Then, nutrients derive from the catabolism of macromolecules, such as proteins, fatty acids and nucleic acids, by the respective enzymes and they are transferred to newly developed organs (Luoni *et al.*, 2019). The list of SAGs included many representatives of catabolic enzymes. Among those involved in the breakdown of the photosynthetic apparatus during developmental leaf senescence are the protein STAY-GREEN, a chlorophyllide *b* reductase NONYELLOW COLORING 1 (NYC1), a chlorophyllide *b* reductase NONYELLOW COLORING 1-LIKE (NOL) and a pheophytinase. Briefly, protein STAY-GREEN is a Mg-dechelatase, which converts Chl *a* to pheophytin *a* at the first step of Chl degradation (Christ & Hörtensteiner, 2014). Chl *b* cannot enter this process directly and it needs to be converted to Chl *a* (Hörtensteiner, 2009). The chlorophyllide *b* reductase isoforms NYC1 and NOL are responsible for reconverting Chl *b* to Chl *a* for its subsequent degradation (Horie *et al.*, 2009). After Chl *a* is turned to pheophytin *a* by protein STAY-GREEN, a pheophytinase functions in the conversion of pheophytin *a* to pheophorbide *a* downstream in the Chl catabolic process (Shimoda *et al.*, 2016). Interestingly, the PSII 10 kDa polypeptide family protein, a light-independent protochlorophyllide reductase iron-sulfur ATP-binding protein and a 1,4-dihydroxy-2-naphthoyl-CoA thioesterase were significantly upregulated in the middle stage of leaf senescence. The first one is part of the oxygen-evolving complex of PSII and is necessary for water splitting and electron transfer in PSII (Suorsa *et al.*, 2006). Then, the second one probably functions in Chl biosynthesis pathway, at the step of light independent reduction of protochlorophyllide to chlorophyllide (Fujita & Bauer, 2000). Finally, the thioesterase is involved in phylloquinone biosynthesis, which carries electrons to PSI, but also accepts electrons for the formation of disulfide bonds (Widhalm *et al.*, 2012). The reason why these genes of photosynthetic function were upregulated, while most genes encoding components of the photosynthetic apparatus were downregulated (see next chapter) is not clear. One might speculate that their specific functions are still needed to ensure a coordinated and efficient nutrient recycling. But this has to be clarified in future experiments.

Major sources of nitrogen are amino acids and proteins. Many genes encoding for proteases are highly upregulated during leaf senescence. The majority of proteases include cysteine proteases, also in the form of metacaspases, aspartic proteases, PPPDE thiol peptidases and serine proteases in the form of subtilisin-like proteases and serine carboxypeptidases. In addition, vacuolar processing enzymes were found in the list of SAGs and it has been proposed that some proteases are stored in vacuoles during senescence in order to function during the evolution of this process (Kinoshita *et al.*, 1999). Interestingly, two protease inhibitors, a Bowman Birk type bran trypsin inhibitor and a subtilisin-chymotrypsin inhibitor-2A were also upregulated during developmental leaf senescence.

After protein degradation, the processing of amino acids is followed. Many amino acids are further degraded by the corresponding enzymes for nutrient utilization, while others are used for nitrogen mobilization from senescing cells to new developing organs through phloem (Buchanan-Wollaston *et al.*, 2005). In barley senescing primary leaves, five members of aminotransferases were upregulated. Aminotransferases are enzymes, which bind pyridoxal-5'-phosphate and catalyse reactions between amino acids and α -keto (2-oxo) acids

(Parthasarathy *et al.*, 2019). Briefly, some of the aminotransferases in the SAG list were one alanine glyoxylate aminotransferase, which catalyzes the conversion of glyoxylate and L-alanine to glycine and pyruvate. Then, an acetylornithine aminotransferase is involved in L-arginine biosynthesis (Frémont *et al.*, 2013). One tryptophan aminotransferase converts 2-oxoglutarate (2OG) and L-tryptophan to indole-3-pyruvate and L-glutamate in the auxin biosynthesis pathway (Stepanova *et al.*, 2008). The chloroplastic LL-diaminopimelate aminotransferase functions in lysine biosynthesis pathway (Hudson *et al.*, 2005), while one branched-chain-amino-acid amino-transferase is involved in leucine, isoleucine and valine biosynthesis (Knill *et al.*, 2008). On the other hand, one lysine ketoglutarate reductase/saccharopine dehydrogenase acts in lysine catabolism and glutamate is formed in various steps of this pathway (Zhu *et al.*, 2001). Glutamate can be utilized for the formation of L-glutamyl 5-phosphate by P5CS, which is also known as gamma-glutamyl phosphate reductase. This is the first step in proline biosynthesis pathway (Székely *et al.*, 2008). Here, two genes encoding for gamma-glutamyl phosphate reductase were upregulated. Another enzyme, which influences the biosynthesis of proline, but also of other amino acids, is glutamate carboxypeptidase (Shi *et al.*, 2013). This gene was upregulated here and was probably involved in sugar and amino acid metabolism during leaf senescence. One of the multiple genes encoding for glutamine synthetase was upregulated in the present work in response to senescence. This enzyme is involved in glutamine biosynthesis from glutamate and is important for nitrogen assimilation, not only during development, but also during stress responses (Ji *et al.*, 2019).

The list of SAGs, which were related to amino acid metabolism included also one L-allo-threonine aldolase, one 4-hydroxy-tetrahydrodipicolinate reductase, one serine decarboxylase, one arginine aminohydrolase and one argogenate dehydrogenase. The L-allo-threonine aldolase is involved in the conversion of threonine to glycine (Joshi *et al.*, 2007), while the 4-hydroxy-tetrahydrodipicolinate reductase is member of the lysine biosynthesis pathway through diaminopimelic acid (Hudson *et al.*, 2006). Serine decarboxylase functions in serine catabolism for the synthesis of ethanolamine. The latter is then used for the synthesis of membrane phospholipids (Kwon *et al.*, 2012). Then, arginine amidohydrolase catabolizes arginine for the production of ornithine and urea (Patel *et al.*, 2017). Ornithine is a precursor for the production of putrescine and subsequent polyamines. Finally, argogenate dehydrogenase acts in the carboxylation of argogenate to tyrosine (Rippert & Matringe, 2002). It is obvious that during developmental leaf senescence, there is a well-coordinated organisation of amino acids and other molecules for the better utilization of nutrients, but also for the optimal regulation of this process.

Proteins and amino acids are not the only source of nitrogen. Nucleic acids become important source of carbon, nitrogen and phosphorus for the new developing leaves and organs. The enzymes, which are responsible for nucleic acid catabolism, were found in the list of SAGs. Those include pyrimidine-specific ribonucleoside hydrolases, ribonucleases, endonucleases, exonucleases, but also enzymes of the broader pyrimidine and purine metabolic pathways, such as the dihydroorotate dehydrogenase and uricase, respectively. Finally, the 7-cyano-7-deazaguanine synthase is involved in the formation of queosines nucleosides, while an RNA ligase/cyclic nucleotide phosphodiesterase has ligase activity for the metabolism of cyclic nucleotides.

As the process of leaf senescence is progressing, the organelles lose their structure and the membranes are breaking down. Lipids are major components of cellular membranes

in various forms, such as glycerolipids (phospholipids, galactolipids, triacylglycerols and sulfolipids), sphingolipids and sterols (Reszczyńska & Hanaka, 2020). During leaf senescence, the degradation of lipids begins with the enzymes called lipases. Here, there were 13 genes encoding for various forms of lipases and were upregulated during senescence. Of them, five genes corresponded to GDSL esterases/lipases and three to lipases. Then, one esterase/lipase/thioesterase family protein was found in the SAGs and it is known to function during stress and senescence (Lippold *et al.*, 2012). Briefly, the degradation of cellular membranes leads to accumulation of toxic intermediates, like free fatty acids and free phytols. This member of the esterase/lipase/thioesterase family converts those free toxic intermediates into fatty acid phytol esters (Lippold *et al.*, 2012). Interestingly, two genes were found in the list of barley SAGs, but are known to be involved in bacteria metabolism, like the D-(-)-3-hydroxybutyrate oligomer hydrolase for butanoate metabolism (Sugiyama *et al.*, 2004) and the UDP-2,3-diacetylglucosamine hydrolase for lipid A biosynthesis (Li *et al.*, 2011). Besides the catabolism of lipids, there are processes involving the biosynthesis of lipid molecules, which are important during senescence. One well-known example is the group of JA and its derivatives. Here, one allene oxide cyclase was upregulated and is involved in 12-oxophytodienoic acid (OPDA) production, which is precursor in JA biosynthesis (Stenzel *et al.*, 2003). Similarly, the 12-oxophytodienoate reductase-like protein was upregulated and is involved in oxylipin/JA biosynthesis (Schaller *et al.*, 2000).

Other metabolic processes involve the methylation of specific molecules by groups of methyltransferases. Three O-methyltransferases were upregulated here in senescing leaves with general function in transferring methyl-groups on a molecule. In addition, one calmodulin-lysine N-methyltransferase acts on the methylation of Ca²⁺ binding protein calmodulin for the regulation of multiple aspects of plant development, such as root development and stress responses (Banerjee *et al.*, 2013). Two S-adenosyl-L-methionine-dependent methyltransferases function with the S-adenosyl-L-methionine (SAM) as cofactor for the methylation of other compounds, like lipids and nucleic acids. This is in line with the function of the arginine N-methyltransferase, which was also found in barley SAGs. This enzyme transfers methyl groups from SAM to arginine residues of histones for chromatin organization (Yan *et al.*, 2007). The reverse reaction is catalyzed by methyl-esterases and four of those genes were also included in the SAG list. They hydrolyze methyl groups from methyl ester residues and participates in many regulatory functions, such as activation of auxin during multiple aspects of plant development (Yang *et al.*, 2008). Finally, three members of alpha/beta-hydrolases superfamily were found in the list of SAGs. One of them is known as pimeloyl-acyl-carrier protein methyl ester esterase and is involved in biotin biosynthesis (Shi *et al.*, 2016).

3.5.1.3. Carbon remobilization and cell wall organization

Leaf senescence involves a number of internal catabolic processes, ending with total collapse of plant cells. These processes demand energy and since the photosynthetic activity of senescing cells is compromised, cells obtain the required energy by increasing the respiratory rate (Bhat *et al.*, 2019). Here, an upregulation of components of respiratory machinery was observed. Specifically, two electron transfer flavoproteins were induced: one corresponds to alpha subunit of mitochondrial electron transfer flavoprotein and one to beta subunit of electron transfer flavoprotein. These proteins are responsible for transferring electrons to dehydrogenases of the membrane-bound respiratory chain (Toogood *et al.*, 2007).

Another SAG was one chain of NADH-ubiquinone oxidoreductase, which corresponds to one subunit of the NADH dehydrogenase for the transfer of electrons from NADH to components of the respiratory chain (Walker, 1992). Finally, leaf senescence leads to induction of ubiquinol oxidase, which is another component involved in further electron transfer during respiration.

An increase in respiration is accompanied by a higher demand in reduced carbon. Plant cells are wrapped in a structure of cell wall, which comprises of proteins and polysaccharides in the form of pectin, cellulose and hemicellulose (Loix *et al.*, 2017). The latter consists of xylans, mannoglycans (mannans), xyloglucans and mixed linkase β -glucans (Ebringerová, 2005). As leaf senescence is progressing, cells are broken down and, in parallel, are recycling their nutrients. Many genes involved in metabolic processes of cell wall polysaccharides were found in the list of SAGs. Main representatives were enzymes of pectin metabolism (pectate lyase, pectin acetyltransferase, pectin lyase-like protein, omega-hydroxy-palmitate *O*-feruloyl transferase), cellulose metabolism (sucrose-UDP glucosyltransferase, endo-1,4-beta glucanase, cellulose synthase), lignin metabolism (laccase, caffeoylshikimate esterase, hydroxycinnamoyl-CoA shikimate) and metabolism of hemicellulose components (cinnamoyl-CoA reductase, endo-1,4-beta-xylanase, xyloglucan endotransglucosylase, trichome birefringence-like proteins, glucan 1,3-beta-glucosidase and arabinogalactan peptide-like protein). Additionally, many CASP-like proteins and one beta-expansin are functioning in cell wall reorganization or loosening during senescence. Here, the list of SAGs included multiple enzymes, which function in carbohydrate metabolic process, such as a mannan endo-1,4-beta-mannosidase, a phosphoglycerate mutase-like protein, a beta-galactosidase and multiple beta-glucosidases.

It is worth mentioning that the highest upregulation was observed for isocitrate lyase and malate synthase, two enzymes of glyoxylate cycle. In fact, the strong induction of those two enzymes in barley senescing leaves was first reported by Gut & Matile (1988). Both enzymes function in glyoxysomes, where plastidial lipids are reutilized via beta-oxidation for their conversion to succinate. The latter enters mitochondria and at the end is converted oxaloacetate and eventually to sugar molecules (Gut & Matile, 1988; De Bellis *et al.*, 2020). It is obvious that one important parameter during leaf senescence is to ensure an energy reservoir in the form of sugar, which will be used in order to fuel this highly coordinated process.

3.5.1.4. Transporters

It has been discussed in depth that the major goal of leaf senescence is the recycling and relocation of nutrients to new developing organs. After the degradation of proteins, amino acids, lipids and nucleic acids, the nutrients are transferred by the appropriate transporters. Thus, there was a long list of transporters, which were induced during developmental leaf senescence in barley. These nutrients are used either in the senescing cells for the biosynthesis of other molecules, such as secondary metabolites and in processes like respiration or are transferred to younger cells in new developing leaves and organs (Rentsch *et al.*, 2007; Thakur *et al.*, 2016).

Major complexes for transportation of macromolecules, which were upregulated here in senescence, are ABC transporters, lipid-transfer proteins, amino acid permeases,

oligopeptide transporters, and nucleobases transporters The adenosine triphosphate (ATP)-binding cassette (ABC) transporters are found in all organisms and act as importers and exporters. They have an expanded function in plant development and stress responses and in transferring nutrients and phytohormones (Kang *et al.*, 2011). Our data suggest also a function during leaf senescence, as two ABC transporters were highly induced in senescing samples. Then, lipid transfer protein family consists of multiple members across many plant species and they transfer fatty acids and phospholipids between membranes. One interesting finding was the role of one lipid transfer protein in ethylene mediated response and signaling in *Arabidopsis* (Wang *et al.*, 2016). Here, six members of this protein family were found as SAGs, expanding the function of those lipid transporters in developmental leaf senescence. At the same time, amino acids and peptides from degraded proteins are transferred through phloem to new developing leaves by amino acid permeases and oligopeptide transporters (Hörtensteiner & Feller, 2002). Total five genes for amino acid permeases and two genes for oligopeptide transporters were induced during barley leaf senescence. Finally, one adenine/guanine permease and one purine permease-like protein are responsible for purine transport through membranes and could possibly function in CK export during leaf senescence (van der Graaff *et al.*, 2006).

It has been discussed that during leaf senescence, the photosynthetic efficiency is reduced and the respiratory rate is enhanced (Bhat *et al.*, 2019). The latter requires an input of carbon and sugar molecules. Thus, sugar transporter proteins, such as SWEET transporters and one UDP-galactose transporter were highly upregulated in the present work. At the same time, the catabolism of proteins and amino acids produces nitrogen, which is remobilized by the corresponding transporters. Three high affinity nitrate transporters were considered as SAGs here and function in nitrate transport and assimilation during leaf senescence. Additionally, other nutrients are imported and exported by one sodium transporter and one FXFD domain-containing ion transport regulator for sodium transport and potassium regulation, one K⁺ uptake permease and one Cation/H⁺ antiporter for potassium transport and one voltage-dependent calcium channel and one putative vacuolar cation/proton exchanger for regulation of calcium homeostasis and transmembrane transport in calcium-mediated signaling cascades. Interestingly, one auxin influx and one auxin efflux transporter were induced here and are involved in auxin homeostasis and signaling pathway in regulation of leaf senescence, even though it has been reported that auxin transporters are downregulated in red clover during leaf senescence (Chao *et al.*, 2018). Finally, one metal transporter, one S-type anion channel, one organic cation transporter protein, one member of the major facilitator superfamily, two transporter-related family proteins and one mitochondrial import inner membrane translocase function in transport of ions and other molecules across plasma membranes or mitochondrial membranes.

3.5.1.5. Phytohormones and signaling cascades

Phytohormones are known to be positive or negative regulators of many aspects of plant development, including leaf senescence. One major phytohormone for the regulation of senescence initiation is ethylene. Cells perceive ethylene as a signal in the endoplasmic reticulum and then a signaling cascade is activated for the transcriptional regulation of SAGs (J. Kim *et al.*, 2015). It has already been discussed that six ethylene-responsive TFs were

induced in the present work during developmental leaf senescence. In the same list, protein REVERSION-TO-ETHYLENE SENSITIVITY1 was also present and it is a positive regulator of ethylene receptors (Resnick *et al.*, 2008) for ethylene perception and downstream transmission. Many studies have reported a combined activity of ethylene and JA on regulating the timing of senescence (for review Song *et al.*, 2014; J. Kim *et al.*, 2015). In fact, J. Kim *et al.* (2015) summarized the interplay between those two phytohormones and concluded that the function of JA in leaf senescence is dependent on ethylene perception and downstream signaling. In addition, JA was found in conjugation with ACC, which is a precursor of ethylene biosynthesis (Staswick & Tiriyaki, 2004; J. Kim *et al.*, 2015). This observation links JA with the biosynthesis of ethylene during leaf senescence. Furthermore, one JAZ protein was strongly induced here in senescing samples. This gene is a transcriptional repressor of JA signaling pathway and results in induction of leaf senescence (Pauwels & Goossens, 2011).

Then, five SAUR-like auxin-responsive family proteins were induced in barley developmental leaf senescence. The family of small auxin up RNA (SAUR) genes is involved in many aspects of plant development (reviewed in Ren & Gray, 2015) and is regulated by auxin. It has been reported that auxin is a positive regulator of SAUR genes in shoots, but a negative regulator of those genes in roots (Paponov *et al.*, 2008). The role of SAUR genes in leaf senescence is controversial, but it is known that specific SAUR genes, such as AtSAUR36, AtSAUR49, AtSAUR30, AtSAUR39, AtSAUR41 and AtSAUR72 (Hou *et al.*, 2013; Wen *et al.*, 2020) promote leaf senescence probably through downstream interaction with senescence regulated phosphatases and kinases. Additionally, two indole-3-acetic acid-amidosynthetases and one indole-3-acetic acid-amino acid hydrolase ILR1 were upregulated here and function in the regulation of auxin metabolism and homeostasis during various plant processes (Ding *et al.*, 2008; Böttcher *et al.*, 2010). It is known that the function of auxin is correlated with CKs in a quantity based manner (Moubayidin *et al.*, 2009). Besides the enzymes, which are involved in regulation of auxin biosynthesis and homeostasis, two enzymes for CKs biosynthesis from nucleotides were found in the list of SAGs. These are two CK riboside 5'-monophosphate phosphoribohydrolases, which produce CK nucleobases from CK riboside 5'-monophosphates in the direct pathway for active CK production (Kuroha *et al.*, 2009). In contrast to auxin, CKs are negative regulators of leaf senescence and improve the antioxidant capacity of plants during this process (reviewed in Hönig *et al.*, 2018). This contradictory function between auxin and CK is well-studied during many aspects of plant development.

Another well-studied phytohormone is the ABA, which is considered as abiotic stress response phytohormone. Many stress responses are regulated by ABA, such as the stomatal closure under drought and salt stress (Lee & Luan, 2012). In addition, ABA regulates TFs for the induction of stress related genes, like the ABA-responsive NAC TF VNI2 which regulates a number of *COR* and *RD* genes for conferring stress resistance and leaf longevity (Yang *et al.*, 2011). This is one example of the complex role of ABA in plants. In the present work, an upregulation of ABA-deficient gene, which is involved in neoxanthin synthesis (North *et al.*, 2007), was observed. Neoxanthin is a precursor molecule in the ABA biosynthesis pathway. This implies an accumulation of ABA during developmental leaf senescence in barley. Then, ABA downstream activates a signaling cascade for the transcriptional regulation of ABA

responsive genes. Thus, two ABA responsive element-binding factors and one ABA-regulated RNA-binding protein were upregulated here during leaf senescence, as was already discussed.

It is worth mentioning that a GA 2-oxidase, which is involved in the catabolism of GA, was induced in barley senescing leaves (van der Graaff *et al.*, 2006). GAs are negative regulators of leaf senescence. As a result, during this process, GA 2-oxidase is responsible for catabolism of GAs and further induction of senescence. Overall, it is obvious that there is a strong regulation and crosstalk among plant hormones, which function in a coordinated way for the optimal regulation of developmental leaf senescence.

Phytohormones are molecular signals, which activate multiple signaling cascades for the induction or inhibition of specific plants responses and developmental processes. The signal is transduced by a number of signaling components, such as kinases, phosphatases and calcium-binding proteins (Wang *et al.*, 2002; Demidchik *et al.*, 2018). During barley developmental leaf senescence, total 32 genes encoding for protein kinases, 4 genes of phosphatases and 4 calmodulins and calcium binding proteins were induced. It is known that protein kinases, including receptor-like kinases and mitogen-activated protein kinases and phosphatases, such as PP2C proteins, are intermediates in the signaling cascades activated by various phytohormones during plant development (reviewed in Ahmad & Guo, 2019). Other intermediates in the signal transduction are inositol 1,4,5-trisphosphate receptor-interacting proteins and leucine-rich repeat (LRR) proteins, which were found in the list of SAGs.

3.5.1.6. Redox regulation

As the process of leaf senescence is progressing, there are various changes in cell metabolism and organization. As mentioned above, there is an induction of catabolic enzymes, including proteases, lipases and nucleases, which degrade macromolecules and structural components of the cell, resulting in the production of ROS, such as superoxide radicals (O_2^-), hydroxyl radicals ($\cdot OH$), singlet oxygen (1O_2) and hydrogen peroxide (H_2O_2). An accumulation of ROS results in oxidative damage of cell membranes and accelerates cell death (van Breusegem & Dat, 2006). Part of the free carbon and nitrogen molecules, after the degradation of macromolecules in senescing leaves, are used for the biosynthesis of secondary metabolites, including phenylpropanoids and flavonoids, which function in the regulation of cellular redox state. In the present work, seven genes encoding for glycosyltransferases were upregulated in senescing barley leaves. In general, plant glycosyltransferases function in attaching sugar molecules to other acceptor molecules through a glycosidic bond (Keegstra & Raikhel, 2001). One example is the accumulation of anthocyanins in cell vacuoles for the protection of senescing leaves from oxidative damage (reviewed in Thakur *et al.*, 2016). Here, one anthocyanidin 3-*O*-glucosyltransferase and one UDP glucose:anthocyanidin 5,3-*O*-glucosyltransferase, which are involved in anthocyanin biosynthesis (Ogata *et al.*, 2005), were found in SAG list. In the same list, two 7-deoxyloganetin glycosyltransferases were found, which function in accumulation of geniposide for iridoid biosynthesis (Nagatoshi *et al.*, 2011). Other glycosyltransferases are the UDP-glucose:2-hydroxyflavanone C-glucosyltransferase, which is involved in isoorientin biosynthesis (Sun *et al.*, 2021), and the glycosyltransferase 64 protein C5, which is probably involved in protein and lipid glycosylation. Finally, one polyphenol oxidase for polyphenol

biosynthesis and one 4-coumarate:CoA ligase for phenylpropanoid metabolism were induced during developmental leaf senescence.

The protection of plant cells from oxidative damage is ensured by the positive regulation of components of cellular antioxidant system, in order to scavenge an excess of ROS and avoid premature leaf senescence. Here, two peroxidases were induced in barley senescing leaves and probably function in removal of H₂O₂. Oxidative damage can occur during exposure to stress factors, as well. Thus, there is often an overlap in the gene regulation during stress and senescence. Indeed, two aldehyde dehydrogenases were upregulated here in response to senescence, but they are also known to be involved in stress tolerance of *Arabidopsis* plants (Sunkar *et al.*, 2003). Aldehyde dehydrogenases function for the detoxification of toxic aldehydes, which are produced as by-products of lipid peroxidation. Other well-known ROS scavenging enzymes are glutathione S-transferases (Mittler *et al.*, 2004). Here, there was a strong induction of eight genes encoding for glutathione S-transferases. This protein family responds to many abiotic and biotic stress factors, which result to oxidative stress (reviewed in Hernández Estévez & Rodríguez Hernández, 2020), but is also involved in leaf senescence (Kunieda *et al.*, 2005). In addition, two lactoylglutathione lyases, which are also known as glyoxalases, were induced in barley senescing leaves. This enzyme is involved in methylglyoxal metabolism through the glyoxalate pathway. Methylglyoxal is a toxic compound, which is accumulated in cells due to stress exposure or age. More specifically, lactoylglutathione lyases act in the second step of glyoxalate pathway for the conversion of *S*-lactoylglutathione to *D*-lactate and the release of glutathione (reviewed in Singla-Pareek *et al.*, 2020). Another glutathione-dependent enzyme is glutaredoxin. The latter is involved in regulating the ratio of reduced and oxidized glutathione (GSH/GSSG) in order to maintain a stable cellular redox state (Kalinina *et al.*, 2014). In the present work, two genes encoding for members of the glutaredoxin family were upregulated.

One of the major groups of enzymes with oxidoreductase activity, which use a heme-thiolate molecule as cofactor, is the family of cytochrome P450s. Their main mode of action involves a NADPH- and/or O₂-dependent hydroxylation of specific molecules. These enzymes function in plant abiotic and biotic stress responses, biosynthesis of antioxidants and secondary metabolites, metabolism of fatty acids and xenobiotics and in hormone regulation (reviewed in Pandian *et al.*, 2020). Christ *et al.* (2013) reported a function of the cytochrome P450 enzyme CYP89A9 in leaf senescence of *Arabidopsis* plants, especially in the formation of major Chl catabolites. In the present work, the involvement of this protein family in leaf senescence is obvious, as 13 genes encoding for cytochrome P450 enzymes were upregulated in barley senescing primary leaves. Another family of enzymes with hydroxylation/oxygenation activity are the 2OG and Fe(II)-dependent oxygenases, which require 2OG and O₂ as co-substrates and Fe(II) as cofactor. These enzymes function in many aspects of plant development in biosynthetic processes, including the biosynthesis of phytohormones and secondary metabolites, but also in DNA demethylation (Kawai *et al.*, 2014). These processes are important in the regulation of developmental leaf senescence and five members of the 2OG and Fe(II)-dependent oxygenase family were found here as SAGs.

One interesting protein family, which had three representatives in the list of SAGs, was that of calcium-binding caleosins/peroxygenases. Caleosins are found in barley developing grains as part of oil bodies and they are also suspected to engage in lipid

trafficking and membrane expansion (Liu *et al.*, 2005). In addition, their function is expanding to plant responses to environmental stress and oxylipin signaling pathway (Partridge & Murphy, 2009). Another enzyme with oxidoreductase activity, which is positively regulated in barley senescing primary leaves, is one HIPL1 protein, but its exact function is not known yet. Then, one isoflavone reductase-like protein is associated with defense mechanisms against oxidative stress (S.G. Kim *et al.*, 2010), which is often observed during leaf senescence. Finally, it is interesting that four genes encode for blue copper proteins were considered here as SAGs. These small copper-binding proteins function in shuttling electrons from various donor proteins to acceptor proteins (De Rienzo *et al.*, 2000). This trait is utilized here from barley leaves during developmental leaf senescence.

3.5.1.7. Stress responses and other genes

The process of developmental leaf senescence is highly regulated and involves a well-coordinated reprogramming of gene expression. Many factors act in signaling cascades or in the interplay among various pathways, which lead to the activation or inhibition of specific responses. As a result, genes, which are usually regulated under unfavorable conditions, were found to be differentially regulated during developmental leaf senescence, as well. This was observed in the present transcriptomic analysis, where many stress response genes were induced during normal leaf senescence. ABA regulates the expression of genes during various steps of development and stress responses (Jibrán *et al.*, 2013; Dar *et al.*, 2017). Here, three members of the LEA protein family and one Cor protein, whose regulation is dependent on ABA (Battaglia *et al.*, 2008; Mikkelsen & Thomashow, 2009), were found in the list of SAGs. Then, one member of the family with domain of unknown function 584 (DUF584) was upregulated here. This gene shares homology and belongs to the same family with the ABA-induced and senescence associated gene *HvS40* (Jehanzeb *et al.*, 2017), which was strongly induced during the progress of leaf senescence (Fig. 22A). The desiccation-induced 1VOC protein was also found in the same list. This is a vicinaloxygen chelate metalloenzyme, which is involved in osmotic and water deprivation stress (Mulako *et al.*, 2008). Other abiotic stress related genes, which were induced during leaf senescence as well, encode for a plant cadmium resistance protein, an O-acyltransferase WSD1, a zinc finger A20 and AN1 domain stress-associated protein and protein UPF0496. These genes act in cadmium resistance and heavy metal efflux (Song *et al.*, 2010), in cuticular wax synthesis under various stress conditions (Abdullah *et al.*, 2021), in various abiotic stress treatments (Ben Saad *et al.*, 2019) and in water deprivation, respectively.

Interestingly, genes involved in biotic stress responses were also found in the list of SAGs. More specifically, these are one MACPF domain-containing protein, three members of thaumatin family and three disease resistance proteins of NBS-LRR class. The motif of MACPF is conserved among all kingdoms and is found in proteins involved in defense responses and programmed cell death (Morita-Yamamuro *et al.*, 2005; Noutoshi *et al.*, 2006). Thaumatin and thaumatin-like proteins belong to pathogenesis related protein family and mainly induce plant resistance to biotic and abiotic stress responses (Rajam *et al.*, 2007). The class of NBS-LRR proteins, including those with TIR-NBS-LRR and NB-ARC domains, functions in signaling cascades for recognizing pathogen effectors and, through ATP to ADP exchange, they transmit the signal for the activation of the appropriate stress response (Dubey & Singh, 2018). Similarly, a cysteine-rich/transmembrane domain protein confers resistance

against biotrophic pathogens and increases the growth of hypocotyl in *A. thaliana* (Pereira Mendes *et al.*, 2021), but was also induced during leaf senescence in the present work. Additionally, developmental leaf senescence induces the expression of two germin-like proteins and two wound-induced protease inhibitors. The family of germin-like proteins has variable functions in biotic stress responses, conferring resistance against fungi, viruses and insects, but also in salt, drought, light and mechanical stress (Ilyas *et al.*, 2016). The wound-induced protease inhibitors are serine-type endopeptidases, which inhibit chymotrypsin and trypsin and function against herbivores or wounding (Cipollini & Bergelson, 2001). Finally, three universal stress proteins were found in the list of SAGs. This protein family is well-known in prokaryotic organisms, but similar proteins are found in *A. thaliana* and other plant species and have functions in various environmental stress factors (Chi *et al.*, 2019; Kerk *et al.*, 2003).

One major aspect of the present work was the study of HvFP1, which belongs to HIPP family protein. It was shown that this gene was induced in response to a number of abiotic stress treatments, including drought, a combination of cold and high light, high salinity and dark (Fig. 6), but also during developmental leaf senescence (Fig. 7). As expected, *HvFP1* was found in the list of SAGs of senescing leaves, as well. It is interesting that more members of the HIPP family were upregulated in the process of leaf senescence. Total three genes of heavy metal transport/detoxification proteins were found in the list of SAGs: two of them were annotated as AtHIPP39, while the third was annotated as AtFP5.

The process of leaf senescence is only one part of plant development, where nutrients are recycled to new leaves and reproductive organs. As a result, genes involved in other aspects of plant development are expected to be induced in the present transcriptomic analysis. Indeed, there was an upregulation of a number of developmental genes with diverse functions, which are provided in Table 4 in appx. 6.2.3., but their function is not further analyzed in the present work. In the same list, multiple genes of nucleic acid replication, transcription or translation processes, as well as of posttranscriptional and posttranslational modifications and maintenance of cellular structure and metabolism were found to be upregulated during barley developmental leaf senescence. Finally, the fact that barley genome annotation is still incomplete, resulted in a number of DEGs with known domains, but not exact function in leaf senescence. Future improvement of barley genome will unravel the exact annotation of those genes, thus they were not further analyzed and are only provided in Table 4 in appx. 6.2.3.

3.5.2. Senescence Downregulated Genes (SDGs)

3.5.2.1. Transcription factors

The transcriptomic analysis of leaf senescence in barley revealed a long list of TFs, which were induced in order to regulate a number of downstream processes in a highly organized manner. On the other hand, there are TFs, which are negatively regulated during leaf senescence. This was the case here for five members of the basic helix-loop-helix (bHLH) family. This is one of the largest families of TFs in eukaryotic organisms. It is known that they form homo- or hetero-dimers and function in multiple aspects of plant development, including flavonoid metabolism, phytochrome signaling, phytohormone regulation and various abiotic stress responses (Castilhos *et al.*, 2014; Qian *et al.*, 2021). Some members of

bHLH TF family are involved in JA signaling for the activation of JA-induced leaf senescence, while others have an antagonistic effect for the attenuation of JA-induced leaf senescence (Qi *et al.*, 2015). In the same work, a controversial function of bHLHs for the optimal conduction of leaf senescence is discussed. Here, it can be assumed, that a downregulation of bHLHs was necessary for the evolution of this process in barley primary leaves.

Moreover, one CONSTANS-like zinc finger protein, one Bell-like homeodomain protein and one RADIALIS TFs were found in the list of SDGs. The CONSTANS-like genes are involved in the regulation of flowering time with respect to photoperiod (Putterill *et al.*, 1995). Especially, the CONSTANS-like 16, which was downregulated here, is known to positively regulate Chl biosynthesis for Chl accumulation (Ohmiya *et al.*, 2019). Thus, the inhibition of this gene here is in line with the suspension of Chl biosynthesis during leaf senescence. Then, the Bell-like homeodomain protein family is involved in shoot apical meristem initiation and maintenance (Rutjens *et al.*, 2009) and determination of leaf morphology (Kumar *et al.*, 2007). During the last phase of leaf development, this TF was negatively regulated. Finally, the RADIALIS-like 3, which belongs to RADIALIS protein family, was downregulated during senescence. The rice RADIALIS-like 3 is a MYB TF with function in salt stress responses and dark induced leaf senescence in an ABA-dependent way (Park *et al.*, 2018).

Interestingly, one member of the scarecrow TF family and one homeobox leucine zipper protein were also downregulated here. Members of the same family of TFs were found in the list of SAG. This counteraction among members of the same gene family shows how diverse and highly regulated is the process of leaf senescence. Especially for the scarecrow TF family, the downregulation of one member, which is homologous to *Arabidopsis* scarecrow-like protein 23, was observed in the present work. This gene is important for plant growth and leaf development. Briefly, *Arabidopsis* scarecrow-like protein 23 is expressed in xylem-associated bundle sheath cells and is involved in fate specification of bundle sheath cells and in transport of inorganic compounds (Cui *et al.*, 2014). As expected, the function of this gene was inhibited here during leaf senescence. Similarly, one member of the homeobox leucine zipper protein, the homeobox-leucine zipper protein ROC6-like, was downregulated during senescence. This family of TFs has multiple members with diverse functions in plant growth. ROC6 is classified in the same subgroup with ROC5 in rice and the latter is involved in epidermal cell fate and development (Zou *et al.*, 2011). Some other examples are the *A. thaliana* homeobox 12, which is involved in stress responses and leaf development regulation (Hur *et al.*, 2015) and the *O. sativa* Hox33, which influences the embryonic shoot meristem formation, leaf pattern and leaf senescence (Luan *et al.*, 2013).

Similar counter regulation was observed for two auxin responsive proteins and one AP2-like ethylene-responsive TF. Even though there was a strong representation of ethylene responsive TFs in the list of SAGs, one AP2/ERF-like gene was downregulated here. There are 121 members of the AP2/ERF family of TFs in barley and they have diverse functions in plant development and stress responses (Guo *et al.*, 2016). In the present work, one member was negatively regulated during developmental leaf senescence. In the same list of SDGs, two auxin-responsive proteins were found. In fact, it was shown that auxin-responsive factors are regulators of multiple aspects of plant development, including leaf senescence (Lim *et al.*,

2010). Finally, the function of one abscisic stress ripening gene is inhibited during leaf senescence. This gene is involved in ABA signaling during fruit ripening (Jia *et al.*, 2016) and abiotic stress responses (Li *et al.*, 2017).

3.5.2.2. Components of photosynthetic apparatus

A compromised photosynthetic apparatus is accompanying the process of leaf senescence, as shown by the yellow color of leaves. The action of catabolic enzymes leads to the degradation of chloroplasts and their components. A strong reduction of five genes encoding for Chl *a/b* binding proteins of light harvesting complex and five genes of small chain of ribulose-1,5-bisphosphate carboxylase/oxygenase (RuBisCO) was observed in senescing leaves. Then, four subunits of NADPH-quinone oxidoreductases, one 1,4-dihydroxy-2-naphthoate polyprenyl-transferase, one ferric reduction oxidase and one subunit of Cytb₆/f complex, which function in electron transport chain of photosynthetic machinery (Shimada *et al.*, 2005) were negatively regulated, as well. At the same time, one tetrapyrrole-binding protein, one glutamyl-tRNA reductase and one subunit of magnesium-chelatase, which have additional functions in Chl biosynthesis and the BURP domain of protein RD22, which is a suppressor of Chl degradation were inhibited during leaf senescence. Finally, the protein WEAK CHLOROPLAST MOVEMENT UNDER BLUE LIGHT, which is necessary for chloroplast movement and accumulation and the curvature thylakoid chloroplastic-like protein, which determines the architecture of grana in thylakoid membranes of chloroplasts (Armbruster *et al.*, 2013) were also found in the list of SDGs.

3.5.2.3. Anabolic and catabolic enzymes

The nutrient acquisition and recycling is one major goal of developmental leaf senescence and is accompanied by a number of anabolic and catabolic processes. Even though a strong induction of anabolic and catabolic enzymes has been observed in the present work, there was a negative regulation of some of such enzymes as well. One interesting finding was the strong downregulation of two acid phosphatases and two purple acid phosphatases during leaf senescence. Such enzymes are known to function in phosphorus remobilization in plants, especially during senescence (Robinson *et al.*, 2012; Gao *et al.*, 2017). In fact, an inhibition of those phosphatases had a negative impact on the successful remobilization of phosphorus to new organs (Robinson *et al.*, 2012). However, here, a downregulation of such phosphatases was observed, implying a different mode of action of these enzymes in the middle stage of barley leaf senescence. Further work is needed to understand their role in barley.

Moreover, a strong downregulation of four members of aspartic proteinases nepenthesins and three carboxypeptidases was observed. The first are classified as atypical aspartic proteinases and are involved in plant stress responses as well as in chloroplast metabolism and reproduction (Soares *et al.*, 2019). Thus, their function was inhibited in leaf senescence. As for the carboxypeptidases, it was shown that they are involved in nitrogen remobilization in barley senescing leaves (Yang *et al.*, 2004), but their mode of action is more complex, as some members are negatively regulated here in response to leaf senescence. Furthermore, members of enzymatic families of cysteine proteases, aspartyl proteases, subtilisin-like proteases and metacaspases were found in both SAG and SDG lists. Then, one nucleoporin autopeptidase was downregulated here. The exact mode of its action is not clear,

but could be involved in nuclear transport and root elongation (H. Guo *et al.*, 2021). A negative regulation of trypsin was noted, which is a serine protease and could be linked to the upregulation of two trypsin inhibitors under the same experimental conditions. Another interesting observation is the downregulation of two genes with annotation as phage capsid scaffolding protein serine peptidase and ATP-dependent protease (ATPase). These genes are studied for their function in phages and bacteria in the correct assembly of the icosahedric procapsid of bacteriophage P2 (Chang *et al.*, 2009) and in the proteasome-like degradation complex of *Escherichia coli* (Burton *et al.*, 2005), respectively. However, the reason for their presence in barley SDG list is not yet clear.

A further processing takes place by enzymes of amino acid metabolism. Again, one tryptophan aminotransferase for conversion of 2OG and L-tryptophan to indole-3-pyruvate and L-glutamate in the auxin biosynthesis pathway and one L-allo-threonine aldolase for conversion of threonine to glycine were found in both lists of SAGs and SDGs. Then, one serine incorporator and three tryptophan decarboxylases were downregulated in barley senescing leaves. The first is probably involved in serine biosynthesis, but also in incorporating serine in lipids during lipid biosynthesis and membrane formation (Inuzuka *et al.*, 2005). The second is involved in serotonin biosynthesis in eukaryotic organisms. Even though serotonin is mostly studied in mammals, research in plants shows a function in various aspects of plant development and especially during reproduction and seed maturation (Kang *et al.*, 2009). Thus, a downregulation of both genes was observed during developmental leaf senescence in barley. Finally, one aspartokinase and one branched-chain-amino-acid aminotransferase were found in the list of SDGs and are involved in amino acid biosynthesis pathways. Specifically, the first is part of the L-lysine, L-methionine and L-threonine biosynthesis, while the second is part of L-isoleucine, L-leucine and L-valine biosynthesis.

An interesting observation was the negative regulation of specific catabolic enzymes, which have already been discussed in the section of SAGs. These are members of lipases, GDSL esterases/lipases, methyltransferases and ribonucleases. Then, one cyclopropane-fatty-acyl-phospholipid synthase, which has methyltransferase and oxidoreductase activity and one omega-3 fatty acid desaturase are involved in lipid biosynthesis and were downregulated in barley leaf senescence. Finally, one S-ribonuclease binding protein with proposed function in ubiquitin degradation system, and especially in E3-ubiquitin ligase complex (O'Brien *et al.*, 2004), was negatively regulated in leaf senescence.

3.5.2.4. Carbon remobilization and cell wall organization

The last phase of leaf development refers to age-induced senescence. By definition, many biosynthetic processes are inhibited, including cell proliferation and expansion, by an induction in JA and/or inhibition of CKs (Danisman *et al.*, 2012; Zhang & Zhou, 2013). As a result, a downregulation of enzymes of cell shaping and expansion and cell wall formation was observed. These were one endoglucanase, one expansin, one glutamate racemase for cell wall biosynthesis (Hwang *et al.*, 1999), one trehalose-6-phosphate synthase for regulation of cell architecture (Chary *et al.*, 2008) and six (glucan)-endo-1,3-beta-glucanases. In addition, three dirigent proteins with function in pinoresinol biosynthesis pathway for the formation of lignin were negatively regulated during leaf senescence. Interestingly, enzymes, which are involved in degradation of cell wall components and have been reported to be upregulated in

senescing samples (Breeze *et al.*, 2011), were found in the list of SDGs here. These refer to catabolic enzymes of cell wall components, including one pectinesterase, one pectinesterase inhibitor, one laccase, one beta-galactosidase, one protein trichome birefringence and two glycosyltransferases. Obviously, components for cell wall degradation during senescence was specifically regulated in a time-dependent manner.

Furthermore, photosynthesis and other biological processes are impaired. Due to that, two carbonic anhydrases were downregulated during leaf senescence. These chloroplastic enzymes are involved in stomatal density and stomatal movement in a CO₂ dependent way (Engineer *et al.*, 2014). Then, the function of one chloroplastic fructose-bisphosphate aldolase, which acts in Calvin-Benson cycle for CO₂ fixation, was inhibited in senescing barley primary leaves (Carrera *et al.*, 2021). Same pattern was observed for one alpha-1,4 glucan phosphorylase, which was involved in carbohydrate metabolism and especially in catabolism of glycogen.

3.5.2.5. Transporters

The significance of transporters during developmental leaf senescence has already been discussed above. Many members of transporter families were positive regulated and function in nutrient and phytohormone transfer during leaf senescence. It was noted that some members of the aforementioned families were downregulated under the same conditions. This was the case for two ABC transporters, various amino acid transporters, one peptide transporter, one nitrate NRT1/ PTR transporter, one Cation/H⁺ antiporter and three lipid transfer proteins. On the contrary, a number of transporters were found only in the SDG list. Briefly, a negative regulation of nutrient transporters was observed, including a Zn²⁺-transporting ATPase, a boron transporter, a TauE/SafE sulfite exporter, one ammonium transporter, one sodium/bile acid symporter, one vacuolar iron transporter, two nodulin-like/major facilitator proteins for transport of inorganic ions and one glutamate receptor. Then, one mechanosensitive ion channel, which probably functions in plant development by determining plastid shape and size and protecting from osmotic shock (Haswell & Meyerowitz, 2006) and one protein DETOXIFICATION, which serves as efflux carrier of toxic heavy metals and other compounds (Li *et al.*, 2002) were negatively regulated in barley senescing primary leaves. It is worth mentioning that the members of the aquaporin protein family were present in the list of SDGs. These proteins form channels and ensure water transportation through plasma membrane for various physiological and biochemical processes (Ahmed *et al.*, 2021). Many of these processes, including photosynthesis, cell expansion and plant growth, are impaired during leaf senescence, justifying the downregulation of aquaporins.

3.5.2.6. Phytohormones and signaling cascades

Main regulators of senescence initiation are phytohormones and especially a combined function of JA and ethylene. The pathway of JA biosynthesis starts in chloroplasts and involves multiple steps, which are catalyzed by phospholipases, lipoxygenases, allene oxide synthases and allene oxide cyclases (Mueller, 1997). In the present work, phospholipase A, which is important for the first step of JA biosynthesis for linolenic acid formation (Ishiguro *et al.*, 2001), was downregulated. Same expression pattern was observed for three

lipoxygenases and two allene oxide synthases. Lipoxygenases are characterized as Fe- or Mn-binding oxidoreductases, with multiple functions in plant development, abiotic and biotic stress responses, leaf senescence and seed maturation, mainly through JA biosynthesis (reviewed in Viswanath *et al.*, 2020). The allene oxide synthases act downstream of lipoxygenases in JA biosynthesis pathway in chloroplasts (Mueller, 1997). As a consequence of negative regulation of JA biosynthesis, one JA-induced protein was found in SDG list. Interestingly, one enzyme involved in ethylene synthesis was also downregulated here. This is the 5'-methylthioadenosine/ *S*-adenosylhomocysteine nucleosidase, which functions in maintaining the homeostasis of *S*-adenosylmethionine. The latter is acquired by ACC synthases for the formation of ACC, which is a precursor in ethylene biosynthesis pathway (Bürstenbinder *et al.*, 2007). Our results indicated that, even though these enzymes are important for JA and ethylene biosynthesis and initiation of leaf senescence, a strong downregulation was observed here, in the middle stage of this process. It would be interesting to analyze in future experiments whether these JA and ethylene related enzymes are also downregulated at early time points of senescence, when chloroplasts are still intact.

Moreover, SAM functions in the transfer of methyl groups in nicotianamine and polyamine biosynthesis pathways (Sauter *et al.*, 2013). Nicotianamine is important for acquisition of metal ions from the roots and their reallocation to shoot parts (Klatte *et al.*, 2009). The suppressed function of nicotianamine during leaf senescence is supported, not only by the reduction of SAM, but also by the inhibition of nicotianamine synthase. On the other hand, one polyamine oxidase (PAO), which is responsible for polyamine catabolism, was strongly downregulated here. One explanation is that a limitation in polyamine biosynthesis precursor leads to a negative regulation of polyamine catabolic enzyme. The amount of polyamines is important for the regulation of leaf senescence, even though it is not clear whether their effect is positive or negative (Cai *et al.*, 2015; Sobieszczuk-Nowicka, 2017). Another suggestion is that the inhibition of PAO controls the amount of H₂O₂, which is produced during the catabolism of spermine and spermidine to putrescine and constitutes a signal for regulation of programmed cell death (Sobieszczuk-Nowicka, 2017).

Another group of phytohormones, the CKs, have many roles in cell division and expansion, shoot apical meristem formation and other developmental processes, including regulation of leaf senescence (reviewed in Höning *et al.*, 2018). The amount of endogenous CKs is important for the regulation of the aforementioned processes and CKX enzyme is responsible for the catabolism of CKs (Werner *et al.*, 2003). Here, this enzyme was downregulated.

It is obvious that phytohormones have a critical and interactive role in regulation of leaf senescence in a quantity-dependent manner. An increase or a decrease in the amount of a specific phytohormone triggers a downstream signal transmission for the activation or suppression of the respective biological process. The signal transduction involves various players, such as kinases and phosphatases. The positive regulation of those molecules during leaf senescence has been discussed earlier. A negative regulation of other kinases and phosphatases is also part of the signal transduction. Here, two cysteine-rich receptor-like kinases, one protein kinase, two receptor kinases, one PB1-domain-containing protein with possible kinase activity, one phosphatase and one leucine carboxyl methyltransferase were downregulated.

3.5.2.7. Redox regulation

The involvement of secondary metabolites in plant development, stress responses and redox regulation is well-established, but whether they are positive or negative regulators of leaf senescence is a matter of debate (Korankye *et al.*, 2017). All groups of aromatic, alkaloid and terpene metabolites are involved in plant defence against biotic stress and especially the group of terpenes has important roles in abiotic stress responses and senescence. In fact, their regulation is dependent on the coordinated action of various phytohormones, including CKs, JA and ethylene (Horiuchi *et al.*, 2001; Dani *et al.*, 2016). Here, one terpene synthase and two linalool synthases for the biosynthesis of terpenoids were downregulated. One argument is that the biosynthesis of secondary metabolites requires a carbon source from photosynthesis, which is compromised during leaf senescence, but other studies show an opposite trend (Korankye *et al.*, 2017). Same expression pattern is observed for enzymes of flavonoid and carotenoid biosynthetic pathways. The first includes one anthocyanidin reductase which is involved in the biosynthesis of condensed tannins (Xie *et al.*, 2003). An inhibition of these enzymes leads to ROS accumulation and induction of leaf senescence (Harding, 2019). The carotenoid pathway involves one xylulose kinase (Hemmerlin *et al.*, 2006), one lycopene cyclase (Cunningham *et al.*, 1996) and one beta-carotene isomerase (Alder *et al.*, 2012) and is known to be altered during leaf senescence (Dhami & Cazzonelli, 2020). Finally, one polyphenol oxidase, which is a chloroplastic enzyme that acts in oxidation of phenols to *o*-quinones (Taranto *et al.*, 2017), was found in the list of SDGs, as well.

The adverse impact of ROS on developmental processes and responses of plants is a subject of many studies. Nevertheless, the positive role of ROS as signaling compounds has also been discussed (Khanna-Chopra, 2012). It is obvious that cells regulate the homeostasis of ROS on an optimum level according to their state, by regulating ROS scavenging enzymes. A decrease in the antioxidant system leads to accumulation of ROS, promoting lipid peroxidation, membrane degradation and protease activation (Khanna-Chopra, 2012; Zentgraf & Hemleben, 2008). In the present work, the positive regulation of such enzymes was noted, but a negative regulation was also observed. This was the case for eleven genes encoding for peroxidases, one ascorbate peroxidase and three glutaredoxins. In general, plant peroxidases are involved in multiple aspects of plant development, with a focus on ROS generation and regulation (Abarca *et al.*, 2001; Passardi *et al.*, 2005). Then, ascorbate peroxidase is well-known for its function in H₂O₂ scavenging through the ascorbate-glutathione cycle and in leaf senescence (Hossain *et al.*, 2006; Ribeiro *et al.*, 2017). Similarly, glutaredoxins are involved in many aspects of ROS regulation during plant development (Mittler *et al.*, 2004; Rouhier *et al.*, 2004; Kalinina *et al.*, 2014). In the present work, a downregulation of ROS generation and scavenging enzymes was observed, maintaining a balance for the optimum senescence regulation.

Interestingly, eleven genes of cytochrome P450 and one for cytochrome b561 were found in the list of SDGs, confirming the diverse function of those enzymes. Briefly, cytochrome P450s are heme binding molecules acting as electron carriers in various cellular processes (Bolwell *et al.*, 1994). Similar function is observed for cytochrome b561, which uses ascorbate as electron donor (Griesen *et al.*, 2004). Finally, one aldehyde dehydrogenase and one lactoylglutathione lyase were downregulated during developmental leaf senescence.

The function of both enzymes in metabolizing toxic by-products of cell metabolism (Stiti *et al.*, 2011) and in glutathione release from *S*-lactoylglutathione (Singla-Pareek *et al.*, 2020), respectively, has already been discussed.

3.5.2.8. Stress responses and other genes

The stages of leaf and plant development are well-coordinated by the interplay among various genes. The time of leaf development and senescence and the transition from vegetative to reproductive state are predetermined, unless external factors affect the regulation of those processes. That implies that during leaf senescence, which is the subject of the present work, there is a regulation of genes, which are involved in other plant responses. This regulation may be positive or negative, in order to maintain plant homeostasis and achieve the optimal performance under certain conditions. Indeed, genes with known functions in abiotic and biotic stress responses were also found in the list of SDGs. Especially for abiotic stress, one LEA protein, which is regulated by ABA under various abiotic stress responses (Battaglia *et al.*, 2008), was downregulated here. Members of this gene family were found in the list of SAGs, as well, implying a counter action of LEA proteins during leaf senescence. Similar expression pattern is observed for members of HIPP family. It is well-established that HvFP1 was upregulated during senescence of barley primary leaves (Fig. 7). On the other hand, another member with homology to *Arabidopsis* AtFP3 was strongly downregulated in the RNA Seq analysis. Additionally, a leucine carboxyl methyltransferase was found in the list of SDGs and is involved in abiotic stress responses of plants (Creighton *et al.*, 2017).

Regarding the biotic stress, one universal stress protein, one disease resistance protein of TIR-NBS-LRR class and one pathogenesis related thaumatin were negatively regulated and their mode of action in biotic stress has been discussed before (Kerk *et al.*, 2003; Rajam *et al.*, 2007; Dubey & Singh, 2018; Chi *et al.*, 2019). In addition, one thionin and two MLO-like proteins are also involved in biotic stress responses and were downregulated during leaf senescence. Thionin accumulates in cell wall of infected plant cells (Iwai *et al.*, 2002) and studies showed that it is induced in *Arabidopsis* after wounding or fungal infection (Vignutelli *et al.*, 1998) and conferred resistance against bacterial infection in transgenic rice lines (Iwai *et al.*, 2002). On the other hand, MLO-like proteins are targets of powdery mildew for establishment of fungal infection in plant tissues and *loss-of-function* of those genes results in plant resistance against fungal infection (Kusch & Panstruga, 2017; Reilly *et al.*, 2021). Furthermore, one Hessian fly responsive-2-like protein, which has a role in plant defence against insects and pathogens (Puthoff *et al.*, 2005) and one formate dehydrogenase, which is involved in responses against bacterial infection (Marzorati *et al.*, 2021), were negatively regulated in the middle stage of leaf senescence. Finally, the downregulation of one FAD-binding Berberine family protein was noted here. This protein has a function in protecting plant cells from oligogalacturonides. Even though low levels of those molecules act as signal for the activation of defense responses after wounding or microbial infection, high levels disrupt normal plant development (Benedetti *et al.*, 2018).

As discussed in the section of SAGs, genes involved in other developmental processes are differentially regulated during leaf senescence. Here, those downregulated genes are provided in Table 5 in appx. 6.2.3., as their function is diverse and a conclusion regarding their role in middle stage of leaf senescence cannot be made. Similarly, genes involved in regulation of nucleic acid replication, transcription and translation, posttranscriptional and

posttranslational modifications and cytoskeleton organization were found in SDG list in Table 5 in appx. 6.2.3. Finally, a number of genes with known domains, but unknown mode of function was also included in the same section and future improvement of barley genome annotation may unravel their role in leaf senescence. Thus, the possible function of those gene families was not further analyzed in the present work.

3.6. Identification of target genes in *HvFP1* regulatory pathways

In this work, it could be shown that OE of *HvFP1* has an impact on different processes in plants. Both *HvFP1* OE lines exhibited a delayed leaf senescence process, but also a negative regulation of several ABA- and senescence-related marker genes, in both control and senescent leaves (Fig. 13, 14 and 22). To globally identify DEGs due to OE of *HvFP1*, an RNA Seq approach was performed to compare differences in transcriptomes of control and senescent WT and OE primary leaves. Analysis of the identified DEGs could give information of how *gain-of-function* of *HvFP1* affects gene expression at different developmental stages and allow the identification of possible target genes regulated via *HvFP1*-dependent regulatory pathways. Thus, it will give a deeper understanding of the function of *HvFP1*.

3.6.1. Differentially expressed genes in *HvFP1* OE lines in both control and senescing states

A comprehensive analysis of gene expression in primary leaves of OE line with that in WT resulted in 52 DEGs in both control and senescence stages (Fig. 34). Interestingly, only two genes were downregulated (Fig. 34B) and 50 genes were upregulated (Fig. 34A). This observation implies a rather positive gene regulation downstream of *HvFP1* functional network, indicating that under normal developmental conditions, *HvFP1* acts mainly as a positive regulator. Regarding the two downregulated genes, one was annotated as an F-box family protein and one as protein DETOXIFICATION. It is known, from studies in other model organisms, that F-box proteins might be involved in protein-protein interactions in regulatory processes. Then, protein DETOXIFICATION is probably involved in detoxification of cadmium or other heavy metals and toxic compounds (Li *et al.*, 2002). The exact function of both genes in barley is not yet clear. Nevertheless, it is interesting that the transcript level of an F-box protein was further reduced in senescing samples of OE line.

The list of 50 upregulated genes in *HvFP1* OE line in control as well as in senescent leaves included various representatives, which were manually sorted according to their predicted function. The group of TFs and TAs was of great interest. That included one ARF, one FRS, one Zn²⁺ finger C3H12, one MSANTD, one fibronectin type III domain protein and one cheY-like two-component responsive regulator protein. The ARF binds specifically to the auxin-responsive promoter elements for activation or inhibition of transcription. Especially the *Solanum lycopersicum* ARF10 is a positive regulator of a protochlorophyllide oxidoreductase that catalyses the formation of chlorophyllide from protochlorophyllide, a key step in Chl biosynthesis (Yuan *et al.*, 2018). Then, the FRS5 is a Zn²⁺ binding transcription activator, which was originally described to regulate light responses during development (Wang & Wang, 2015; Ma & Li, 2018). In fact, FAR1, together with FHY3, which derived from transposases, function in phyA signaling and downstream for light responses, Chl and chloroplast formation, plant circadian rhythm, ROS homeostasis, ABA and abiotic stress

responses and leaf senescence (reviewed in Wang & Wang, 2015). Another heavy metal binding TF is the C3H12, which functions in plant growth, development, abiotic and biotic stress responses (Peng *et al.*, 2012; Pi *et al.*, 2018; Xie *et al.*, 2019). The function of MSANTD TF is not clear, but their domains are linked with chromatin remodelling complexes (Barg *et al.*, 2005). Finally, the fibronectin type III domain protein resembles a PHD-finger protein that is involved in MP-dependent embryonic root meristem initiation (Saiga *et al.*, 2012), while the function of cheY-like two-component responsive regulator protein is not clear. As mentioned above, ARF10 and FRS5 are part of Chl biosynthesis and light regulation, respectively. More genes with similar functions were found in the same list of upregulated genes. These correspond to one chloroplastic phytychromobilin:ferredoxin oxidoreductase, the subunit PSI-N of PSI reaction center, the subunit S of NAD(P)H-quinone oxidoreductase and one TPR-like protein. The subunit PSI-N of PSI reaction center and the subunit S of NAD(P)H-quinone oxidoreductase are part of the photosynthetic apparatus (Yamamoto *et al.*, 2011). Then, the TPR-like protein family has members with diverse functions, including the assembly and repair of PSII of photosynthetic apparatus (Zeytuni & Zarivach, 2012; Rast *et al.*, 2016; Yang *et al.*, 2017). Finally, the phytychromobilin:ferredoxin oxidoreductase is a PFB synthase with important role in chromophore formation and downstream activation of phytychromes (Kobayashi & Masuda, 2016; Piao *et al.*, 2021). Members of FRS family and PFB synthases have distinct roles in phytychrome activation and downstream regulation of multiple aspects of plant development (Wang & Wang, 2015; Gavassi *et al.*, 2017; Junior *et al.*, 2021).

The constant induction of *HvFPI* obviously influences diverse processes in cellular organization and metabolism. These processes involve well-structured and coordinated signaling pathways. Here, a positive regulation of components of signaling cascades is observed. Among them, multiple receptors for signal perception were found, including one wall-associated receptor kinase, one muscarinic acetylcholine receptor M3 and one glutamate receptor. The latter probably acts as non-selective cation channel and could transport sodium, potassium, and Ca^{2+} ions. Then, the signal transduction is achieved through other kinases, such as one serine/threonine kinase and one cysteine-rich receptor-like protein kinase, one 1-phosphatidylinositol 4,5-bisphosphate phosphodiesterase, a SH3 domain-binding protein and an RCC1 family with FYVE Zn^{2+} finger domain. In fact, the transcript level of signal transduction genes was quite high in both mature and senescing conditions.

Another group of genes is related to metabolism of carbohydrates. That involves one glycosyl hydrolase, one phosphoenolpyruvate carboxylase for the carboxylation of phosphoenolpyruvate and the formation of oxaloacetate of tricarboxylic acid cycle (Nimmo, 2000) and one phospho-N-acetylmuramoyl-pentapeptide-transferase, which acts in glycosylation events. Furthermore, one callose synthase, one laccase and one 1,4-alpha-D-glucan maltohydrolase were strongly induced and function in callose synthesis during cytokinesis and cell wall and cell plate organization, lignin metabolism and detoxification of lignin-derived products (Xie *et al.*, 2018) and hydrolysis of (1->4)-alpha-D-glucosidic linkages in polysaccharides to remove successive maltose units from the non-reducing ends of the chains, respectively. In fact, the organization of cell wall and cell shape is regulated by components of cytoskeleton (Cai *et al.*, 2011). Here, such proteins were found to be positively regulated in *HvFPI* OE line, including a dynein assembly factor, a microtubule-associated

RP/EB protein and the heavy chain of kinesin. Moreover, genes with functions in gene replication and transcription, protein translation and in posttranslational modifications were found in the same list. Briefly, these are the histone H3, the 40S ribosomal protein, DNA and RNA polymerases, a DNA ligase, an elongation factor and components of ubiquitin proteasome pathway for protein degradation. Then, a DNL-type Zn²⁺ finger and a chaperone DnaJ-domain protein act in protein folding and stability (Zhai *et al.*, 2011; Liu & Whitham, 2013), while a DHHC-type Zn²⁺ finger protein, a SUMO-activating enzyme and a sentrin-specific protease are involved in posttranslational modifications, in the pathway of protein acylation/ palmitoylation or sumoylation, respectively. Such protein posttranslational modifications regulate abiotic stress responses (Ghimire *et al.*, 2020) and plant development (Xiang *et al.*, 2010; Zhou *et al.*, 2017).

Finally, a number of genes with distinct function were found in the list of upregulated genes in control and senescing samples of *HvFPI* OE line. Those are one acyl-[acyl-carrier-protein] desaturase, which has a role in lipid metabolism and their subsequent role in biotic stress responses (Kazaz *et al.*, 2021), a pyridoxal-5'-phosphate-dependent enzyme and an XH/XS domain-containing protein. It is worth mentioning the presence of multiple genes with annotation as transposons. These are repetitive DNA sequences, which add genetic variation to plant genome and are evolved to important functional genes, such as the FAR1/FHY components in phytochrome formation (Quesneville, 2020). Interestingly, it was shown earlier that such transposable elements are induced during senescence in *Arabidopsis* (Guo *et al.*, 2004), but also in human senescing cells (Colombo *et al.*, 2018). The exact function of these transposons is not yet clear, however evidence is increasing, showing that transposable elements have functions in regulating gene expression (Quesneville, 2020).

3.6.2. Differentially expressed genes in *HvFPI* OE lines in either control or senescing states

The constant and high expression of *HvFPI* influences the expression of some specific genes regardless of the nature of the samples, i.e. control or senescing leaves. On the other hand, there were other DEGs only in control or senescing samples, reflecting a correlation between *HvFPI* OE with the function of those genes either in control leaves or exclusively during developmental leaf senescence. Starting with the first group, 18 genes were upregulated in OE line (Fig. 34A), while no downregulated genes were detected in this comparison (Fig. 34B). Interestingly, again one member of FRS proteins and the subunit C of NADH-quinone oxidoreductase were also found here. Then, one Werner syndrome-like exonuclease, one La-related protein and four components of ubiquitin proteasome complex are involved in nucleic acid regulation and protein degradation, respectively (Merret *et al.*, 2013; Xu & Xue, 2019; Dock-Bregeon *et al.*, 2021). Other enzymes were one dihydroflavonol -4-reductase of flavonoid metabolism and one hydrolase. Two genes with function in biotic stress response were also upregulated in control leaves of OE line. Specifically, these were one rp1-like protein and one disease resistance protein. Finally, the rest of upregulated genes included one muscle calcium channel and one nitrate transporter, one dynamin for organization of cytoskeleton and two components of signaling cascades.

The comparison between senescing samples of WT and OE lines resulted in 43 upregulated (Fig. 34A) and 10 downregulated genes (Fig. 34B). Focusing on the latter, a

strong reduction in the transcript level of two RNA polymerase transcription mediators, which are involved in transcriptional regulation via gene-specific positioning of RNA polymerase II, the histone H3 and rRNA N-glycosidase, which is a negative regulator of protein translation, was observed. Same expression pattern was noted for two senescence associated proteins, with no specified known function. This correlates with the observed delay in leaf senescence in the OE lines. Then, the FGGY family of carbohydrate kinase and one peroxidase probably function in metabolic processes, while the ras-related protein RHN1, which might be involved in vesicular traffic, and the GA production enzyme GA 3-beta-dioxygenase were also found in the list of SDGs.

Focusing on the 43 upregulated genes in oe-S samples, in comparison to wt-S samples, again two members of the FRS5 TF family and one Zn²⁺ finger C3H43 protein were also found here. Other TFs and TAs were one ARIA-interacting double AP2 domain protein, one dentin sialophosphoprotein-related protein and one helicase SEN1. Again, genes involved in nucleic acid and protein modification were found, such as a helicase-like protein, the DNA topoisomerase 2, one probable staphylococcal-like nuclease CAN3, one tRNA pseudouridine synthase and one tRNA guanine-N(7)-methyltransferase, but also an inter-alpha-trypsin inhibitor, a sentrin-specific protease and members of the ubiquitin catabolic process. Then, genes involved in chromatin organization, homologous recombination and cell cycle were significantly induced. These are a 70 kDa DNA-binding replication protein, one kinesin-like protein, one regulator protein of cell division and apoptosis, one MAR-binding filament-like protein, the Zn²⁺-binding tripartite terminase, an animal RPA1 domain protein and two proteins for structural maintenance of chromosomes. It is worth noted that, again, six representatives of transposons were found in the list of upregulated genes in oe-S samples and their possible function was discussed above (Guo *et al.*, 2004; Colombo *et al.*, 2018; Quesneville, 2020).

In *HvFPI* OE line, the signaling pathways for the regulation of leaf senescence involve three protein kinases and one calmodulin protein. In addition, defense response genes were also upregulated, including the calmodulin binding MLO-like protein, the modifier of *snc1,4* protein and the disease resistance RPP13-like protein for response to bacterial infection. Then, genes with distinguished functions complete the list of upregulated genes. Specifically, those are two genes for vesicle formation and transfer, one endoglucanase of cellulose metabolism and cell wall formation, the TPR-like protein and one subunit of NAD(P)H-quinone oxidoreductase for the structure and function of photosynthetic machinery, the ACBD4 protein for lipid metabolism, modification and repair and one F-box protein with unknown function.

Overall, it seems that the state of leaf, i.e. mature or senescing, affects the number of genes, which were differentially regulated in *HvFPI* OE lines. Nevertheless, members of the same families or genes with the same functions were found in both states, implying that excess of *HvFPI* alone influences their expression pattern, independently of the developmental stage of the leaf.

3.7. Proposed model for the function of *HvFPI*

The present work showed that *HvFPI* was significantly induced in barley primary leaves in response to a number of abiotic stress conditions and during developmental leaf

senescence (Fig. 6 and 7). Furthermore, *HvFP1* was regulated by internal factors, i.e. upregulated by ABA and downregulated by CKs (Fig. 8). Even though the study of *HvFP1* KO lines did not give any notable results (Fig. 23 to 26), study of *HvFP1* OE lines showed that those plants behaved similar to WT under abiotic stress conditions, only in terms of PSII efficiency and Chl content. On a molecular level, the expression of some ABA-related genes, i.e. *HvS40*, *HvNCED* and *HvDhn1*, was suppressed in the case of drought-induced leaf senescence (Fig. 13 and 14). In the absence of stress, OE of *HvFP1* favored a delay in developmental leaf senescence, in a physiological and molecular level (Fig. 20, 21 and 22). Taking the above results together, a proposed mode of action for this protein is summarized in Fig. 37. As discussed above, various stress and developmental factors, as well as ABA, induce the expression of *HvFP1*. Then, transcriptomic data from qRT-PCR showed a suppression of *HvNCED* (Fig. 13B and 14B), which is key enzyme in ABA biosynthesis pathway (Iuchi *et al.*, 2001). One idea is that, under specific stress conditions and developmental stages, *HvFP1* acts in a negative feedback loop, which suppresses ABA accumulation and the downstream regulation of ABA-related genes, like *HvS40* (Jehanzeb *et*

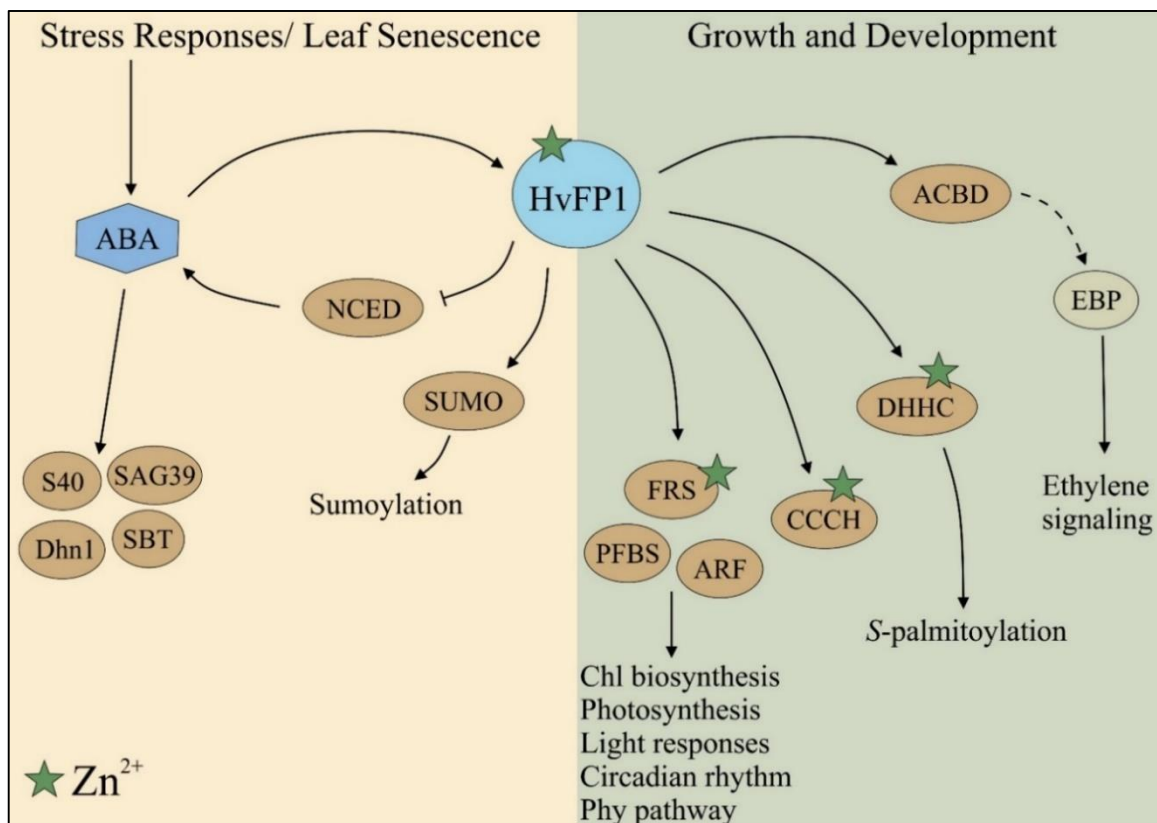


Figure 37: Schematic representation of the proposed model for the mode of function of *HvFP1*. Various abiotic stress factors, phytohormones and developmental leaf senescence influence the expression of *HvFP1*, implying a function as crosstalk factor among those processes. Study of *HvFP1* OE lines and an RNA Seq analysis revealed a positive regulation of Zn^{2+} -domain containing TFs, which downstream regulate genes with specific function in plants. A negative regulation by *HvFP1* is noted only for some stress- and senescence-marker genes and a small number of single genes, which derived from RNA Seq analysis. Positive regulations are indicated by arrows, negative regulations are indicated by bars, dashed line indicate information from literature and green stars represent the Zn^{2+} molecules.

al., 2017), *HvDhn1* (Suprunova *et al.*, 2004), *HvSAG39* (Liu *et al.*, 2010) and *HvSBT* (Wang *et al.*, 2018) (Fig. 13, 14 and 22). Such negative feedback loops in ABA signaling have already been described (Liu *et al.*, 2016; Jamsheer *et al.*, 2022) and are important for balancing major developmental processes and stress responses and for improving the fitness of the plants. The fact that CKs downregulate *HvFP1* (Fig. 8B), but also other HIPPs (T. Guo *et al.*, 2021), could enhance this hypothesis, as it is known that ABA and CK signaling pathways function in an antagonistic way (Zhang *et al.*, 2021).

In parallel, transcriptomic data from RNA Seq showed a positive regulation of stress- and growth-related genes in excess of *HvFP1*. Many of those genes include various Zn²⁺ finger C3H- and FRS5 families of TFs and Zn²⁺ binding components for protein palmitoylation, which can be associated with the presence of HMA domain in *HvFP1*. One mode of action of *HvFP1* could be the transfer of Zn²⁺ to Zn²⁺-domain containing factors, resulting in the downstream regulation of other target genes or proteins, which are involved in photosynthesis, light responses, plant growth and various stress responses (Xiang *et al.*, 2010; Peng *et al.*, 2012; Tang *et al.*, 2012; Wang & Wang, 2015; Zhou *et al.*, 2017; Ma & Li, 2018; Pi *et al.*, 2018; Xie *et al.*, 2019). This observation is in line with the work of Barth *et al.* (2009), where they confirmed an interaction between *AtHIPP26* with the Zn²⁺ finger homeodomain TF *ATHB29* for the downstream activation of stress responsive genes and of Sun *et al.* (2022), where they found that *CqHIPP34*, which is the *AtHIPP26* homolog in quinoa plants, interacts with Zn²⁺ finger-homeodomain TF *CqZF-HD14* to improve plant tolerance under drought stress. As *HvFP1* is homologous to *AtHIPP26*, a similar mode of action can be assumed. In addition, Zschiesche *et al.* (2015) could show that *AtHIPP3* indeed binds Zn²⁺ via its HMA domains. Whether this ability to bind Zn²⁺ with the HMA domain, which could be transferred to target proteins, e.g. Zn²⁺ finger TFs, is central for the regulatory function of *HvFP1* should be addressed in future experiments. One way could be to specifically mutate the cysteine residues in the HMA domain and then to test whether this modified *HvFP1* has lost its regulatory function.

Finally, another interesting outcome of the RNA Seq analysis was the positive regulation of *HvACBD4* in *HvFP1* OE lines (Fig. 36F). This is not the first report, which correlates HIPPs with the family of ACBDs, also known as ACBPs. Gao *et al.* (2009) showed that *AtACBP2*, interacts with *AtFP6* (also known as *HIPP26*), which is the closest homolog of *HvFP1* in *Arabidopsis* (Barth *et al.*, 2009). Both *AtFP6* and *AtACBP2* bind Cd²⁺ *in vivo* and they may confer resistance to Cd²⁺ stress (Gao *et al.*, 2009). Furthermore, *AtACBP2* binds [¹⁴C]linoleoyl-CoA and [¹⁴C]linolenoyl-CoA *in vitro* and could provide these acyl-CoAs for phospholipid repair after lipid peroxidation due to heavy metal stress (Gao *et al.*, 2009). The same team suggested that specific ACBPs possess additional ankyrin or kelch domains to promote protein-protein interactions in order to provide acyl-CoA esters to enzymes without acyl-CoA binding domains or, interestingly, to transfer heavy metals to TFs through interaction with HMA domain containing proteins, such as *AtHIPP26* (Li *et al.*, 2008; Gao *et al.*, 2009) or, in the present work, *HvFP1*. Then, *AtACBP2* and *AtACBP4* are known to have one mutual interaction partner, the ethylene binding protein (EBP) (Li & Chye, 2004; Li *et al.*, 2008). One hypothesis is that the interaction of ACBPs with heavy metal binding proteins could have a regulatory function by affecting the Cu²⁺-mediated ethylene binding and signaling through *AtEBP* (Li & Chye, 2004; Gao *et al.*, 2009). Finally, some members

of ACBP family are involved in abiotic stress responses and leaf senescence (reviewed in Lai & Chye, 2021), through regulation of specific phytohormones. Specifically, *AtACBP2* is induced by ABA and confers resistance to drought stress and enhances the ABA-mediated leaf senescence (Du *et al.*, 2013), while other ACBPs are involved in the biosynthesis and accumulation of JA and its derivatives (Ye *et al.*, 2016; Hu *et al.*, 2021), which then function in signal transduction during stress responses and plant defence (Truman *et al.*, 2007; Hu *et al.*, 2021).

Taking our results together, it is suggested that HvFP1 is involved in fine-tuning and balancing of stress- and development-related pathways and acts directly as a crosstalk factor in hubs among those signaling pathways or indirectly by regulating other components, such as Zn²⁺ binding TFs and TAs or a member of the ACBP family, which have similar multifunctions in regulatory hubs.

4. Materials and Methods

4.1. Materials

4.1.1. Chemicals, solvents, kits and enzymes

The chemicals and organic solvents, which were used in the present work, were provided by Carl Roth GmbH & Co. KG (Karlsruhe, Germany), AppliChem GmbH (Darmstadt, Germany), SERVA Electrophoresis GmbH (Heidelberg, Germany), MerckKGaA (Darmstadt, Germany), Th. Geyer GmbH & Co. KG (Renningen, Germany), Sigma-Aldrich GmbH (owned by MerckKGaA, Darmstadt, Germany), Duchefa Biochemie B.V. (Haarlem, Netherlands), Qiagen GmbH (Hilden, Germany), Roche Diagnostics GmbH (Mannheim, Germany), Honeywell (North Carolina, USA) and Genaxxon bioscience GmbH (Ulm, Germany). The enzymes and kits for molecular biology techniques were provided by Thermo Fisher Scientific GmbH (Massachusetts, USA), KAPA Biosystems (Massachusetts, USA), EURx Sp. z o.o. (Gdańsk, Poland), Promega (Madison, USA), Qiagen GmbH (Hilden, Germany), Biozym (Hessisch Oldendorf, Germany) and Agilent Technologies (Santa Clara, USA).

4.1.2. Vectors

The barley OE lines were constructed with pENTR™/D-TOPO® vector (Thermo Fisher Scientific), pGEM®-T vector (Promega) and pIPKb004 vector (Himmelbach *et al.*, 2007). For barley KO lines, improved shuttle vectors pMGE625, 626, 628 and 629 with scaffold sequences (Dang *et al.*, 2015; Kumar *et al.*, 2018) and gene editing vector pMGE634 (Kumar *et al.*, 2018) were utilized. Description and references for the vectors are provided in Table 11 in appx. 6.4.1.

4.1.3. Microorganisms

The *Escherichia coli* strains TOP10 and XL1-Blue MRF' and the *Agrobacterium tumefaciens* strain AGL-1 were used during the genetic transformation of barley plants.

Strains	Genotypes
<i>Escherichia coli</i> TOP10	F <i>mcrA</i> Δ(<i>mrr-hsdRMS-mcrBC</i>) φ80 <i>lacZ</i> ΔM15 Δ <i>lacX74 recA1 araD139</i> Δ(<i>ara-leu</i>) 7697 <i>galU galK rpsL Str^R endA1 nupG</i>
<i>Escherichia coli</i> XL1-Blue MRF'	Δ(<i>mcrA</i>) 183 Δ(<i>mcrCB-hsdSMR-mrr</i>) 173 <i>endA1 supE44 thi-1 recA1 gyrA96 relA1 lac</i> [F' <i>proAB lac^qZΔM15 Tn10 (Tet^R)</i>]
<i>Agrobacterium tumefaciens</i> AGL-1	AGL0 <i>recA::bla pTiBo542ΔT Mop⁺ Cb^R</i>

4.1.4. Primers

The primer sequences were designed with the Primer3web v4.1.0 software (Koressaar & Remm, 2007; Untergasser *et al.*, 2012; Koressaar *et al.*, 2018), NCBI Primer-BLAST tool (Ye *et al.*, 2012) and PrimerSelect program of Lasergene 10 Expert Sequence Analysis Software (DNASTAR Inc., Wisconsin, USA). The oligonucleotide sequences for KO lines were selected according to CRISPR-Gene Editing (<http://skl.scau.edu.cn/>) website (Xie *et al.*, 2017). Primers and oligos were provided by Eurofins genomics (Ebersberg, Germany). Primer information is provided in Table 12 in appx. 6.4.2.

4.1.5. Plant material

4.1.5.1. Overexpression lines 21.3I and 21.2A

The transformation of barley plants was done by the working group of Prof. Dr. Edgar Peiter (Institute of Agricultural and Nutrition Sciences, Martin Luther University Halle-Wittenberg) and Steffan Enhert. Barley *H. vulgare* L. cv. Golden Promise embryos were transformed via the *A. tumefaciens* system. Briefly, the genomic sequence of *HvFPI* was amplified with a forward primer containing an EcoRI site, a TOPO[®] cloning sequence and the StrepII[®] sequence, and a reverse primer containing a BamHI site. Then, the sequence was ligated into the pGEM[®]-T vector (Promega) and the vector was transformed into competent *E. coli* XL1-Blue MRF' cells. The positive colonies were sequenced for their inserts and the latter were ligated into the pENTR[™]/D-TOPO[®] vector (Thermo Fisher Scientific) by TOPO[®] cloning reaction. Competent *E. coli* TOP10 cells were transformed with the OE vector. Then, OE vectors were isolated from positive *E. coli* cultures, the insert was sequenced and ligated into the pIPKb004 vector by GATEWAY[®]Clonase reaction (Thermo Fisher Scientific). The vectors were transformed into competent *E. coli* XL1-Blue MRF' cells, isolated from *E. coli* cultures and transformed into *A. tumefaciens* strain AGL1 cells. After barley embryos were inoculated with *A. tumefaciens* culture, formation of calli and development of roots and shoots was induced.

4.1.5.2. Knock out lines 20.1At and 20.17M

The CRISPR-Cas9 system was used to transform barley *H. vulgare* L. cv. Golden Promise embryos, according to the protocol of Ordon *et al.* (2017), which was adjusted for monocots by Kumar *et al.* (2018). The procedure was carried out in a collaboration with the working group of Prof. Dr. Edgar Peiter (Institute of Agricultural and Nutrition Sciences, Martin Luther University Halle-Wittenberg). Two components are introduced into the genome: The Cas9 nuclease and synthetic single guide RNAs (sgRNA), with similarity to the target gene, together with a scaffold sequence. The sgRNAs were designed in CRISPR-GE website (Xie *et al.*, 2017) and possible off-targets were estimated with the CRISPR-GE (<http://skl.scau.edu.cn/>) website and an IPK blast (https://webblast.ipk-gatersleben.de/barley_ibsc/). The forward and reverse oligos of each sgRNA were hybridized together and cloned into the shuttle vectors pMGE625, 626, 628 and 629, under the regulation of HvU3 small nuclear RNA promoter. The vectors were inserted into *E. coli* cells and isolated from *E. coli* cultures with a Miniprep DNA purification kit (PROMEGA). Purified vectors were used in a cut/ligation reaction in order to assemble all sgRNAs in the genome editing vector pMGE634, which contains the complete gene sequence of *ZmCas9* nuclease. The pMGE634 vector was inserted in *E. coli* cells and isolated from *E. coli* cultures with a Miniprep DNA purification kit (PROMEGA). The *A. tumefaciens* strain AGL-1 cells were transformed with the vector pMGE634 and used for the transformation of barley embryos. Afterwards, transformed embryos formed calli and development of roots and shoots was induced.

4.2. Methods

4.2.1. Barley plant cultivation

Barley *H. vulgare* L. cv. Golden Promise WT or transgenic plants were used in all experimental approaches. Barley seeds were spread on wet paper and covered with aluminum foil. They were stratified at 4 °C for 96 h and germinated at 23 °C/ 18 °C in a 16 h/ 8 h

thermoperiod for 48 h in dark. Germinated seeds were sowed in 5 L Mitscherlich pots containing soil 'Werkverband typ ED73', pH 5.8 (Einheitserdewerke Werkverband e.V., Sinnatal-Altengronau, Germany) without fertilizers. Plants were grown under controlled, long day conditions in greenhouse cabinets with 16 h light 23 °C/ 8 h dark 18 °C, light intensity of 100 $\mu\text{mol m}^{-2} \text{s}^{-1}$ and 45 % relative humidity.

4.2.2. Phenotypic characterization of barley plants

Total 10 plants of each barley line were sowed in soil (ED73) and grown in a phytochamber under controlled, long-day conditions. Plants were monitored throughout their development, until the production of seeds. Photos of whole plants were taken at specific time points. Mean values and standard deviations of the length of primary leaves, the plant height, the day of flag leaf formation and the number of tillers were calculated.

4.2.3. Experimental Design/ Abiotic Stress Treatments

4.2.3.1. Drought stress

For drought stress, 10 germinated barley seeds of WT or transgenic lines were sowed in 1.5 kg soil (ED73) in each Mitscherlich pot and irrigated with 0.6 L water to reach a soil RWC of 65 % at the beginning of the experiment. Plants were grown in greenhouse cabinets and drought stress was applied after the 11th DAS by withholding water. Control plants were irrigated every two days, by weighting the pots and adding the same amount of missing water in order to maintain the soil RWC at 65 %. Every two days, Mitscherlich pots were rotated around the cabinet, in order to eliminate the effect of location on the results. At the same time points, changes in physiological parameters were monitored by measuring the PSII efficiency and the Chl content of 20 primary leaves. Samples of 4 - 5 primary leaves were taken at each time point, frozen in liquid nitrogen and stored at -80 °C.

4.2.3.2. Cold and high light stress

For cold stress, germinated barley seeds of WT or transgenic lines were sowed in 1.5 kg soil (ED73) in Mitscherlich pots and were grown in greenhouse cabinets. On the 13th DAS, plants were transferred in a phytochamber at 4 °C and 780 $\mu\text{mol m}^{-2} \text{s}^{-1}$ light intensity. Control plants remained in the greenhouse cabinets. Changes in physiological parameters were monitored by measuring the PSII efficiency and the Chl content of 10 primary leaves every 2 to 3 h for the first 24 h and then once a day for 4 days. Samples of 4 - 5 primary leaves were taken at each time point, frozen in liquid nitrogen and stored at -80 °C.

4.2.3.3. Salt stress

For salt stress, 10 germinated barley seeds of WT or transgenic lines were sowed in 1.5 kg soil (ED73) in Mitscherlich pots and were grown in greenhouse cabinets. On the 13th DAS, plants were treated with 750 mM NaCl. Control plants were irrigated with fresh water. Changes in physiological parameters were monitored by measuring the PSII efficiency and the Chl content of 10 primary leaves every 2 to 4 h for the first 24 h and then once a day for 4 days. Samples of 4 - 5 primary leaves were taken at each time point, frozen in liquid nitrogen and stored at -80 °C.

4.2.3.4. Dark induced leaf senescence

For monitoring the dark induced leaf senescence, germinated barley seeds of WT or transgenic lines were sowed in 1.5 kg soil (ED73) and were grown in greenhouse cabinets.

On the 11th DAS, the primary leaves were covered with aluminum foil, in order to apply dark conditions. Changes in physiological parameters were monitored by measuring the PSII efficiency and the Chl content of 10 primary leaves every one or two days, until the senescence of primary leaves. Samples of 4 - 5 primary leaves were taken at each time point, frozen in liquid nitrogen and stored at -80°C .

4.2.3.5. Developmental leaf senescence

For monitoring the developmental leaf senescence, 10 germinated barley seeds of WT or transgenic lines were sowed in 1.5 kg soil (ED73) in Mitscherlich pots and were grown in greenhouse cabinets. Every two days, Mitscherlich pots were rotated around the cabinet, in order to eliminate the effect of location on the results. At the same time points, changes in physiological parameters were monitored by measuring the PSII efficiency and the Chl content of 20 primary leaves, until the senescence of primary leaves. Samples of 4 - 5 primary leaves were taken at each time point, frozen in liquid nitrogen and stored at -80°C .

4.2.3.6. Phytohormone treatments

Germinated barley seeds of WT plants were sowed in soil (ED73) in Mitscherlich pots and were grown in greenhouse cabinets. On the 13th DAS, primary leaves were cut and incubated in 50 ml of phytohormone solution. The following phytohormones were first dissolved in pure EtOH and then diluted in tap water for the appropriate final concentration: 100 μM ABA, 1 mM SA, 200 μM MeJA. The following phytohormones were first dissolved in 1 M KOH and then diluted in tap water for the appropriate final concentration: 50 μM 6-BAP, 50 μM Kinetin, 50 μM Zeatin. In control primary leaves, either water with pure EtOH or water with KOH was applied. Primary leaves were harvested at 0, 4 and 24 h after incubation in phytohormone solution. Samples of 4 - 5 primary leaves were taken at each time point, frozen in liquid nitrogen and stored at -80°C .

4.2.4. Measurement of physiological parameters

4.2.4.1. Photosystem II efficiency

A MINI-PAM fluorometer (Walz GmbH, Effeltrich, Germany) was used to measure the photosynthetic efficiency of primary leaves in different treatments. The leaf area was covered with appropriate clips for 5 min for dark adaptation. Then, MINI-PAM provides saturated light and the PSII efficiency is calculated as the ratio F_v/F_m , where F_m is the maximum fluorescence and F_v is the variable fluorescence ($F_v=F_m-F_0$).

4.2.4.2. Chlorophyll content

A SPAD-502 instrument (Soil Plant Analysis Development, Konica Minolta Sensing Europe B.V., Munich, Germany) was used to measure the Chl content of primary leaves in different treatments. The Chl content is expressed in SPAD units.

4.2.5. Isolation of total RNA

Total RNA was isolated with TRIzol reagent according to the method described by Chomczynski & Mackey (1995). Plant material was ground to a fine powder using liquid nitrogen. Then, ~ 300 mg of ground plant material were mixed with 1,100 μl preheated at 60°C TRIzol reagent (38% acidic, water-saturated phenol, 0.8 M guanidinium thiocyanate, 0.4 M ammonium thiocyanate, 0.1 M Na-acetate pH 5.0 and 5% glycerol), incubated at 60°C for 10 min and centrifuged at 13,000 rpm for 10 min. Supernatant was mixed with 220 μl

chloroform by vortexing for at least 1 min. Phase separation was achieved with centrifugation at 13,000 rpm for 20 min. The upper aqueous phase, which contains the RNA, was transferred to new 1.5-ml Eppendorf tubes. For the precipitation of the RNA, 250 μ l 0.8M Na-citrate/ 1.2 M NaCl and 250 μ l isopropanol were added. Samples were mixed well, incubated for approximately 30 min at room temperature (RT) and centrifuged at 13,000 rpm for 20 min. Pellets were washed with 1 ml 70% EtOH, dried completely and dissolved in 50 μ l DEPC-treated water, by incubating at 65 °C for 10 min and vortexing. A second precipitation was applied by adding 1:10 vol. 4 M NaCl and 2 vol. pure EtOH and incubating at RT for 20 min. RNA was precipitated by centrifuging at 13,000 rpm for 20 min and washed with 190 μ l 70 % EtOH. RNA pellets were dried completely and dissolved in 30 μ l DEPC- treated water, by incubating at 65 °C for 10 min and vortexing. The concentration of total RNA was estimated by using a NanoPhotometer[®] NP80 (Implen, Munich, Germany).

4.2.6. Synthesis of complementary DNA

Complementary DNA (cDNA) synthesis was performed with the RevertAid[™] H Minus First Strand cDNA Synthesis kit (Thermo Fisher Scientific, Massachusetts, USA) in a Thermocycler Professional Trio, Biometra (Analytik, Jena, Germany). According to the protocol, 1 μ g RNA was mixed with nuclease-free water to a final volume of 10.8 μ l. Then, 1 μ l 0.5 μ g/ μ l Oligo(dT)₁₈ Primer and 0.5 μ l 0.2 μ g/ μ l Random Hexamer Primer were added and the samples were incubated at 65 °C for 5 min. Then, 4 μ l 5X Reaction Buffer (250 mM Tris-HCl pH 8.3, 250 mM KCl, 20 mM MgCl₂, 50 mM DTT), 2 μ l 10 mM dNTP mix, 1 μ l RiboLock RNase Inhibitor (20 units/ μ l) and 0.7 μ l RevertAid H Minus M-MuLV Reverse Transcriptase (200 units/ μ l) were added and the reverse transcription reaction was carried out at 25 °C for 5 min, then at 45 °C for 60 min and finally at 70 °C for 5 min.

4.2.7. Quantitative Real-Time PCR

The quantitative real-time PCR (qRT-PCR) was performed with four dilution series for each sample, corresponding to 1:4, 1:16, 1:64 or 1:256, in order to calculate and verify the efficiency of the primers. In each reaction, 2 μ l template cDNA was mixed with 2.2 μ l DEPC-treated water, 5 μ l SYBR green master mix (KAPA SYBR FAST Universal, KAPA BIOSYSTEMS) and 0.4 μ l of each gene-specific primer (5 μ M). The qRT-PCR reaction was carried out using a CFX Connect Real-Time PCR Detection System (Bio-Rad, Laboratories GmbH, CA, USA). The software of the cycler estimated the C_p values and the slopes of regression line for calculating the PCR efficiency. The relative expression level and standard errors were calculated using the REST-384[®]v2 2006 software (Relative Expression Software Tool-384, v2; Pfaffl *et al.*, 2002, Qiagen GmbH, Hilden, Germany), normalized to the reference genes *HvPP2A* (Chen *et al.*, 2015; Sudhakar Reddy *et al.*, 2016), *HvActin* (Chen *et al.*, 2015; Gines *et al.*, 2018) and *HvGCN5* (which showed a stable expression under all tested conditions).

4.2.8. DNA isolation

Isolation of DNA was performed by adapting the protocol from Brandstädter *et al.* (1994). Plant material was ground to a fine powder using liquid nitrogen. Then, ~500 mg of ground plant material were mixed with 1 ml extraction buffer (100 mM Tris-HCl pH 8.0, 500 mM NaCl, 50 mM EDTA, 1.5 % w/v SDS and 10 mM β -mercaptoethanol), homogenized well and incubated at 65 °C for 10 min. Subsequently, 300 μ l acetous potassium acetate (3 M

potassium acetate and 2 M acetic acid) were added, mixed gently and incubated at 4 °C for 10 min. Samples were centrifuged at 20,000 g for 10 min and supernatant was mixed with 300 µl phenol/ chloroform/ isomyl alcohol solution (25:24:1, equilibrated with TE buffer, pH 7.5-8.0). After brief vortex, phase separation was achieved by centrifugation at 6,000 g for 5 min. The upper phase was transferred to new 2-ml eppendorfs and nucleic acids were precipitated by adding 500 µl isopropanol, incubating at -20 °C for 10 min and centrifugation at 20,000 rcf for 20 min. The pellets were washed with 1 ml 70 % EtOH by centrifugation at 20,000 g for 5 min. Pellets were dried completely at 37 °C for 30 min and dissolved in 100 µl 10 mM Tris-HCl pH 8.0. RNA was removed by adding 100 µg/ ml RNase A (Thermo Fisher Scientific). Free RNA nucleotides were removed with a second precipitation step. Each sample was mixed with 0.1 vol. 3 M Na-acetate pH 5.0 and 2.5 vol pure EtOH. Samples were centrifuged at 20,000 g for 20 min. The pellets were washed with 1 ml 70 % EtOH, then dried at 37 °C for 30 min and dissolved in 100 µl 10 mM Tris-HCl pH 8.0. DNA concentration was estimated using a NanoPhotometer® NP80 (Implen, Munich, Germany).

4.2.9. Polymerase Chain Reaction

For Polymerase Chain Reaction (PCR), specific primers were designed to target the gene of interest. Approximately 500 ng DNA was used as template for the PCR reaction. In addition, 2 µl 10X Buffer B, 0.4 µl 25 mM MgCl₂, 1 µl 2.5 mM dNTPs, 1.2 µl 5 µM forward primer, 1.2 µl 5 µM reverse primer, 0.1 µl 5 units/ µl Taq Pol (EURx) and dH₂O were added in a final volume of 20 µl. The reaction was performed in a Thermocycler Professional Trio, Biometra (Analytik, Jena, Germany) starting at 95 °C for 30 s. Then, 35 cycles were repeated, starting at 95 °C for 30 s, then at each primer pair's T_m for 30 s and at 72 °C for X s [X=60*(product size in bp)/1000].

4.2.10. Agarose gel

Total 20 µl of the PCR reaction was mixed with 4 µl 6xDNA loading dye (Thermo Fisher Scientific) and loaded on 1 % agarose gel in 1x TAE buffer (40 mM Tris base, 20 mM acetic acid, 1 mM EDTA disodium salt) containing DNA Stain Clear G (SERVA). A GeneRuler DNA ladder mix (Thermo Fisher Scientific) was also loaded. The electrophoresis was carried out at 100 Volt for ~1 h with an Electrophoresis Power Supply instrument (Pharmacia Biotech). An E-Box Gel Documentation Imaging (Vilber, HQ France or Eberhardzell, Germany) instrument was used for gel visualization.

4.2.11. Gel extraction and DNA sequencing

Specific PCR products were extracted from 0.8 % extra pure agarose gel according to GeneJET Gel Extraction Kit (Thermo Fisher Scientific). The concentration of extracted DNA was estimated with a NanoPhotometer® NP80 (Implen, Munich, Germany). Total 5 µl of DNA with concentration up to 50 ng/ µl and total 5 µl of 5 µM primers were mixed, according to the guidelines of the company, and sent to Genewiz (Leipzig, Germany) for sequencing. The resulted sequences were visualized with the SeqMan program of Lasergene 10 Expert Sequence Analysis Software (DNASTAR Inc., Madison, WI, USA).

4.2.12. Protein isolation

Protein isolation was performed with 100 mg grounded with liquid nitrogen plant material, mixed with 500 µl 2x SDS-PAGE sample buffer (60 mM Tris-HCl pH 6.8; 20 %

Glycerol, 4 % SDS and 10 % 2-Mercaptoethanol). Samples were incubated for 3 min at 93 °C, placed on ice for 2 min and then centrifuged at 16,000 g for 10 min, at RT. Total proteins in supernatant were purified using the method adapted from Wessel & Flügge (1984). Briefly, 600 µl methanol were added to protein solution, mixed and centrifuged at 9,000 g for 5 s, at RT. Then, samples were mixed with 300 µl chloroform and centrifuged at 9,000 g for 5 s, at RT. For phase separation, 450 µl ddH₂O were added, mixed well for 30 s and centrifuged at 9,000 g for 1 min, at RT. The aqueous upper phase was carefully removed. The protein-containing inter- and lower phases were precipitated by adding 450 µl methanol and centrifugation at 16,000 g for 10 min at RT. Protein pellets dried completely at 37 °C under a fume hood and resolved in 60 µl 2x SDS-PAGE sample buffer.

4.2.13. Protein quantification

Total 3 µl were used for quantification of total proteins. Additionally, samples of Bovine Serum Albumin protein in amounts of 5 µg to 30 µg were measured in order to make a reference curve. All samples were mixed with ddH₂O to a final volume of 200 µl. Then, 800 µl amidoblack staining solution (0.1 % amidoblack, 10 % acetic acid, 90 % methanol) was added and samples were centrifuged at 20,000 g for 20 min. Pellets were washed twice with 1 ml amidoblack destaining solution (10 % acetic acid, 90 % methanol) by centrifugation at 20,000 g for 10 min. Pellets were dried completely and resuspended in 1 ml 0.2 M NaOH. Protein concentration was estimated photometrically (Specord®200 plus, Analytik Jena, Germany) by measuring the absorbance at 615 nm (maximum absorbance of amidoblack) and 750 nm (opacity correction).

4.2.14. SDS Polyacrylamide Gel Electrophoresis

Total 60 µg proteins were separated in an SDS-PAGE, which includes two polyacrylamide gels. The 4 % stacking gel consists of 625 µl 2 M Tris-HCl pH 6.8, 1.5 ml 37.5:1 Acrylamide:Bis, 100 µl 10% SDS, 10 µl TEMED, 100 µl 10 % APS and 7.65 ml dH₂O and packs the proteins together before their separation. Then, proteins enter a 14 % running gel, which consists of 3.75 ml 2 M Tris-HCl pH 8.8, 9.35 ml 37.5:1 Acrylamide:Bis, 200 µl 10% SDS, 20 µl TEMED, 200 µl 10 % APS and 6.5 ml dH₂O. Protein samples were mixed 0.5 µl 0.005 % bromophenol blue solution and were loaded on the gel. The electrophoresis took place in 1x SDS electrophoresis buffer (25 mM Tris, 192 mM Glycin, 0.1 % SDS) at 90-140 Volt. Protein bands were visible by incubating the gel in a coomassie staining solution (20 % Methanol, 20 % 5x Roti®-blue) overnight and then in a coomassie destaining solution (25 % Methanol) for ~4h.

4.2.15. Antibody production/ Western blot analysis

Specific antibodies for HvFP1 were used for detecting the protein of interest among the total plant proteins. A custom anti-HvFP1 antiserum was developed by Innovagen AB (Lund, Sweden) in rabbit. Specifically, 6xHis-HvFP1 was heterologously expressed in *E. coli* and purified with affinity chromatography. Total 1 mg of purified 6xHis-HvFP1 was used as antigene in order to produce anti-HvFP1 antibodies. Indeed, highly specific anti-HvFP1 antibodies were purified out of 9 ml anti-HvFP1 antiserum using 6xHis-HvFP1 coupled to NHS-activated Sepharose beads in combination with the purification protocol suggested by Narhi *et al.* (1997). The dialysed 7 M urea and 50 mM sodium acetate, pH 4.0 elution fraction of anti-HvFP1 antibodies was used in a western blot analysis.

For the immunoblot analysis, total 60 µg proteins were separated in a 14 % SDS-PAGE and then transferred on a PVDF membrane. The protocol includes a semi-dry transfer, using transfer buffer with methanol and 1x WBB (25 mM Tris pH 8.3, 192 mM Glycin, 20 % Methanol), at 38 mA for 1.5 h. For blocking non-specific interactions of the antibody, the membrane was incubated in blocking solution with 1x TBS-Tween20 (50 mM Tris-HCl, pH 8.0, 150 mM NaCl, 0.1 % Tween20) and 5 % non-fat milk powder at 4 °C, overnight. Then, the membrane was washed with 1x TBS-Tween20 twice for 15 min and three times for 5 min and incubated with the anti-HvFP1 primary antibodies (0.91 µg/ml in 1x TBS-Tween20) for 1.5 h at RT. The washing steps were repeated and the membrane was incubated with the secondary antibody [1:15,000 dilution of goat anti-rabbit IgG (H+L) conjugated to horseradish peroxidase (170-6515, BIO-RAD Laboratories, California, USA) in 1x TBS-Tween20] for 1 h at RT. The washing steps were repeated and the protein of interest was photochemically detected on the membrane by using a WesternBright Chemiluminescence Substrate Quantum kit (Biozym) and high performance chemiluminescence films (28906837, Cytiva Sweden AB, Sweden).

4.2.16. RNA Sequencing

4.2.16.1. Sample preparation

Total RNA of selected samples was extracted with TRIzol reagent, as described above (Chomczynski & Mackey, 1995). Then, one additional purification step was performed with the RNeasy® Mini Kit, RNA Cleanup protocol (Qiagen), in order to increase the purity of RNA. The quantity and quality of samples was estimated with a NanoPhotometer® NP80 (Implen, Munich, Germany) and an Agilent RNA 6000 Pico Kit (Agilent Technologies, CA, USA) in a Bioanalyzer2100 system (Agilent Technologies, CA, USA). An electropherogram summarized the concentration of RNA, the subunits of ribosomal RNA, the ratio of 25S and 18S rRNA and the RNA Integrity Number (RIN) value for each sample and the ladder. After the quality control, total 20 µl of each sample with concentration >40 ng/ µl were sent to Novogene Co., Ltd (United Kingdom) for the library preparation and sequencing.

4.2.16.2. Library preparation and sequencing

The NEBNext®Ultra™ RNA Library Prep Kit for Illumina® (NEB, USA) was used for generating the sequencing libraries, according to manufacturer's recommendations and each sample's sequence was assigned with index codes. More specifically, poly-T oligo-attached magnetic beads were utilized to purify mRNA from total RNA and divalent cations were used under high temperature in a NEBNext First Strand Synthesis Reaction Buffer (5x) for the fragmentation of RNA. An M-MuLV reverse transcriptase (RNase H-) and random hexamers were used for the synthesis of first strand cDNA, while a DNA pol I and an RNase H were recruited in the next step for the synthesis of second strand cDNA. Remaining overhangs were converted into blunt ends via exonuclease/polymerase activities. The 3' ends of DNA fragments were adenylated and ligated with NEBNext adaptors with hairpin loop structure to prepare for hybridization. Then, the library fragments were purified with AMPure XP system (Beckman Coulter, Beverly, USA) in order to select only those with 150-200 bp length. Before PCR, 3 µl of USER Enzyme (NEB, USA) were mixed with size-selected, adaptor-ligated cDNA at 37 °C for 15 min, followed by 5 min at 95 °C. Afterwards, Phusion High-Fidelity DNA polymerase, Universal PCR primers and Index (X) Primer were used for

the PCR. The products of PCR were purified with the AMPure XP system and the quality of the libraries was estimated with a Bioanalyzer 2100 system (Agilent Technologies). After the quality control of the libraries, a PE Cluster Kit cBot-HS (Illumina) was used in order to cluster the index-coded samples on a cBot Cluster Generation System, according to the manufacturer's instructions. Then, the libraries were sequenced using an Illumina platform and paired-end reads were generated.

4.2.16.3. Data Analysis

4.2.16.3.1. Quality control

Each step in RNA Seq was monitored in terms of quality. That applies to the raw data after the sequencing of the libraries. The raw reads were visualized in FASTQ format and processed through the fastp tool. This algorithm performs a quality control, in which adapter sequences, poly-N sequences and reads with low quality are removed from raw data and clean reads are obtained. The latter are used for the calculation of GC content and Phred quality score (Q score) for base call accuracy. Only clean data were used for downstream analysis.

4.2.16.3.2. Mapping to reference genome, novel gene prediction and quantification

Next step was mapping the paired-end clean reads to the reference genome. In the present work, the v2 of *H. vulgare* L. cv. Morex genome annotation (Mascher, 2019) was recruited as reference genome and the HISAT2 software (D. Kim *et al.*, 2015; Kim *et al.*, 2019) was used for the mapping. The sequence alignment data were visualized with the Integrative Genomics Viewer software (Robinson *et al.*, 2011). This software displayed the positions of single or multiple reads in the reference genome, and read distribution between annotated exons, introns or intergenic regions, both in adjustable scale, respectively. Additionally, it displayed the read abundance of different regions to demonstrate their expression levels in adjustable scale and provided annotation information for both, genes and splicing isoforms. The mapping information was also used as input into the regular Cufflinks assembler, which compares transcript fragments to the reference transcripts to determine if they were sufficiently different to be considered as novel. In this process, novel genes could be identified, but not further analyzed. The quantification of total novel and known transcripts was accomplished by counting the number of reads mapped to each gene with the featurecounts program. Furthermore, the gene length and sequencing depth are taken into consideration and the FPKM (Fragments Per Kilobase of transcript per Million mapped reads) value was estimated (Mortazavi *et al.*, 2008). These values reflect the gene expression level.

4.2.16.3.3. Differential expression analysis

In the present work, samples from three independent biological replicates were used for the RNA Seq analysis. For this reason, the DESeq2R package was used for the calculation of differential expression level (Anders *et al.*, 2010). DESeq2 depends on a model based on the negative binomial distribution in order to determine the differential expression and the statistical significance. The estimated *p*-values were further adjusted with the Benjamini and Hochberg's approach for False Discovery Rate: if the readcount of the *i*-th gene in *j*-th sample is K_{ij} , there is $K_{ij} \sim \text{NB}(\mu_{ij}, \sigma_{ij}^2)$. Only genes with $\log_2\text{FoldChange} < 2$ and *padj* value < 0.05 were included in the lists with differentially expressed genes. Venn diagrams were

created for the presentation of DEGs by using the online page of InteractiVenn (Heberle *et al.*, 2015).

4.2.16.3.4. Functional analysis

The functional annotation of each genes was analysed for its homologies and biological processes with Uniprot (<https://www.uniprot.org/>), Barlex (https://apex.ipk-gatersleben.de/apex/f?p=284:10:::HOME_LINK#), TAIR (<https://www.arabidopsis.org/>) and NCBI blast (<https://blast.ncbi.nlm.nih.gov/Blast.cgi>).

4.2.17. Statistical analysis

Each experimental approach included at least two or three independent biological replicates and ten to twenty technical replicates. The qRT-PCR analysis was performed at least three times, with four analytical replicates for each sample. For qRT-PCR results, the statistical analysis and the *p*-values were determined by using the Pair Wise Fixed Reallocation Randomisation Test[®], included in REST-384[®] 2006 (Relative Expression Software Tool - 384, v2.; Pfaffl *et al.* 2002).The RNA sequencing analysis was performed with samples from three independent biological replicates and the *p*-values of differential gene expression were calculated with the DESeq2R package and adjusted with the Benjamini and Hochberg's approach for False Discovery Rate.

5. References

- Abarca, D., Martín, M., & Sabater, B.** (2001). Differential leaf stress responses in young and senescent plants. *Physiologia Plantarum* **113**(3):409–415.
- Abdullah, H.M., Rodriguez, J., Salacup, J.M., Castañeda, I.S., Schnell, D.J., Pareek, A., & Dhankher, O.P.** (2021). Increased Cuticle Waxes by Overexpression of WSD1 Improves Osmotic Stress Tolerance in *Arabidopsis thaliana* and *Camelina sativa*. *International Journal of Molecular Sciences* **22**(10):5173.
- Acosta-Motos, J.R., Ortuño, M.F., Bernal-Vicente, A., Diaz-Vivancos, P., Sanchez-Blanco, M.J., & Hernandez, J.A.** (2017). Plant Responses to Salt Stress: Adaptive Mechanisms. *Agronomy* **7**(18):38.
- Ahmad, S., & Guo, Y.** (2019). Signal Transduction in Leaf Senescence: Progress and Perspective. *Plants* **8**(10):405.
- Ahmed, S., Kouser, S., Asgher, M., & Gandhi, S.G.** (2021). Plant aquaporins: A frontward to make crop plants drought resistant. *Physiologia Plantarum* **172**(2):1089–1105.
- Alder, A., Jamil, M., Marzorati, M., Bruno, M., Vermathen, M., Bigler, P., Ghisla, S., Bouwmeester, H., Beyer, P., & Al-Babili, S.** (2012) The path from β -carotene to carlactone, a strigolactone-like plant hormone. *Science* **335**(6074):1348–1351.
- An, C., & Mou, Z.** (2011). Salicylic Acid and its Function in Plant Immunity. *Journal of Integrative Plant Biology* **53**(6):412–428.
- Anders, S., & Huber, W.** (2010). Differential expression analysis for sequence count data. *Genome Biology* **11**:R106.
- Armbruster, U., Labs, M., Pribil, M., Viola, S., Xu, W., Scharfenberg, M., Hertle, A.P., Rojahn, U., Jensen, P.E., Rappaport, F., Joliot, P., Dörmann, P., Wanner, G., & Leister, D.** (2013) *Arabidopsis* CURVATURE THYLAKOID1 Proteins Modify Thylakoid Architecture by Inducing Membrane Curvature, *The Plant Cell* **25**(7):2661–2678.
- Avila-Ospina, L., Marmagne, A., Talbotec, J., Krupinska, K., & Masclaux-Daubresse, C.** (2015). The identification of new cytosolic glutamine synthetase and asparagine synthetase genes in barley (*Hordeum vulgare* L.), and their expression during leaf senescence. *Journal of Experimental Botany* **66**(7):2013–2026.
- Badr, A., Müller, K., Schäfer-Pregl, R., Rabey, H.E., Effgen, S., Ibrahim, H.H., Pozzi, C., Rohde, W., & Salamini, F.** (2000). On the Origin and Domestication History of Barley (*Hordeum vulgare*). *Molecular Biology and Evolution* **17**(4):499–510.
- Banerjee, J., Magnani, R., Nair, M., Dirk, L.M., DeBolt, S., Maiti, I.B., & Houtz, R.L.** (2013). Calmodulin-Mediated Signal Transduction Pathways in *Arabidopsis* Are Fine-Tuned by Methylation. *The Plant Cell* **25**(11):4493–4511.
- Barg, R., Sobolev, I., Eilon, T., Gur, A., Chmelnitsky, I., Shabtai, S., Grotewold, E., & Salts, Y.** (2005). The tomato early fruit specific gene *Lefsm1* defines a novel class of plant-specific SANT/MYB domain proteins. *Planta* **221**(2):197–211.
- Barth, O., Vogt, S., Uhlemann, R., Zschiesche, W., & Humbeck, K.** (2009). Stress induced and nuclear localized HIP26 from *Arabidopsis thaliana* interacts via its heavy metal associated domain with the drought stress related zinc finger transcription factor ATHB29. *Plant Molecular Biology* **69**:213–226.
- Barth, O., Zschiesche, W., Siersleben, S., & Humbeck, K.** (2004). Isolation of a novel barley cDNA encoding a nuclear protein involved in stress response and leaf senescence. *Physiologia Plantarum* **121**(2):282–293.
- Battaglia, M., Olvera-Carrillo, Y., Garcarrubio, A., Campos, F., & Covarrubias, A.A.** (2008). The Enigmatic LEA Proteins and Other Hydrophilins. *Plant Physiology* **148**(1):6–24.
- Baweja, P., & Kumar, G.** (2020). Abiotic Stress in Plants: An Overview. In *Plant Stress Biology*. Giri, B., Sharma, M.P., Eds.: Plant Stress Biology. Springer, Singapore.
- Ben Saad, R., Safi, H., Ben Hsouna, A., Brini, F., & Ben Romdhane, W.** (2019). Functional domain analysis of LmSAP protein reveals the crucial role of the zinc-finger A20 domain in abiotic stress tolerance. *Protoplasma* **256**(5):1333–1344.
- Benedetti, M., Verrascina, I., Pontiggia, D., Locci, F., Mattei, B., De Lorenzo, G., & Cervone, F.** (2018). Four *Arabidopsis* berberine bridge enzyme-like proteins are specific oxidases that inactivate the elicitor-active oligogalacturonides. *The Plant Journal* **94**(2):260–273.

- Bhat, M.A., Lone, H.A., & Mehraj, S.S.** (2019). Nutrient Remobilization During Senescence. In *Senescence Signalling and Control in Plants*. Sarwat, M., Tuteja, N., Eds.: Academic Press: London, UK pp. 227–237.
- Bolwell, G.P., Bozak, K., & Zimmerlin, A.** (1994). Plant cytochrome P450. *Phytochemistry* **37**(6):1491–1506.
- Böttcher, C., Keyzers, R.A., Boss, P.K., & Davies, C.** (2010) Sequestration of auxin by the indole-3-acetic acid-amido synthetase GH3-1 in grape berry (*Vitis vinifera* L.) and the proposed role of auxin conjugation during ripening. *Journal of Experimental Botany* **61**(13):3615–3625.
- Brady, S.M., Sarkar, S.F., Bonetta, D., & McCourt, P.** (2003). The *ABSCISIC ACID INSENSITIVE 3* (*ABI3*) gene is modulated by farnesylation and is involved in auxin signaling and lateral root development in *Arabidopsis*. *The Plant Journal* **34**(1):67–75.
- Brandstädter, J., Rollbach, C., & Theres, K.** (1994). The pattern of histone H4 expression in the tomato shoot apex changes during development. *Planta* **192**:69–74.
- Breeze, E., Harrison, E., McHattie, S., Hughes, L., Hickman, R., Hill, C., Kiddle, S., Kim, Y., Penfold, C.A., Jenkins, D., Zhang, C., Morris, K., Jenner, C., Jackson, S., Thomas, B., Tabrett, A., Legaie, R., Moore, J.D., Wild, D.L., Ott, S.; Rand, D., Beynon, J., Denby, K., Mead, A., & Buchanan-Wollaston, V.** (2011). High-Resolution Temporal Profiling of Transcripts during *Arabidopsis* Leaf Senescence Reveals a Distinct Chronology of Processes and Regulation. *The Plant Cell* **23**(3):873–894.
- Buchanan-Wollaston, V., Page, T., Harrison, E., Breeze, E., Lim, P.O., Nam, H.G., Lin, J.-F., Wu, S.-H., Swidzinski, J., Ishizaki, K., & Leaver, C.J.** (2005). Comparative transcriptome analysis reveals significant differences in gene expression and signalling pathways between developmental and dark/starvation-induced senescence in *Arabidopsis*. *The Plant Journal* **42**(4):567–585.
- Bürstenbinder, K., Rzewuski, G., Wirtz, M., Hell, R. and Sauter, M.** (2007), The role of methionine recycling for ethylene synthesis in *Arabidopsis*. *The Plant Journal* **49**:238–249.
- Burton, R.E., Baker, T.A., & Sauer, R.T.** (2005). Nucleotide-dependent substrate recognition by the AAA+ HslUV protease. *Nature Structural & Molecular Biology* **12**(3):245–251.
- Cai, G., Faleri, C., Del Casino, C., Emons, A.M.C., & Cresti, M.** (2011). Distribution of Callose Synthase, Cellulose Synthase, and Sucrose Synthase in Tobacco Pollen Tube Is Controlled in Dissimilar Ways by Actin Filaments and Microtubules. *Plant Physiology* **155**(3):1169–1190.
- Cai, G., Sobieszczuk-Nowicka, E., Aloisi, I., Fattorini, L., Serafini-Fracassini, D., & Del Duca, S.** (2015). Polyamines are common players in different facets of plant programmed cell death. *Amino Acids* **47**(1):27–44.
- Carrera, D.Á., George, G.M., Fischer-Stettler, M., Galbier, F., Eicke, S., Truernit, E., Streb, S., & Zeeman, S. C.** (2021). Distinct plastid fructose biphosphate aldolases function in photosynthetic and non-photosynthetic metabolism in *Arabidopsis*. *Journal of Experimental Botany* **72**(10):3739–3755.
- Castilhos, G., Lazzarotto, F., Spagnolo-Fonini, L., Bodanese-Zanettini, M.H., & Margis-Pinheiro, M.** (2014). Possible roles of basic helix-loop-helix transcription factors in adaptation to drought. *Plant Science* **223**:1–7.
- Chandra Babu, R., Zhang, J., Blum, A., David Ho, T.-H., Wu, R., & Nguyen, H. T.** (2004). *HVA1*, a LEA gene from barley confers dehydration tolerance in transgenic rice (*Oryza sativa* L.) via cell membrane protection. *Plant Science* **166**(4):855–862.
- Chang, J.R., Spilman, M.S., Rodenburg, C. M., & Dokland, T.** (2009). Functional domains of the bacteriophage P2 scaffolding protein: Identification of residues involved in assembly and protease activity. *Virology* **384**(1):144–150.
- Chao, Y., Xie, L., Yuan, J., Guo, T., Li, Y., Liu, F., & Han, L.** (2018). Transcriptome analysis of leaf senescence in red clover (*Trifolium pratense* L.). *Physiology and Molecular Biology of Plants* **24**(5):753–765.
- Chary, S.N., Hicks, G.R., Choi, Y.G., Carter, D., & Raikhel, N.V.** (2008). Trehalose-6-Phosphate Synthase/Phosphatase Regulates Cell Shape and Plant Architecture in *Arabidopsis*. *Plant Physiology* **146**(1):97–107.
- Chen, Y., Hu, B., Tan, Z., Liu, J., Yang, Z., Li, Z., & Huang, B.** (2015). Selection of Reference Genes for Quantitative Real-Time PCR Normalization in Creeping Bentgrass Involved in Four Abiotic Stresses. *Plant Cell Reports* **34**:1825–1834.

- Cheng, D., Tan, M., Yu, H., Li, L., Zhu, D., Chen, Y., & Jiang, M.** (2018). Comparative analysis of Cd-responsive maize and rice transcriptomes highlights Cd co-modulated orthologs. *BMC Genomics* **19**(1):709.
- Chi, Y.H., Koo, S.S., Oh, H.T., Lee, E.S., Park, J.H., Phan, K.A. T., Wi, S.D., Bae, S.B., Paeng, S.K., Chae, H.B., Kang, C.H., Kim, M.G., Kim, W.-Y., Yun, D.-J., & Lee, S.Y.** (2019). The Physiological Functions of Universal Stress Proteins and Their Molecular Mechanism to Protect Plants From Environmental Stresses. *Frontiers in Plant Science* **10**:750.
- Chomczynski, P., & Mackey, K.** (1995) Short technical reports. Modification of the TRI reagent procedure for isolation of RNA from polysaccharide- and proteoglycan-rich sources. *Biotechniques* **19**(6):942–945.
- Christ, B., & Hörtensteiner, S.** (2014) Mechanism and Significance of Chlorophyll Breakdown. *Journal of Plant Growth Regulation* **33**:4–20.
- Christ, B., Süßenbacher, I., Moser, S., Bichsel, N., Egert, A., Müller, T., Kräutler, B., & Hörtensteiner, S.** (2013). Cytochrome P450 CYP89A9 Is Involved in the Formation of Major Chlorophyll Catabolites during Leaf Senescence in *Arabidopsis*. *The Plant Cell* **25**(5):1868–1880.
- Cipollini, D.F., & Bergelson, J.** (2001). Plant Density and Nutrient Availability Constrain Constitutive and Wound-induced Expression of Trypsin Inhibitors in *Brassica napus*. *Journal of Chemical Ecology* **27**(3):593–610.
- Cobbett, C., & Goldsbrough, P.** (2002). PHYTOCHELATINS AND METALLOTHIONEINS: Roles in Heavy Metal Detoxification and Homeostasis. *Annual Review of Plant Biology* **53**(1):159-182.
- Colombo, A.R., Elias, H.K., & Ramsingh, G.** (2018). Senescence induction universally activates transposable element expression. *Cell Cycle* **17**(14):1846–1857.
- Cowan, G.H., Roberts, A.G., Jones, S., Kumar, P., Kalyandurg, P.B., Gil, J.F., Savenkoy, E.I., Hemsley, P.A., & Torrance, L.** (2018). Potato Mop-Top Virus Co-opts the Stress Sensor HIP26 for Long-Distance Movement. *Plant Physiology* **176**:2052-2070.
- Creighton, M.T., Koltun, A., Kataya, A.R.A., Maple-Grødem, J., Averkina, I.O., Heidari, B., & Lillo, C.** (2017). Methylation of protein phosphatase 2A-Influence of regulators and environmental stress factors. *Plant, Cell & Environment* **40**(10):2347–2358.
- Crowell, D.N.** (2000). Functional implications of protein isoprenylation in plants. *Progress in Lipid Research* **39**:393-408.
- Crowell, D.N., & Huizinga, D.H.** (2009). Protein isoprenylation: The fat of the matter. *Trends in Plant Science*, **14**(3):163-170.
- Cui, H., Kong, D., Liu, X., & Hao, Y.** (2014). SCARECROW, SCR-LIKE 23 and SHORT-ROOT control bundle sheath cell fate and function in *Arabidopsis thaliana*. *The Plant Journal* **78**(2):319–327.
- Cunningham, F.X.Jr., Pogson, B., Sun, Z., McDonald, K.A., DellaPenna, D., & Gantt, E.** (1996). Functional analysis of the β and ϵ lycopene cyclase enzymes of *Arabidopsis* reveals a mechanism for control of cyclic carotenoid formation. *Plant Cell* **8**(9):1613–1626.
- Cutler, S.R., Rodriguez, P.L., Finkelstein, R.R., & Abrams, S.R.** (2010). Abscisic Acid: Emergence of a Core Signaling Network. *Annual Review of Plant Biology* **61**(1):651-679.
- DalCorso, G., Farinati, S., Maistri, S., & Furini, A.** (2008). How Plants Cope with Cadmium: Staking All on Metabolism and Gene Expression. *Journal of Integrative Plant Biology* **50**(10):1268-1280.
- Dang, Y., Jia, G., Choi, J., Ma, H., Anaya, E., Ye, C., Shankar, P., & Wu, H.** (2015). Optimizing sgRNA structure to improve CRISPR-Cas9 knockout efficiency. *Genome Biology* **16**(1):280.
- Dani, K.G.S., Fineschi, S., Michelozzi, M., & Loreto, F.** (2016). Do cytokinins, volatile isoprenoids and carotenoids synergically delay leaf senescence? *Plant, Cell & Environment* **39**:1103– 1111.
- Danisman, S., van der Wal, F., Dhondt, S., Waites, R., de Folter, S., Bimbo, A., van Dijk, A.D., Muino, J.M., Cutri, L., Dornelas, M.C., Angenent, G.C., & Immink, R.G.H.** (2012). *Arabidopsis* Class I and Class II TCP Transcription Factors Regulate Jasmonic Acid Metabolism and Leaf Development Antagonistically. *Plant Physiology* **159**(4):1511–1523.
- Danquah, A., de Zelicourt, A., Colcombet, J., & Hirt, H.** (2014). The role of ABA and MAPK signaling pathways in plant abiotic stress responses. *Biotechnology Advances* **32**(1):40–52.
- Dar, N.A., Amin, I., Wani, W., Wani, S. A., Shikari, A. B., Wani, S. H., & Masoodi, K. Z.** (2017). Abscisic acid: A key regulator of abiotic stress tolerance in plants. *Plant Gene* **11**:106–111.

- de Abreu-Neto, J.B., Turchetto-Zolet, A.C., de Oliveira, L.F.V., Bodanese Zanettini, M.H., & Margis-Pinheiro, M. (2013). Heavy metal-associated isoprenylated plant protein (HIPP): Characterization of a family of proteins exclusive to plants. *FEBS Journal* **280**(7):1604-1616.
- De Bellis, L., Luvisi, A., & Alpi, A. (2020). Aconitase: To Be or not to Be Inside Plant Glyoxysomes, That Is the Question. *Biology* **9**(7):162.
- De Rienzo, F., Gabdoulline, R.R., Menziani, M.C., & Wade, R.C. (2000). Blue copper proteins: A comparative analysis of their molecular interaction properties. *Protein Science* **9**(8):1439–1454.
- Demidchik, V., Shabala, S., Isayenkov, S., Cuin, T.A., & Pottosin, I. (2018). Calcium transport across plant membranes: Mechanisms and functions. *New Phytologist* **220**(1):49–69.
- Dhami, N., & Cazzonelli, C.I. (2020) Environmental impacts on carotenoid metabolism in leaves. *Plant Growth Regulation* **92**:455–477.
- Ding, X., Cao, Y., Huang, L., Zhao, J., Xu, C., Li, X., & Wang, S. (2008). Activation of the Indole-3-Acetic Acid–Amido Synthetase GH3-8 Suppresses Expansin Expression and Promotes Salicylate- and Jasmonate-Independent Basal Immunity in Rice. *The Plant Cell* **20**(1):228–240.
- Dock-Bregeon, A.-C., Lewis, K.A., & Conte, M.R. (2021). The La-related proteins: Structures and interactions of a versatile superfamily of RNA-binding proteins. *RNA Biology* **18**(2):178–193.
- Du, Z.-Y., Chen, M.-X., Chen, Q.-F., Xiao, S., & Chye, M.-L. (2013). Overexpression of Arabidopsis acyl-CoA-binding protein ACBP2 enhances drought tolerance. *Plant, Cell & Environment* **36**(2):300–314.
- Du, H., Liu, H., & Xiong, L. (2013). Endogenous auxin and jasmonic acid levels are differentially modulated by abiotic stresses in rice. *Frontiers in Plant Science* **4**:397.
- Dubey, N., & Singh, K. (2018). Role of NBS-LRR Proteins in Plant Defense. In *Molecular Aspects of Plant-Pathogen Interaction*. Singh, A., Singh, I., Eds.: Springer, Singapore, pp 115–138.
- Dubos, C., Stracke, R., Grotewold, E., Weisshaar, B., Martin, C., & Lepiniec, L. (2010). MYB transcription factors in *Arabidopsis*. *Trends in Plant Science* **15**(10):573–581.
- Dykema, P.E., Sipes, P.R., Marie, A., Biermann, B.J., Crowell, D.N., & Randall, S.K. (1999). A new class of proteins capable of binding transition metals. *Plant Molecular Biology* **41**:139-150.
- Ebringerová, A. (2005). Structural Diversity and Application Potential of Hemicelluloses. *Macromolecular Symposia* **232**(1):1–12.
- Engineer, C.B., Ghassemian, M., Anderson, J.C., Peck, S.C., Hu, H., & Schroeder, J.I. (2014). Carbonic anhydrases, *EPF2* and a novel protease mediate CO₂ control of stomatal development. *Nature* **513**(7517):246–250.
- Fichman, Y., & Mittler, R. (2020). Rapid systemic signaling during abiotic and biotic stresses: Is the ROS wave master of all trades? *The Plant Journal* **102**(5):887–896.
- Fiorucci, A.-S., & Fankhauser, C. (2017). Plant Strategies for Enhancing Access to Sunlight. *Current Biology* **27**:931-940.
- Fischer-Kilbiński, I., Miao, Y., Roitsch, T., Zschiesche, W., Humbeck, K., & Krupinska, K. (2010). Nuclear targeted AtS40 modulates senescence associated gene expression in *Arabidopsis thaliana* during natural development and in darkness. *Plant Molecular Biology* **73**:379–390.
- Frémont, N., Riefler, M., Stolz, A., & Schmölling, T. (2013). The Arabidopsis *TUMOR PRONE5* Gene Encodes an Acetylornithine Aminotransferase Required for Arginine Biosynthesis and Root Meristem Maintenance in Blue Light. *Plant Physiology* **161**:1127–1140.
- Fujita, Y., & Bauer, C.E. (2000). Reconstitution of Light-independent Protochlorophyllide Reductase from Purified Bchl and BchN-BchB Subunits. *Journal of Biological Chemistry* **275**(31):23583–23588.
- Gan, S., & Amasino, R.M. (1995). Inhibition of Leaf Senescence by Autoregulated Production of Cytokinin. *Science* **270**:1986-1988.
- Gao, W., Lu, L., Qiu, W., Wang, C., & Shou, H. (2017). *OsPAP26* Encodes a Major Purple Acid Phosphatase and Regulates Phosphate Remobilization in Rice. *Plant and Cell Physiology* **58**(5):885–892.
- Gao, W., Xiao, S., Li, H.-Y., Tsao, S.-W., & Chye, M.-L. (2009). *Arabidopsis thaliana* acyl-CoA-binding protein ACBP2 interacts with heavy-metal-binding farnesylated protein AtFP6. *New Phytologist* **181**(1):89-102.

- Garcia-Molina, A., Altmann, M., Alkofer, A., Epple, P.M., Dangl, J.L., & Falter-Braun, P.** (2017). LSU network hubs integrate abiotic and biotic stress responses via interaction with the superoxide dismutase FSD2. *Journal of Experimental Botany* **68**(5):1185-1197.
- Gavassi, M.A., Monteiro, C.C., Campos, M.L., Melo, H.C., & Carvalho, R.F.** (2017). Phytochromes are key regulators of abiotic stress responses in tomato. *Scientia Horticulturae* **222**:126–135.
- Ghimire, S.; Tang, X.; Zhang, N.; Liu, W., & Si, H.** (2020) SUMO and SUMOylation in plant abiotic stress. *Plant Growth Regulation* **91**:317–325.
- Ghori, N.-H., Ghori, T., Hayat, M.Q., Imadi, S.R., Gul, A., Altay, V., & Ozturk, M.** (2019). Heavy metal stress and responses in plants. *International Journal of Environmental Science and Technology* **16**:1807-1828.
- Gilmour, S.J., Zarka, D.G., Stockinger, E.J., Salazar, M.P., Houghton, J.M., & Thomashow, M.F.** (1998). Low temperature regulation of the *Arabidopsis* CBF family of AP2 transcriptional activators as an early step in cold-induced *COR* gene expression. *The Plant Journal* **16**(4):433–442.
- Gines, M., Baldwin, T., Rashid, A., Bregitzer, P., Maughan, P.J., Jellen, E.N., & Klos, K.E.** (2018). Selection of Expression Reference Genes with Demonstrated Stability in Barley among a Diverse Set of Tissues and Cultivars. *Crop Science* **58**:332–341.
- Giraldo, P., Benavente, E., Manzano-Agugliaro, F., & Gimenez, E.** (2019). Worldwide Research Trends on Wheat and Barley: A Bibliometric Comparative Analysis. *Agronomy* **9**:352.
- Gray, S.B., & Brady, S.M.** (2016). Plant developmental responses to climate change. *Developmental Biology* **419**(1):64-77.
- Gregersen, P. L., Culetic, A., Boschian, L., & Krupinska, K.** (2013). Plant senescence and crop productivity. *Plant Mol Biol* **82**(6):603–22.
- Gregersen, P.L., Holm, P.B., & Krupinska, K.** (2008). Leaf senescence and nutrient remobilisation in barley and wheat. *Plant Biology* **10**:37–49.
- Griesen, D., Su, D., Bérczi, A., & Asard, H.** (2004). Localization of an Ascorbate-Reducible Cytochrome b561 in the Plant Tonoplast. *Plant Physiology* **134**(2):726–734.
- Guo, B., Wei, Y., Xu, R., Lin, S., Luan, H., Lv, C., Zhang, X., Song, X., & Xu, R.** (2016). Genome-Wide Analysis of APETALA2/Ethylene-Responsive Factor (AP2/ERF) Gene Family in Barley (*Hordeum vulgare* L.). *PLOS ONE* **11**(9):e0161322.
- Guo, H., Ayalew, H., Seethepalli, A., Dhakal, K., Griffiths, M., Ma, X.-F., & York, L.M.** (2021). Functional phenomics and genetics of the root economics space in winter wheat using high-throughput phenotyping of respiration and architecture. *New Phytologist* **232**(1):98–112.
- Guo, P., Baum, M., Grando, S., Ceccarelli, S., Bai, G., Li, R., von Korff, M., Varshney, R.K., Graner, A., & Valkoun, J.** (2009). Differentially expressed genes between drought-tolerant and drought-sensitive barley genotypes in response to drought stress during the reproductive stage. *Journal of Experimental Botany* **60**(12):3531–3544.
- Guo, T., Weber, H., Niemann, M.C.E., Theisl, L., Leonte, G., Novák, O., & Werner, T.** (2021). *Arabidopsis* HIPPI proteins regulate endoplasmic reticulum-associated degradation of CKX proteins and cytokinin responses. *Molecular Plant* **14**(11):1918-1934.
- Guo, Y., Ren, G., Zhang, K., Li, Z., Miao, Y., & Guo, H.** (2021). Leaf senescence: Progression, regulation, and application. *Molecular Horticulture* **1**(5):1-25.
- Guo, Y., Cai, Z., & Gan, S.** (2004). Transcriptome of *Arabidopsis* leaf senescence. *Plant, Cell and Environment* **27**(5):521–549.
- Gupta, A., Andrés, R.-M., & Caño-Delgado, A.I.** (2020). The physiology of plant responses to drought. *Science* **368**:266-269.
- Gut, H., & Matile, P.** (1988). Apparent induction of key enzymes of the glyoxylic acid cycle in senescent barley leaves. *Planta* **176**(4):548–550.
- Harding, S.A.** (2019). Condensed tannins: arbiters of abiotic stress tolerance? *Tree Physiology* **39**(3):341–344.
- Hare, P.D., Cress, W.A., & van Staden, J.** (1997). The involvement of cytokinins in plant responses to environmental stress. *Plant Growth Regulation* **23**:79–103.
- Harwood, W.A.** (2019). An Introduction to Barley: The Crop and the Model. In *Barley: Methods and protocols*. Walker, J. M., Eds.: Humana Press. Vol. 1900.

- Haswell, E.S., & Meyerowitz, E.M. (2006). MscS-like Proteins Control Plastid Size and Shape in *Arabidopsis thaliana*. *Current Biology* **16**(1):1–11.
- He, Y., Fukushige, H., Hildebrand, D.F., & Gan, S. (2002). Evidence Supporting a Role of Jasmonic Acid in Arabidopsis Leaf Senescence. *Plant Physiology* **128**:876–884.
- Heberle, H., Meirelles, G.V., da Silva, F.R., Telles, G.P., & Minghim, R. (2015). InteractiVenn: A web-based tool for the analysis of sets through Venn diagrams. *BMC Bioinformatics* **16**(1):169.
- Heidarvand, L., & Maali Amiri, R. (2010). What happens in plant molecular responses to cold stress? *Acta Physiologiae Plantarum* **32**(3), 419–431.
- Hemmerlin, A., Tritsch, D., Hartmann, M., Pacaud, K., Hoeffler, J.F., van Dorselaer, A., Rohmer, M., & Bach, T.J. (2006). A cytosolic Arabidopsis D-xylulose kinase catalyzes the phosphorylation of 1-deoxy-D-xylulose into a precursor of the plastidial isoprenoid pathway. *Plant Physiology* **142**(2):441–457.
- Hernández Estévez, I., & Rodríguez Hernández, M. (2020). Plant Glutathione S-transferases: An overview. *Plant Gene* **23**:100233.
- Hill, D.R. & Bendall, F. (1960). Function of the two cytochrome components in chloroplasts: a working hypothesis. *Nature* **186**: 136–137.
- Himmelbach, A., Zierold, U., Hensel, G., Riechen, J., Douchkov, D., Schweizer, P., & Kumlehn, J. (2007). A Set of Modular Binary Vectors for Transformation of Cereals. *Plant Physiology* **145**:1192–1200.
- Holub, J., Hanuš, J., Hanke, D.E., & Strnad, M. (1998). Biological activity of cytokinins derived from *Ortho*- and *Meta*-Hydroxybenzyladenine. *Plant Growth Regulation* **26**:109–115.
- Hönig, M., Plíhalová, L., Husičková, A., Nisler, J., & Doležal, K. (2018). Role of Cytokinins in Senescence, Antioxidant Defence and Photosynthesis. *International Journal of Molecular Sciences* **19**(12):4045.
- Horie, Y., Ito, H., Kusaba, M., Tanaka, R., & Tanaka, A. (2009). Participation of Chlorophyll *b* Reductase in the Initial Step of the Degradation of Light-harvesting Chlorophyll *a/b*-Protein Complexes in Arabidopsis. *Journal of Biological Chemistry* **284**(26):17449–17456.
- Horiuchi, J., Arimura, G., Ozawa R., Shimoda T., Takabayashi, J., & Nishioka, T. (2001). Exogenous ACC enhances volatiles production mediated by jasmonic acid in lima bean leaves. *FEBS Letters* **509**(2):332–336.
- Hörtensteiner, S. (2009) Stay-green regulates chlorophyll and chlorophyll-binding protein degradation during senescence. *Trends in Plant Science* **14**(3):155–162.
- Hörtensteiner, S., & Feller, U. (2002). Nitrogen metabolism and remobilization during senescence. *Journal of Experimental Botany* **53**(370):927–937.
- Hossain, Z., Kalam Azad Mandal, A., Kumar Datta, S., & Krishna Biswas, A. (2006). Decline in ascorbate peroxidase activity—A prerequisite factor for tepal senescence in gladiolus. *Journal of Plant Physiology* **163**(2):186–194.
- Hou, K., Wu, W., & Gan, S.-S. (2013). *SAUR36*, a SMALL AUXIN UP RNA Gene, Is Involved in the Promotion of Leaf Senescence in Arabidopsis. *Plant Physiology* **161**(2):1002–1009.
- Hsiao, A.-S., Haslam, R.P., Michaelson, L.V., Liao, P., Chen, Q.-F., Sooriyaarachchi, S., Mowbray, S.L., Napier, J.A., Tanner, J.A., & Chye, M.-L. (2014). Arabidopsis cytosolic acyl-CoA-binding proteins ACBP4, ACBP5 and ACBP6 have overlapping but distinct roles in seed development. *Bioscience Reports* **34**(6):e00165.
- Hu, T.-H., Lung, S.-C., Ye, Z.-W., & Chye, M.-L. (2021). Corrigendum: Depletion of Arabidopsis ACYL-COA-BINDING PROTEIN3 Affects Fatty Acid Composition in the Phloem. *Frontiers in Plant Science* **12**:632503.
- Huang, Y., Guo, Y., Liu, Y., Zhang, F., Wang, Z., Wang, H., Wang, F., Li, D., Mao, D., Luan, S., Liang, M., & Chen, L. (2018). 9-*cis*-Epoxy-carotenoid Dioxygenase 3 Regulates Plant Growth and Enhances Multi-Abiotic Stress Tolerance in Rice. *Frontiers in Plant Science* **9**:162.
- Hudson, A.O., Bless, C., Macedo, P., Chatterjee, S.P., Singh, B.K., Gilvarg, C., & Leustek, T. (2005). Biosynthesis of lysine in plants: evidence for a variant of the known bacterial pathways. *Biochimica et Biophysica Acta* **1721**(1–3):27–36.
- Hudson, A.O., Singh, B.K., Leustek, T., & Gilvarg, C. (2006). An LL -Diaminopimelate Aminotransferase Defines a Novel Variant of the Lysine Biosynthesis Pathway in Plants. *Plant Physiology* **140**(1):292–301.

- Huner, N.P.A., Öquist, G., & Sarhan, F. (1998). Energy balance and acclimation to light and cold. *Trends in Plant Science* **3**(6):224–230.
- Hur, Y.-S., Um, J.-H., Kim, S., Kim, K., Park, H.-J., Lim, J.-S., Kim, W.-Y., Jun, S.E., Yoon, E.K., Lim, J., Ohme-Takagi, M., Kim, D., Park, J., Kim, G.-T., & Cheon, C.-I. (2015). *Arabidopsis thaliana* homeobox 12 (ATHB 12), a homeodomain-leucine zipper protein, regulates leaf growth by promoting cell expansion and endoreduplication. *New Phytologist* **205**(1):316–328.
- Hwang, K.Y., Cho, C.-S., Suk, S., Sung, H.-C., Yu, Y.G., & Cho, Y. (1999). Structure and mechanism of glutamate racemase from *Aquifex pyrophilus*. *Nature structural biology* **6**(5):422–426.
- Ilyas, M., Rasheed, A., & Mahmood, T. (2016). Functional characterization of germin and germin-like protein genes in various plant species using transgenic approaches. *Biotechnology Letters* **38**(9):1405–1421.
- Inuzuka, M., Hayakawa, M., & Ingi, T. (2005). Serinc, an Activity-regulated Protein Family, Incorporates Serine into Membrane Lipid Synthesis. *Journal of Biological Chemistry* **280**(42):35776–35783.
- Ishiguro, S., Kawai-Oda, A., Ueda, J., Nishida, I., & Okada, K. (2001). The *DEFECTIVE IN ANTHER DEHISCENCE1* Gene Encodes a Novel Phospholipase A1 Catalyzing the Initial Step of Jasmonic Acid Biosynthesis, Which Synchronizes Pollen Maturation, Anther Dehiscence, and Flower Opening in *Arabidopsis*. *The Plant Cell* **13**:2191–2209.
- Iuchi, S., Kobayashi, M., Taji, T., Naramoto, M., Seki, M., Kato, T., Tabata, S., Kakubari, Y., Yamaguchi-Shinozaki, K., & Shinozaki, K. (2001). Regulation of drought tolerance by gene manipulation of 9-*cis*-epoxycarotenoid dioxygenase, a key enzyme in abscisic acid biosynthesis in *Arabidopsis*. *The Plant Journal* **27**(4):325–333.
- Iwai, T., Kaku, H., Honkura, R., Nakamura, S., Ochiai, H., Sasaki, T., & Ohashi, Y. (2002). Enhanced Resistance to Seed-Transmitted Bacterial Diseases in Transgenic Rice Plants Overproducing an Oat Cell-Wall-Bound Thionin. *Molecular Plant-Microbe Interactions* **15**(6):515–521.
- Jamsheer, M.K., Jindal, S., Sharma, M., Awasthi, P., Sreejath, S., Sharma, M., Mannully, C.T., & Laxmi, A. (2022). A negative feedback loop of TOR signaling balances growth and stress-response trade-offs in plants. *Cell Reports* **39**(1):110631.
- Janack, B., Sosoi, P., Krupinska, K., & Humbeck, K. (2016). Knockdown of WHIRLY1 Affects Drought Stress-Induced Leaf Senescence and Histone Modifications of the Senescence-Associated Gene *HvS40*. *Plants* **5**(3):37.
- Janská, A., Maršík, P., Zelenková, S., & Ovesná, J. (2009). Cold stress and acclimation - What is important for metabolic adjustment? *Plant Biology* **12**(3):395–405.
- Jaradat, M.R., Feurtado, J.A., Huang, D., Lu, Y., & Cutler, A.J. (2013). Multiple roles of the transcription factor AtMYBR1/AtMYB44 in ABA signaling, stress responses, and leaf senescence. *BMC Plant Biology* **13**(1):192.
- Jehanzeb, M., Zheng, X., & Miao, Y. (2017). The Role of the *S40* Gene Family in Leaf Senescence. *International Journal of Molecular Sciences* **18**(10):2152.
- Ji, Y., Li, Q., Liu, G., Selvaraj, G., Zheng, Z., Zou, J., & Wei, Y. (2019). Roles of Cytosolic Glutamine Synthetases in *Arabidopsis* Development and Stress Responses. *Plant and Cell Physiology* **60**(3):657–671.
- Jia, H., Jiu, S., Zhang, C., Wang, C., Tariq, P., Liu, Z., Wang, B., Cui, L., & Fang, J. (2016). Abscisic acid and sucrose regulate tomato and strawberry fruit ripening through the abscisic acid-stress-ripening transcription factor. *Plant Biotechnology Journal* **14**(10):2045–2065.
- Jibrán, R., Hunter, D.A., & Dijkwel, P.P. (2013). Hormonal regulation of leaf senescence through integration of developmental and stress signals. *Plant Molecular Biology*, **82**(6), 547–561.
- Jing, H.-C., Schippers, J.H.M., Hille, J., & Dijkwel, P.P. (2005). Ethylene-induced leaf senescence depends on age-related changes and OLD genes in *Arabidopsis*. *Journal of Experimental Botany* **56**(421):2915–2923.
- Jones, J.D.G., & Dangl, J.L. (2006). The plant immune system. *Nature* **444**(7117):323–329.
- Joshi, V., Laubengayer, K.M., Schauer, N., Fernie, A.R., & Jander, G. (2007). Two *Arabidopsis* Threonine Aldolases Are Nonredundant and Compete with Threonine Deaminase for a Common Substrate Pool. *The Plant Cell* **18**(12):3564–3575.
- Junior, C.A.S., D’Amico-Damião, V., & Carvalho, R.F. (2021). Phytochrome type B family: The abiotic stress responses signaller in plants. *Annals of Applied Biology* **178**(2):135–148.

- Kalinina, E.V., Chernov, N.N., & Novichkova, M.D.** (2014). Role of glutathione, glutathione transferase, and glutaredoxin in regulation of redox-dependent processes. *Biochemistry (Moscow)* **79**(13):1562–1583.
- Kang, J., Park, J., Choi, H., Burla, B., Kretzschmar, T., Lee, Y., & Martinoia, E.** (2011). Plant ABC Transporters. *The Arabidopsis Book* **9**:e0153.
- Kang, K., Kim, Y.-S., Park, S., & Back, K.** (2009). Senescence-Induced Serotonin Biosynthesis and Its Role in Delaying Senescence in Rice Leaves. *Plant Physiology* **150**(3):1380–1393.
- Kawai, Y., Ono, E., & Mizutani, M.** (2014). Evolution and diversity of the 2-oxoglutarate-dependent dioxygenase superfamily in plants. *The Plant Journal* **78**(2):328–343.
- Kazaz, S., Miray, R., & Baud, S.** (2021). Acyl–Acyl Carrier Protein Desaturases and Plant Biotic Interactions. *Cells* **10**(3):674.
- Keegstra, K., & Raikhel, N.** (2001). Plant glycosyltransferases. *Current Opinion in Plant Biology* **4**(3):219–224.
- Kerk, D., Bulgrien, J., Smith, D.W., & Gribskov, M.** (2003). Arabidopsis Proteins Containing Similarity to the Universal Stress Protein Domain of Bacteria. *Plant Physiology* **131**(3):1209–1219.
- Khan, M.I.R., Fatma, M., Per, T.S., Anjum, N.A., & Khan, N.A.** (2015). Salicylic acid-induced abiotic stress tolerance and underlying mechanisms in plants. *Frontiers in Plant Science* **6**:462.
- Khan, I.U., Rono, J.K., Liu, X.S., Feng, S.J., Li, H., Chen, X., & Yang, Z.M.** (2020). Functional characterization of a new metallochaperone for reducing cadmium concentration in rice crop. *Journal of Cleaner Production* **272**:123152.
- Khan, I.U., Rono, J.K., Zhang, B.Q., Liu, X.S., Wang, M.Q., Wang, L.L., Wu, X.C., Chen, X., Cao, W.H., & Yang, Z.M.** (2019). Identification of novel rice (*Oryza sativa*) HPP and HIPP genes tolerant to heavy metal toxicity. *Ecotoxicology and Environmental Safety* **175**:8–18.
- Khanna-Chopra, R.** (2012). Leaf senescence and abiotic stresses share reactive oxygen species-mediated chloroplast degradation. *Protoplasma* **249**(3):469–481.
- Kim, D., Langmead, B., & Salzberg, S.L.** (2015). HISAT: A fast spliced aligner with low memory requirements. *Nature Methods* **12**(4):357–360.
- Kim, D., Paggi, J.M., Park, C., Bennett, C., & Salzberg, S.L.** (2019). Graph-based genome alignment and genotyping with HISAT2 and HISAT-genotype. *Nature Biotechnology* **37**(8):907–915.
- Kim, J., Chang, C., & Tucker, M.L.** (2015). To grow old: Regulatory role of ethylene and jasmonic acid in senescence. *Frontiers in Plant Science* **6**(20):1–7.
- Kim, S.G., Kim, S.T., Wang, Y., Kim, S.-K., Lee, C.H., Kim, K.-K., Kim, J.-K., Lee, S.Y., & Kang, K.Y.** (2010). Overexpression of rice isoflavone reductase-like gene (*OsIRL*) confers tolerance to reactive oxygen species. *Physiologia Plantarum* **138**(1):1–9.
- Kim, T.-H., Böhmer, M., Hu, H., Nishimura, N., & Schroeder, J.I.** (2010). Guard Cell Signal Transduction Network: Advances in Understanding Abscisic Acid, CO₂, and Ca²⁺ Signaling. *Annual Review of Plant Biology* **61**:561–591.
- Kinoshita, T., Yamada, K., Hiraiwa, N., Kondo, M., Nishimura, M., & Hara-Nishimura, I.** (1999). Vacuolar processing enzyme is up-regulated in the lytic vacuoles of vegetative tissues during senescence and under various stressed conditions. *The Plant Journal* **19**(1):43–53.
- Kissoudis, C., van de Wiel, C., Visser, R.G.F., & van der Linden, G.** (2014). Enhancing crop resilience to combined abiotic and biotic stress through the dissection of physiological and molecular crosstalk. *Frontiers in Plant Science* **5**:207.
- Klatte, M., Schuler, M., Wirtz, M., Fink-Straube, C., Hell, R., & Bauer, P.** (2009). The Analysis of Arabidopsis Nicotianamine Synthase Mutants Reveals Functions for Nicotianamine in Seed Iron Loading and Iron Deficiency Responses. *Plant Physiology* **150**(1):257–271.
- Knill, T., Schuster, J., Reichelt, M., Gershenzon, J., & Binder, S.** (2008). Arabidopsis Branched-Chain Aminotransferase 3 Functions in Both Amino Acid and Glucosinolate Biosynthesis. *Plant Physiology* **146**(3):1028–1039.
- Kobayashi, K., & Masuda, T.** (2016). Transcriptional Regulation of Tetrapyrrole Biosynthesis in *Arabidopsis thaliana*. *Frontiers in Plant Science* **7**:1811.
- Kohno, M., Takato, H., Horiuchi, H., Fujita, K., & Suzuki, S.** (2012). Auxin-nonresponsive grape *Aux/IAA19* is a positive regulator of plant growth. *Molecular Biology Reports* **39**(2):911–917.

- Korankye, E.A., Lada, R., Asiedu, S., & Caldwell, C.** (2017). Plant Senescence: The Role of Volatile Terpene Compounds (VTCs). *American Journal of Plant Sciences* **8**:3120-3139.
- Koressaar, T., Lepamets, M., Kaplinski, L., Raime, K., Andreson, R., & Remm, M.** (2018). Primer3_masker: Integrating masking of template sequence with primer design software. *Bioinformatics* **34**(11):1937–1938.
- Koressaar, T., & Remm, M.** (2007). Enhancements and modifications of primer design program Primer3. *Bioinformatics* **23**(10):1289–1291.
- Koyama, T.** (2014). The roles of ethylene and transcription factors in the regulation of onset of leaf senescence. *Frontiers in Plant Science* **5**:650.
- Krieger-Liszkay, A., Krupinska, K., & Shimakawa, G.** (2019). The impact of photosynthesis on initiation of leaf senescence. *Physiologia Plantarum* **166**: 148-164.
- Krupinska, K., Dähnhardt, D., Fischer-Kilbienski, I., Kucharewicz, W., Scharrenberg, C., Trösch, M., & Buck, F.** (2014). Identification of WHIRLY1 as a Factor Binding to the Promoter of the Stress- and Senescence-Associated Gene *HvS40*. *Journal of Plant Growth Regulation* **33**(1):91–105.
- Krupinska, K., Haussühl, K., Schäfer, A., van der Kooij, T.A.W., Leckband, G., Lörz, H., & Falk, J.** (2002). A Novel Nucleus-Targeted Protein Is Expressed in Barley Leaves during Senescence and Pathogen Infection. *Plant Physiology* **130**(3):1172–1180.
- Kucharewicz, W., Distelfeld, A., Bilger, W., Müller, M., Munné-Bosch, S., Hensel, G., & Krupinska, K.** (2017). Acceleration of leaf senescence is slowed down in transgenic barley plants deficient in the DNA/RNA-binding protein WHIRLY1. *Journal of Experimental Botany* **68**(5):983–996.
- Kumar, M., Lee, S.-C., Kim, J.-Y., Kim, S.-J., Aye, S.S., & Kim, S.-R.** (2014). Over-expression of dehydrin gene, *OsDhn1*, improves drought and salt stress tolerance through scavenging of reactive oxygen species in rice (*Oryza sativa* L.). *Journal of Plant Biology* **57**(6):383–393.
- Kumar, N., Galli, M., Ordon, J., Stuttmann, J., Kogel, K.-H. & Imani, J.** (2018). Further analysis of barley MORC1 using a highly efficient RNA-guided Cas9 gene-editing system. *Plant Biotechnology Journal* **16**(11):1–12.
- Kumar, R., Kushalappa, K., Godt, D., Pidkowich, M.S., Pastorelli, S., Hepworth, S.R., & Haughn, G.W.** (2007). The *Arabidopsis* BEL1-LIKE HOMEODOMAIN Proteins SAW1 and SAW2 Act Redundantly to Regulate *KNOX* Expression Spatially in Leaf Margins. *The Plant Cell* **19**(9):2719–2735.
- Kunieda, T., Fujiwara, T., Amano, T., & Shioi, Y.** (2005). Molecular Cloning and Characterization of a Senescence-induced Tau-class Glutathione S-transferase from Barley Leaves. *Plant and Cell Physiology* **46**(9):1540–1548.
- Kuroha, T., Tokunaga, H., Kojima, M., Ueda, N., Ishida, T., Nagawa, S., Fukuda, H., Sugimoto, K., & Sakakibara, H.** (2009). Functional Analyses of *LONELY GUY* Cytokinin-Activating Enzymes Reveal the Importance of the Direct Activation Pathway in *Arabidopsis*. *The Plant Cell* **21**(10):3152–3169.
- Kusch, S., & Panstruga, R.** (2017). *mlo* -Based Resistance: An Apparently Universal “Weapon” to Defeat Powdery Mildew Disease. *Molecular Plant-Microbe Interactions* **30**(3):179–189.
- Kwon, Y., Yu, S., Lee, H., Yim, J. H., Zhu, J.-K., & Lee, B.** (2012). *Arabidopsis* Serine Decarboxylase Mutants Implicate the Roles of Ethanolamine in Plant Growth and Development. *International Journal of Molecular Sciences* **13**(3):3176–3188.
- Lai, S.-H., & Chye, M.-L.** (2021). Plant Acyl-CoA-Binding Proteins-Their Lipid and Protein Interactors in Abiotic and Biotic Stresses. *Cells* **10**(5):1064.
- Lee, S.C., & Luan, S.** (2012). ABA signal transduction at the crossroad of biotic and abiotic stress responses. *Plant, Cell & Environment* **35**(1):53–60.
- Lemoine, R., Camera, S.L., Atanassova, R., Dédaldéchamp, F., Allario, T., Pourtau, N., Bonnemain, J.-L., Laloi, M., Coutos-Thévenot, P., Maurousset, L., Faucher, M., Girousse, C., Lemonnier, P., Parrilla, J., & Durand, M.** (2013). Source-to-sink transport of sugar and regulation by environmental factors. *Frontiers in Plant Science* **272**(4).
- Li, C., Guan, Z., Liu, D., & Raetz, C.R.H.** (2011). Pathway for lipid A biosynthesis in *Arabidopsis thaliana* resembling that of *Escherichia coli*. *Proceedings of the National Academy of Sciences* **108**(28):11387–11392.
- Li, H.-Y., & Chye, M.-L.** (2003). Membrane Localization of Arabidopsis Acyl-CoA Binding Protein ACBP2. *Plant Molecular Biology* **51**:483-492.

- Li, H.-Y., & Chye, M.-L.** (2004). *Arabidopsis* Acyl-CoA-Binding Protein ACBP2 Interacts With an Ethylene-Responsive Element-Binding Protein, AtEBP, via its Ankyrin Repeats. *Plant Molecular Biology* **54**:233–243.
- Li, H.-Y., Xiao, S., & Chye, M.-L.** (2008). Ethylene- and pathogen-inducible *Arabidopsis* acyl-CoA-binding protein 4 interacts with an ethylene-responsive element binding protein. *Journal of Experimental Botany* **59**(14):3997–4006.
- Li, J., Li, Y., Yin, Z., Jiang, J., Zhang, M., Guo, X., Ye, Z., Zhao, Y., Xiong, H., Zhang, Z., Shao, Y., Jiang, C., Zhang, H., An, G., Paek, N.-C., Ali, J., & Li, Z.** (2017). *OsASR5* enhances drought tolerance through a stomatal closure pathway associated with ABA and H₂O₂ signalling in rice. *Plant Biotechnology Journal* **15**(2):183–196.
- Li, L., He, Z., Pandey, G.K., Tsuchiya, T., & Luan, S.** (2002). Functional Cloning and Characterization of a Plant Efflux Carrier for Multidrug and Heavy Metal Detoxification. *Journal of Biological Chemistry* **277**(7):5360–5368.
- Li, Z., Zhang, Y., Zou, D., Zhao, Y., Wang, H.-L., Zhang, Y., Xia, X., Luo, J., Guo, H., & Zhang, Z.** (2020). LSD 3.0: A comprehensive resource for the leaf senescence research community. *Nucleic Acids Research* **48**: D1069–D1075.
- Lim, C.W., & Lee, S.C.** (2020). ABA-Dependent and ABA-Independent Functions of RCAR5/PYL11 in Response to Cold Stress. *Frontiers in Plant Science* **11**:587620.
- Lim, P.O., Kim, H.J., & Nam, G.H.** (2007). Leaf Senescence. *Annual Review of Plant Biology* **58**(1):115–136.
- Lim, P.O., Lee, I.C., Kim, J., Kim, H.J., Ryu, J.S., Woo, H.R., & Nam, H.G.** (2010). Auxin response factor 2 (ARF2) plays a major role in regulating auxin-mediated leaf longevity. *Journal of Experimental Botany* **61**(5):1419–1430.
- Lippold, F., vom Dorp, K., Abraham, M., Hölzl, G., Wewer, V., Yilmaz, J.L., Lager, I., Montandon, C., Besagni, C., Kessler, F., Stymne, S., & Dörmann, P.** (2012). Fatty Acid Phytol Ester Synthesis in Chloroplasts of *Arabidopsis*. *The Plant Cell* **24**(5):2001–2014.
- Liu, H., Hedley, P., Cardle, L., Wright, K.M., Hein, I., Marshall, D., & Waugh, R.** (2005). Characterisation and functional analysis of two barley caleosins expressed during barley caryopsis development. *Planta* **221**(4):513–522.
- Liu, J., Liao, S., Li, M., & Du, X.** (2022). *Arabis paniculata* ApHIPP3 increases Cd tolerance by interacting with ApCHC1. *Journal of Genetics* **101**(1):21.
- Liu, J.-Z., & Whitham, S.A.** (2013). Overexpression of a soybean nuclear localized type-III DnaJ domain-containing HSP40 reveals its roles in cell death and disease resistance. *The Plant Journal* **74**(1):110–121.
- Liu, L., Zhou, Y., Szczerba, M.W., Li, X., & Lin, Y.** (2010). Identification and Application of a Rice Senescence-Associated Promoter. *Plant Physiology* **153**(3):1239–1249.
- Liu, S., Li, M., Su, L., Ge, K., Li, L., Li, X., Liu, X., & Li, L.** (2016). Negative feedback regulation of ABA biosynthesis in peanut (*Arachis hypogaea*): A transcription factor complex inhibits *AhNCED1* expression during water stress. *Scientific Reports* **6**(1):37943.
- Loix, C., Huybrechts, M., Vangronsveld, J., Gielen, M., Keunen, E., & Cuypers, A.** (2017). Reciprocal Interactions between Cadmium-Induced Cell Wall Responses and Oxidative Stress in Plants. *Frontiers in Plant Science* **8**:1867.
- Luan, W., Shen, A., Jin, Z., Song, S., Li, Z., & Sha, A.** (2013). Knockdown of *OsHox33*, a member of the class III homeodomain-leucine zipper gene family, accelerates leaf senescence in rice. *Science China Life Sciences*, **56**(12):1113–1123.
- Luoni, S.B., Astigueta, F.H., Nicosia, S., Moschen, S., Fernandez, P., & Heinz, R.** (2019). Transcription Factors Associated with Leaf Senescence in Crops. *Plants* **8**(10):411.
- Ma, L., & Li, G.** (2018). FAR1-RELATED SEQUENCE (FRS) and FRS-RELATED FACTOR (FRF) Family Proteins in *Arabidopsis* Growth and Development. *Frontiers in Plant Science* **9**:692.
- Mahlooji, M., Sharifi, R.S., Razmjoo, J., Sabzalian, M.R., & Sedghi, M.** (2018). Effect of salt stress on photosynthesis and physiological parameters of three contrasting barley genotypes. *Photosynthetica* **56**(2):549–556.

- Manara, A., Fasani, E., Molesini, B., DalCorso, G., Pennisi, F., Pandolfini, T., & Furini, A.** (2020). The Tomato Metalloprotease Inhibitor I, which Interacts with a Heavy Metal-Associated Isoprenylated Protein, Is Implicated in Plant Response to Cadmium. *Molecules* **25**:700.
- Marthe, C., Kumlehn, J., & Hensel, G.** (2015). Barley (*Hordeum vulgare* L.) Transformation Using Immature Embryos. In *Agrobacterium Protocols Methods in Molecular Biology*. Wang, K., Eds.: Springer Science+Business Media New York, New York, Vol. 1223.
- Marzorati, F., Vigani, G., Morandini, P., & Murgia, I.** (2021). Formate dehydrogenase contributes to the early *Arabidopsis thaliana* responses against *Xanthomonas campestris* pv *campestris* infection. *Physiological and Molecular Plant Pathology* **114**:101633.
- Mascher, M.** (2019). Source of the TRITEX assembly pipeline. e!DAL - Plant Genomics & Phenomics Research Data Repository 2019, doi: <https://doi.org/10.5447/IPK/2019/19>.
- Merret, R., Martino, L., Bousquet-Antonelli, C., Fneich, S., Descombin, J., Billey, É., Conte, M.R., & Deragon, J.-M.** (2013). The association of a La module with the PABP-interacting motif PAM2 is a recurrent evolutionary process that led to the neofunctionalization of La-related proteins. *RNA* **19**(1):36–50.
- Mikkelsen, M.D., & Thomashow, M.F.** (2009). A role for circadian evening elements in cold-regulated gene expression in *Arabidopsis*. *The Plant Journal* **60**(2):328–339.
- Mitra, A., Katak, S., Singh, A. N., Gaur, A., Razafindrabe, B.H.N., Kumar, P., Chatterjee, S., & Gupta, D.K.** (2021). Plant Stress, Acclimation, and Adaptation: A Review. In *Plant Growth and Stress Physiology*. Gupta, D.K., Palma J.M., Eds.: Plant in Challenging Environments; Springer International Publishing: Cham, Switzerland, Vol. 3.
- Mittler, R., Vanderauwera, S., Gollery, M., & Van Breusegem, F.** (2004). Reactive oxygen gene network of plants. *Trends in Plant Science* **9**(10):490–498.
- Morita-Yamamuro, C., Tsutsui, T., Sato, M., Yoshioka, H., Tamaoki, M., Ogawa, D., Matsuura, H., Yoshihara, T., Ikeda, A., Uyeda, I., & Yamaguchi, J.** (2005). The *Arabidopsis* Gene CAD1 Controls Programmed Cell Death in the Plant Immune System and Encodes a Protein Containing a MACPF Domain. *Plant and Cell Physiology* **46**(6):902–912.
- Mortazavi, A., Williams, B.A., McCue, K., Schaeffer, L., & Wold, B.** (2008). Mapping and quantifying mammalian transcriptomes by RNA-Seq. *Nature Methods* **5**(7):621–628.
- Moubayidin, L., Di Mambro, R., & Sabatini, S.** (2009). Cytokinin–auxin crosstalk. *Trends in Plant Science* **14**(10):557–562.
- Mueller, M.J.** (1997). Enzymes involved in jasmonic acid biosynthesis. *Physiologia Plantarum* **100**:653–663.
- Mulako, I., Farrant, J.M., Collett, H., & Illing, N.** (2008). Expression of *Xhdsi-1^{VOC}*, a novel member of the vicinal oxygen chelate (VOC) metalloenzyme superfamily, is up-regulated in leaves and roots during desiccation in the resurrection plant *Xerophyta humilis* (Bak) Dur and Schinz. *Journal of Experimental Botany* **59**(14):3885–3901.
- Munns, R.** (2005). Genes and salt tolerance: Bringing them together. *New Phytologist* **167**(3):645–663.
- Nagatoshi, M., Terasaka, K., Nagatsu, A., & Mizukami, H.** (2011). Iridoid-specific Glucosyltransferase from *Gardenia jasminoides*. *Journal of Biological Chemistry* **286**(37):32866–32874.
- Nakamoto, H., & Vigh, L.** (2007). The small heat shock proteins and their clients. *Cellular and Molecular Life Sciences* **64**:294–306.
- Nakashima, K., Fujita, Y., Katsura, K., Maruyama, K., Narusaka, Y., Seki, M., Shinozaki, K., & Yamaguchi-Shinozaki, K.** (2006). Transcriptional Regulation of ABI3- and ABA-responsive Genes Including RD29B and RD29A in Seeds, Germinating Embryos, and Seedlings of *Arabidopsis*. *Plant Molecular Biology* **60**(1):51–68.
- Narhi, L.O., Caughey, D.J., Horan, T.P., Kita, Y., Chang, D., & Arakawa, T.** (1997). Fractionation and Characterization of Polyclonal Antibodies Using Three Progressively More Chaotropic Solvents. *Analytical Biochemistry* **253**(2):246–252.
- Nimmo, H.G.** (2000). The regulation of phosphoenolpyruvate carboxylase in CAM plants. *Trends in Plant Science* **5**(2):75–80.

- North, H.M., Almeida, A.D., Boutin, J.-P., Frey, A., To, A., Botran, L., Sotta, B., & Marion-Poll, A. (2007). The *Arabidopsis* ABA-deficient mutant *aba4* demonstrates that the major route for stress-induced ABA accumulation is via neoxanthin isomers. *The Plant Journal* **50**(5):810–824.
- Noutoshi, Y., Kuromori, T., Wada, T., Hirayama, T., Kamiya, A., Imura, Y., Yasuda, M., Nakashita, H., Shirasu, K., & Shinozaki, K. (2006). Loss of *NECROTIC SPOTTED LESIONS 1* associates with cell death and defense responses in *Arabidopsis thaliana*. *Plant Molecular Biology* **62**:29–42.
- O'Brien, M., Major, G., Chantha, S.-C., & Matton, D.P. (2004). Isolation of S-RNase binding proteins from *Solanum chacoense*: Identification of an SBP1 (RING finger protein) orthologue. *Sexual Plant Reproduction* **17**(2):81–87.
- Ogata, J., Kanno, Y., Itoh, Y., Tsugawa, H., Suzuki, M. (2005). Anthocyanin biosynthesis in roses. *Nature* **435**:757–758.
- Ohmiya, A., Oda-Yamamizo, C., & Kishimoto, S. (2019). Overexpression of *CONSTANS-like 16* enhances chlorophyll accumulation in petunia corollas. *Plant Science* **280**:90–96.
- Ordon, J., Gantner, J., Kemna, J., Schwalgun, L., Reschke, M., Streubel, J., Boch, J. & Stuttmann, J. (2017). Generation of chromosomal deletions in dicotyledonous plants employing a user-friendly genome editing toolkit. *The Plant Journal* **89**:155–168.
- Orendi, G., Zimmermann, P., Baar, C., & Zentgraf, U. (2001). Loss of stress-induced expression of catalase3 during leaf senescence in *Arabidopsis thaliana* is restricted to oxidative stress. *Plant Science* **161**(2):301–314.
- Pandian, B.A., Sathishraj, R., Djanaguairaman, M., Prasad, P.V.V., & Jugulam, M. (2020). Role of Cytochrome P450 Enzymes in Plant Stress Response. *Antioxidants* **9**(5):454.
- Paponov, I.A., Paponov, M., Teale, W., Menges, M., Chakrabortee, S., Murray, J.A.H., & Palme, K. (2008). Comprehensive Transcriptome Analysis of Auxin Responses in *Arabidopsis*. *Molecular Plant* **1**(2):321–337.
- Park, D.-Y., Shim, Y., Gi, E., Lee, B.-D., An, G., Kang, K., & Paek, N.-C. (2018). The MYB-related transcription factor RADIALIS-LIKE3 (OsRL3) functions in ABA-induced leaf senescence and salt sensitivity in rice. *Environmental and Experimental Botany* **156**:86–95.
- Parthasarathy, A., Adams, L.E., Savka, F.C., & Hudson, A.O. (2019). The *Arabidopsis thaliana* gene annotated by the locus tag At3g08860 encodes alanine aminotransferase. *Plant Direct* **3**:1–10.
- Partridge, M., & Murphy, D.J. (2009). Roles of a membrane-bound caleosin and putative peroxygenase in biotic and abiotic stress responses in *Arabidopsis*. *Plant Physiology and Biochemistry* **47**(9):796–806.
- Passardi, F., Cosio, C., Penel, C., & Dunand, C. (2005). Peroxidases have more functions than a Swiss army knife. *Plant Cell Reports* **24**(5):255–265.
- Patel, J., Ariyaratne, M., Ahmed, S., Ge, L., Phuntumart, V., Kalinoski, A., & Morris, P.F. (2017). Dual functioning of plant arginases provides a third route for putrescine synthesis. *Plant Science* **262**:62–73.
- Pauwels, L., & Goossens, A. (2011). The JAZ Proteins: A Crucial Interface in the Jasmonate Signaling Cascade. *The Plant Cell* **23**(9):3089–3100.
- Pei, Z.-M., Ghassemian, M., Kwak, C.M., McCourt, P., & Schroeder, J.I. (1998). Role of Farnesyltransferase in ABA Regulation of Guard Cell Anion Channels and Plant Water Loss. *Science* **282**:287–290.
- Peng, X., Zhao, Y., Cao, J., Zhang, W., Jiang, H., Li, X., Ma, Q., Zhu, S., & Cheng, B. (2012). CCCH-Type Zinc Finger Family in Maize: Genome-Wide Identification, Classification and Expression Profiling under Abscisic Acid and Drought Treatments. *PLoS ONE* **7**(7):e40120.
- Pereira Mendes, M., Hickman, R., Van Verk, M.C., Nieuwendijk, N.M., Reinstädler, A., Panstruga, R., Pieterse, C.M.J., & Van Wees, S.C.M. (2021). A family of pathogen-induced cysteine-rich transmembrane proteins is involved in plant disease resistance. *Planta* **253**(5):102.
- Pfaffl, M.W., Horgan, G.W., & Dempfle, L. (2002). Relative expression software tool (REST[®]) for group-wise comparison and statistical analysis of relative expression results in real-time PCR. *Nucleic Acids Research* **30**(9):e36.
- Pi, B., He, X., Ruan, Y., Jang, J.-C., & Huang, Y. (2018). Genome-wide analysis and stress-responsive expression of CCCH zinc finger family genes in *Brassica rapa*. *BMC Plant Biology* **18**(1):373.

- Piao, M., Zou, J., Li, Z., Zhang, J., Yang, L., Yao, N., Li, Y., Li, Y., Tang, H., Zhang, L., Yang, D., Yang, Z., Du, X., & Zuo, Z. (2021). The *Arabidopsis* HY2 Gene Acts as a Positive Regulator of NaCl Signaling during Seed Germination. *International Journal of Molecular Sciences* **22**(16):9009.
- Podzimska-Sroka, D., O'Shea, C., Gregersen, P.L., & Skriver, K. (2015). NAC Transcription Factors in Senescence: From Molecular Structure to Function in Crops. *Plants* **4**(3):412–448.
- Pružinská, A., Tanner, G., Aubry, S., Anders, I., Moser, S., Müller, T., Ongania, K.-H., Kräutler, B., Youn, J.-Y., Liljegren, S.J., & Hörtensteiner, S. (2005). Chlorophyll Breakdown in Senescent *Arabidopsis* Leaves. Characterization of Chlorophyll Catabolites and of Chlorophyll Catabolic Enzymes Involved in the Degreening Reaction. *Plant Physiology* **139**(1): 52–63.
- Puthoff, D.P., Sardesai, N., Subramanyam, S., Nemacheck, J.A., & Williams, C.E. (2005). *Hfr-2*, a wheat cytolytic toxin-like gene, is up-regulated by virulent Hessian fly larval feeding. *Molecular Plant Pathology* **6**(4):411–423.
- Putterill, J., Robson, F., Lee, K., Simon, R., & Coupland, G. (1995). The *CONSTANS* gene of *Arabidopsis* promotes flowering and encodes a protein showing similarities to zinc finger transcription factors. *Cell* **80**(6):847–857.
- Qi, T., Wang, J., Huang, H., Liu, B., Gao, H., Liu, Y., Song, S., & Xie, D. (2015). Regulation of Jasmonate-Induced Leaf Senescence by Antagonism between bHLH Subgroup IIIe and IIId Factors in *Arabidopsis*. *The Plant Cell* **27**(6):1634–1649.
- Qian, Y., Zhang, T., Yu, Y., Gou, L., Yang, J., Xu, J., & Pi, E. (2021). Regulatory Mechanisms of bHLH Transcription Factors in Plant Adaptive Responses to Various Abiotic Stresses. *Frontiers in Plant Science* **12**:677611.
- Quesneville, H. (2020). Twenty years of transposable element analysis in the *Arabidopsis thaliana* genome. *Mobile DNA* **11**(1):28.
- Radakovic, Z.S., Anjam, M.S., Escobar, E., Chopra, D., Cabrera, J., Silva, A.C., Escobar, C., Sobczak, M., Grundler, F.M.W., & Siddique, S. (2018). *Arabidopsis* *HIPP27* is a host susceptibility gene for the beet cyst nematode *Heterodera schachtii*. *Molecular Plant Pathology* **19**(8):1917-1928.
- Raghavendra, A.S., Gonugunta, V.K., Christmann, A., & Grill, E. (2010). ABA perception and signalling. *Trends in Plant Science* **15**(7):395-401.
- Rajam, M.V., Chandola, N., Goud, S.P., Singh, D., Kashyap, V., Choudhary, M.L., & Sihachakr, D. (2007). Thaumatin gene confers resistance to fungal pathogens as well as tolerance to abiotic stresses in transgenic tobacco plants. *Biologia Plantarum* **51**(1):135–141.
- Ranty, B., Aldon, D., Cotellet, V., Galaud, J.-P., Thuleau, P., & Mazars, C. (2016). Calcium Sensors as Key Hubs in Plant Responses to Biotic and Abiotic Stresses. *Frontiers in Plant Science* **7**:327.
- Rast, A., Rengstl, B., Heinz, S., Klingl, A., & Nickelsen, J. (2016). The Role of Slr0151, a Tetratricopeptide Repeat Protein from *Synechocystis* sp. PCC 6803, during Photosystem II Assembly and Repair. *Frontiers in Plant Science* **7**:605.
- Reilly, A., Gibriel, H.A.Y., Karki, S.J., Twamley, A., Finnan, J., Kildea, S., & Feechan, A. (2021). Genome-wide identification of the oat *MLO* family and identification of a candidate *AsMLO* associated with powdery mildew susceptibility. *Plant Biology*. [Preprint]
- Ren, H., & Gray, W.M. (2015). SAUR Proteins as Effectors of Hormonal and Environmental Signals in Plant Growth. *Molecular Plant* **8**(8):1153–1164.
- Rentsch, D., Schmidt, S., & Tegeder, M. (2007). Transporters for uptake and allocation of organic nitrogen compounds in plants. *FEBS Letters* **581**:2281–2289.
- Resnick, J.S., Rivarola, M., & Chang, C. (2008). Involvement of *RTE1* in conformational changes promoting ETR1 ethylene receptor signaling in *Arabidopsis*. *The Plant Journal* **56**(3):423–431.
- Reszczyńska, E., & Hanaka, A. (2020). Lipids Composition in Plant Membranes. *Cell Biochemistry and Biophysics* **78**:401–414.
- Ribeiro, C.W., Korbes, A.P., Garighan, J.A., Jardim-Messeder, D., Carvalho, F.E.L., Sousa, R.H.V., Caverzan, A., Teixeira, F.K., Silveira, J.A.G., & Margis-Pinheiro, M. (2017). Rice peroxisomal ascorbate peroxidase knockdown affects ROS signaling and triggers early leaf senescence. *Plant Science* **263**:55–65.

- Rippert, P., & Matringe, M.** (2002). Purification and kinetic analysis of the two recombinant arogenate dehydrogenase isoforms of *Arabidopsis thaliana*. *European Journal of Biochemistry* **269**(19):4753–4761.
- Roberts, I.N., Veliz, C.G., Criado, M.V., Signorini, A., Simonetti, E., & Caputo, C.** (2017). Identification and expression analysis of 11 subtilase genes during natural and induced senescence of barley plants. *Journal of Plant Physiology* **211**:70–80.
- Robinson, J.T., Thorvaldsdóttir, H., Winckler, W., Guttman, M., Lander, E., Getz, G., & Mesirov, J.** (2011). Integrative genomics viewer. *Nature biotechnology* **29**(1):24–26.
- Robinson, W.D., Carson, I., Ying, S., Ellis, K. and Plaxton, W.C.** (2012). Eliminating the purple acid phosphatase AtPAP26 in *Arabidopsis thaliana* delays leaf senescence and impairs phosphorus remobilization. *New Phytologist* **196**:1024–1029.
- Rochaix, J.-D.** (2011). Regulation of photosynthetic electron transport. *Biochim Biophysica Acta Bioenergetics* **1807**(3): 375–383.
- Rouhier, N., Gelhaye, E., & Jacquot, J.-P.** (2004). Plant glutaredoxins: Still mysterious reducing systems. *Cellular and Molecular Life Sciences* **61**(11):1266–1277.
- Rushton, P.J., Somssich, I.E., Ringler, P., & Shen, Q.J.** (2010). WRKY transcription factors. *Trends in Plant Science* **15**(5):247–258.
- Rutjens, B., Bao, D., van Eck-Stouten, E., Brand, M., Smeekens, S., & Proveniers, M.** (2009). Shoot apical meristem function in *Arabidopsis* requires the combined activities of three BEL1-like homeodomain proteins. *The Plant Journal* **58**(4):641–654.
- Saiga, S., Möller, B., Watanabe-Taneda, A., Abe, M., Weijers, D., & Komeda, Y.** (2012). Control of embryonic meristem initiation in *Arabidopsis* by PHD-finger protein complexes. *Development* **139**(8):1391–1398.
- Sakellariou, M., & Mylona, P.V.** (2020). New Uses for Traditional Crops: The Case of Barley Biofortification. *Agronomy* **10**(12): 1964–1976.
- Sauter, M., Moffatt, B., Saechao, M.C., Hell, R., & Wirtz, M.** (2013). Methionine salvage and *S*-adenosyl-methionine: Essential links between sulfur, ethylene and polyamine biosynthesis. *Biochemical Journal* **451**(2):145–154.
- Schaller, F., Biesgen, C., Müssig, C., Altmann, T., & Weiler, E.W.** (2000). 12-Oxophytodienoate reductase 3 (OPR3) is the isoenzyme involved in jasmonate biosynthesis. *Planta* **210**(6):979–984.
- Schmidt, T.G., & Skerra, A.** (2007). The Strep-tag system for one-step purification and high-affinity detection or capturing of proteins. *Nature Protocols*, **2**(6):1528–1535.
- Schreiber, M., Mascher, M., Wright, J., Padmarasu, S., Himmelbach, A., Heavens, D., Milne, L., Clavijo, B.J., Stein, N., & Waugh, R.** (2020). A Genome Assembly of the Barley ‘Transformation Reference’ Cultivar Golden Promise. *G3 Genes|Genomes|Genetics*, **10**(6):1823–1827.
- Shi, J., Cao, X., Chen, Y., Cronan, J.E., & Guo, Z.** (2016). An Atypical α/β -Hydrolase Fold Revealed in the Crystal Structure of Pimeloyl-Acyl Carrier Protein Methyl Esterase BioG from *Haemophilus influenzae*. *Biochemistry* **55**(48):6705–6717.
- Shi, Y., Wang, Z., Meng, P., Tian, S., Zhang, X., & Yang, S.** (2013). The glutamate carboxypeptidase AMP 1 mediates abscisic acid and abiotic stress responses in *A. thaliana*. *New Phytologist* **199**(1):135–150.
- Shimada, H., Ohno, R., Shibata, M., Ikegami, I., Onai, K., Ohto, M., and Takamiya, K.** (2005). Inactivation and deficiency of core proteins of photosystems I and II caused by genetical phylloquinone and plastoquinone deficiency but retained lamellar structure in a T-DNA mutant of *Arabidopsis*. *The Plant Journal* **41**:627–637.
- Shimoda, Y., Ito, H., & Tanaka, A.** (2016). *Arabidopsis* *STAY-GREEN*, Mendel’s Green Cotyledon Gene, Encodes Magnesium-Dechelataase. *The Plant Cell* **28**(9):2147–2160.
- Singla-Pareek, S.L., Kaur, C., Kumar, B., Pareek, A., & Sopory, S.K.** (2020). Reassessing plant glyoxalases: Large family and expanding functions. *New Phytologist* **227**(3):714–721.
- Soares, A., Ribeiro Carlton, S.M., & Simões, I.** (2019). Atypical and nucellin-like aspartic proteases: Emerging players in plant developmental processes and stress responses. *Journal of Experimental Botany* **70**(7):2059–2076.
- Sobieszczuk-Nowicka, E.** (2017). Polyamine catabolism adds fuel to leaf senescence. *Amino Acids* **49**(1):49–56.

- Sobieszczuk-Nowicka, E., Kubala, S., Zmienko, A., Malecka, A., & Legocka, J. (2016). From Accumulation to Degradation: Reprogramming Polyamine Metabolism Facilitates Dark-Induced Senescence in Barley Leaf Cells. *Frontiers in Plant Science* **6**:1198.
- Song, S., Qi, T., Wasternack, C., & Xie, D. (2014). Jasmonate signaling and crosstalk with gibberellin and ethylene. *Current Opinion in Plant Biology* **21**:112–119.
- Song, W.-Y., Choi, K.S., Kim, D.Y., Geisler, M., Park, J., Vincenzetti, V., Schellenberg, M., Kim, S.H., Lim, Y.P., Noh, E.W., Lee, Y., & Martinoia, E. (2010). *Arabidopsis* PCR2 Is a Zinc Exporter Involved in Both Zinc Extrusion and Long-Distance Zinc Transport. *The Plant Cell* **22**(7):2237–2252.
- Staswick, P.E., & Tiryaki, I. (2004). The Oxylinin Signal Jasmonic Acid Is Activated by an Enzyme That Conjugates It to Isoleucine in *Arabidopsis*. *The Plant Cell* **16**(8):2117–2127.
- Stenzel, I., Hause, B., Maucher, H., Pitzschke, A., Miersch, O., Ziegler, J., Ryan, C.A., & Wasternack, C. (2003). Allene oxide cyclase dependence of the wound response and vascular bundle-specific generation of jasmonates in tomato - amplification in wound signalling. *The Plant Journal* **33**(3):577–589.
- Stepanova, A.N., Robertson-Hoyt, J., Yun, J., Benavente, L.M., Xie, D.-Y., Doležal, K., Schlereth, A., Jürgens, G., & Alonso, J.M. (2008). *TAA1*-Mediated Auxin Biosynthesis Is Essential for Hormone Crosstalk and Plant Development. *Cell* **133**(1):177–191.
- Stiti, N., Missihoun, T.D., Kotchoni, S.O., Kirch, H.-H., & Bartels, D. (2011). Aldehyde Dehydrogenases in *Arabidopsis thaliana*: Biochemical Requirements, Metabolic Pathways, and Functional Analysis. *Frontiers in Plant Science* **2**:265.
- Sudhakar Reddy, P., Srinivas Reddy, D., Sivasakthi, K., Bhatnagar-Mathur, P., Vadez, V., & Sharma, K.K. (2016). Evaluation of Sorghum [*Sorghum bicolor* (L.)] Reference Genes in Various Tissues and under Abiotic Stress Conditions for Quantitative Real-Time PCR Data Normalization. *Frontiers in Plant Science* **7**:529.
- Sugiyama, A., Kobayashi, T., Shiraki, M., & Saito, T. (2004). Roles of Poly(3-Hydroxybutyrate) Depolymerase and 3HB-Oligomer Hydrolase in Bacterial PHB Metabolism. *Current Microbiology* **48**:424–427.
- Sun, W., Wei, J., Wu, G., Xu, H., Chen, Y., Yao, M., Zhan, J., Yan, J., Wu, N., Chen, H., Bu, T., Tang, Z., & Li, Q. (2022). CqZF-HD14 enhances drought tolerance in quinoa seedlings through interaction with CqHIP34 and CqNAC79. *Plant Science* **323**:111406.
- Sun, X., Sun, C., Li, Z., Hu, Q., Han, L., & Luo, H. (2016). AsHSP17, a creeping bentgrass small heat shock protein modulates plant photosynthesis and ABA-dependent and independent signalling to attenuate plant response to abiotic stress. *Plant, Cell & Environment* **39**(6):1320–1337.
- Sun, X., Xue, X., Wang, X., Zhang, C., Zheng, D., Song, W., Zhao, J., Wei, J., Wu, Z., & Zhang, Z. (2021). Natural variation of *ZmCGT1* is responsible for isoorientin accumulation in maize silk. *The Plant Journal* **109**(1):64–76.
- Sunkar, R., Bartels, D., & Kirch, H.-H. (2003). Overexpression of a stress-inducible aldehyde dehydrogenase gene from *Arabidopsis thaliana* in transgenic plants improves stress tolerance. *The Plant Journal* **35**(4):452–464.
- Suorsa, M., Sirpiö, S., Allahverdiyeva, Y., Paakkarinen, V., Mamedov, F., Styring, S., & Aro, E.-M. (2006). PsbR, a Missing Link in the Assembly of the Oxygen-evolving Complex of Plant Photosystem II. *Journal of Biological Chemistry* **281**(1):145–150.
- Suprunova, T., Krugman, T., Fahima, T., Chen, G., Shams, I., Korol, A., & Nevo, E. (2004). Differential expression of dehydrin genes in wild barley, *Hordeum spontaneum*, associated with resistance to water deficit. *Plant, Cell and Environment* **27**(10):1297–1308.
- Székely, G., Ábrahám, E., Cséplő, Á., Rigó, G., Zsigmond, L., Csiszár, J., Ayaydin, F., Strizhov, N., Jásik, J., Schmelzer, E., Koncz, C., & Szabados, L. (2008). Duplicated *P5CS* genes of *Arabidopsis* play distinct roles in stress regulation and developmental control of proline biosynthesis. *The Plant Journal* **53**:11–28.
- Szymańska, R., Ślesak, I., Orzechowska, A., & Kruk, J. (2017). Physiological and biochemical responses to high light and temperature stress in plants. *Environmental and Experimental Botany* **139**:165–177.
- Tang, W., Wang, W., Chen, D., Ji, Q., Jing, Y., Wang, H., & Lin, R. (2012). Transposase-Derived Proteins FHY3/FAR1 Interact with PHYTOCHROME-INTERACTING FACTOR1 to Regulate Chlorophyll Biosynthesis by Modulating *HEMB1* during Deetiolation in *Arabidopsis*. *The Plant Cell* **24**(5):1984–2000.

- Taranto, F., Pasqualone, A., Mangini, G., Tripodi, P., Miazzi, M.M., Pavan, S., & Montemurro, C.** (2017). Polyphenol Oxidases in Crops: Biochemical, Physiological and Genetic Aspects. *International Journal of Molecular Sciences* **18**(2):377.
- Tehseen, M., Cairns, N., Sherson, S., & Cobbett, C.S.** (2010). Metallochaperone-like genes in *Arabidopsis thaliana*. *Metallomics* **2**:556-564.
- Temel, A., Janack, B., & Humbeck, K.** (2017). Drought Stress-Related Physiological Changes and Histone Modifications in Barley Primary Leaves at *HSP17* Gene. *Agronomy* **7**(2):43.
- Thakur, N., Sharma, V., & Kishore, K.** (2016). Leaf senescence: An overview. *Indian Journal of Plant Physiology* **21**(3):225–238.
- Thomas, H., Huang, L., Young, M., & Ougham, H.** (2009). Evolution of plant senescence. *BMC Evolutionary Biology* **9**(1):163.
- Tommasini, L., Svensson, J.T., Rodriguez, E.M., Wahid, A., Malatrasi, M., Kato, K., Wanamaker, S., Resnik, J., & Close, T.J.** (2008). Dehydrin gene expression provides an indicator of low temperature and drought stress: Transcriptome-based analysis of Barley (*Hordeum vulgare* L.). *Functional & Integrative Genomics* **8**(4):387–405.
- Toogood, H.S., Leys, D., & Scrutton, N.S.** (2007). Dynamics driving function – new insights from electron transferring flavoproteins and partner complexes. *FEBS Journal* **274**(21):5481–5504.
- Tran, L.-S.P., Nakashima, K., Sakuma, Y., Osakabe, Y., Qin, F., Simpson, S.D., Maruyama, K., Fujita, Y., Shinozaki, K., & Yamaguchi-Shinozaki, K.** (2006). Co-expression of the stress-inducible zinc finger homeodomain ZFHD1 and NAC transcription factors enhances expression of the *ERD1* gene in *Arabidopsis*. *The Plant Journal* **49**:46-63.
- Truman, W., Bennett, M.H., Kubigsteltig, I., Turnbull, C., & Grant, M.** (2007). *Arabidopsis* systemic immunity uses conserved defense signaling pathways and is mediated by jasmonates. *Proceedings of the National Academy of Sciences* **104**(3):1075–1080.
- Turchetto-Zolet, A.C., Margis-Pinheiro, M., & Margis, R.** (2009). The evolution of pyrroline-5-carboxylate synthase in plants: A key enzyme in proline synthesis. *Molecular Genetics and Genomics* **281**(1):87–97.
- Untergasser, A., Cutcutache, I., Koressaar, T., Ye, J., Faircloth, B.C., Remm, M., & Rozen, S.G.** (2012). Primer3—New capabilities and interfaces. *Nucleic Acids Research* **40**(15):e115.
- van Breusegem, F., & Dat, J.F.** (2006). Reactive Oxygen Species in Plant Cell Death. *Plant Physiology* **141**(2):384–390.
- van der Graaff, E., Schwacke, R., Schneider, A., Desimone, M., Flügge, U.-I., & Kunze, R.** (2006). Transcription Analysis of *Arabidopsis* Membrane Transporters and Hormone Pathways during Developmental and Induced Leaf Senescence. *Plant Physiology* **141**(2):776–792.
- Verma, S., Nizam, S., & Verma, P.K.** (2013). Biotic and Abiotic Stress Signaling in Plants. In: *Stress Signaling in Plants: Genomics and Proteomics Perspective*. Sarwat, M., Ahmad, A., Abdin, M., Eds.: Springer, New York, Vol. 1.
- Vignutelli, A., Wasternack, C., Apel, K., & Bohlmann, H.** (1998). Systemic and local induction of an *Arabidopsis* thionin gene by wounding and pathogens. *The Plant Journal* **14**(3):285–295.
- Villao, L., Sánchez, E., Romero, C., Galarza, L., Flores, J., & Santos-Ordóñez, E.** (2019). Activity characterization of the plantain promoter from the heavy metal-associated isoprenylated plant gene (MabHIPP) using the luciferase reporter gene. *Plant Gene* **19**:100187.
- Viswanath, K.K., Varakumar, P., Pamuru, R.R., Basha, S.J., Mehta, S., & Rao, A.D.** (2020). Plant Lipxygenases and Their Role in Plant Physiology. *Journal of Plant Biology* **63**(2):83–95.
- Walker, J.E.** (1992). The NADH:ubiquinone oxidoreductase (complex I) of respiratory chains. *Quarterly Reviews of Biophysics* **25**(3):253–324.
- Wang, H., Sun, Y., Chang, J., Zheng, F., Pei, H., Yi, Y., Chang, C., & Dong, C.-H.** (2016). Regulatory function of *Arabidopsis* lipid transfer protein 1 (LTP1) in ethylene response and signaling. *Plant Molecular Biology* **91**:471–484.
- Wang, H., & Wang, H.** (2015). Multifaceted roles of *FHY3* and *FAR1* in light signaling and beyond. *Trends in Plant Science* **20**(7):453–461.
- Wang, K.L.-C., Li, H., & Ecker, J.R.** (2002). Ethylene Biosynthesis and Signaling Networks. *The Plant Cell* **14**:131–151.

- Wang, Q., Guo, Q., Guo, Y., Yang, J., Wang, M., Duan, X., Niu, J., Liu, S., Zhang, J., Lu, Y., Hou, Z., Miao, W., Wang, X., Kong, W., Xu, X., Wu, Y., Rui, Q., & La, H. (2018). Arabidopsis Subtilase SASP is involved in the regulation of ABA signaling and drought tolerance by interacting with OPEN STOMATA 1. *Journal of Experimental Botany* **69**(18):4403–4417.
- Wani, S.H., Kumar, V., Shriram, V., & Sah, S.K. (2016). Phytohormones and their metabolic engineering for abiotic stress tolerance in crop plants. *The Crop Journal* **4**(3):162–176.
- Wasternack, C. (2007). Jasmonates: An Update on Biosynthesis, Signal Transduction and Action in Plant Stress Response, Growth and Development. *Annals of Botany* **100**(4):681–697.
- Wen, Z., Mei, Y., Zhou, J., Cui, Y., Wang, D., & Wang, N.N. (2020). SAUR49 Can Positively Regulate Leaf Senescence by Suppressing SSPP in Arabidopsis. *Plant and Cell Physiology* **61**(3):644–658.
- Werner, T., Motyka, V., Laucou, V., Smets, R., Van Onckelen, H., & Schmülling, T. (2003). Cytokinin-Deficient Transgenic Arabidopsis Plants Show Multiple Developmental Alterations Indicating Opposite Functions of Cytokinins in the Regulation of Shoot and Root Meristem Activity. *The Plant Cell* **15**(11):2532–2550.
- Wessel, D., & Flüggé, U.I. (1984). A method for the quantitative recovery of protein in dilute solution in the presence of detergents and lipids. *Analytical Biochemistry* **138**(1):141–143.
- Widhalm, J.R., Ducluzeau, A.-L., Buller, N.E., Elowsky, C.G., Olsen, L.J., & Basset, G.J.C. (2012). Phylloquinone (vitamin K1) biosynthesis in plants: two peroxisomal thioesterases of lactobacillales origin hydrolyze 1,4-dihydroxy-2-naphthoyl-coa. *The Plant Journal* **71**(2):205–215.
- Woo, H.R., Kim, H.J., Lim, P.O., & Nam, H.G. (2019). Leaf Senescence: Systems and Dynamics Aspects. *Annual Review of Plant Biology* **70**:347–76.
- Xiang, J., Lin, J., Tang, D., Zhou, B., Guo, M., He, R., Huang, X., Zhao, X., & Liu, X. (2010). A DHHC-type zinc finger protein gene regulates shoot branching in *Arabidopsis*. *African Journal of Biotechnology* **9**(45):7759–7766.
- Xie, D.-Y., Sharma, S.B., Paiva, N.L., Ferreira, D., & Dixon, R.A. (2003). Role of anthocyanidin reductase, encoded by BANYULS in plant flavonoid biosynthesis. *Science* **299**(5605):396–399.
- Xie, M., Zhang, J., Tschaplinski, T.J., Tuskan, G.A., Chen, J.-G., & Muchero, W. (2018). Regulation of Lignin Biosynthesis and Its Role in Growth-Defense Tradeoffs. *Frontiers in Plant Science* **9**:1427.
- Xie, X., Ma, X., Zhu, Q., Zeng, D., Li, G., & Liu, Y.-G. (2017). CRISPR-GE: A Convenient Software Toolkit for CRISPR-Based Genome Editing. *Molecular Plant* **10**(9):1246–1249.
- Xie, Z., Lin, W., Yu, G., Cheng, Q., Xu, B., & Huang, B. (2019). Improved cold tolerance in switchgrass by a novel CCCH-type zinc finger transcription factor gene, *PvC3H72*, associated with ICE1–CBF–COR regulon and ABA-responsive genes. *Biotechnology for Biofuels* **12**(1):224.
- Xing, Y., & Zhang, Q. (2010). Genetic and Molecular Bases of Rice Yield. *Annual Review of Plant Biology* **61**:421–442.
- Xu, F.-Q., & Xue, H.-W. (2019). The ubiquitin-proteasome system in plant responses to environments. *Plant, Cell & Environment* **42**(10):2931–2944.
- Yadav, S.K. (2010). Heavy metals toxicity in plants: An overview on the role of glutathione and phytochelatin in heavy metal stress tolerance of plants. *South African Journal of Botany* **76**:167–179.
- Yamamoto, H., Peng, L., Fukao, Y., & Shikanai, T. (2011). An Src Homology 3 Domain-Like Fold Protein Forms a Ferredoxin Binding Site for the Chloroplast NADH Dehydrogenase-Like Complex in *Arabidopsis*. *The Plant Cell* **23**(4):1480–1493.
- Yan, D., Zhang, Y., Niu, L., Yuan, Y., & Cao, X. (2007). Identification and characterization of two closely related histone H4 arginine 3 methyltransferases in *Arabidopsis thaliana*. *Biochemical Journal* **408**(1):113–121.
- Yang, H., Li, P., Zhang, A., Wen, X., Zhang, L., & Lu, C. (2017). Tetratricopeptide repeat protein Pyg7 is essential for photosystem I assembly by interacting with PsaC in Arabidopsis. *The Plant Journal* **91**(6):950–961.
- Yang, L., Mickelson, S., See, D., Blake, T.K., Fischer, A.M. (2004). Genetic analysis of the function of major leaf proteases in barley (*Hordeum vulgare* L.) nitrogen remobilization. *Journal of Experimental Botany* **55**(408):2607–2616.

- Yang, S.-D., Seo, P.J., Yoon, H.-K., & Park, C.-M. (2011). The *Arabidopsis* NAC Transcription Factor VNI2 Integrates Abscisic Acid Signals into Leaf Senescence via the *COR/RD* Genes. *The Plant Cell* **23**(6):2155–2168.
- Yang, Y., Xu, R., Ma, C., Vlot, A.C., Klessig, D.F., & Pichersky, E. (2008). Inactive Methyl Indole-3-Acetic Acid Ester Can Be Hydrolyzed and Activated by Several Esterases Belonging to the *AtMES* Esterase Family of *Arabidopsis*. *Plant Physiology* **147**(3):1034–1045.
- Ye, J., Coulouris, G., Zaretskaya, I., Cutcutache, I., Rozen, S., & Madden, T.L. (2012). Primer-BLAST: A tool to design target-specific primers for polymerase chain reaction. *BMC Bioinformatics* **13**(1):134.
- Ye, Z.-W., Lung, S.-C., Hu, T.-H., Chen, Q.-F., Suen, Y.-L., Wang, M., Hoffmann-Benning, S., Yeung, E., & Chye, M.-L. (2016). *Arabidopsis* acyl-CoA-binding protein ACBP6 localizes in the phloem and affects jasmonate composition. *Plant Molecular Biology* **92**(6):717–730.
- Yoshida, T., Mogami, J., & Yamaguchi-Shinozaki, K. (2014). ABA-dependent and ABA-independent signaling in response to osmotic stress in plants. *Current Opinion in Plant Biology* **21**:133–139.
- Yu, S.-M., Lo, S.-F., & Ho, T.-H.D. (2015). Source–Sink Communication: Regulated by Hormone, Nutrient, and Stress Cross-Signaling. *Trends in plant science* **20**(12):844–857.
- Yuan, Y., Mei, L., Wu, M., Wei, W., Shan, W., Gong, Z., Zhang, Q., Yang, F., Yan, F., Zhang, Q., Luo, Y., Xu, X., Zhang, W., Miao, M., Lu, W., Li, Z., & Deng, W. (2018). SlARF10, an auxin response factor, is involved in chlorophyll and sugar accumulation during tomato fruit development. *Journal of Experimental Botany* **69**(22):5507–5518.
- Zentgraf, U., & Hemleben, V. (2008). Molecular Cell Biology: Are Reactive Oxygen Species Regulators of Leaf Senescence? In *Progress in Botany*; Lüttge, U., Beyschlag, W., & Murata J., Eds.: Springer, Berlin, Heidelberg, Vol. **69**:117–138.
- Zeytuni, N., & Zarivach, R. (2012). Structural and Functional Discussion of the Tetra-Trico-Peptide Repeat, a Protein Interaction Module. *Structure* **20**(3):397–405.
- Zhai, P., Vu, M.T., Hoff, K.G., & Silberg, J.J. (2011). A conserved histidine in human DNLZ/HEP is required for stimulation of HSPA9 ATPase activity. *Biochemical and Biophysical Research Communications* **408**(4):589–594.
- Zhang, B. Q., Liu, X.S., Feng, S.J., Zhao, Y.N., Wang, L.L., Rono, J.K., Li, H., & Yang, Z.M. (2020). Developing a cadmium resistant rice genotype with *OsHIPP29* locus for limiting cadmium accumulation in the paddy crop. *Chemosphere* **247**:125958.
- Zhang, H., Li, Y., & Zhu, J.-K. (2018). Developing naturally stress-resistant crops for a sustainable agriculture. *Nature Plants* **4**:989–996.
- Zhang, H., Zhang, X., Liu, J., Niu, Y., Chen, Y., Hao, Y., Zhao, J., Sun, L., Wang, H., Xiao, J., & Wang, X. (2020). Characterization of the Heavy-Metal-Associated Isoprenylated Plant Protein (*HIPP*) Gene Family from *Triticeae* Species. *International Journal of Molecular Sciences* **21**(17):6191.
- Zhang, H., Zhao, M., Song, Q., Zhao, L., Wang, G., & Zhou, C. (2016). Identification and function analyses of senescence-associated *WRKYs* in wheat. *Biochemical and Biophysical Research Communications* **474**(4):761–767.
- Zhang, H., & Zhou, C. (2013). Signal transduction in leaf senescence. *Plant Molecular Biology* **82**(6):539–545.
- Zhang, K., & Gan, S.-S. (2012). An Abscisic Acid-AtNAP Transcription Factor-SAG113 Protein Phosphatase 2C Regulatory Chain for Controlling Dehydration in Senescing *Arabidopsis* Leaves. *Plant Physiology* **158**(2):961–969.
- Zhang, L., Zhao, G., Jia, J., Liu, X., & Kong, X. (2012). Molecular characterization of 60 isolated wheat MYB genes and analysis of their expression during abiotic stress. *Journal of Experimental Botany* **63**(1):203–214.
- Zhang, W., Peng, K., Cui, F., Wang, D., Zhao, J., Zhang, Y., Yu, N., Wang, Y., Zeng, D., Wang, Y., Cheng, Z., & Zhang, K. (2021). Cytokinin oxidase/dehydrogenase OsCKX11 coordinates source and sink relationship in rice by simultaneous regulation of leaf senescence and grain number. *Plant Biotechnology Journal* **19**(2):335–350.
- Zhang, X., Feng, H., Feng, C., Xu, H., Huang, X., Wang, Q., Duan, X., Wang, X., Wei, G., Huang, L., & Kang, Z. (2015). Isolation and characterisation of cDNA encoding a wheat heavy metal-associated isoprenylated protein involved in stress responses. *Plant Biology* **17**:1176–1186.

- Zhao, J., Zhou, H., & Li, X.** (2013). UBIQUITIN-SPECIFIC PROTEASE16 interacts with a HEAVY METAL ASSOCIATED ISOPRENYLATED PLANT PROTEIN27 and modulates cadmium tolerance. *Plant Signaling & Behavior* **8**(10):e25680-1.
- Zhou, B., Lin, J.Z., Peng, D., Yang, Y.Z., Guo, M., Tang, D.Y., Tan, X., & Liu, X.M.** (2017). Plant architecture and grain yield are regulated by the novel DHHC-type zinc finger protein genes in rice (*Oryza sativa* L.). *Plant Science* **254**:12–21.
- Zhu, X., Tang, G., Granier, F., Bouchez, D., & Galili, G.** (2001). A T-DNA Insertion Knockout of the Bifunctional Lysine-Ketoglutarate Reductase/Saccharopine Dehydrogenase Gene Elevates Lysine Levels in Arabidopsis Seeds. *Plant Physiology* **126**(4):1539–1545.
- Zou, J., Liu, A., Chen, X., Zhou, X., Gao, G., Wang, W., & Zhang, X.** (2009). Expression analysis of nine rice heat shock protein genes under abiotic stresses and ABA treatment. *Journal of Plant Physiology* **166**(8):851–861.
- Zou, L., Sun, X., Zhang, Z., Liu, P., Wu, J., Tian, C., Qiu, J., & Lu, T.** (2011). Leaf Rolling Controlled by the Homeodomain Leucine Zipper Class IV Gene *Roc5* in Rice. *Plant Physiology* **156**(3):1589–1602.
- Zschiesche, W., Barth, O., Daniel, K., Böhme, S., Rausche, J., & Humbeck, K.** (2015). The zinc-binding nuclear protein HIPP3 acts as an upstream regulator of the salicylate-dependent plant immunity pathway and of flowering time in *Arabidopsis thaliana*. *New Phytologist* **207**(4):1084-1096.
- Zwack, P.J., & Rashotte, A.M.** (2015). Interactions between cytokinin signalling and abiotic stress responses. *Journal of Experimental Botany* **66**(16):4863–4871.

6. Appendix

6.1. Additional information for barley *H. vulgare* L. cv. Golden promise transgenic lines

6.1.1. The constructs for the establishment of OE and KO lines

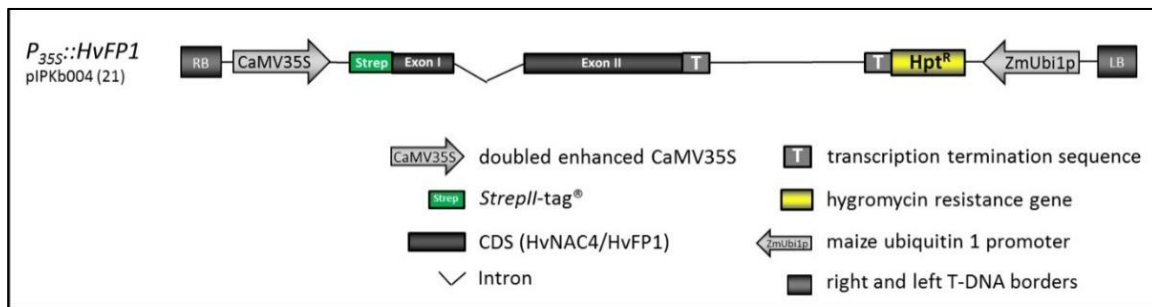


Figure 38: Schematic representation of the gene structure of *HvFP1* overexpressing construct in lines 21.3I and 21.2A. The cassette contained the hygromycin phosphotransferase gene (*Hpt*), which gives the transformed plants resistance to hygromycin. The *P_{35S}::HvFP1* construct contained an N-terminal *StreptII*[®] tag. The expression of the target gene was regulated by the double enhanced constitutive viral promoter CaMV35S.

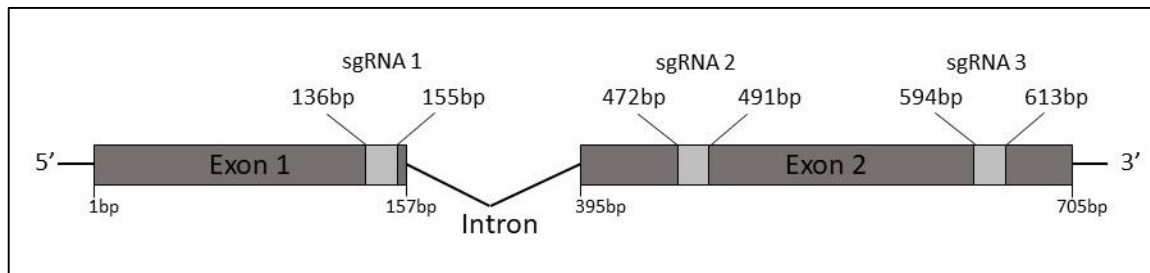


Figure 39: Schematic representation of *HvFP1* sequence and the targets of CRISPR-Cas9 system for the establishment of knock out lines 20.1At and 20.17M. The three points of sgRNA targeting were marked with light grey.

6.1.2. Polymerase Chain Reaction (PCR) for genotyping of OE and KO lines

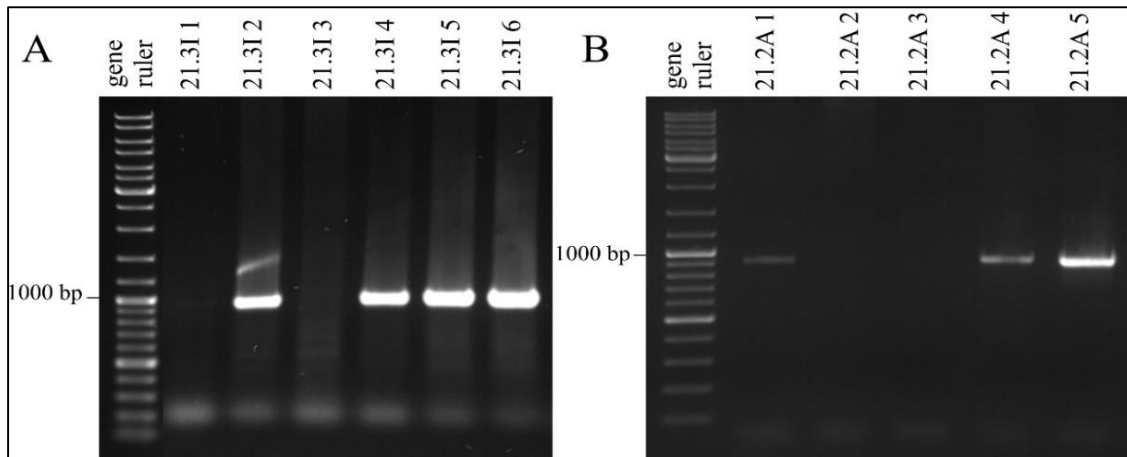


Figure 40: Polymerase Chain Reaction for the detection of inserted *Strep-HvFP1* transgene in OE lines for selected barley plants of T1 generation. (A) for 21.3I line and (B) for 21.2A line. Product size was estimated at 886 bp.

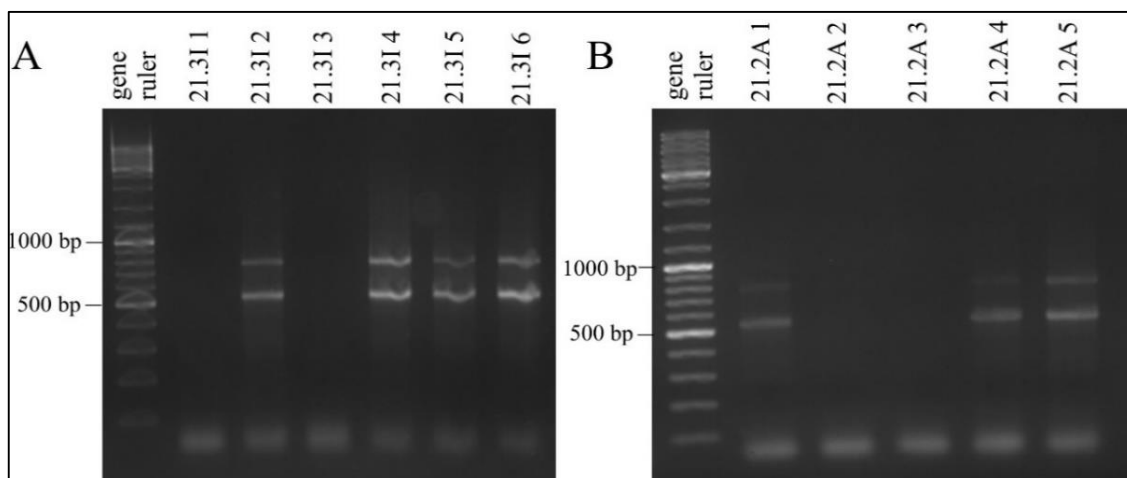


Figure 41: Polymerase Chain Reaction for the detection of full and spliced transcribed products of *HvFP1* in OE lines. (A) 21.3I and (B) 21.2A. Full length transcript had a size of 771 bp, while spliced transcript of 468 bp.

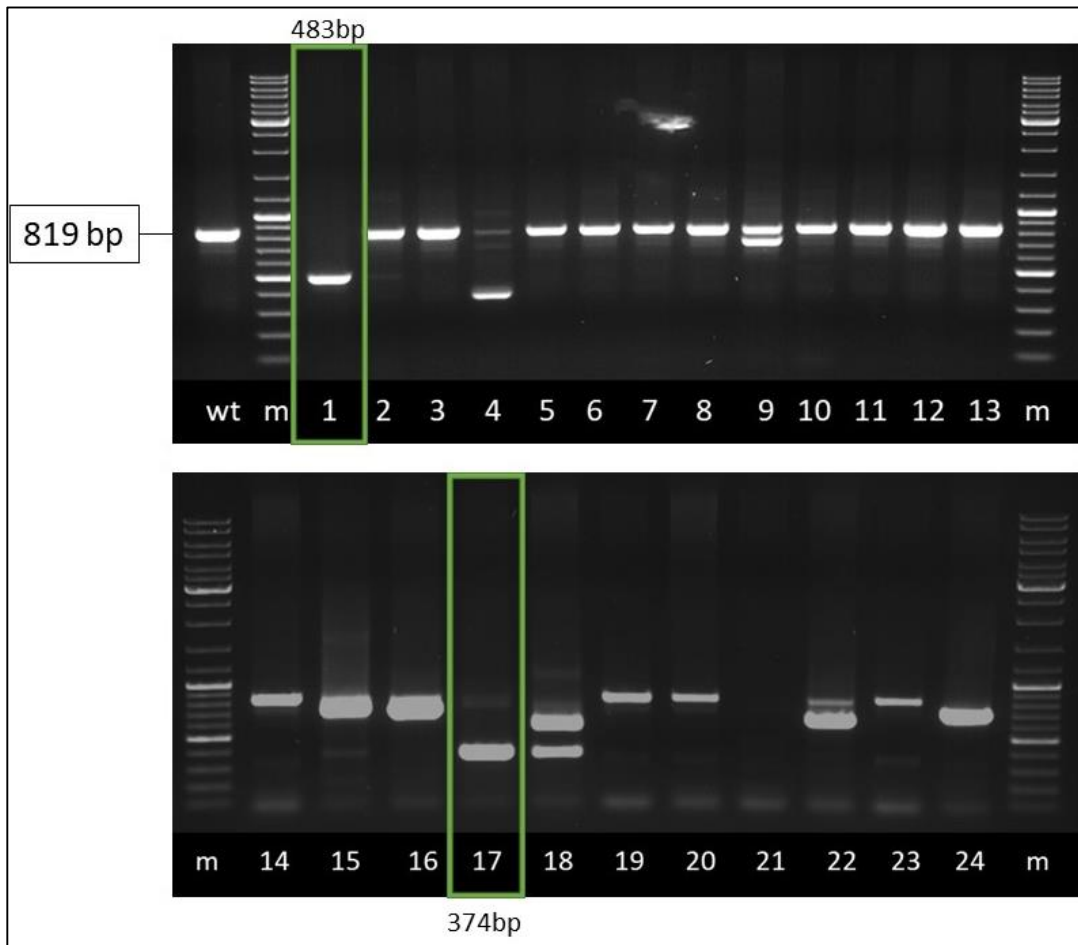


Figure 42: Polymerase Chain Reaction reaction for detecting *HvFPI* KO plants in 24 samples, after transformation with the CRISPR-Cas9 system. WT product was estimated at 819 bp, while plants 1 and 17 gave products at 483 bp and 374 bp, respectively

6.1.3. Phenotypic characterization of OE and KO lines

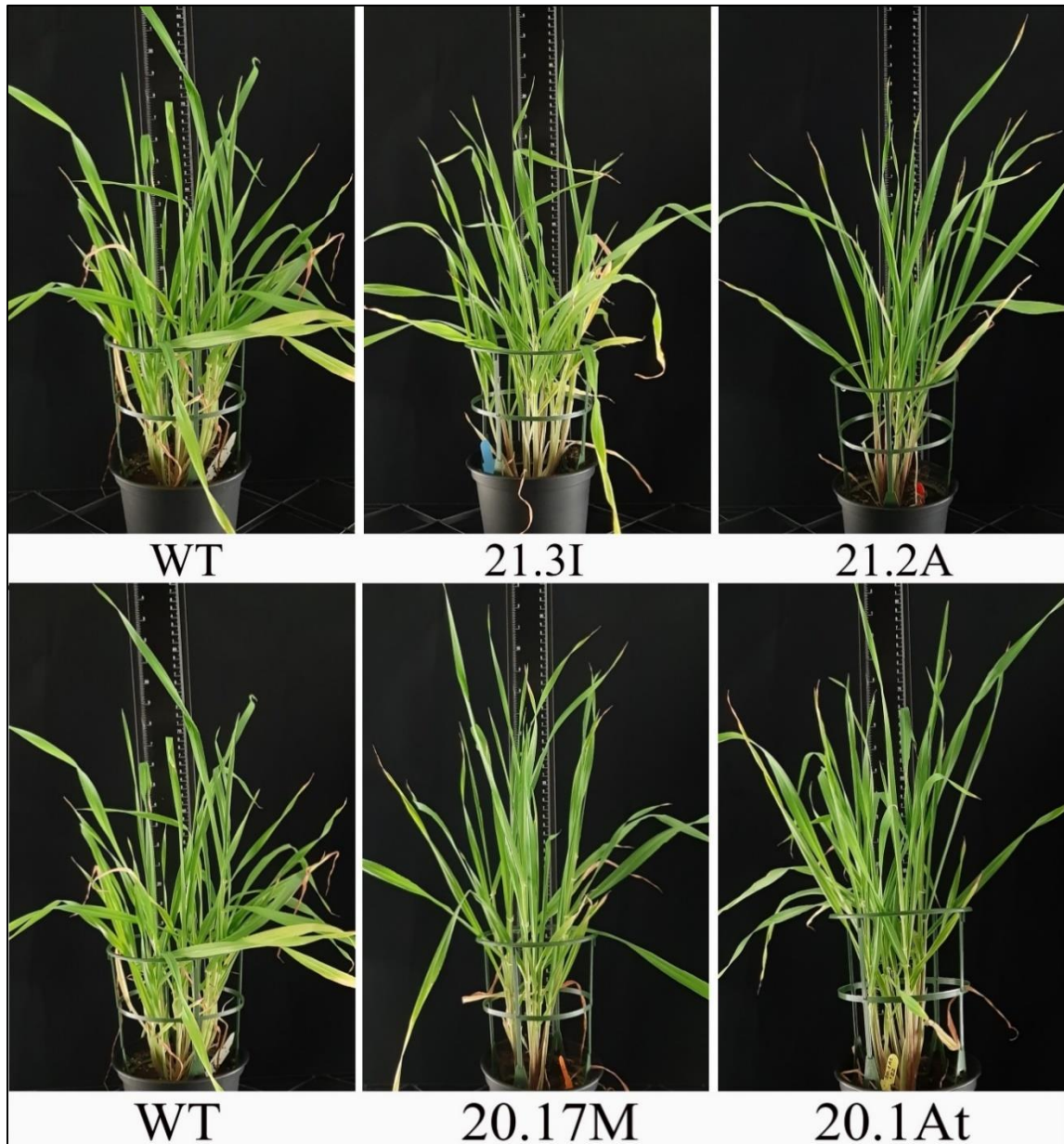


Figure 43: Photos of selected plants of WT, OE lines 21.3I and 21.2A and KO lines 20.1At and 20.17M on the 43rd day after sowing.

6.2. Additional information for RNA Seq analysis in barley primary leaves

6.2.1. Example of quality control of the RNA samples with a Bioanalyzer

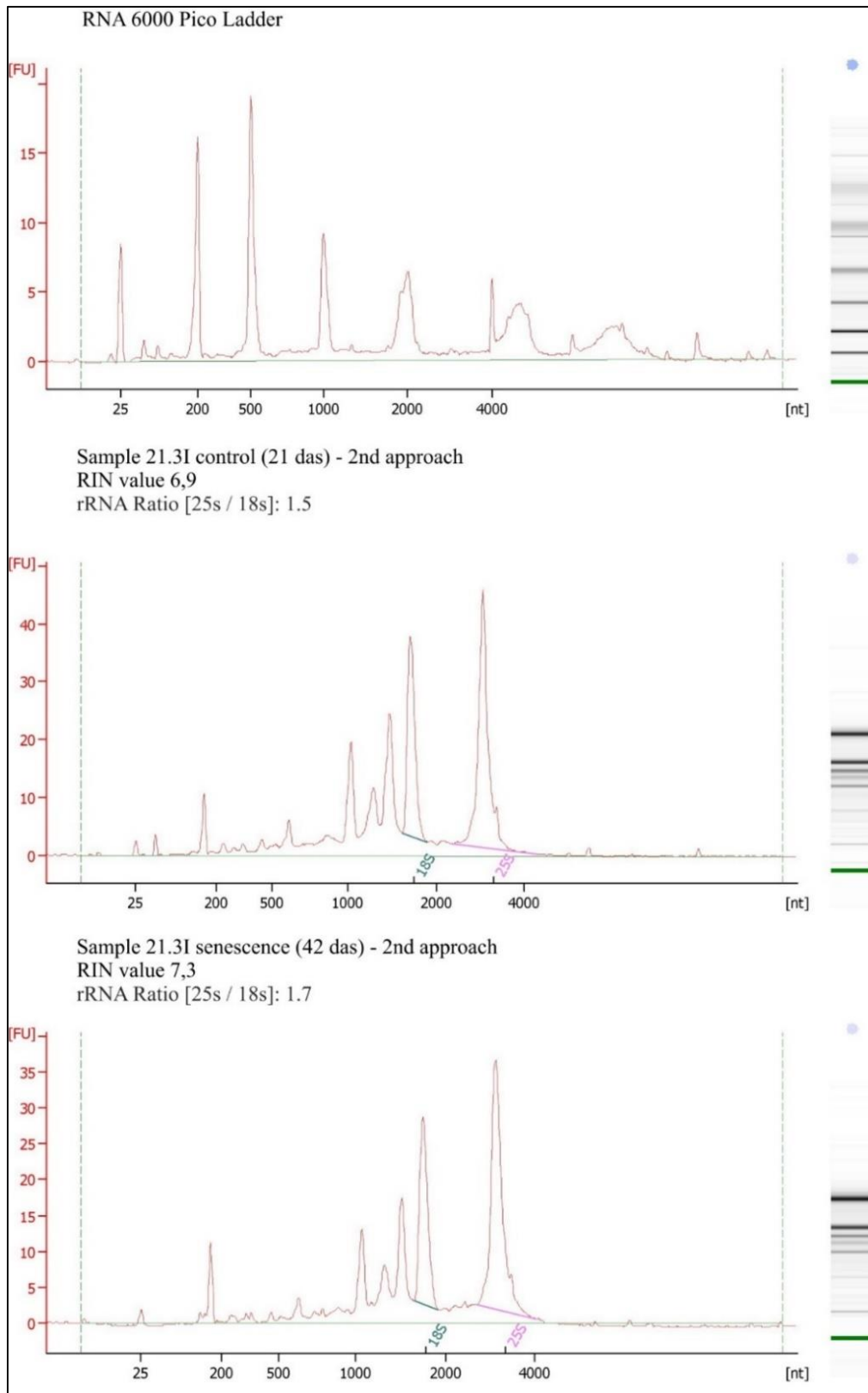


Figure 44: Example of an electropherogram profile, showing the quality of the ladder and two RNA samples as derived from Bioanalyzer 2100. The five peaks of ribosomal RNA are displayed and the RNA Integrity Number (RIN) is calculated.

6.2.2. Number of reads and total mapping rate of the 12 samples

Table 2: Data quality summary for each sequenced sample. Raw reads: reads count from the raw data; Clean reads: Clean data are read counts filtered from raw data. All the following analysis is based on clean data; Raw bases: Base number of raw data. (number of raw reads) * (sequence length), converting unit to G; Clean bases: Base number of raw data after filtering. (number of clean reads) * (sequence length), converting unit to G; Error rate (%): base error rate of whole sequencing; Q30(%): The percentage of the bases whose Q Phred values is greater than 30. (Number of bases with Q Phred value > 30) / (Number of total bases) *100; GC content (%): The percentage of G&C base numbers of total bases. (G&C base number) / (Total base number) *100.

Sample name	Raw reads	Clean reads	Raw bases	Clean bases	Error rate(%)	Q30(%)	GC content(%)
wt_C_1	33495522	33098549	10.0	9.9	0.02	94.28	58.35
wt_C_2	26781332	26423353	8.0	7.9	0.02	94.23	55.53
wt_C_3	29674393	29358173	8.9	8.8	0.02	95.87	60.77
wt_S_1	29105921	28831384	8.7	8.6	0.03	94.19	55.27
wt_S_2	26851116	26542775	8.1	8.0	0.02	94.51	56.56
wt_S_3	30718363	30496261	9.2	9.1	0.02	95.71	60.20
oe_C_1	26026452	25827802	7.8	7.7	0.03	93.92	51.69
oe_C_2	30912426	30444351	9.3	9.1	0.02	95.61	57.38
oe_C_3	25772946	25395774	7.7	7.6	0.02	95.65	57.04
oe_S_1	23110142	22542891	6.9	6.8	0.03	94.24	49.71
oe_S_2	29184626	28806268	8.8	8.6	0.02	95.93	57.62
oe_S_3	27213589	26837846	8.2	8.1	0.02	95.32	56.63

Table 3: Summary of mapping results and the distribution of clean reads in reference genome. Total reads: total clean reads used for analysis; Total mapped reads: numbers of reads being mapped on the genome; Uniquely mapped reads: numbers of reads being mapped on single position of the genome; Total mapping rate: (mapped reads)/ (total reads) *100; Uniquely mapping rate: (uniquely mapped reads)/ (total reads) *100; Exonic, intronic, intergenic regions: percentage of clean reads mapped in exonic, intronic or intergenic regions of reference genome.

Sample name	Total reads	Total mapped reads	Uniquely mapped reads	Total mapping rate	Uniquely mapping rate	Exonic region	Intronic region	Intergenic region
wt_C_1	66197098	63151158	61372976	95.40 %	92.71 %	93.14 %	1.15 %	5.71%
wt_C_2	52846706	50395633	48939192	95.36 %	92.61 %	90.92 %	1.39 %	7.69 %
wt_C_3	58716346	56341034	54708212	95.95 %	93.17 %	94.50 %	4.80 %	0.71 %
wt_S_1	57662768	54767999	53562154	94.98 %	92.89 %	90.06 %	1.34 %	8.60 %
wt_S_2	53085550	50828046	49629405	95.75 %	93.49 %	92.07 %	0.94 %	6.99 %
wt_S_3	60992522	56364070	54735413	92.41 %	89.74 %	93.12 %	0.67 %	6.22 %
oe_C_1	51655604	48725822	46982374	94.33 %	90.95 %	86.32 %	1.92 %	11.76 %
oe_C_2	60888702	58089178	56422869	95.40 %	92.67 %	92.17 %	1.26 %	6.57 %
oe_C_3	50791548	48717572	47362583	95.92 %	93.25 %	90.86 %	1.17 %	7.97 %
oe_S_1	45085782	42559903	41499560	94.40 %	92.05 %	81.26 %	2.09 %	16.65 %
oe_S_2	57612536	55039247	53697221	95.53 %	93.20 %	92.56 %	1.41 %	6.03 %
oe_S_3	53675692	51406271	50364243	95.77 %	93.83 %	92.57 %	1.36 %	6.07 %

6.2.3. Complete lists of SAGs and SDGs

Table 4: List of SAGs in WT barley primary leaves. Gene IDs, log₂FC and gene annotations are provided.

Gene ID	log ₂ FC	gene annotation
HORVU.MOREX.r2.2HG0114820	14.993	Isocitrate lyase (ICL) - Isocitrase; Isocitratase
HORVU.MOREX.r2.4HG0336950	11.378	Hydrolase, alpha/beta fold family protein, expressed
HORVU.MOREX.r2.2HG0146360	9.261	Malate synthase
HORVU.MOREX.r2.5HG0417580	9.248	Cytokinin riboside 5'-monophosphate phosphoribohydrolase (LONELY GUY-like 9)
HORVU.MOREX.r2.2HG0159200	8.928	Homeobox-leucine zipper protein / lipid-binding START domain-containing protein
HORVU.MOREX.r2.2HG0098550	8.912	GDSL esterase/lipase (Sinapine esterase-BnSCE3)
HORVU.MOREX.r2.1HG0056670	8.771	Cation/H(+) antiporter (Protein CATION/H+ EXCHANGER 15)
HORVU.MOREX.r2.7HG0607580	8.370	Ribonuclease H-like protein
HORVU.MOREX.r2.5HG0433920	8.288	Lipid transfer protein (Protein YELLOW-LEAF-SPECIFIC GENE 3)
HORVU.MOREX.r2.7HG0570060	8.129	ABC transporter family protein (Pleiotropic drug resistance protein 1)
HORVU.MOREX.r2.2HG0159210	7.956	Protein kinase superfamily protein
HORVU.MOREX.r2.6HG0509740	7.818	Laccase - Putative laccase-9; Benzenediol:oxygen oxidoreductase 9
HORVU.MOREX.r2.1HG0058240	7.624	GDSL esterase/lipase
HORVU.MOREX.r2.2HG0170060	7.231	Cysteine protease (Oryzain alpha chain)
HORVU.MOREX.r2.4HG0339910	7.107	LOB domain-containing protein (ASYMMETRIC LEAVES 2like protein 16)
HORVU.MOREX.r2.2HG0159410	7.067	Sodium transporter (Probable cation transporter HKT7)
HORVU.MOREX.r2.7HG0620670	7.033	UPF0496 protein
HORVU.MOREX.r2.1HG0074010	7.031	UvrABC system protein C
HORVU.MOREX.r2.UnG0633870	7.022	Cytochrome P450 (4-hydroxyphenylacetaldehyde oxime monooxygenase)
HORVU.MOREX.r2.6HG0459020	6.943	Pectin lyase-like superfamily protein (Probable polygalacturonase)
HORVU.MOREX.r2.2HG0159220	6.897	HXXXD-type acyl-transferase protein, (Omega-hydroxypalmitate O-feruloyl transferase)
HORVU.MOREX.r2.1HG0036340	6.888	Ripening-related protein
HORVU.MOREX.r2.4HG0346510	6.872	Pentatricopeptide repeat (PPR) superfamily protein (Endoglucanase 15)
HORVU.MOREX.r2.2HG0114670	6.829	Aspartic proteinase nepenthesin-1
HORVU.MOREX.r2.3HG0244950	6.772	Methyl esterase (Salicylic acid binding protein 2)
HORVU.MOREX.r2.6HG0519910	6.771	Vesicle-associated membrane protein
HORVU.MOREX.r2.2HG0139100	6.747	Subtilisin-like protease (SBT1.7)
HORVU.MOREX.r2.7HG0550410	6.733	Ethylene-responsive transcription factor
HORVU.MOREX.r2.5HG0351990	6.696	Thaumatococcus-like protein
HORVU.MOREX.r2.2HG0114720	6.671	Late embryogenesis abundant (LEA) hydroxyproline-rich glycoprotein
HORVU.MOREX.r2.2HG0094100	6.660	Lipid transfer protein
HORVU.MOREX.r2.4HG0315030	6.652	TPX2 (targeting protein for Xklp2) protein family
HORVU.MOREX.r2.3HG0269610	6.600	UDP-glycosyltransferase (Anthocyanidin 3-O-glucosyltransferase)
HORVU.MOREX.r2.6HG0502090	6.594	ABC transporter ATP-binding protein
HORVU.MOREX.r2.5HG0435670	6.590	7-cyano-7-deazaguanine synthase
HORVU.MOREX.r2.6HG0513870	6.574	Lipase
HORVU.MOREX.r2.6HG0513950	6.529	Mannan endo-1,4-beta-mannosidase 4
HORVU.MOREX.r2.5HG0370290	6.521	ARM repeat superfamily protein
HORVU.MOREX.r2.1HG0067780	6.463	Auxin-responsive protein (Indole-acetic acidinduced protein 19)
HORVU.MOREX.r2.6HG0471520	6.404	Histone H3
HORVU.MOREX.r2.4HG0344810	6.388	12-oxophytodienoate reductase-like protein
HORVU.MOREX.r2.2HG0168640	6.343	RECEPTOR LIKE PROTEIN KINASE-like 2.2
HORVU.MOREX.r2.UnG0625150	6.320	NADH-ubiquinone oxidoreductase chain 1
HORVU.MOREX.r2.5HG0382610	6.309	Metacaspase
HORVU.MOREX.r2.2HG0150360	6.303	NAC domain protein
HORVU.MOREX.r2.2HG0168200	6.287	xyloglucan endotransglucosylase/hydrolase 5
HORVU.MOREX.r2.7HG0619190	6.277	RING/U-box superfamily protein (NEP1 interacting protein 2)
HORVU.MOREX.r2.3HG0244150	6.274	ARM repeat superfamily protein
HORVU.MOREX.r2.2HG0135070	6.228	cysteine-rich/transmembrane domain protein A
HORVU.MOREX.r2.3HG0224140	6.225	Translation initiation factor IF-2
HORVU.MOREX.r2.1HG0074610	6.195	Protein phosphatase 2c, putative
HORVU.MOREX.r2.4HG0347720	6.160	Heavy metal transport/detoxification superfamily protein (AtHIP39)
HORVU.MOREX.r2.1HG0068230	6.151	Ethylene-responsive transcription factor ERF109
HORVU.MOREX.r2.3HG0242240	6.147	Coiled-coil domain-containing protein 18, putative isoform 2
HORVU.MOREX.r2.1HG0012530	6.102	Endoglucanase(Endo-1,4-beta glucanase 14)

HORVU.MOREX.r2.3HG0206320	6.087	Cytochrome P450
HORVU.MOREX.r2.1HG0067180	6.076	senescence regulator (Protein of unknown function, DUF584) HvS40
HORVU.MOREX.r2.4HG0326510	6.050	Auxin influx transporter (Auxin transporterlike protein 2)
HORVU.MOREX.r2.3HG0186520	6.035	Protein NEN4; NAC45/NAC86-dependent exonuclease-domain protein 4
HORVU.MOREX.r2.2HG0151290	5.986	Pectin acetyltransferase
HORVU.MOREX.r2.1HG0056650	5.983	Scarecrow transcription factor family protein
HORVU.MOREX.r2.1HG0020940	5.981	Tryptophan aminotransferase
HORVU.MOREX.r2.6HG0490010	5.933	High affinity nitrate transporter
HORVU.MOREX.r2.2HG0158210	5.879	Armadillo/beta-catenin-like repeat family protein, expressed
HORVU.MOREX.r2.7HG0546820	5.844	Bidirectional sugar transporter SWEET
HORVU.MOREX.r2.5HG0414050	5.793	Calmodulin-lysine N-methyltransferase
HORVU.MOREX.r2.2HG0169380	5.780	Nuclease S1 (endonuclease 4)
HORVU.MOREX.r2.7HG0550540	5.765	Lipase (Triacylglycerol lipase)
HORVU.MOREX.r2.3HG0186220	5.740	RING/FYVE/PHD zinc finger superfamily protein
HORVU.MOREX.r2.2HG0149820	5.720	Caleosin (Peroxygenase)
HORVU.MOREX.r2.7HG0529950	5.718	Seed maturation protein
HORVU.MOREX.r2.2HG0108560	5.645	vacuolar sorting-associated protein (DUF946)
HORVU.MOREX.r2.6HG0506530	5.608	Amino acid permease
HORVU.MOREX.r2.5HG0424600	5.600	Cysteine protease (Protein SENESCENCE-ASSOCIATED-GENE 39)
HORVU.MOREX.r2.3HG0270900	5.579	Glutathione S-transferase (cold-induced protein)
HORVU.MOREX.r2.2HG0128360	5.577	Ribonuclease
HORVU.MOREX.r2.2HG0153170	5.568	Aldehyde dehydrogenase
HORVU.MOREX.r2.7HG0592210	5.515	with no lysine (K) kinase 6
HORVU.MOREX.r2.2HG0090150	5.500	DnaJ
HORVU.MOREX.r2.7HG0592200	5.493	Cytochrome P450
HORVU.MOREX.r2.6HG0462680	5.474	Myb-like transcription factor family protein
HORVU.MOREX.r2.2HG0128660	5.437	Cytochrome P450 (Isoflavone 2'-hydroxylase)
HORVU.MOREX.r2.3HG0254170	5.396	Cysteine proteinase (Thiol protease SEN102)
HORVU.MOREX.r2.3HG0226510	5.395	S-type anion channel (SLAC1-homolog protein 3)
HORVU.MOREX.r2.7HG0607010	5.392	Ras family protein (Ras related protein RHN1)
HORVU.MOREX.r2.UnG0634040	5.367	T-box transcription factor TBX1
HORVU.MOREX.r2.4HG0318270	5.363	Mitochondrial import inner membrane translocase subunit Tim17/Tim22/Tim23 protein
HORVU.MOREX.r2.7HG0595850	5.351	SWIM zinc finger family protein/ mitogen-activated protein kinase kinase kinase-related
HORVU.MOREX.r2.3HG0240680	5.338	Gibberellin 2-oxidase
HORVU.MOREX.r2.1HG0066530	5.312	Serine/threonine-protein kinase (Putative receptor protein kinase ZmPK1)
HORVU.MOREX.r2.3HG0242100	5.304	GH3.3 (Probable indole-3-acetic acid-amido synthetase GH3.2)
HORVU.MOREX.r2.5HG0367070	5.297	MYB transcription factor (Transcription factor MYB108)
HORVU.MOREX.r2.1HG0005380	5.267	Zinc finger protein (Zinc finger protein ZAT5)
HORVU.MOREX.r2.6HG0476390	5.260	Glutamyl-tRNA(Gln) amidotransferase subunit A
HORVU.MOREX.r2.6HG0450240	5.249	Glycosyltransferase (7-deoxyloganetin glucosyltransferase; Genipin glucosyltransferase)
HORVU.MOREX.r2.5HG0383660	5.244	NAC domain protein (NAC transcription factor 56)
HORVU.MOREX.r2.1HG0063020	5.242	Dof zinc finger protein (Cyclic dof factor 4; Dof zinc finger protein)
HORVU.MOREX.r2.5HG0438910	5.215	Cycloeculanol cycloisomerase
HORVU.MOREX.r2.2HG0150280	5.151	L-allo-threonine aldolase
HORVU.MOREX.r2.1HG0067320	5.131	Chaperone DnaJ
HORVU.MOREX.r2.1HG0073870	5.121	Sugar transporter protein (Sugar transporter ERD6-like 4)
HORVU.MOREX.r2.6HG0448620	5.111	Protein kinase (Probable LRR receptor-like serine/threonine-protein kinase)
HORVU.MOREX.r2.5HG0437420	5.078	Zinc finger protein (Zinc finger protein ZAT5)
HORVU.MOREX.r2.1HG0060640	4.999	transcription repressor (Transcription repressor OFP6)
HORVU.MOREX.r2.7HG0586150	4.980	transmembrane protein, putative (DUF679 domain membrane protein 2)
HORVU.MOREX.r2.7HG0607660	4.979	Beta-glucosidase, putative (Beta-glucosidase 25)
HORVU.MOREX.r2.6HG0454080	4.964	MOB kinase activator-like 1A
HORVU.MOREX.r2.1HG0005370	4.957	Zinc finger family protein (Zinc finger protein ZAT5)
HORVU.MOREX.r2.3HG0264530	4.926	Homoserine kinase
HORVU.MOREX.r2.1HG0010160	4.920	LOB domain-containing protein (ASYMMETRIC LEAVES 2like protein 7)
HORVU.MOREX.r2.6HG0496810	4.891	Trihelix transcription factor GT-2 (Trihelix transcription factor GTL1)
HORVU.MOREX.r2.7HG0555330	4.860	Jasmonate zim-domain protein (Protein TIFY 11e)
HORVU.MOREX.r2.7HG0555570	4.853	Caleosin (Probable peroxygenase 5)
HORVU.MOREX.r2.5HG0431470	4.851	Inositol 1,4,5-trisphosphate receptor-interacting protein (CASP-like protein)

HORVU.MOREX.r2.4HG0323980	4.816	neuronal PAS domain protein
HORVU.MOREX.r2.4HG0322480	4.777	dessication-induced 1VOC superfamily protein
HORVU.MOREX.r2.1HG0074930	4.705	histone deacetylase-like protein
HORVU.MOREX.r2.3HG0207730	4.703	Isoflavone reductase-like protein
HORVU.MOREX.r2.2HG0112190	4.684	Cyclin family protein
HORVU.MOREX.r2.5HG0395660	4.673	U-box domain-containing protein (Plant Ubox protein 19)
HORVU.MOREX.r2.2HG0149810	4.670	Clavamate synthase-like protein
HORVU.MOREX.r2.4HG0335550	4.661	DUF1997 family protein
HORVU.MOREX.r2.2HG0127410	4.661	4-hydroxy-tetrahydrodipicolinate reductase
HORVU.MOREX.r2.6HG0513660	4.628	Ethylene-responsive transcription factor (ERF013)
HORVU.MOREX.r2.7HG0588810	4.586	Arogenate dehydrogenase
HORVU.MOREX.r2.7HG0587680	4.586	Lectin-like protein kinase
HORVU.MOREX.r2.7HG0553480	4.584	Serine/threonine kinase WNK-related (Transcription factor bHLH155)
HORVU.MOREX.r2.1HG0058960	4.583	2-oxoglutarate (2OG) and Fe(II)-dependent oxygenase (Protein iron deficiency specific 3)
HORVU.MOREX.r2.1HG0072130	4.567	50S ribosomal protein L16
HORVU.MOREX.r2.6HG0515810	4.559	Lysine ketoglutarate reductase/saccharopine dehydrogenase
HORVU.MOREX.r2.2HG0142330	4.554	Histidine protein kinase SaeS
HORVU.MOREX.r2.3HG0246960	4.552	Transmembrane protein, putative
HORVU.MOREX.r2.3HG0256100	4.515	Pectate lyase
HORVU.MOREX.r2.5HG0363420	4.508	Zinc finger protein (COLD INDUCED ZINC FINGER PROTEIN 2, Zinc finger ZAT6)
HORVU.MOREX.r2.4HG0294380	4.490	Methyl esterase 17 (Methyl indole-3-acetic acid esterase)
HORVU.MOREX.r2.1HG0058730	4.471	Cytochrome P450 98A8
HORVU.MOREX.r2.6HG0461750	4.448	Plant regulator RWP-RK family protein (NINlike protein 3)
HORVU.MOREX.r2.2HG0159860	4.443	Xyloglucan endotransglucosylase/hydrolase
HORVU.MOREX.r2.4HG0290030	4.433	arginine N-methyltransferase, putative (DUF688)
HORVU.MOREX.r2.3HG0250370	4.430	MYB transcription factor (Transcription factor DIVARICATA)
HORVU.MOREX.r2.1HG0074130	4.426	transmembrane protein
HORVU.MOREX.r2.5HG0413910	4.413	Protein STAY-GREEN, chloroplastic
HORVU.MOREX.r2.5HG0410240	4.385	Esterase/lipase/thioesterase family protein (Acyl-transferase-like protein)
HORVU.MOREX.r2.7HG0607560	4.385	Glycosyltransferase (Cyanidin 3-O-rutinoside 5-O-glucosyltransferase)
HORVU.MOREX.r2.6HG0513330	4.374	Chaperone dnaJ-like protein
HORVU.MOREX.r2.4HG0281260	4.371	Glutamine synthetase (Glutamate ammonia ligase GLN1)
HORVU.MOREX.r2.1HG0044630	4.355	Expansin protein (Beta expansin 2)
HORVU.MOREX.r2.6HG0496860	4.324	Homeobox protein, putative (Homeoboxleucine zipper protein HOX24)
HORVU.MOREX.r2.5HG0360560	4.310	Cinnamoyl-CoA reductase 4 (Protein IRREGULAR XYLEM 4)
HORVU.MOREX.r2.7HG0562700	4.305	BTB/POZ domain-containing protein
HORVU.MOREX.r2.3HG0190020	4.288	Cytochrome P450 (Protein benzoxazineless 2, indole-2-monooxygenase)
HORVU.MOREX.r2.7HG0556530	4.279	Cytochrome P450 (Flavonoid 3' monooxygenase)
HORVU.MOREX.r2.3HG0203620	4.279	Trichome birefringence-like protein
HORVU.MOREX.r2.4HG0299650	4.239	dicer-like 2
HORVU.MOREX.r2.1HG0014960	4.217	Phosphatidylinositol 4-kinase beta 1
HORVU.MOREX.r2.1HG0068220	4.214	Ethylene-responsive transcription factor (ERF109)
HORVU.MOREX.r2.5HG0400700	4.203	Non-specific serine/threonine kinase (CBL-interacting protein kinase 16)
HORVU.MOREX.r2.7HG0603220	4.193	Ankyrin repeat family protein, putative (Protein ACCELERATED CELL DEATH)
HORVU.MOREX.r2.1HG0000660	4.190	APOLLO (Protein NEN4; NAC45/NAC86-dependent exonuclease-domain protein 4)
HORVU.MOREX.r2.6HG0512400	4.189	Calcium binding family protein
HORVU.MOREX.r2.5HG0437540	4.172	Actin depolymerizing factor
HORVU.MOREX.r2.1HG0021430	4.167	Lactoylglutathione lyase
HORVU.MOREX.r2.4HG0337670	4.163	Trypsin inhibitor (Bowman Birk type bran trypsin inhibitor)
HORVU.MOREX.r2.1HG0052100	4.155	DUF538 family protein (Protein of unknown function, DUF538)
HORVU.MOREX.r2.1HG0061390	4.147	Ethylene-responsive transcription factor
HORVU.MOREX.r2.3HG0273830	4.116	Cytochrome P450 (4-hydroxyphenylacetaldehyde oxime monooxygenase)
HORVU.MOREX.r2.7HG0533970	4.109	ABA-responsive binding factor (Dehydration-responsive element-binding protein 1C)
HORVU.MOREX.r2.5HG0356660	4.106	Glutathione S-transferase (28 kDa cold induced protein)
HORVU.MOREX.r2.2HG0144230	4.090	Heavy metal transport/detoxification superfamily protein, putative (AtFP5)
HORVU.MOREX.r2.6HG0508650	4.081	Dihydroorotate dehydrogenase (Quinone)
HORVU.MOREX.r2.UnG0630520	4.058	Cytochrome P450 (4-hydroxyphenylacetaldehyde oxime monooxygenase)
HORVU.MOREX.r2.1HG0053740	4.057	P-loop containing nucleoside triphosphate hydrolases superfamily protein
HORVU.MOREX.r2.1HG0065280	4.057	Late embryogenesis abundant protein (ABA-inducible protein PHV A1)

HORVU.MOREX.r2.3HG0197030	4.039	WRKY family transcription factor (WRKY DNA-binding protein 72)
HORVU.MOREX.r2.5HG0392460	4.031	transmembrane protein, putative (Protein of unknown function, DUF599)
HORVU.MOREX.r2.7HG0604750	4.019	High-affinity nitrate transporter 2.2
HORVU.MOREX.r2.4HG0326020	4.007	Ankyrin repeat protein-like (Alpha-latroinsectotoxinLt1a;)
HORVU.MOREX.r2.1HG0017950	3.984	Cytochrome P450 (indole-2-monooxygenase, Protein benzoxazineless)
HORVU.MOREX.r2.3HG0260290	3.982	Glutathione S-transferase (28 kDa cold-induced protein)
HORVU.MOREX.r2.3HG0184690	3.972	Abscisic acid-deficient 4 (Protein MAO HUZI 4, chloroplastic)
HORVU.MOREX.r2.5HG0418660	3.962	11S globulin seed storage protein
HORVU.MOREX.r2.1HG0075680	3.962	FAD-binding Berberine family protein
HORVU.MOREX.r2.4HG0344320	3.958	Protein PLANT CADMIUM RESISTANCE 2
HORVU.MOREX.r2.1HG0007880	3.957	Bidirectional sugar transporter SWEET (Bidirectional sugar transporter SWEET14)
HORVU.MOREX.r2.6HG0526450	3.957	Sucrose synthase (Sucrose-UDP glucosyltransferase 7)
HORVU.MOREX.r2.1HG0057620	3.947	Aminotransferase like protein (Alanine glyoxylate aminotransferase 2 homolog 3)
HORVU.MOREX.r2.3HG0192020	3.942	NAC domain protein
HORVU.MOREX.r2.5HG0365590	3.910	ATP-dependent RNA helicase HCA4
HORVU.MOREX.r2.2HG0158730	3.866	transmembrane protein, putative (DUF247)
HORVU.MOREX.r2.1HG0062610	3.864	Shugoshin C terminus
HORVU.MOREX.r2.2HG0135520	3.851	Ethylene-responsive transcription factor ERF113
HORVU.MOREX.r2.5HG0424220	3.848	Beta-glucosidase (Lysosomal beta glucosidase)
HORVU.MOREX.r2.4HG0331810	3.842	Endo-1,4-beta-xylanase
HORVU.MOREX.r2.3HG0238350	3.834	Glycosyltransferase (UDPglucose: anthocyanidin 5,3-O-glucosyltransferase)
HORVU.MOREX.r2.6HG0474180	3.825	Protein trichome birefringence
HORVU.MOREX.r2.3HG0190050	3.814	Cytochrome P450 (indole-2-monooxygenase; Protein benzoxazineless 2)
HORVU.MOREX.r2.5HG0424190	3.784	Beta-glucosidase (Glycosyl hydrolase family protein 3B)
HORVU.MOREX.r2.6HG0505500	3.767	2-oxoglutarate (2OG) and Fe(II)-dependent oxygenase
HORVU.MOREX.r2.2HG0106570	3.759	Proline-rich nuclear receptor coactivator 2
HORVU.MOREX.r2.5HG0430520	3.754	Lipid transfer protein
HORVU.MOREX.r2.5HG0360620	3.743	WRKY transcription factor (WRKY DNAbinding protein 11)
HORVU.MOREX.r2.4HG0335580	3.742	Major facilitator superfamily protein
HORVU.MOREX.r2.1HG0021410	3.721	Lactoylglutathione lyase
HORVU.MOREX.r2.2HG0161460	3.716	Polyphenol oxidase
HORVU.MOREX.r2.1HG0031680	3.709	Plant/T7N9-9 protein
HORVU.MOREX.r2.2HG0105590	3.686	IgA FC receptor
HORVU.MOREX.r2.6HG0476540	3.684	BZip transcription factor
HORVU.MOREX.r2.7HG0615690	3.680	DNA polymerase III PolC-type
HORVU.MOREX.r2.6HG0462660	3.672	Vacuolar cation/proton exchanger, putative (Ca(2+)/H(+) exchanger 4)
HORVU.MOREX.r2.2HG0149830	3.662	Caleosin (Peroxygenase)
HORVU.MOREX.r2.5HG0405550	3.662	Type 2 phosphatidylinositol 4,5-bisphosphate 4-phosphatase
HORVU.MOREX.r2.1HG0058030	3.657	Glutaredoxin-like
HORVU.MOREX.r2.2HG0141720	3.650	Protein kinase superfamily protein
HORVU.MOREX.r2.4HG0348600	3.648	Heat shock transcription factor (C2b)
HORVU.MOREX.r2.1HG0020770	3.640	Arabinogalactan peptide-like protein
HORVU.MOREX.r2.7HG0614180	3.634	4-coumarate:CoA ligase
HORVU.MOREX.r2.6HG0511920	3.632	RNA-binding protein (ABA-regulated RNA-binding protein 1)
HORVU.MOREX.r2.2HG0169050	3.623	Leucine-rich repeat protein kinase family protein
HORVU.MOREX.r2.3HG0223690	3.618	Inorganic pyrophosphatase 2 (Pyrophosphatespecific phosphatase 3)
HORVU.MOREX.r2.2HG0139750	3.616	Amino acid permease (Amino acid permease BAT1)
HORVU.MOREX.r2.3HG0233790	3.611	Receptor-like protein kinase
HORVU.MOREX.r2.3HG0203250	3.604	Flowering locus T (Protein HEADING DATE 3A; FT-like protein A)
HORVU.MOREX.r2.1HG0070660	3.580	Eukaryotic aspartyl protease family protein
HORVU.MOREX.r2.3HG0246620	3.570	Late embryogenesis abundant (LEA) hydroxyproline-rich glycoprotein
HORVU.MOREX.r2.4HG0334350	3.560	Histone H2B
HORVU.MOREX.r2.5HG0397860	3.535	Kinase family protein (Serine/threonine protein kinase At5g01020)
HORVU.MOREX.r2.2HG0153370	3.516	Kinase family protein (Probable receptor like protein kinase)
HORVU.MOREX.r2.2HG0174300	3.504	Dof zinc finger protein (Dof zinc finger protein DOF5.8)
HORVU.MOREX.r2.5HG0357350	3.485	2-oxoglutarate and Fe(II)-dependent oxygenase (Protein DMR6-LIKE OXYGENASE 1)
HORVU.MOREX.r2.5HG0434720	3.467	abscisic acid responsive elements-binding factor 2
HORVU.MOREX.r2.7HG0593520	3.460	Receptor-kinase, putative
HORVU.MOREX.r2.1HG0050960	3.460	CASP-like protein
HORVU.MOREX.r2.7HG0610860	3.456	SAUR-like auxin-responsive family protein (SMALL AUXIN UP RNA 72)

HORVU.MOREX.r2.4HG0328360	3.446	Branched-chain-amino-acid aminotransferase
HORVU.MOREX.r2.7HG0553050	3.443	GDSL esterase/lipase (Extracellular lipase At1g74460)
HORVU.MOREX.r2.6HG0509890	3.433	Kelch repeat-containing protein (SKP-1-interacting partner 11)
HORVU.MOREX.r2.3HG0224130	3.406	Chaperone protein DnaJ
HORVU.MOREX.r2.7HG0615710	3.400	RNA-directed DNA polymerase-related family protein
HORVU.MOREX.r2.3HG0201000	3.392	Alpha/beta-Hydrolases superfamily protein (Probable carboxyl-esterase 15)
HORVU.MOREX.r2.4HG0326540	3.387	Thaumatococin (Thaumatococin-like protein 1)
HORVU.MOREX.r2.3HG0206740	3.381	Transducin/WD40 repeat-like superfamily protein (Putative E3 ubiquitin protein ligase)
HORVU.MOREX.r2.2HG0157690	3.375	Lipid transfer protein
HORVU.MOREX.r2.1HG0070240	3.370	2-oxoglutarate (2OG) and Fe(II)-dependent oxygenase superfamily protein
HORVU.MOREX.r2.4HG0296980	3.365	Lipid-transfer protein
HORVU.MOREX.r2.6HG0452100	3.365	High affinity nitrate transporter
HORVU.MOREX.r2.2HG0105290	3.350	IgA FC receptor
HORVU.MOREX.r2.6HG0502370	3.349	Xyloglucan endotransglucosylase/hydrolase
HORVU.MOREX.r2.2HG0141340	3.339	F-box protein family-like
HORVU.MOREX.r2.7HG0598020	3.334	Zinc finger, B-box (Protein SALT TOLERANCE HOMOLOG)
HORVU.MOREX.r2.1HG0048110	3.311	Alpha/beta-Hydrolases superfamily protein (Caffeoylshikimate esterase;)
HORVU.MOREX.r2.2HG0083230	3.308	Phosphoglycerate mutase-like protein
HORVU.MOREX.r2.2HG0147850	3.303	Peroxidase 18
HORVU.MOREX.r2.2HG0144950	3.276	C2 and GRAM domain-containing protein
HORVU.MOREX.r2.1HG0012520	3.275	Aminotransferase like protein (Acetylornithine aminotransferase)
HORVU.MOREX.r2.7HG0533490	3.266	Oligopeptide transporter
HORVU.MOREX.r2.3HG0262310	3.266	Methyl esterase 1, putative (Probable esterase PIR7A)
HORVU.MOREX.r2.2HG0154440	3.260	FXYD domain-containing ion transport regulator 3
HORVU.MOREX.r2.3HG0256140	3.257	Cyclophilin-like peptidyl-prolyl cis-trans isomerase family protein
HORVU.MOREX.r2.5HG0384680	3.256	Pentatricopeptide repeat-containing protein
HORVU.MOREX.r2.7HG0556520	3.252	HIPL1 protein
HORVU.MOREX.r2.3HG0202770	3.245	Lachrymatory factor synthase
HORVU.MOREX.r2.6HG0474220	3.216	transmembrane protein, putative (DUF247)
HORVU.MOREX.r2.5HG0430510	3.211	Lipid transfer protein
HORVU.MOREX.r2.2HG0168980	3.209	Hydroxycinnamoyl-CoA shikimate/quinate hydroxycinnamoyltransferase
HORVU.MOREX.r2.3HG0260390	3.207	NAC domain protein (Protein VND-INTERACTING 2)
HORVU.MOREX.r2.5HG0436790	3.206	Pathogenesis-related thaumatin family protein
HORVU.MOREX.r2.3HG0196880	3.189	WRKY transcription factor (WRKY DNA binding protein 50)
HORVU.MOREX.r2.1HG0000390	3.180	Glucan 1,3-beta-glucosidase (Exo-1,3-beta-glucanase)
HORVU.MOREX.r2.7HG0598660	3.154	Germin-like protein
HORVU.MOREX.r2.6HG0479630	3.144	NIMA-related kinase 4
HORVU.MOREX.r2.2HG0160590	3.120	Ubiquinol oxidase
HORVU.MOREX.r2.2HG0082080	3.119	Glycosyltransferase (7-deoxyloganetin glucosyltransferase; Genipin glucosyltransferase)
HORVU.MOREX.r2.3HG0234530	3.113	Protein kinase-like (Mitogenactivated protein kinase kinase kinase ANP1)
HORVU.MOREX.r2.3HG0271660	3.110	Histidine decarboxylase (Serine decarboxylase 1)
HORVU.MOREX.r2.3HG0241980	3.107	Blue copper protein
HORVU.MOREX.r2.7HG0610870	3.107	SAUR-like auxin-responsive protein family (SMALL AUXIN UP RNA 72)
HORVU.MOREX.r2.3HG0253930	3.103	Cysteine proteinase (KDEL tailed cysteine endopeptidase CEP1)
HORVU.MOREX.r2.3HG0241870	3.100	Glutathione S-transferase
HORVU.MOREX.r2.1HG0002490	3.097	O-methyltransferase-like protein
HORVU.MOREX.r2.5HG0417090	3.097	Calmodulin-like protein
HORVU.MOREX.r2.5HG0359910	3.096	Non-specific serine/threonine kinase (CBL-interacting protein kinase 4)
HORVU.MOREX.r2.5HG0398150	3.086	Aldehyde dehydrogenase (Antiquitin-1)
HORVU.MOREX.r2.7HG0610820	3.078	Cytochrome P450 (indole-2-monooxygenase)
HORVU.MOREX.r2.2HG0105580	3.073	IgA FC receptor
HORVU.MOREX.r2.5HG0407610	3.068	SIN3-like 1
HORVU.MOREX.r2.3HG0238860	3.064	Glutamate carboxypeptidase 2
HORVU.MOREX.r2.2HG0086370	3.059	Heavy metal-associated domain containing protein, expressed (AtHIPP27)
HORVU.MOREX.r2.1HG0068690	3.046	Homeobox associated leucine zipper protein
HORVU.MOREX.r2.5HG0405180	3.038	F-box protein (F-box/LRR-repeat protein At2g43260)
HORVU.MOREX.r2.6HG0497990	3.034	Cell division cycle 23-like protein
HORVU.MOREX.r2.6HG0524590	3.021	Electron transfer flavoprotein beta-subunit
HORVU.MOREX.r2.3HG0236180	3.018	Protein phosphatase 2C (Probable protein phosphatase 2C 50)
HORVU.MOREX.r2.1HG0002200	3.016	Ras-related protein, expressed (Ras-related protein RABA2a)

HORVU.MOREX.r2.5HG0430070	3.014	Purine permease-like protein
HORVU.MOREX.r2.7HG0552980	3.013	Amino acid permease
HORVU.MOREX.r2.5HG0439330	3.012	Mannan endo-1,4-beta-mannosidase 4
HORVU.MOREX.r2.3HG0226300	2.999	Amino acid transporter family protein (Probable GABA transporter 2)
HORVU.MOREX.r2.1HG0053260	2.984	Wound-induced protease inhibitor
HORVU.MOREX.r2.7HG0588290	2.981	RING/U-box protein (RING-type E3 ubiquitin transferase ATL43)
HORVU.MOREX.r2.3HG0235880	2.974	Voltage-dependent calcium channel subunit alpha-2/delta-1
HORVU.MOREX.r2.2HG0111800	2.971	MYB transcription factor (Myb related protein 39)
HORVU.MOREX.r2.7HG0594280	2.968	Beta-galactosidase (Lactase 9)
HORVU.MOREX.r2.3HG0251960	2.964	Gamma-glutamyl phosphate reductase (Delta-1-pyrroline-5-carboxylate synthase P5CS)
HORVU.MOREX.r2.3HG0260200	2.956	SAUR-like auxin-responsive family protein
HORVU.MOREX.r2.6HG0508630	2.914	MACPF domain-containing protein
HORVU.MOREX.r2.6HG0514200	2.906	Allene oxide cyclase (Protein COLEOPTILE PHOTOMORPHOGENESIS)
HORVU.MOREX.r2.2HG0126480	2.904	Photosystem II 10 kDa polypeptide family protein
HORVU.MOREX.r2.2HG0150960	2.899	Leguminosin group485 secreted peptide
HORVU.MOREX.r2.7HG0537910	2.897	Glutathione S-transferase (Heat shock protein 26A)
HORVU.MOREX.r2.3HG0248580	2.897	F-box protein
HORVU.MOREX.r2.1HG0046990	2.889	Calcium binding family protein (Probable calcium-binding protein CML15)
HORVU.MOREX.r2.5HG0418820	2.886	Auxin Efflux Carrier family protein
HORVU.MOREX.r2.5HG0425850	2.877	K ⁺ uptake permease 9
HORVU.MOREX.r2.7HG0544640	2.877	CASP-like protein
HORVU.MOREX.r2.1HG0040480	2.869	Glutathione s-transferase (Protein EARLY RESPONSIVE TO DEHYDRATION 9)
HORVU.MOREX.r2.5HG0401270	2.867	Vacuolar-processing enzyme
HORVU.MOREX.r2.1HG0047430	2.866	Diacylglycerol kinase
HORVU.MOREX.r2.7HG0614190	2.864	CASP-like protein
HORVU.MOREX.r2.3HG0232910	2.846	RING/FYVE/PHD zinc finger superfamily protein
HORVU.MOREX.r2.2HG0083970	2.843	S-adenosylmethionine-dependent methyltransferase
HORVU.MOREX.r2.2HG0102730	2.842	Cold regulated protein 27
HORVU.MOREX.r2.2HG0107530	2.832	Transferase (Omega-hydroxy-palmitate O-feruloyl transferase)
HORVU.MOREX.r2.1HG0023260	2.819	nuclease
HORVU.MOREX.r2.2HG0165780	2.817	Organic cation transporter protein (Organic cation/carnitine transporter 4)
HORVU.MOREX.r2.2HG0172140	2.813	Nuclease S1 (Single-strand-ednucleate endonuclease ENDO1)
HORVU.MOREX.r2.5HG0396930	2.811	54S ribosomal protein L4, mitochondrial
HORVU.MOREX.r2.5HG0383600	2.807	Zinc finger family protein
HORVU.MOREX.r2.7HG0571920	2.806	Squamosa promoter-binding protein-like (SBP domain) transcription factor
HORVU.MOREX.r2.6HG0511260	2.806	Universal stress protein
HORVU.MOREX.r2.1HG0059580	2.804	Legume-specific protein
HORVU.MOREX.r2.3HG0235580	2.803	Cytokinin riboside 5'-monophosphate phosphoribohydrolase (LONELY GUY-like 1)
HORVU.MOREX.r2.5HG0368350	2.785	Universal stress family protein
HORVU.MOREX.r2.1HG0006680	2.776	TOX high mobility group box protein, putative (DUF1635)
HORVU.MOREX.r2.6HG0497420	2.775	Blue copper protein
HORVU.MOREX.r2.5HG0428390	2.773	Leguminosin group485 secreted peptide
HORVU.MOREX.r2.3HG0235870	2.771	Protein REVERSION-TO-ETHYLENE SENSITIVITY1
HORVU.MOREX.r2.7HG0549240	2.767	Zinc-finger protein (COLD INDUCED ZINC FINGER PROTEIN 2)
HORVU.MOREX.r2.7HG0535170	2.765	F-box protein PP2 (Protein PHLOEM PROTEIN 2LIKE B10)
HORVU.MOREX.r2.1HG0051960	2.765	NAC domain-containing protein 48
HORVU.MOREX.r2.6HG0509110	2.761	VQ motif family protein
HORVU.MOREX.r2.1HG0059270	2.751	Histone H2B
HORVU.MOREX.r2.2HG0144330	2.741	Amino acid permease (Amino acid transporter AAP7)
HORVU.MOREX.r2.3HG0248920	2.738	Myb transcription factor
HORVU.MOREX.r2.4HG0321820	2.736	Plant protein 1589 of Uncharacterized protein function
HORVU.MOREX.r2.3HG0203750	2.735	Cellulose synthase
HORVU.MOREX.r2.3HG0209970	2.731	D-(-)-3-hydroxybutyrate oligomer hydrolase
HORVU.MOREX.r2.7HG0598650	2.731	Germin-like protein
HORVU.MOREX.r2.2HG0094120	2.728	GDSL esterase/lipase
HORVU.MOREX.r2.4HG0335860	2.720	SAUR-like auxin-responsive family protein
HORVU.MOREX.r2.3HG0186310	2.714	GDSL esterase/lipase (Extracellular lipase At5g14450)
HORVU.MOREX.r2.2HG0163510	2.712	Methyl esterase
HORVU.MOREX.r2.1HG0039410	2.707	DUF538 family protein (Protein of unknown function, DUF538)

HORVU.MOREX.r2.3HG0224260	2.697	Emb CAB62340.1
HORVU.MOREX.r2.2HG0154950	2.680	F-box protein PP2-A13 (Protein PHLOEM PROTEIN 2LIKE A13)
HORVU.MOREX.r2.7HG0548470	2.672	LL-diaminopimelate aminotransferase
HORVU.MOREX.r2.3HG0206270	2.670	Short-chain dehydrogenase/reductase (Probable chlorophyll(ide) b reductase NYC1)
HORVU.MOREX.r2.2HG0104130	2.665	Nuclear transcription factor Y subunit
HORVU.MOREX.r2.7HG0550180	2.656	RNA ligase/cyclic nucleotide phosphodiesterase family protein
HORVU.MOREX.r2.2HG0096000	2.654	Auxin-induced in root cultures protein 12
HORVU.MOREX.r2.3HG0210160	2.651	Lipase
HORVU.MOREX.r2.4HG0285500	2.650	Adenine/guanine permease (Protein AZAGUANINE RESISTANT 2)
HORVU.MOREX.r2.3HG0271750	2.648	Glutathione S-transferase (28 kDa cold induced protein)
HORVU.MOREX.r2.5HG0349880	2.648	Kinase, putative (L-type lectin domain containing receptor kinase IX.1)
HORVU.MOREX.r2.1HG0053690	2.626	Wound-induced protease inhibitor
HORVU.MOREX.r2.7HG0593530	2.623	Visual system homeobox 1
HORVU.MOREX.r2.5HG0403080	2.617	Calmodulin
HORVU.MOREX.r2.3HG0195620	2.605	Lectin receptor kinase (L-type lectin domain containing receptor kinase)
HORVU.MOREX.r2.5HG0445120	2.597	NAD-dependent malic enzyme (DNA repair RAD52 like protein 2)
HORVU.MOREX.r2.7HG0569760	2.595	DUF936 family protein
HORVU.MOREX.r2.7HG0558340	2.593	Glycosyltransferase (UDP-glucose:2-hydroxyflavanone C-glucosyl-transferase)
HORVU.MOREX.r2.2HG0100030	2.586	Cytochrome P450
HORVU.MOREX.r2.3HG0236590	2.578	Zinc finger A20 and AN1 domain stress-associated protein
HORVU.MOREX.r2.3HG0265150	2.567	Pimeloyl-[acyl-carrier protein] methyl ester esterase
HORVU.MOREX.r2.7HG0533390	2.555	Oligopeptide transporter
HORVU.MOREX.r2.4HG0279600	2.555	DUF538 family protein, putative (Protein of unknown function, DUF538)
HORVU.MOREX.r2.1HG0042390	2.543	CASP-like protein
HORVU.MOREX.r2.5HG0382780	2.534	Gamma-glutamyl phosphate reductase
HORVU.MOREX.r2.6HG0479090	2.523	Ran-binding zinc finger protein
HORVU.MOREX.r2.7HG0557310	2.522	Peroxidase
HORVU.MOREX.r2.3HG0193390	2.515	Pyrimidine-specific ribonucleoside hydrolase
HORVU.MOREX.r2.3HG0262580	2.506	Homeobox-leucine zipper protein / lipid-binding START domain-containing protein
HORVU.MOREX.r2.2HG0173010	2.472	Light-independent protochlorophyllide reductase iron-sulfur ATP-binding protein
HORVU.MOREX.r2.3HG0249890	2.454	Transcription factor (Gbox binding factor 4, bZIP transcription factor 40)
HORVU.MOREX.r2.3HG0237610	2.443	UDP-2,3-diacetylglucosamine hydrolase
HORVU.MOREX.r2.2HG0167340	2.441	Protein kinase (Abscisic acid-inducible protein kinase)
HORVU.MOREX.r2.1HG0040640	2.437	Glutathione S-transferase
HORVU.MOREX.r2.6HG0496470	2.428	SAUR-like auxin-responsive family protein
HORVU.MOREX.r2.6HG0496150	2.428	MYB transcription factor (Transcription factor LAF1)
HORVU.MOREX.r2.4HG0325680	2.425	Transcription initiation factor IIF subunit alpha
HORVU.MOREX.r2.3HG0203880	2.423	Ring finger protein, putative (RING type E3 ubiquitin transferase ATL5)
HORVU.MOREX.r2.4HG0344600	2.419	UDP-galactose transporter
HORVU.MOREX.r2.1HG0066900	2.417	NBS-LRR-like resistance protein (disease resistance RPP13-like protein 1)
HORVU.MOREX.r2.1HG0053820	2.412	NB-ARC domain-containing disease resistance protein
HORVU.MOREX.r2.2HG0105550	2.407	IgA FC receptor
HORVU.MOREX.r2.4HG0331160	2.402	Metal transporter
HORVU.MOREX.r2.5HG0391510	2.386	IAA-amino acid hydrolase ILR1
HORVU.MOREX.r2.1HG0032670	2.378	PPPDE thiol peptidase family protein (Desumoylating isopeptidase 1)
HORVU.MOREX.r2.2HG0082480	2.378	Arginase (Arginine amidohydrolase 1)
HORVU.MOREX.r2.7HG0572820	2.368	Carboxypeptidase (Serine carboxypeptidase like 51)
HORVU.MOREX.r2.7HG0591450	2.367	Alpha/beta hydrolase, putative (Pheophytinase, chloroplastic)
HORVU.MOREX.r2.7HG0611170	2.364	two-component response regulator (putative Myb transcription factor)
HORVU.MOREX.r2.5HG0441010	2.332	Electron transfer flavoprotein subunit alpha, mitochondrial
HORVU.MOREX.r2.1HG0033820	2.315	Transporter-related family protein
HORVU.MOREX.r2.3HG0270060	2.313	Disease resistance protein (TIR-NBS-LRR class) family
HORVU.MOREX.r2.7HG0620680	2.310	Blue copper protein
HORVU.MOREX.r2.1HG0073980	2.297	O-methyltransferase (Probable inactive methyltransferase)
HORVU.MOREX.r2.1HG0073880	2.296	O-methyltransferase (Flavonoid O-methyl-transferase like protein)
HORVU.MOREX.r2.6HG0512770	2.292	Universal stress protein family protein
HORVU.MOREX.r2.3HG0250200	2.288	Uricase (Urate oxidase)
HORVU.MOREX.r2.6HG0477640	2.271	Protein kinase family protein (PTI1-like tyrosineprotein kinase At3g15890)
HORVU.MOREX.r2.3HG0232400	2.262	O-acyltransferase WSD1 (Wax synthase)

HORVU.MOREX.r2.6HG0449500	2.258	Receptor-like protein kinase (Wall associated receptor kinase 4)
HORVU.MOREX.r2.6HG0521020	2.244	Receptor-like protein kinase (Wall-associated receptor kinase 3)
HORVU.MOREX.r2.3HG0225070	2.238	Ubiquitin-like modifier-activating enzyme atg7
HORVU.MOREX.r2.6HG0508410	2.237	Blue copper protein
HORVU.MOREX.r2.2HG0091480	2.224	NAC domain protein (NAC transcription factor NAMB1)
HORVU.MOREX.r2.5HG0445480	2.220	Hydroxyproline-rich glycoprotein family protein
HORVU.MOREX.r2.4HG0289360	2.219	Protein BPS1, chloroplastic
HORVU.MOREX.r2.1HG0014140	2.211	Thioesterase family protein (1,4-dihydroxy-2-naphthoyl-CoA thioesterase 1)
HORVU.MOREX.r2.4HG0277430	2.205	Chlorophyll-(ide) b reductase NOL; Protein NONYELLOW COLORING 1-LIKE
HORVU.MOREX.r2.3HG0200070	2.195	Plant/MSJ1 1-3 protein, putative
HORVU.MOREX.r2.7HG0618650	2.195	Protein kinase, putative (E3 ubiquitin protein ligase KEG)
HORVU.MOREX.r2.7HG0539640	2.191	WRKY family transcription factor (WRKY transcription factor 61)
HORVU.MOREX.r2.2HG0141090	2.190	S-adenosyl-L-methionine-dependent methyltransferases superfamily protein
HORVU.MOREX.r2.2HG0159810	2.173	Leucine-rich repeat (LRR) family protein
HORVU.MOREX.r2.2HG0173550	2.163	Heavy metal transport/detoxification superfamily protein (AtHIP39)
HORVU.MOREX.r2.4HG0279030	2.158	Exostosin-2 (Glycosyltransferase family protein 64 protein C5)
HORVU.MOREX.r2.1HG0061930	2.136	Cysteine protease family protein
HORVU.MOREX.r2.5HG0422550	2.133	Transporter-related family protein (Organic cation/carnitine transporter 7)
HORVU.MOREX.r2.6HG0504490	2.126	Protein kinase (G-type lectin Sreceptorlike serine/threonine-protein kinase)
HORVU.MOREX.r2.6HG0460340	2.110	F-box family protein
HORVU.MOREX.r2.3HG0194250	2.103	Inhibitor protein (Subtilisin-chymotrypsin inhibitor-2A)
HORVU.MOREX.r2.4HG0335560	2.064	plant/protein
HORVU.MOREX.r2.3HG0198580	2.059	embryo defective 2410
HORVU.MOREX.r2.5HG0407490	2.035	Protein Iojap/ribosomal silencing factor RsfS
HORVU.MOREX.r2.7HG0572250	2.032	Pyrimidine-specific ribonucleoside hydrolase
HORVU.MOREX.r2.2HG0125570	2.023	Glutaredoxin family protein, putative
HORVU.MOREX.r2.3HG0195030	2.017	neuronal PAS domain protein
HORVU.MOREX.r2.3HG0263430	2.004	Receptor protein kinase-like

Table 5: List of SDGs in WT barley primary leaves. Gene IDs, log₂FC and gene annotations are provided.

Gene ID	log ₂ FC	gene annotation
HORVU.MOREX.r2.7HG0534180	-10.968	Acid phosphatase 1
HORVU.MOREX.r2.5HG0351680	-10.087	Terpene synthase
HORVU.MOREX.r2.7HG0597270	-8.999	Polyamine oxidase
HORVU.MOREX.r2.5HG0415670	-8.419	Aquaporin-like protein
HORVU.MOREX.r2.2HG0171870	-8.396	Lipoxygenase
HORVU.MOREX.r2.2HG0092490	-7.773	Peroxidase
HORVU.MOREX.r2.5HG0350050	-7.730	Lipoxygenase
HORVU.MOREX.r2.2HG0142270	-7.536	Phage capsid scaffolding protein (GPO) serine peptidase
HORVU.MOREX.r2.1HG0004420	-7.447	Cytochrome P450, putative
HORVU.MOREX.r2.3HG0206750	-6.928	5'-methylthioadenosine/S-adenosylhomocysteine nucleosidase
HORVU.MOREX.r2.UnG0628730	-6.729	Thionin
HORVU.MOREX.r2.2HG0085980	-6.660	Ribulose bisphosphate carboxylase small chain
HORVU.MOREX.r2.6HG0517650	-6.555	Purple acid phosphatase
HORVU.MOREX.r2.1HG0068790	-6.524	Lipid transfer protein
HORVU.MOREX.r2.3HG0191820	-6.502	Cytochrome P450 family protein, expressed
HORVU.MOREX.r2.1HG0077160	-6.498	Ribonuclease
HORVU.MOREX.r2.1HG0041050	-6.471	XRI1-like protein
HORVU.MOREX.r2.2HG0171910	-6.319	Lipoxygenase
HORVU.MOREX.r2.6HG0454160	-6.258	Peroxidase
HORVU.MOREX.r2.7HG0593770	-6.160	Receptor-kinase, putative
HORVU.MOREX.r2.4HG0288490	-6.088	Dirigent protein
HORVU.MOREX.r2.5HG0382290	-6.057	F-box/kelch-repeat protein
HORVU.MOREX.r2.2HG0174220	-6.006	Cytochrome P450 family protein, expressed
HORVU.MOREX.r2.UnG0635360	-5.682	NAD(P)H-quinone oxidoreductase subunit 6, chloroplastic
HORVU.MOREX.r2.7HG0539180	-5.645	Early nodulin 93
HORVU.MOREX.r2.1HG0077150	-5.633	Ribonuclease
HORVU.MOREX.r2.6HG0493550	-5.552	Ammonium transporter
HORVU.MOREX.r2.1HG0076290	-5.528	Glucan endo-1,3-beta-glucosidase 3
HORVU.MOREX.r2.7HG0621990	-5.472	Cysteine protease, putative

HORVU.MOREX.r2.2HG0177070	-5.315	GDSL esterase/lipase
HORVU.MOREX.r2.2HG0092440	-5.263	Peroxidase
HORVU.MOREX.r2.4HG0345840	-5.258	Acid phosphatase 1
HORVU.MOREX.r2.UnG0624330	-5.232	Cytochrome P450
HORVU.MOREX.r2.1HG0073470	-5.166	Chlorophyll a-b binding protein, chloroplastic
HORVU.MOREX.r2.6HG0476900	-5.129	Kinase family protein
HORVU.MOREX.r2.6HG0456280	-5.060	Linalool synthase, chloroplastic
HORVU.MOREX.r2.2HG0092860	-5.051	ABC transporter G family member
HORVU.MOREX.r2.4HG0339950	-5.047	WAT1-related protein
HORVU.MOREX.r2.1HG0073660	-4.997	Subtilisin-like protease
HORVU.MOREX.r2.2HG0086010	-4.996	Ribulose bisphosphate carboxylase small chain
HORVU.MOREX.r2.3HG0269820	-4.973	Phospholipase A1
HORVU.MOREX.r2.6HG0508300	-4.925	cysteine-rich repeat secretory-like protein
HORVU.MOREX.r2.3HG0181490	-4.862	basic helix-loop-helix (bHLH) DNA-binding superfamily protein
HORVU.MOREX.r2.1HG0057310	-4.849	Expansin
HORVU.MOREX.r2.2HG0085320	-4.824	Aspartic proteinase nepenthesin-1
HORVU.MOREX.r2.3HG0275510	-4.820	Jasmonate-induced protein
HORVU.MOREX.r2.5HG0410540	-4.772	Plant/MAC12-16 protein
HORVU.MOREX.r2.3HG0235080	-4.764	ABC transporter G family member
HORVU.MOREX.r2.7HG0621180	-4.651	GDSL esterase/lipase
HORVU.MOREX.r2.3HG0243630	-4.639	Cytokinin oxidase/dehydrogenase
HORVU.MOREX.r2.6HG0459100	-4.625	Phototropic-responsive NPH3 family protein
HORVU.MOREX.r2.6HG0450600	-4.607	Pathogenesis-related thaumatin superfamily protein
HORVU.MOREX.r2.6HG0505970	-4.561	DUF506 family protein
HORVU.MOREX.r2.5HG0429680	-4.535	phosphoglucose isomerase 1
HORVU.MOREX.r2.7HG0529200	-4.516	MLO-like protein
HORVU.MOREX.r2.UnG0630690	-4.513	NAD(P)H-quinone oxidoreductase subunit J, chloroplastic
HORVU.MOREX.r2.3HG0208840	-4.452	Carboxypeptidase
HORVU.MOREX.r2.5HG0367400	-4.446	Lysine/histidine transporter
HORVU.MOREX.r2.3HG0210370	-4.439	Pectinesterase
HORVU.MOREX.r2.4HG0337410	-4.391	Cyanate hydratase
HORVU.MOREX.r2.4HG0322380	-4.341	Cysteine-rich receptor-kinase-like protein
HORVU.MOREX.r2.4HG0336620	-4.335	O-methyltransferase
HORVU.MOREX.r2.UnG0633650	-4.311	NADH-quinone oxidoreductase subunit B
HORVU.MOREX.r2.7HG0596360	-4.304	Peroxidase
HORVU.MOREX.r2.5HG0411230	-4.299	Glutamate racemase
HORVU.MOREX.r2.2HG0134510	-4.273	Heavy metal-associated protein
HORVU.MOREX.r2.4HG0288340	-4.244	translation initiation factor
HORVU.MOREX.r2.7HG0561650	-4.243	Basic helix-loop-helix transcription factor
HORVU.MOREX.r2.1HG0007840	-4.220	Tryptophan decarboxylase
HORVU.MOREX.r2.4HG0346630	-4.195	Aspartic proteinase nepenthesin-1
HORVU.MOREX.r2.4HG0346330	-4.192	Cortical cell-delineating protein
HORVU.MOREX.r2.5HG0413450	-4.190	Cytochrome P450, putative
HORVU.MOREX.r2.2HG0158490	-4.179	Histone-lysine N-methyltransferase 2C
HORVU.MOREX.r2.4HG0289000	-4.077	FAD-binding Berberine family protein
HORVU.MOREX.r2.6HG0456270	-4.055	Linalool synthase, chloroplastic
HORVU.MOREX.r2.4HG0277800	-4.027	Auxin responsive protein
HORVU.MOREX.r2.5HG0438580	-4.014	Protein NRT1/ PTR FAMILY 5.5
HORVU.MOREX.r2.6HG0454180	-3.991	Peroxidase
HORVU.MOREX.r2.UnG0634460	-3.987	NAD(P)H-quinone oxidoreductase subunit 3, chloroplastic
HORVU.MOREX.r2.3HG0260970	-3.969	Basic helix-loop-helix (BHLH) Transcription Factor
HORVU.MOREX.r2.6HG0503810	-3.962	Transcription factor RADIALIS
HORVU.MOREX.r2.6HG0454170	-3.959	Peroxidase
HORVU.MOREX.r2.5HG0440710	-3.951	Glucan endo-1,3-beta-glucosidase 1
HORVU.MOREX.r2.2HG0137090	-3.950	Carbonic anhydrase
HORVU.MOREX.r2.3HG0225660	-3.936	Lipase
HORVU.MOREX.r2.1HG0073510	-3.925	Chlorophyll a-b binding protein, chloroplastic
HORVU.MOREX.r2.4HG0291520	-3.813	Egg cell-secreted protein 1.1
HORVU.MOREX.r2.3HG0188690	-3.813	Non-specific lipid-transfer protein
HORVU.MOREX.r2.5HG0410520	-3.806	Plant/MAC12-16 protein
HORVU.MOREX.r2.5HG0401720	-3.785	Zinc finger protein-like
HORVU.MOREX.r2.4HG0343090	-3.779	Mechanosensitive ion channel
HORVU.MOREX.r2.6HG0504120	-3.776	Formate dehydrogenase, mitochondrial
HORVU.MOREX.r2.3HG0254560	-3.751	Peptide transporter
HORVU.MOREX.r2.1HG0076230	-3.732	Glucan endo-1,3-beta-glucosidase 3

HORVU.MOREX.r2.2HG0158500	-3.707	Bifunctional inhibitor/lipid-transfer protein/seed storage 2Salbumin superfamily protein
HORVU.MOREX.r2.3HG0245140	-3.670	Polyphenol oxidase
HORVU.MOREX.r2.2HG0127000	-3.665	Amino acid permease
HORVU.MOREX.r2.2HG0084360	-3.661	Sulfotransferase
HORVU.MOREX.r2.4HG0348610	-3.620	Metacaspase-1
HORVU.MOREX.r2.7HG0571590	-3.561	Chlorophyll a-b binding protein, chloroplastic
HORVU.MOREX.r2.5HG0407340	-3.557	NAD(P)-binding Rossmann-fold superfamily protein
HORVU.MOREX.r2.6HG0451460	-3.548	Flowering promoting factor-like 1
HORVU.MOREX.r2.3HG0265860	-3.546	Endo-1,3-beta-glucanase
HORVU.MOREX.r2.5HG0441740	-3.501	Protein DETOXIFICATION
HORVU.MOREX.r2.3HG0271390	-3.496	Abscisic stress ripening
HORVU.MOREX.r2.1HG0073480	-3.495	Chlorophyll a-b binding protein, chloroplastic
HORVU.MOREX.r2.2HG0083680	-3.457	Cyclopropane-fatty-acyl-phospholipid synthase
HORVU.MOREX.r2.2HG0092470	-3.452	Peroxidase
HORVU.MOREX.r2.4HG0328590	-3.449	Allene oxide synthase
HORVU.MOREX.r2.4HG0348300	-3.431	Protein WEAK CHLOROPLAST MOVEMENT UNDER BLUE LIGHT 1
HORVU.MOREX.r2.4HG0329070	-3.352	Cytochrome P450 family protein, expressed
HORVU.MOREX.r2.4HG0346110	-3.341	Basic helix-loop-helix (BHLH) Transcription Factor
HORVU.MOREX.r2.2HG0163720	-3.334	disease resistance protein (TIR-NBS-LRR class)
HORVU.MOREX.r2.5HG0371220	-3.328	LIM domain protein
HORVU.MOREX.r2.7HG0546850	-3.274	Dirigent protein
HORVU.MOREX.r2.4HG0345700	-3.272	Branched-chain-amino-acid aminotransferase
HORVU.MOREX.r2.5HG0408540	-3.251	Glucan endo-1,3-beta-glucosidase-like protein
HORVU.MOREX.r2.3HG0261990	-3.244	Laccase
HORVU.MOREX.r2.7HG0585720	-3.234	Auxin-responsive protein
HORVU.MOREX.r2.4HG0346050	-3.225	basic helix-loop-helix (bHLH) DNA-binding superfamily protein
HORVU.MOREX.r2.5HG0427010	-3.199	Leucine carboxyl methyltransferase
HORVU.MOREX.r2.2HG0161630	-3.189	Gag-Pro-Pol polyprotein
HORVU.MOREX.r2.1HG0075880	-3.189	Plant basic secretory protein family protein, putative
HORVU.MOREX.r2.1HG0009540	-3.160	Xylulose kinase
HORVU.MOREX.r2.5HG0428780	-3.158	Hfr-2-like protein
HORVU.MOREX.r2.6HG0523360	-3.156	Chlorophyll a-b binding protein, chloroplastic
HORVU.MOREX.r2.2HG0155090	-3.150	Cytochrome P450
HORVU.MOREX.r2.3HG0198350	-3.148	Serine incorporator
HORVU.MOREX.r2.7HG0551870	-3.139	Homeobox leucine zipper protein
HORVU.MOREX.r2.7HG0613110	-3.133	Aspartic proteinase nepenthesin-2
HORVU.MOREX.r2.4HG0343900	-3.131	Purple acid phosphatase
HORVU.MOREX.r2.1HG0046920	-3.130	Cation/H(+) antiporter
HORVU.MOREX.r2.7HG0561530	-3.109	Transmembrane protein, putative
HORVU.MOREX.r2.4HG0338680	-3.102	1,4-dihydroxy-2-naphthoate polyprenyltransferase, chloroplastic
HORVU.MOREX.r2.2HG0079620	-3.099	ATP-dependent protease ATPase subunit HslU
HORVU.MOREX.r2.5HG0369230	-3.098	Glutaredoxin family protein
HORVU.MOREX.r2.5HG0436740	-3.060	Amino acid transporter, putative
HORVU.MOREX.r2.6HG0522030	-3.053	ARF-GAP domain 13
HORVU.MOREX.r2.2HG0150390	-3.051	Protodermal factor 1
HORVU.MOREX.r2.4HG0345780	-3.038	Apyrase
HORVU.MOREX.r2.6HG0462950	-3.032	Glucan endo-1,3-beta-glucosidase 3
HORVU.MOREX.r2.2HG0110340	-3.027	Scarecrow transcription factor family protein
HORVU.MOREX.r2.1HG0005850	-3.014	Protein trichome birefringence
HORVU.MOREX.r2.1HG0046390	-3.013	AP2-like ethylene-responsive transcription factor
HORVU.MOREX.r2.3HG0255670	-2.983	Trigger factor
HORVU.MOREX.r2.7HG0603370	-2.956	Beta-carotene isomerase D27, chloroplastic
HORVU.MOREX.r2.5HG0369380	-2.947	Glutaredoxin family protein
HORVU.MOREX.r2.2HG0142780	-2.941	C2 calcium/lipid-binding domain, CaLB
HORVU.MOREX.r2.1HG0017110	-2.908	Peroxidase
HORVU.MOREX.r2.2HG0086020	-2.888	Ribulose biphosphate carboxylase small chain
HORVU.MOREX.r2.2HG0165600	-2.857	Anthocyanidin reductase
HORVU.MOREX.r2.7HG0533890	-2.850	Glycosyltransferase
HORVU.MOREX.r2.3HG0246030	-2.846	UDP-glycosyltransferase
HORVU.MOREX.r2.1HG0029020	-2.835	Ribulose bisphosphate carboxylase small chain
HORVU.MOREX.r2.6HG0521950	-2.829	Nicotianamine synthase
HORVU.MOREX.r2.3HG0257370	-2.829	Proline transporter
HORVU.MOREX.r2.7HG0620050	-2.821	BURP domain protein RD22
HORVU.MOREX.r2.2HG0139610	-2.819	zinc finger homeodomain 1
HORVU.MOREX.r2.3HG0194100	-2.804	Tryptophan aminotransferase

HORVU.MOREX.r2.2HG0093280	-2.801	Universal stress protein
HORVU.MOREX.r2.3HG0248650	-2.777	Beta-galactosidase
HORVU.MOREX.r2.5HG0403320	-2.772	Alpha/beta-Hydrolases superfamily protein
HORVU.MOREX.r2.7HG0603650	-2.758	Zinc-transporting ATPase
HORVU.MOREX.r2.7HG0560190	-2.750	Nucleoporin autopeptidase
HORVU.MOREX.r2.4HG0288540	-2.740	Carboxypeptidase
HORVU.MOREX.r2.7HG0533270	-2.711	Eukaryotic aspartyl protease family protein, putative
HORVU.MOREX.r2.4HG0344460	-2.707	L-allo-threonine aldolase
HORVU.MOREX.r2.1HG0011280	-2.701	neuronal PAS domain protein
HORVU.MOREX.r2.3HG0202810	-2.666	Lachrymatory-factor synthase
HORVU.MOREX.r2.7HG0587300	-2.659	Cytochrome b561
HORVU.MOREX.r2.2HG0170780	-2.649	Tryptophan decarboxylase
HORVU.MOREX.r2.6HG0496790	-2.627	Aldehyde dehydrogenase
HORVU.MOREX.r2.6HG0517410	-2.626	Clustered mitochondria protein
HORVU.MOREX.r2.1HG0038700	-2.603	Aquaporin-1
HORVU.MOREX.r2.4HG0276750	-2.601	O-methyltransferase
HORVU.MOREX.r2.6HG0507730	-2.598	Protein curvature thylakoid chloroplastic-like
HORVU.MOREX.r2.2HG0096630	-2.587	Magnesium-chelatase subunit H
HORVU.MOREX.r2.3HG0251940	-2.583	Bel1-like homeodomain protein 1
HORVU.MOREX.r2.2HG0086070	-2.581	Ribulose biphosphate carboxylase small chain
HORVU.MOREX.r2.2HG0160100	-2.576	GDSL esterase/lipase
HORVU.MOREX.r2.2HG0170800	-2.563	Tryptophan decarboxylase
HORVU.MOREX.r2.3HG0249410	-2.558	Pectinesterase inhibitor, putative
HORVU.MOREX.r2.6HG0515620	-2.551	Glycosyltransferase
HORVU.MOREX.r2.5HG0369340	-2.549	Glutaredoxin family protein
HORVU.MOREX.r2.1HG0070490	-2.549	Sodium Bile acid symporter family
HORVU.MOREX.r2.2HG0092580	-2.516	Peroxidase
HORVU.MOREX.r2.1HG0015910	-2.502	GDSL esterase/lipase
HORVU.MOREX.r2.7HG0547970	-2.493	Glutamate receptor
HORVU.MOREX.r2.5HG0426190	-2.491	Cytochrome b6-f complex subunit 7
HORVU.MOREX.r2.7HG0597710	-2.491	Fructose-bisphosphate aldolase
HORVU.MOREX.r2.2HG0092500	-2.475	Peroxidase
HORVU.MOREX.r2.5HG0396740	-2.468	Vacuolar iron transporter-like protein
HORVU.MOREX.r2.2HG0141130	-2.462	Ferric reduction oxidase 7
HORVU.MOREX.r2.1HG0062600	-2.448	Trehalose-6-phosphate synthase
HORVU.MOREX.r2.2HG0160340	-2.437	Ascorbate peroxidase
HORVU.MOREX.r2.7HG0556340	-2.436	CONSTANS-like zinc finger protein
HORVU.MOREX.r2.4HG0277350	-2.428	Methyltransferase
HORVU.MOREX.r2.1HG0066390	-2.414	30S ribosomal protein S1
HORVU.MOREX.r2.5HG0434150	-2.411	Lactoylglutathione lyase
HORVU.MOREX.r2.1HG0038750	-2.410	Cytochrome P450 family protein
HORVU.MOREX.r2.2HG0081530	-2.408	Glutamyl-tRNA (Gln) amidotransferase subunit A
HORVU.MOREX.r2.1HG0073300	-2.395	Receptor-like kinase
HORVU.MOREX.r2.3HG0199870	-2.376	Boron transporter
HORVU.MOREX.r2.1HG0057610	-2.371	Nodulin-like / Major Facilitator Superfamily protein
HORVU.MOREX.r2.2HG0088630	-2.361	Omega-3 fatty acid desaturase
HORVU.MOREX.r2.3HG0251700	-2.361	Alpha-1,4 glucan phosphorylase
HORVU.MOREX.r2.2HG0174370	-2.323	Cytochrome P450
HORVU.MOREX.r2.2HG0176170	-2.316	polyadenylate-binding protein 1-B-binding protein
HORVU.MOREX.r2.5HG0443070	-2.315	Methyltransferase
HORVU.MOREX.r2.6HG0451570	-2.301	Allene oxide synthase
HORVU.MOREX.r2.3HG0227720	-2.301	Carbonic anhydrase
HORVU.MOREX.r2.4HG0286480	-2.289	Tetrapyrrole-binding protein, chloroplastic
HORVU.MOREX.r2.6HG0475080	-2.272	MLO-like protein
HORVU.MOREX.r2.2HG0128880	-2.268	Peroxidase
HORVU.MOREX.r2.4HG0336650	-2.239	O-methyltransferase
HORVU.MOREX.r2.5HG0399230	-2.230	Zinc finger protein
HORVU.MOREX.r2.4HG0290380	-2.221	Dirigent protein
HORVU.MOREX.r2.5HG0435830	-2.216	transmembrane protein
HORVU.MOREX.r2.5HG0363510	-2.209	Aspartic proteinase nepenthesin-1
HORVU.MOREX.r2.5HG0414480	-2.201	Endoglucanase
HORVU.MOREX.r2.3HG0255040	-2.151	Late embryogenesis abundant protein
HORVU.MOREX.r2.1HG0015070	-2.127	Carboxypeptidase
HORVU.MOREX.r2.6HG0456940	-2.120	Inhibitor protein
HORVU.MOREX.r2.7HG0552870	-2.120	Aquaporin-1
HORVU.MOREX.r2.7HG0546030	-2.112	Nodulin-like / Major Facilitator Superfamily protein

HORVU.MOREX.r2.4HG0278580	-2.066	Octicosaepptide/Phox/BemIp (PB1) / tetratricopeptide repeat (TPR)-containing protein
HORVU.MOREX.r2.3HG0221970	-2.065	Lycopene cyclase family
HORVU.MOREX.r2.1HG0037430	-2.048	Glutamyl-tRNA reductase
HORVU.MOREX.r2.2HG0157960	-2.045	Trypsin family protein
HORVU.MOREX.r2.3HG0244860	-2.037	Sulfite exporter TauE/SafE family protein
HORVU.MOREX.r2.7HG0606510	-2.024	SBP (S-ribonuclease binding protein) family protein
HORVU.MOREX.r2.5HG0443800	-2.016	Aspartokinase

6.2.4. Lists of five DEGs groups in control and/or senescence samples of *HvFPI* OE line

Table 6: List of downregulated genes in control and senescence primary leaves of OE line. Gene IDs, log2FC and gene annotations are provided.

Gene ID	log2FC C	log2FC S	Gene annotation
HORVU.MOREX.r2.6HG0461250	-3.126	-6.293	F-box family protein
HORVU.MOREX.r2.4HG0277340	-2.646	-3.296	Protein DETOXIFICATION

Table 7: List of downregulated genes in senescence primary leaves of OE line. Gene IDs, log2FC and gene annotations are provided.

Gene ID	log2FC S	Gene description
HORVU.MOREX.r2.5HG0436300	-7.400	RNA polymerase II transcription mediator
HORVU.MOREX.r2.6HG0471520	-6.673	Histone H3
HORVU.MOREX.r2.UnG0635260	-6.206	Mediator of RNA polymerase II transcription subunit 12
HORVU.MOREX.r2.4HG0345940	-5.482	60 kDa jasmonate-induced protein; rRNA N-glycosidase
HORVU.MOREX.r2.UnG0634520	-5.273	Senescence-associated protein, putative
HORVU.MOREX.r2.UnG0635170	-4.428	Protein TAR1; FGGY family of carbohydrate kinase
HORVU.MOREX.r2.UnG0632300	-4.346	Senescence-associated protein, putative
HORVU.MOREX.r2.7HG0607010	-3.847	Ras-related protein RHN1
HORVU.MOREX.r2.3HG0242690	-3.263	Peroxidase 2
HORVU.MOREX.r2.UnG0628140	-2.818	Gibberellin 3-beta-dioxygenase 1

Table 8: List of upregulated genes in control and senescence primary leaves of OE line. Gene IDs, log2FC and gene annotations are provided.

Gene ID	log2FC C	log2FC S	Gene annotation
HORVU.MOREX.r2.3HG0209440	10.098	6.331	40S ribosomal protein
HORVU.MOREX.r2.3HG0224010	9.341	9.040	DNL-type zinc finger
HORVU.MOREX.r2.1HG0051090	9.239	5.604	Kinesin heavy chain
HORVU.MOREX.r2.5HG0376190	9.169	9.220	1-phosphatidylinositol 4,5-bisphosphate phosphodiesterase epsilon-1
HORVU.MOREX.r2.5HG0395730	8.977	9.267	Phytochromobilin:ferredoxin oxidoreductase,
HORVU.MOREX.r2.5HG0351050	8.905	8.287	Phosphoenolpyruvate carboxylase
HORVU.MOREX.r2.6HG0520340	8.765	8.403	Tetratricopeptide repeat (TPR)-like superfamily protein
HORVU.MOREX.r2.5HG0433760	8.657	8.797	Pyridoxal-5'-phosphate-dependent enzyme family protein
HORVU.MOREX.r2.2HG0130560	8.417	7.728	Proteasome subunit beta type (type 3-A; subunit C-1)
HORVU.MOREX.r2.1HG0012690	8.390	8.460	Dynein assembly factor 1, axonemal
HORVU.MOREX.r2.1HG0012700	8.298	8.448	HAT transposon superfamily
HORVU.MOREX.r2.7HG0578290	7.989	5.810	DNA ligase
HORVU.MOREX.r2.1HG0023890	7.918	8.348	Phospho-N-acetylmuramoyl-pentapeptide-transferase
HORVU.MOREX.r2.5HG0397670	7.887	6.975	Transposon protein, putative, CACTA, En/Spm sub-class
HORVU.MOREX.r2.6HG0520330	7.686	7.935	binding protein
HORVU.MOREX.r2.6HG0455790	7.633	7.555	Histone H3
HORVU.MOREX.r2.3HG0249140	7.372	7.171	Elongation factor Ts
HORVU.MOREX.r2.5HG0371730	7.222	6.845	Transposon protein, putative, Pong sub-class
HORVU.MOREX.r2.4HG0320800	7.157	7.028	Chaperone DnaJ-domain superfamily protein
HORVU.MOREX.r2.6HG0478560	7.049	7.124	callose synthase 1

HORVU.MOREX.r2.7HG0608000	7.017	8.846	DNA polymerase alpha subunit B
HORVU.MOREX.r2.3HG0240610	6.947	6.893	Transposon protein, putative, CACTA, En/Spm sub-class
HORVU.MOREX.r2.2HG0085430	6.840	7.148	glycosyl hydrolase protein 10/ carbohydrate-binding protein
HORVU.MOREX.r2.5HG0445070	6.811	4.682	DEAD-box ATP-dependent RNA helicase 52A
HORVU.MOREX.r2.3HG0212390	6.569	6.342	Muscarinic acetylcholine receptor M3
HORVU.MOREX.r2.2HG0164100	6.285	7.116	SH3 domain-binding protein 1, putative
HORVU.MOREX.r2.5HG0399970	6.169	8.980	NAD(P)H-quinone oxidoreductase subunit S, chloroplastic
HORVU.MOREX.r2.4HG0309140	5.919	7.476	Microtubule-associated protein RP/EB family member
HORVU.MOREX.r2.7HG0602190	5.756	7.538	DHHC-type zinc finger family protein
HORVU.MOREX.r2.7HG0578300	5.073	7.644	Glutamate receptor
HORVU.MOREX.r2.5HG0392660	4.971	4.854	XH/XS domain-containing protein
HORVU.MOREX.r2.7HG0578310	4.838	6.792	Sentrin-specific protease 1
HORVU.MOREX.r2.7HG0602170	4.574	4.795	RCC1 family with FYVE zinc finger domain-containing protein
HORVU.MOREX.r2.7HG0531390	4.520	4.056	HAT dimerisation domain-containing protein-like
HORVU.MOREX.r2.7HG0553540	4.230	4.847	SUMO-activating enzyme 2
HORVU.MOREX.r2.1HG0006800	4.130	5.544	RNA polymerase Rpb1, domain 2 family protein
HORVU.MOREX.r2.3HG0207920	4.053	4.827	photosystem I reaction center subunit PSI-N, chloroplast,
HORVU.MOREX.r2.4HG0298030	3.948	5.797	Laccase-22
HORVU.MOREX.r2.6HG0489720	3.669	4.222	Wall-associated receptor kinase 1
HORVU.MOREX.r2.5HG0378770	3.534	4.493	Acyl-[acyl-carrier-protein] desaturase
HORVU.MOREX.r2.3HG0223050	3.291	4.225	protein serine/threonine kinase
HORVU.MOREX.r2.4HG0299360	3.228	2.687	Putative cysteine-rich receptor-like protein kinase 20
HORVU.MOREX.r2.2HG0113950	3.071	4.714	Beta-amylase; 1,4-alpha-D-glucan maltohydrolase
HORVU.MOREX.r2.4HG0314620	2.678	2.960	ATP-dependent DNA helicase MER3 homolog

Table 9: List of upregulated genes in control primary leaves of OE line. Gene IDs, log2FC and gene annotations are provided.

Gene ID	log2FC C	Gene annotation
HORVU.MOREX.r2.3HG0259090	7.532	Muscle calcium channel subunit alpha-1
HORVU.MOREX.r2.7HG0610720	6.603	Werner Syndrome-like exonuclease
HORVU.MOREX.r2.5HG0351060	6.562	Rp1-like protein
HORVU.MOREX.r2.2HG0084340	6.076	La-related protein 7
HORVU.MOREX.r2.1HG0017340	5.745	Dynamin-1
HORVU.MOREX.r2.2HG0086370	5.429	Heavy metal-associated domain containing protein; AtHIPP27
HORVU.MOREX.r2.2HG0171210	4.738	Alpha/beta-Hydrolases superfamily protein
HORVU.MOREX.r2.7HG0531400	3.790	Leucine-rich repeat receptor-like protein kinase family protein
HORVU.MOREX.r2.4HG0324960	3.718	Ubiquitin-60S ribosomal protein L40-2
HORVU.MOREX.r2.4HG0302280	3.578	Sterol 3-beta-glucosyltransferase
HORVU.MOREX.r2.2HG0174650	3.512	Ubiquitin-conjugating enzyme. E2 23
HORVU.MOREX.r2.4HG0325150	3.421	Rho GTPase-activating protein
HORVU.MOREX.r2.5HG0396600	3.209	vacuolar sorting receptor 3
HORVU.MOREX.r2.2HG0105250	2.633	Dihydroflavonol-4-reductase
HORVU.MOREX.r2.5HG0404540	2.498	NADH-quinone oxidoreductase subunit C
HORVU.MOREX.r2.7HG0578320	2.406	Nitrate transporter 1.1; Protein NRT1
HORVU.MOREX.r2.3HG0183540	2.231	Disease resistance protein RPM1
HORVU.MOREX.r2.4HG0304020	2.136	FRS (FAR1 Related Sequences) transcription factor family

Table 10: List of upregulated genes in senescence primary leaves of OE line. Gene IDs, log2FC and gene annotations are provided.

Gene ID	log2FC S	Gene annotation
HORVU.MOREX.r2.5HG0362860	7.598	Inter-alpha-trypsin inhibitor heavy chain H3
HORVU.MOREX.r2.1HG0068030	6.483	Transposon protein Pong sub-class

HORVU.MOREX.r2.2HG0115750	6.437	Tetratricopeptide repeat (TPR)-like superfamily protein
HORVU.MOREX.r2.7HG0578120	6.436	HAT family dimerisation domain containing protein
HORVU.MOREX.r2.2HG0166400	6.408	Sentrin-specific protease
HORVU.MOREX.r2.6HG0471730	6.308	Retrovirus-related Pol polyprotein from transposon TNT 1-94
HORVU.MOREX.r2.1HG0075950	5.952	DNA topoisomerase 2
HORVU.MOREX.r2.6HG0483610	5.484	tRNA pseudouridine synthase D
HORVU.MOREX.r2.7HG0593770	4.700	Receptor kinase-like protein Xa21
HORVU.MOREX.r2.7HG0529200	4.685	MLO-like protein 1
HORVU.MOREX.r2.2HG0169350	4.560	Probable staphylococcal-like nuclease CAN3; Ca(2+)-dependent nuclease
HORVU.MOREX.r2.5HG0405890	4.332	tRNA (guanine-N(7)-)-methyltransferase
HORVU.MOREX.r2.3HG0223070	4.157	Animal RPA1 domain protein
HORVU.MOREX.r2.4HG0302250	4.101	Acyl-CoA-binding domain-containing protein 4
HORVU.MOREX.r2.7HG0534230	3.994	Transposon protein. putative. Mutator sub-class
HORVU.MOREX.r2.6HG0483180	3.986	Protein FAR1-RELATED SEQUENCE 5
HORVU.MOREX.r2.1HG0028670	3.879	Transposon protein. putative. CACTA. En/Spm sub-class. expressed
HORVU.MOREX.r2.6HG0514330	3.872	Protein kinase family protein
HORVU.MOREX.r2.5HG0362360	3.851	Protein FAR1-RELATED SEQUENCE 5
HORVU.MOREX.r2.3HG0223060	3.824	Replication protein A 70 kDa DNA-binding subunit
HORVU.MOREX.r2.3HG0227220	3.801	Auxilin-like protein 1
HORVU.MOREX.r2.2HG0134440	3.796	Zinc finger CCCH domain-containing protein 43
HORVU.MOREX.r2.2HG0111810	3.718	Transposase
HORVU.MOREX.r2.2HG0134450	3.682	Tripartite terminase subunit 1
HORVU.MOREX.r2.7HG0584560	3.623	ARIA-interacting double AP2 domain protein
HORVU.MOREX.r2.6HG0514320	3.539	Cysteine-rich receptor-like protein kinase 24
HORVU.MOREX.r2.3HG0211130	3.486	Kinesin-like protein KIN-14T
HORVU.MOREX.r2.1HG0077060	3.477	Structural maintenance of chromosomes protein 3
HORVU.MOREX.r2.UnG0634460	3.444	NAD(P)H-quinone oxidoreductase subunit 3. chloroplastic
HORVU.MOREX.r2.1HG0032640	3.433	F-box protein
HORVU.MOREX.r2.6HG0460140	3.413	Endoglucanase 11
HORVU.MOREX.r2.7HG0572880	3.238	Helicase-like protein
HORVU.MOREX.r2.7HG0576930	3.092	Structural maintenance of chromosomes protein 1
HORVU.MOREX.r2.4HG0318530	3.065	calmodulin 1
HORVU.MOREX.r2.3HG0183280	2.985	Derlin-2.1
HORVU.MOREX.r2.1HG0022230	2.933	MAR-binding filament-like protein 1-1
HORVU.MOREX.r2.4HG0290210	2.910	Fanconi anemia group M protein; ATP-dependent RNA helicase FANCM
HORVU.MOREX.r2.3HG0240540	2.851	modifier of sncl.4
HORVU.MOREX.r2.2HG0125080	2.781	Protein GRIP
HORVU.MOREX.r2.4HG0338220	2.757	Dentin sialophosphoprotein-related. putative isoform 1
HORVU.MOREX.r2.7HG0595240	2.590	Cell division cycle and apoptosis regulator protein 1
HORVU.MOREX.r2.2HG0174540	2.562	Disease resistance RPP13-like protein 4 (or ZAR1)
HORVU.MOREX.r2.5HG0407770	2.492	Helicase SEN1; tRNA-splicing endonuclease positive effector

6.3. The relative transcript level of six members of barley HIPP family during developmental leaf senescence in WT, OE and KO lines

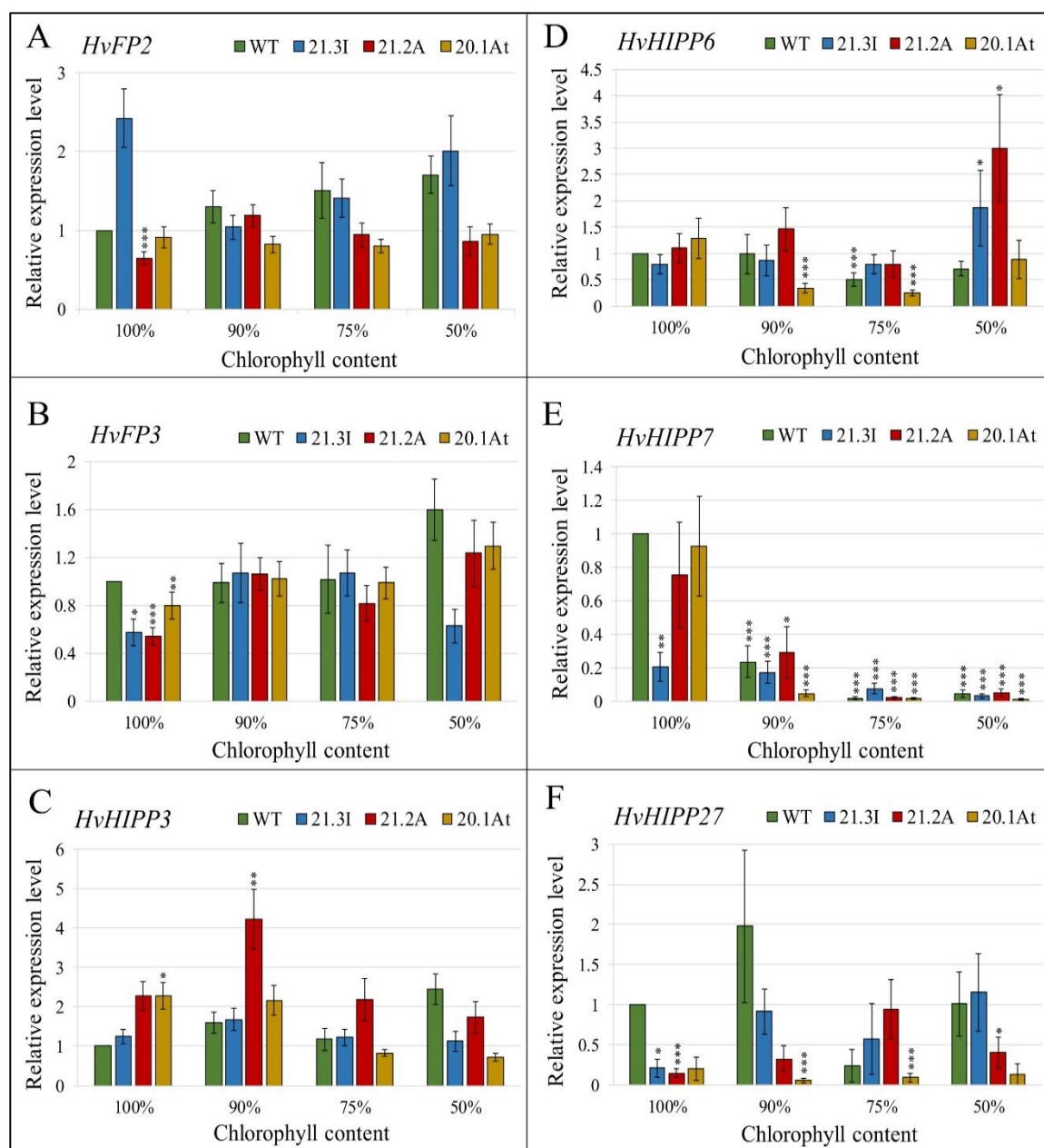


Figure 45: The relative transcript level of six barley HIPP members during developmental leaf senescence in WT and transgenic lines. (A) *HvFP2*; (B) *HvFP3*; (C) *HvHIPP3*; (D) *HvHIPP6*; (E) *HvHIPP7* and (F) *HvHIPP27* in WT, 21.3I, 21.2A and 20.1At lines, in different stages of leaf senescence, defined by the reduction in Chl content. Mean relative expression levels of two independent biological replicates, standard deviations and p -values were determined by REST-384 © 2006 (Pfaffl *et al.*, 2002) and normalized against *HvPP2A*, *HvActin* and *HvGCN5*. Statistically significant differences between WT, OE and KO lines at various stages of developmental leaf senescence, as defined from Chl content, in comparison to WT samples with 100 % Chl content are indicated by asterisks $p < 0.05$ (*), $p < 0.01$ (), $p < 0.001$ (***)**

6.4. Additional information for the primers and vectors used in Materials and Methods

6.4.1. Vectors for genetic transformation of barley embryos

Table 11: Description of the vectors used in genetic transformation of barley embryos.

Vector	Special Feature	Resistance	Reference
pENTR™/D-TOPO®	TOPO®-cloning GATEWAY®-System	Kanamycin (Kan ^R)	Thermo Fisher Scientific
pGEM®-T	β- Galactosidase gene: lac Z	Ampicillin (Amp ^R)	Promega
pIPKb004 (oe-vector)	Promoter: CaMVd35S GATEWAY®-System	Chloramphenicol (Cm ^R), Spectinomycin (Spec ^R), Hygromycin (Hpt ^R)	Himmelbach <i>et al.</i> , 2007 Acc.Nr.:EU161575
pMGE625 (shuttle vector)	Promoter: HvU3. link sequence M13. scaffold sequence. ccdB cassette	Ampicillin (Amp ^R), Chloramphenicol (Cm ^R)	Dang <i>et al.</i> , 2015; Kumar <i>et al.</i> , 2018
pMGE626 (shuttle vector)	Promoter: HvU3. scaffold sequence. ccdB cassette	Ampicillin (Amp ^R), Chloramphenicol (Cm ^R)	Dang <i>et al.</i> , 2015; Kumar <i>et al.</i> , 2018
pMGE628 (shuttle vector)	Promoter: HvU3. link sequence JS838. scaffold sequence. ccdB cassette	Ampicillin (Amp ^R), Chloramphenicol (Cm ^R)	Dang <i>et al.</i> , 2015; Kumar <i>et al.</i> , 2018
pMGE629 (shuttle vector)	Promoter: HvU3. scaffold sequence. ccdB cassette	Ampicillin (Amp ^R), Chloramphenicol (Cm ^R)	Dang <i>et al.</i> , 2015; Kumar <i>et al.</i> , 2018
pMGE634 (gene editing vector)	ZmUbi:Cas9 gene ccdB cassette	Chloramphenicol (Cm ^R), Spectinomycin (Spec ^R), Hygromycin (Hpt ^R)	Kumar <i>et al.</i> , 2018

6.4.2. List of primers and oligos used in PCR, qRT-PCR and CRISPR protocols

Table 12: Information of the primers and oligos used in PCR, qRT-PCR and CRISPR protocols.

Primer for genetic transformation	
Primer name	Primer sequence
d35S_prom_fw	5'-GATGACGCACAATCCCACTATCCT-3'
CaMV35S_01_fw	5'-AAGGCGGAAACGACAATCTG-3'
CaMV35S_01_rev	5'-TGGTGATTCAGCGTGTCTCTC-3'
FP1+TOPO+Tag_fw	5'-caccgaattcATGGCTAGCTGGAGCCACCCGCAGTTCGAAAAAGGCC atggggatcgtgacgtggtgctg-3'
FP1+Bam_rev	5'-ggatccCTACATGACGGAGCAGGCGTTGGG-3'
M13 fw (pENTR)	5'-GTAAAACGACGGCCAG-3'
M13 rev (pENTR)	5'-CAGGAAACAGCTATGAC-3'
SP6 rev (pGEM-T)	5'-AGCTATTTAGGTGACACTATAG-3'
NewT7 for (pGEM-T)	5'-GTAATACGACTCACTATAGGGC-3'
M13F	5'-GTTTTCCAGTCACGAC-3'
JS838	5'-GCCAGTCTCTATGAGTACTGA-3'
JS1132	5'-AACGCTCTTTCTCTTAGGT-3'
Oligos for knock out lines	
sgRNA1_oligo1	5'-agcAAGGCCCTCGACGACATGAA-3'
sgRNA1_oligo2	5'-aacTTCATGTCGTCGAGGGCCT-3'
sgRNA2_oligo1	5'-agcaCGCCGGGTGGCATAACAAGAC-3'

sgRNA2_oligo2	5'-aacGTCTTGTATGCCACCCGGCG-3'		
sgRNA3_oligo1	5'-agcAGGGGTCGCTCATGACGTTG-3'		
sgRNA3_oligo2	5'-aacCAACGTCATGAGCGACCCC-3'		
Primers for genotyping of transgenic lines			
Hyg_fw	5'-TCGGCGAGTACTTCTACACA-3'		
Hyg_rev	5'-GATCGTTATGTTTATCGGCAC-3'		
HvFP1_mut2_fw	5'-GTTTCCTCGTCTCATCCAGCATCC-3'		
HvFP1_mut1_rev	5'-GGAGCAGGCGTTGGGGTTCT-3'		
HvFP1_RT_F2	5'-TTCACCGAATTCATGGCTAGCT-3'		
HvFP1_RT_R1	5'-CCCACCCCTGGATCCCTACATGA-3'		
pIPK004_fw	5'-GGAATTCAAGCTTACGCGTGTC-3'		
pIPK004_rev	5'-AACGATCGGGGAAATTCGAGTC-3'		
Primers for qRT-PCR – stress treatments and leaf senescence			
Gene ID	Gene name	Primer name	Primer sequence
HORVU4Hr1G07 4680	Serine/threonine protein phosphatase 2A	HvPP2A_fw	5'-CACCATTCTCAGCTTGTATTG-3'
		HvPP2A_rev	5'-CACCCCTTGTATTGTTTGTG-3'
HORVU1Hr1G00 2840	Actin 7	HvActin_fw	5'-GGAAATGGCTGACGGTGAGGAC-3'
		HvActin_rev	5'-GGCGACCAACTATGCTAGGGAAAAC-3'
HORVU1Hr1G03 4070	Histone acetyltransferase GCN5	HvGCN5_fw	5'-CAGGCCGCGTCAACCAAGAAC-3'
		HvGCN5_rev	5'-GGACGGCATAACAAGCAAGTCAG-3'
HORVU1Hr1G08 1240	Protein of unknown function, DUF584	HvS40_fw	5'-CGACGGCGACGTCCGATGTA-3'
		HvS40_rev	5'-CTTTGAGCGTCCCTTTC-3'
HORVU4Hr1G06 6860	glutamine synthetase	HvGS2_fw	5'-ATCGTCGTCTCTACGTACTTGC-3'
		HvGS2_rev	5'-AGCGGATCTCACAGGTCG-3'
HORVU5Hr1G00 8050	9-cis-epoxycarotenoid dioxygenase 3	HvNCED_fw	5'-CGCCCTCCATCCCTCCCATCTTCT-3'
		HvNCED_rev	5'-CCGCCGCTAACTGTTTCTCTTCC-3'
HORVU3Hr1G00 7500	16.9 kDa class I heat shock protein 1	HvHsp17_fw	5'-TCGAGATCTCCGGCTGAATGC-3'
		HvHsp17_rev	5'-CGGCAAGAACAACGACACAAC-3'
HORVU2Hr1G09 9820	Cold-responsive protein Wcor15-A	HvCor14b_02_fw	5'-TCTTCCCAGGCCGTGCTTCC-3'
		HvCor14b_02_rev	5'-GCCGCTCTTCGCTTCTC-3'
HORVU5Hr1G09 2160	Dehydrin 7	HvDhn1_RTQ_for02	5'-GAGGAGGAAGAAGGGGATGAAG-3'
		HvDhn1_RTQ_rev02	5'-AGCTTCTCCTTGATCTTGTCCA-3'
HORVU3Hr1G08 5760	Gamma-glutamyl phosphate reductase	HvP5CS2_F2_5	5'-CCCTTCCTCGCCTCGCCCGTCTC-3'
		HvP5CS2_R2_5	5'-GCCATTCCTCCGCTCCCGCTTCTC-3'
HORVU1Hr1G07 9290	Late embryogenesis abundant protein 76	HVA1_RTQ_for03	5'-AAGCAGTCGATCCATTCCAAGT-3'
		HVA1_RTQ_rev03	5'-CATCATCTGCCGGTCTTCTC-3'
HORVU.MOREX .r2.5HG0424600	Cysteine protease	HvCBL_fw01	5'-CCCTGCCTAGCTTTCCTTCT-3'
		HvCBL_rev01	5'-GTGCGAGGATTAACGTGGAC-3'
HORVU.MOREX .r2.2HG0086370	Heavy metal-associated domain containing protein	HvFP1_01_fw	5'-CGCCGGGTGGCATAACAAGAC-3'
		HvFP1_01_rev	5'-CGGCGGAGGGGTCGCTCAT-3'
Primers for qRT-PCR – RNA Seq validation			
Gene ID	Gene name	Primer name	Primer sequence
		HvFRS5_fw01	5'-CCTCTCGCTGTGACGGAACG-3'

HORVU.MOREX .r2.4HG0316380	FAR1-related sequence 5	HvFRS5_rev01	5'-TCGGTGGAGGAACGGTGGG-3'
HORVU.MOREX .r2.5HG0395730	Phytochromobilin:ferredoxin oxidoreductase	HvElm1_fw02	5'-TGGTATGGTCAAGCAAAGCA-3'
		HvElm1_rev02	5'-GATTAGGCATTGCACACCCA-3'
HORVU.MOREX .r2.4HG0302250	Acyl-CoA-binding domain-containing protein 4	HvACBD4_fw01	5'-ACAGTAACTAGAGCAGGCC-3'
		HvACBD4_rev01	5'-TGCAGCAACATGGTTGGATC-3'
HORVU.MOREX .r2.7HG0585880	F-box domain containing protein/ zinc binding CCCH protein	HvC3H12_fw	5'-CTCATGAGACCAGCACAGGA-3'
		HvC3H12_rev	5'-CTAGCTTCTGTGGCCCTCTT-3'
HORVU.MOREX .r2.5HG0352380	Myb/SANT-like DNA-binding domain protein	HvMyb_fw	5'-CATCTCCTCCCTCCATCCAC-3'
		HvMyb_rev	5'-GTCCAGGCCCTCTTTACTCCA-3'
HORVU.MOREX .r2.4HG0305130	Auxin response factor	HvARF10_fw	5'-TGTTGAGCATGACTGGAGGA-3'
		HvARF10_rev	5'-GAGACACGGTAGGGAAGGAG-3'
Primers for qRT-PCR – other barley HIPPs			
Gene ID	Gene name	Primer name	Primer sequence
HORVU.MOREX .r2.2HG0135330	Heavy-metal-associated domain-containing family protein	HvFP2_for	5'-GCATGACAGACACAAAGGCA-3'
		HvFP2_rev	5'-TGCTCATCTTGGGGTTCACT-3'
HORVU.MOREX .r2.3HG0221330	Heavy-metal-associated domain-containing family protein	HvFP3_for	5'-AGAGGAGAGTCAAGAACGCC-3'
		HvFP3_rev	5'-CCGGTGCCTTCTGTGCGTA-3'
HORVU.MOREX .r2.1HG0029940	Heavy metal-associated protein	HvHIPP3-like_for	5'-GGAGCAGGAGACAAGGAGAA-3'
		HvHIPP3-like_rev	5'-CGTCCACCATCACTTCCTTC-3'
HORVU.MOREX .r2.4HG0333490	Heavy metal-associated protein	HvHIPP6-like_for	5'-GCATCAGACGCCGAATCTAC-3'
		HvHIPP6-like_rev	5'-GTTGTCCTTCTTCTCGTCGC-3'
HORVU.MOREX .r2.2HG0134510	Heavy metal-associated protein	HvHIPP7-like_for	5'-CGCCGAAACCTGAAGAGAAG-3'
		HvHIPP7-like_rev	5'-CTTGGTCTCCTCAAACACGC-3'
HORVU.MOREX .r2.7HG0597830	Heavy metal-associated domain containing protein	HvHIPP27-like_for02	5'-CTTCCTAGAAGCCCTGTCCG-3'
		HvHIPP27-like_rev02	5'-TGACGGTCACCCTGTTCTC-3'

List of Figures

Figure 1: A synopsis of abiotic and biotic stress factors and their possible effects on plant development (adapted from Baweja & Kumar, 2020).	5
Figure 2: The ABA-dependent and ABA-independent pathways under osmotic stress.	10
Figure 3: Model sequence of HIPP proteins with the two key components and the optional nuclear localization signal.	13
Figure 4: Study of HvFP1 under various conditions.	14
Figure 5: Top ten producers and total barley production in million tons worldwide for the year 2020.	18
Figure 6: The relative transcript level of <i>HvFP1</i> at different time points of abiotic stress. .	21
Figure 7: The relative transcript level of <i>HvFP1</i> at various developmental stages, compared with samples of 13 th DAS.	22
Figure 8: The relative transcript level of <i>HvFP1</i> in barley primary leaves after treatment with various phytohormones.	23
Figure 9: The relative transcript level of <i>HvFP1</i> in barley transgenic lines.	25
Figure 10: Western blot analysis for detection of HvFP1 in WT, both OE and one KO lines using purified polyclonal α -HvFP1 antibodies.	26
Figure 11: Phenotypic analysis of total 10 plants of each transgenic line.	27
Figure 12: Study of barley <i>HvFP1</i> OE lines under drought stress.	28
Figure 13: The relative transcript level of drought stress marker genes at different time points of drought stress, compared with samples of WT on 11 th DAS.	29
Figure 14: The relative transcript level of drought stress marker genes in drought samples of OE lines at different time points, compared with drought samples of WT at each time point.	30
Figure 15: Study of barley <i>HvFP1</i> OE lines under cold and high light (4°C+HL) stress.	31
Figure 16: Study of barley <i>HvFP1</i> OE lines under salt stress.	32
Figure 17: The relative transcript level of salt stress marker genes at different time points after salt application.	33
Figure 18: Study of barley <i>HvFP1</i> OE lines under dark stress.	34
Figure 19: The relative transcript level of dark stress marker genes at different time points after dark application.	35
Figure 20: Study of barley <i>HvFP1</i> OE lines during developmental leaf senescence.	36
Figure 21: Primary leaves of WT, 21.3I and 21.2A lines during the course of developmental leaf senescence.	37
Figure 22: The relative transcript level of senescence marker genes at various developmental stages, as defined by the Chl content of WT primary leaves.	38
Figure 23: Study of barley <i>HvFP1</i> KO line under drought stress.	40
Figure 24: The relative transcript level of drought stress marker genes in WT and <i>HvFP1</i> KO lines at different time points.	41-42
Figure 25: Study of barley <i>HvFP1</i> KO line during developmental leaf senescence.	42
Figure 26: The relative transcript level of senescence marker genes at various developmental stages, as defined by the Chl content of WT primary leaves.	44

Figure 27: Correlation coefficient matrix among different treatments, lines and biological replicates.....	46
Figure 28: Total number of differentially expressed genes in WT and <i>HvFPI</i> OE lines.	47
Figure 29: Venn diagrams of (A) senescence upregulated (associated) genes and (B) senescence downregulated genes in WT and/or OE line.	47
Figure 30: The major groups of functional annotation and the number of genes in each group for (A) Senescence Upregulated (Associated) Genes and (B) Senescence Downregulated Genes..	49
Figure 31: A summary of functional groups and representative genes, which were upregulated during the reprogramming of gene expression in response to developmental leaf senescence in barley.	50
Figure 32: A summary of functional groups and representative genes, which were downregulated during the reprogramming of gene expression in response to developmental leaf senescence in barley.	51
Figure 33: Total number of genes, which were up- or downregulated in (A) oe-C compared with wt-C samples and (B) oe-S compared with wt-S samples.	52
Figure 34: Venn diagrams of: (A) Upregulated genes in oe-C and oe-S samples in comparison to wt-C and wt-S, respectively and (B) Downregulated genes in oe-C and oe-S samples in comparison to wt-C and wt-S, respectively.	53
Figure 35: The groups of functional annotation and the number of genes in each group for upregulated genes in <i>HvFPI</i> OE line.	53
Figure 36: The relative transcript level of selected genes for RNA Seq validation.....	56
Figure 37: Schematic representation of the proposed model for the mode of function of <i>HvFPI</i>	85
Figure 38: Schematic representation of the gene structure of <i>HvFPI</i> overexpressing construct in lines 21.3I and 21.2A.....	VIII
Figure 39: Schematic representation of <i>HvFPI</i> sequence and the targets of CRISPR-Cas9 system for the establishment of knock out lines 20.1At and 20.17M.	VIII
Figure 40: Polymerase Chain Reaction for the detection of inserted <i>Strep-HvFPI</i> transgene in OE lines for selected barley plants of T1 generation.	IX
Figure 41: Polymerase Chain Reaction for the detection of full and spliced transcribed products of <i>HvFPI</i> in OE lines.	IX
Figure 42: Polymerase Chain Reaction reaction for detecting <i>HvFPI</i> KO plants in 24 samples, after transformation with the CRISPR-Cas9 system.	X
Figure 43: Photos of selected plants of WT, OE lines 21.3I and 21.2A and KO lines 20.1At and 20.17M on the 43 rd day after sowing.	XI
Figure 44: Example of an electropherogram profile, showing the quality of the ladder and two RNA samples as derived from Bioanalyzer 2100.	XII
Figure 45: The relative transcript level of six barley HIPP members during developmental leaf senescence in WT and transgenic lines.	XXVIII

List of Tables

Table 1: The five groups, in which the differentially regulated genes of OE line are classified.....	52
Table 2: Data quality summary for each sequenced sample.	XIII
Table 3: Summary of mapping results and the distribution of clean reads in reference genome.	XIII
Table 4: List of SAGs in WT barley primary leaves.....	XIV
Table 5: List of SDGs in WT barley primary leaves.....	XXI
Table 6: List of downregulated genes in control and senescence primary leaves of OE line.	XXV
Table 7: List of downregulated genes in senescence primary leaves of OE line.	XXV
Table 8: List of upregulated genes in control and senescence primary leaves of OE line.	XXV
Table 9: List of upregulated genes in control primary leaves of OE line.	XXVI
Table 10: List of upregulated genes in senescence primary leaves of OE line.	XXVI
Table 11: Description of the vectors used in genetic transformation of barley embryos.	XXIX
Table 12: Information of the primers and oligos used in PCR, qRT-PCR and CRISPR protocols.....	XXIX

Acknowledgements

At this point, I would like to thank Prof. Dr. Klaus Humbeck for including me in his working group, for giving me the opportunity to work on this new, interesting project and for our excellent collaboration in the last five years. He was always available to discuss the progress of the project, new ideas and future steps, but he also created a positive working environment. His critical comments and input were very valuable for the formulation of the present work.

I kindly thank Prof. Dr. Holger B. Deising for his great suggestions and ideas during our meetings as the co-advisor of my doctoral dissertation.

Prof. Dr. Nicolaus von Wirén and Prof. Dr. Karin Krupinska are thanked for reviewing the present thesis and giving me a very helpful feedback.

The present work was funded as part of the International Graduate School for Agricultural and Polymer Sciences (AGRIPOLY) (Project: ZS/2016/08/80644), which is greatly appreciated. A great thank to the coordinator of this program, PD Dr. Carsten Milkowski, who took care of all financial and bureaucratic matters, as well as to the fellow students/post-docs and their PIs for the productive meetings, exchange of ideas and fun times during our excursions.

Furthermore, I am grateful to the members of the working group of Prof. Dr. Edgar Peiter, especially Dr. Minh Thi Than Hoang and Liane Freitag, for their help to establish and cultivate the knock out barley lines. Members of this working group and Steffan Ehnert are thanked for creating the overexpression barley lines before the beginning of this thesis.

Many thanks to Dr. Olaf Barth for his supervision and guidance during the elaboration of the present thesis. He was always motivated and available to discuss results and new ideas for future experiments. His critical proofreading of this thesis and paper is greatly appreciated. Also, his contribution in generating the a-HvFP1 antibodies, in protein and western blot analysis and other experiments, which were not included in the present work, is greatly appreciated. Dr. Xuan Hieu Cao is thanked for his contribution and guidance during the RNA sequencing performance and analysis. Dipl. Ing. Michael Röser is greatly thanked for his precious technical help in the greenhouse facilities.

I am grateful to all members of plant physiology lab, who created a positive and fun working environment in the last five years. Furthermore, Siska Herklotz and Dr. Nancy Zimmermann are thanked for valuable technical support in my experiments. Dr. Wiebke Zschiesche is thanked for her contribution in formulating the topic of the thesis and her critical comments for the paper. Many thanks to Charlotte Ost and Linh Thuy Nguyen, with whom I shared the office and they really created a relaxed and fun working place. They also provided valuable advice during the elaboration of the thesis. Fellow PhD students Minh Manh Bui, Sylvie Schäfer, Christina Mohr and Ivana Mladenovic are also thanked for the nice meetings and exchange of ideas. The work of the master (at that time) students Paul Winkler, Jessica Li, Cathleen Skupin and Taif Saddawi is greatly appreciated. During our fun collaboration, they provided valuable results.

Last but not least, my sincere gratitude goes to my family and friends, who are not directly linked to the present dissertation, but they offered the greatest support.

Curriculum Vitae

Athina Parasyri

Date of birth: 09.10.1991
 Place of birth: Rethymnon, Crete, Greece
 Nationality: Greek

Education

Nov 2017 – Apr 2023	PhD candidate in Plant Physiology, Institute of Biology Martin-Luther University, Halle-Wittenberg (Halle Saale)
Oct 2014 – Nov 2016	Master studies in Plant Molecular Biology and Biotechnology University of Crete (Heraklion, Greece)
Oct 2009 – Mar 2014	Bachelor studies in Biology University of Crete (Heraklion, Greece)
June 2009	High School Leaving Certificate General High School of Perama (Rethymnon, Greece)

Publications and conferences

- Parasyri, A., Barth, O., Zschiesche, W., & Humbeck, K. (2022). The Barley Heavy Metal Associated Isoprenylated Plant Protein HvFP1 Is Involved in a Crosstalk between the Leaf Development and Abscisic Acid-Related Drought Stress Responses. *Plants* 11:2851.
- Orfanidis, S., Stamatis, N., Parasyri, A., Mente, M.S., Zerveas, S., Pigada, P., Papadimitriou, A., Paschou, M., Nisiforou, O., Papazi, A., Moustaka-Gouni, M., & Kotzabasis, K. (2019). Solving Nuisance Cyanobacteria Eutrophication Through Biotechnology. *Appl. Sci.* 9:2566.
- Parasyri, A., Papazi, A., Stamatis, N., Zerveas, S., Avramidou, E.V., Doulis, A.G., Pirintsos, S., & Kotzabasis, K. (2018). Lichen as Micro-Ecosystem: Extremophilic Behavior with Astrobiotechnological Applications. *Astrobiology* 18:1528-1542.
- Papazi, A., Korelidou, A., Andronis, E., Parasyri, A., Stamatis, N., & Kotzabasis, K. (2018) Bioenergetic reprogramming plasticity under nitrogen depletion by the unicellular green alga *Scenedesmus obliquus*. *Planta* 247:679–692.
- 20th Mitteldeutsche Pflanzenphysiologie-Tagung (June 2022) Dresden: “Barley HvFP1 functions as a crosstalk factor for the regulation of abiotic stress responses and developmental leaf senescence”. (Talk)
- 19th Mitteldeutsche Pflanzenphysiologie-Tagung (September 2021) Wittenberg: “Study of HvFP1 under abiotic stress conditions and leaf development”. (Talk)
- Parasyri, A., Barth, O., Zschiesche, W., & Humbeck, H. (June 2019) 15th Plant Science Student Conference 2019, IPB Halle (Saale): “Heavy metal associated Isoprenylated Plant Proteins (HIPPs): Unravelling their function in plant stress responses”. (Poster Presentation)
- 16th Mitteldeutsche Pflanzenphysiologie-Tagung (February 2018) Dresden: “Identification and functional analyses of putative crosstalk factors of abiotic and biotic stress responses in barley”. (Talk)

Statutory declaration

I heremit declare that with the present thesis, I am applying for the first time to obtain a doctoral degree.

Furthermore, I declare that the work entitled “Barley HIPP protein HvFP1 functions in a crosstalk between abiotic stress responses and developmental signaling pathways, including leaf senescence” was written by me, independently and without external help. All sources and resources, which were used in the thesis, were specified and indicated accordingly. All references to the used works, either verbatim or in content, have been identified and quoted.

Halle (Saale), _____

Athina Parasyri